IMPACTS OF CLIMATE CHANGE AND REFORESTATION ON RAINFALL ONSET AND CESSATION OVER WEST AFRICA USING REGIONAL CLIMATE MODELS

MOUNKAILA SALEY, Moussa
(Bsc, Msc)
MET/11/7677

A THESIS
SUBMITTED TO THE SCHOOL OF POSTGRADUATE STUDIES, FEDERAL UNIVERSITY OF TECHNOLOGY AKURE (FUTA) IN PARTNERSHIP WITH THE WEST AFRICAN SCIENCE SERVICE CENTRE ON CLIMATE CHANGE AND ADAPTED LAND USE (WASCAL), IN PARTIAL FULFILLMENT OF THE REQUIREMENT FOR THE AWARD OF THE DEGREE OF DOCTOR OF PHILOSOPHY IN METEOROLOGY AND CLIMATE SCIENCE

DEPARTMENT OF METEOROLOGY AND CLIMATE SCIENCE
FEDERAL UNIVERSITY OF TECHNOLOGY, AKURE
NIGERIA

FEBRUARY, 2015

ABSTRACT

This study used two observation datasets (the Global Precipitation Climatology Project (GPCP) and the Tropical Rainfall Measuring Mission (TRMM)), to evaluate the ability of nine regional climate models (RCMs) that participated in the Coordinated Regional Climate Downscaling Experiment of Africa (CORDEX-Africa), in simulating the rainfall onset and cessation dates (RODs/RCDs) in West Africa. The study also used two of the RCMs (RegCM and WRF) to examine the potential impacts of climate change and reforestations on RODs and RCDs. All the CORDEX RCMs were driven by ERA-Interim reanalysis (ERAIN), while for impacts studies, RegCM and WRF were driven by general circulation models (GCMs) HadGEM and ECHAM respectively. Four definitions of ROD and one definition of RCD based on rainfall data only are used to compute ROD/RCD. The models evaluation focussed on how well the models simulate the observed mean, standard deviation, and inter-annual variability of ROD and RCD over West Africa when compared to observations (GPCP and TRMM), ERAIN and GCMs. The models were also assessed on how well they link ROD/RCD with the northward movement of the monsoon system over the region. This is because reliable forecasts of the RODs and RCDs are crucial for agricultural planning and food security in West Africa. Results from the observations show that the mean ROD and RCD in West Africa have a zonal distribution with onset dates (ROD) increasing (RCD decreasing) from the Guinea coast northward. ERAIN fails to reproduce the spatial distribution of ROD/RCD as observed in GPCP and TRMM. It was found that the performance of some RCMs in simulating the RODs depends on the ROD definition used, for while ARPEGE, RACMO, PRECIS, and CCLM produce better ROD distributions than ERAIN when the first three ROD definitions were used, they give worse ROD distribution than ERAIN using the fourth definition. However, regardless of the definition used, CCRM5, RCA35, REMO, RegCM3 and WRF show a remarkable improvement over ERAIN. Furthermore, the RCMs (RCA35, PRECIS, CRCM5, REMO, RACMO, RegCM3, and WRF) simulate well the RCDs as observed and perform better than ERAIN; ARPEGE and CCLM fail to simulate the RCD well. This study also shows that the CORDEX RCMs ensemble mean best

simulates the ROD/RCD over West Africa than individual RCMs. The ability of each RCM strongly depends on how well the model reproduces the northward movement of the West African monsoon system and the associated features.

For investigating the potential impacts of climate change and reforestation on the future ROD and RCD over West Africa, RegCM and WRF were used to simulate the present-day climate (1970-2004) and projected future climate (2030-2064) under the representative concentration pathway 4.5 (rcp4.5) conditions. Results show that, for the impacts of climate change due to elevated greenhouse gas (GHGs), the temperature would likely increase over West Africa in both RCMs and also in the GCMs (HadGEM and ECHAM) more consistently over the Sahel. On the other hand, elevated GHGs would lead to a decrease in rainfall as indicated by the RCMs and GCMs although the decrease is much more consistent again over the Sahel. As for the future ROD, increase in GHGs indicates that regardless of the definitions used, northern Nigeria would have delayed RODs. The vertical structure of the monsoon dynamics in the areas where the highest impacts of climate change (i.e. latest ROD) are observed for each definition shows that the elevated GHGs in the future under rcp45 condition would induce shallower monsoon flow essentially over the Sahel. However, there was no agreement between the RCMs (RegCM and WRF) on the potential impact of climate change on the RCDs due to elevated GHGs, for while RegCM indicates delayed RCDs over the Sahel and early RCDs over the Savanna, WRF produces early RCDs in all the areas. From both models, the projected impact of reforestation under the rcp45 condition indicates that West African climate would be cooler in most areas with more rainfall during the rainy season especially over the reforested zone. The cooling effect is more consistent and higher over Savanna but reforestation would induce a warming over some surrounding areas. Regardless of the definitions used, reforestation over Savanna area would induce early ROD over most areas in West Africa as obtained from both models, except over north of Nigeria. The potential impact of reforestation on the RCDs (under rcp45 conditions) again produces divergent results by the RCMs. WRF produces delayed RCDs over all the climatic zones, while RegCM indicates delayed RCDs over the reforested area and early RCDs over Sahel.

CERTIFICATION

a) By the student:

I declare that this is my own work and that it has not been submitted previously as dissertation or thesis elsewhere at any other university for the award of a degree.

Candidate's name: MOUNKAILA SALEY, Moussa

Signature: ……………………………… **Date:** 24/02/2015

b) By the supervisor (s):

We certify that this research work was carried out by Mr. MOUNKAILA SALEY Moussa in the Department of Meteorology, Federal University of Technology Akure under our close supervision, as part of the requirement for the award of PhD in Meteorology and Climate Science and it has not been submitted elsewhere for the award of a degree.

Major supervisor: Prof. J. A. Omotosho

Signature: ……………………………… **Date:** 24/02/2015

Co-supervisor: Dr. Babatunde J. Abiodun

Signature: ……………………………… **Date:** 24/02/2015

Director of WASCAL GRP: Prof. J. A. Omotosho

Signature: ……………………………… **Date:** 24/02/2015

Head of Department: Prof. K. O. Ogunjobi

Signature: ……………………………… **Date:** 24/02/2015

DEDICATION

To my wife Mme Moussa Balkissa ADAMOU and children Tawfiq and Aisha

ACKNOWLEDGEMENTS

This PhD programme is fully sponsored by the German Ministry of Education and Research (BMBF) through the West African Service Center for Climate Change and Adapted Land Use (WASCAL). I am therefore grateful to WASCAL for granting me financial support for the study and my research visit to the University of Cape Town (UCT) South Africa as well as my participation to internationals conferences to present results of the study.

I sincerely thank the Executive Director and the staff of WASCAL Head office, Accra, Ghana and the Director, Prof. J. A. Omotosho and staff of WASCAL GRP-WACS FUTA, Nigeria for their strong support and encouragement throughout the period of the study. I am also grateful to Prof. K.O. Ogunjobi, the Head, and the Staff of Meteorology Department, FUTA, Nigeria, for their cooperation.

I am most grateful to my supervisors Prof. J. A. Omotosho, for his interest, guidance, encouragement and support on the study and to my co-supervisor Dr. Babatunde J. Abiodun whose invitation to UCT, guidance, support and fruitful discussions, both concerning my work and my attempts to write papers, helped me to understand the topic. Many thanks to all my colleagues of the GRP WACS for your valuables contributions, especially to DIASSO Jacques Ulrich with whom I spent my research field work at UCT. I would like also to thank you all the staff members of the Climate Science Analysis Group (Staff) at UCT for their contribution in the achievement of this work.

To my family, I am very grateful for your great patience, supports, never-lacking confidence and prayers. In this respect my beloved wife, Mms Moussa Balkissa Adamou thank you for your infinite support, love and encouragement during the course of this work. I would like to thank you my deceased parents (Mounkaila Saley and Salamatou Garba) for giving me the chance to be educated and my elder sister Fati Mounkaila who passed away during the course of this work, thank you for everything you have done for me. May your souls stay in peace in paradise. Amen. Many thanks, to my brothers, sisters, cousins and uncles for your ever constant supports and prayers. To Mahamadou

Hamini Douada, Moussa Morou and all my friends thank you for your supports.

I am most grateful to Almighty God above all for making this thesis a reality and a success. Thank you ALLAH for everything.

TABLES OF CONTENTS

LISTS OF FIGURES

LISTS OF TABLES

LIST OF ACRONYMS

AEJ	African Easterly Jet
AEW	African Easterly Wave
AMMA	African Monsoon Multidisciplinary Analyses
AOGCM	Atmosphere Ocean General Circulation Model
ARPEGE	Regional climate model of Centre National de Recherches Meteorologiques, France
BATS	Biosphere-Atmosphere Transfer Scheme
CORDEX	Coordinated Regional Climate Downscaling Experiment of Africa
CRCM5	Canadian Regional Climate Model
CSAG	Climate Systems Analysis Group
CPS	Cumulus Parameterization Schemes
CCLM	Climate Limited-Area Modelling Community
CCM3	Community Climate Model version 3
CMIP5	Fifth Coupled Model Inter-comparison Projects
DEF	Definition
ECMWF	European Centre for Medium-Range Weather Forecasts
ECHAM	Max Planck Institute general circulation model, Germany
ERAIN	ERA-Interim reanalysis
GCM	General Circulation Model
GDP	Gross Domestic Products
GHG	Greenhouse gas
GLCC	Global Land Cover Characterization
GPCP	Global Precipitation Climatology Project
HadGEM	Hadley Centre General Environmental Model, UK Met office GCM
ICTP	International Centre for Theoretical Physics
IPCC	Intergovernmental Panel on Climate Change

ITCZ	Inter-Tropical Convergence Zone
ITD	Inter-Tropical Discontinuity
JJA	June July August
LOR	Length Of the Rainy season
LSM	Land Surface Model
MPI-ESM	MPI Earth System Model
MPI-M	Max Planck Institute for Meteorology
MCS	Meso-scale Convective Systems
NCAR	National Center for Atmospheric Research
NOAA	National Oceanic Atmospheric Administration
NOREF	Future climate without reforestation
PBL	Planetary Boundary Layer
PBLS	Planetary Boundary Layer Parameterization Schemes
PRS	Present-day Climate
PRECIS	Regional climate model simulated at UCT within CORDEX framework
RACMO	Koninklijk Nederlands Meteorologisch Instituut, Netherlands
RCA35	Regional climate model of Sveriges Meteorologiska och Hydrologiska Institut (SMHI), Sweden
RCD	Rainfall Cessation Date
RCM	Regional Climate Model
REF	Future climate with reforestation
RegCM	Community Regional Climate Model of the ICTP
REMO	Max Planck Institute regional climate model, Germany
RRTM	Rapid Radiative Transfer Model
ROD	Rainfall Onset Date

SHL	Sahara Heat Low
SL	Squall Lines
SST	Sea Surface Temperature
TEJ	Tropical Easterly Jet
TRMM	Tropical Rainfall Measuring Mission
USGS	United States Geological Survey
WAM	West African Monsoon
WAMME	West African Monsoon Modeling and Evaluation
WASCAL	West African Climate Service Center for Climate Change and Adapted land Use
WMO	World Meteorological Organisation
WRCP	World Climate Research Program
WRF	Weather Regional Forecast model

CHAPTER ONE

INTRODUCTION

1.1 INTRODUCTION

There is a growing evidence of the need for climate change information at the regional to local scale within the debate of global change particularly in Africa (Giorgi *et al.* 2009). Therefore to improve the management of the effects of climate variability and change on society it is fundamental to provide suitable information from climate data, especially with regards to agricultural practices and water resources management. Assessing the impact of climate change in the agriculture sector requires the provision of regional climate change information to farmers and decisions-makers. The farmers need robust translation/prediction of these data to enable the development of suitable adaptation and mitigation strategies to a changing climate at national and regional levels.

This thesis aims to investigate the complexity of assessing the impact of climate change and reforestation on the rainfall onset and cessation over West Africa by using downscaled data from regional climate models (RCMs). The downscaling techniques are explained in Chapter two and this Chapter focuses on the main purpose of the thesis.

1.2 IMPORTANCE OF RAINFALL ONSET AND CESSATION

Agriculture is largely rain-fed in West Africa and plays an important role in the socio-economic life of the people in the region. However its planning is affected by the rainfall onset and cessation. Indeed, the rainfall onset determines the optimal planting time that ensures continuous water availability at the start of germination (e.g. Sivakumar, 1998,1992; Omotosho *et al.*, 2000, Sultan *et al.* 2005; Marteau *et al.* 2011), while the cessation will determine the type of seed to plant depending on the duration of the rainy season. Steward (1991) showed that the rainfall onset is the most important parameter on which depend other related seasonal factors. Both factors (onset and cessation) play an important role in ensuring food security in West Africa (e.g. Omotosho *et al.* 2000, Ingram *et al.*, 2002; Odekunle *et al.* 2006; Abiodun and Omotosho 2007, Marteau *et al.* 2011, Mounkaila *et al.* 2014). Therefore, understanding and predicting the inter-annual variability of the rainfall onset and cessation some weeks or months ahead with regards to agricultural practices or hydroelectricity production becomes as important as the predictions of rainfall amounts (Lima *et al.* 2009). This becomes a great concern for scientists and governments in West Africa. Many recognized Centers of the World Meteorological Organisation (WMO) in the region and National Meteorological Services routinely produce long range forecasts for total rainfall. But Ingram *et al.* (2002), Sultan *et al.* (2005) pointed out that the timing of the rainfall onset is even more important than the rainfall distribution or amount. However, many of the Centers fail to accurately predict the timing of the onset and cessation. Likewise, making a long range forecast of the date of the rainfall onset and cessation is a big challenge despite the huge demand for this information in the region (e.g. Ingram *et al.* 2002). Many methods have been used to investigate the date of the rainfall onset and cessation but there is no agreement among researchers on specific methods that can be applied for a specific region.

However, many definitions of rainfall onset and cessation exist over West Africa. Three main criteria or methods are used to determine the rainfall onset and cessation dates. The first method is called the traditional method which is used generally by traditional farmers. This method has no scientific foundation and consists of observing the behavior of some animals (e.g. birds, insects), trees' flowering prior the first rains. Roncoli *et al.* (2002) showed that this method mostly fails and would benefit from scientific support to improve the decision making by local traditional farmers. The second method used only parameters measured on the surface (synoptic data) and mainly applied to agro-climatological purposes at local scale. The third method used atmospheric dynamics, where the scientists (researchers) defined their own definitions. This present study will focus on the second type of definition designed for agricultural purposes. Thus, the onset of the rainy season is defined for an agricultural farmland as the appropriate time of sowing when sufficient rains are available to keep the soil moist enough to maintain seeds germination to avoid their failure. This will reduce the risk of planting too early or too late (Omotosho *et al.*, 2000). Rainfall cessation can be defined as the end of the rainy season which enables the prediction of the length of the growing season. This parameter is very crucial for the selection of crop varieties, matching and cropping sequences (Omotosho *et al.*, 2000). Therefore, reliable prediction of the RCD will lead to increase in crop yield to fight food security in the region.

1.3 RESEARCH QUESTIONS

Following the outlined problems regarding the rainfall onset dates (RODs) and rainfall cessation dates (RCDs) over West Africa, the following research questions are raised and will be addressed:

i) Which prominent definitions of RODs/RCDs can provide realistic information regarding the sowing and harvesting time for West African farmers?

ii) How well do regional climate models (RCMs) simulate the RODs/RCDs in West Africa?

iii) What are the relationship between the West African monsoon (WAM) systems and the RODs and RCDs?

iv) What are the potential impacts of climate change and reforestation on future RODs/RCDs in the region?

v) Why are the present prediction methods of RODs/RCDs not reliable and challenging in West Africa?

vi) How best can RCMs predict West African rainfall variability, distribution and amounts and therefore reliably capture the best timing of the onset and cessation of the rainy season and their variability (intra seasonal, monthly and inter-annual)?

vii) Which factors contribute to the variability of rainfall in West Africa particularly over the Sahel and what are the relationships between this variability and the Monsoon onset, ITD, AEJ and TEJ?

1.4 AIM AND OBJECTIVES

From the foregoing, the ultimate aim of this thesis is to investigate the ability of RCMs in simulating the rainfall onset and cessation as well as assessing the potential impacts of climate change and reforestation on future ROD/RCD over West Africa. Therefore, the specific objectives of this work are of twofold: To evaluate

- the ability of the Coordinated Regional Climate Downscaling Experiment of Africa (CORDEX-Africa) RCMs in simulating the rainfall onset and cessation over West Africa,
- the potential impacts of climate change and reforestation on future rainfall onset and cessation over West Africa.

1.5 JUSTIFICATION FOR THE PRESENT STUDY

The negative impacts of climate variability and change were projected to be more severe in Africa particularly in West Africa than elsewhere, according to the fifth assessment report of the Intergovernmental Panel on Climate Change reports (IPCC, AR5, 2013 and previous). The region has experienced various changes in rainfall patterns during the summer rainy season from May to October. The main consequences of these drastic changes are droughts, famines and socio-economic problems (Nicholson *et al.*, 2000, Omotosho and Abiodun, 2007). Yet in West Africa, most of the gross domestic products (GDP) activities' are based on the rain-fed agriculture and livestock. However, the planning and activities in those sectors are affected by the time of the rainfall onset and cessation as well as their variability during the rainy season. Unfortunately, many of the approaches by operational forecast centers which use empirical and/or statistical methods show low skills in predicting the factors that influence the timing of the rainfall onset and cessation, and most of them have failed to reliably determine the inter-annual variability. Omotosho (1992) showed that the variability in the date of rainfall onset is for instance as large as the length of the rainy season over the Sahel. Likewise, an early and/or late onset has a significant influence in reducing crop yields if the time of planting is not reliably predicted for agricultural practices. This is one of the strongest reasons why West African countries need a reliable prediction of the rainfall onset and cessation to improve food security. Furthermore, the agriculture sector and water resources strongly depend on the distributions, amount and variability of the rainfall during the rainy season. The consequences of unreliable predictions of the RODs and RCDs are seeds failure, decrease in crop yields, famine and health problems (Sivakumar, 1988, Sarria-Dodd and Jollife 2001). Therefore, predicting the rainfall onset and cessation in West Africa is crucial due to the high variability of the dates of onset/cessation from one region to another. The RODs/RCDs are characterized by a higher irregularity in the regions at sub-seasonal and intra-seasonal time scale and also the mechanisms that underline the RODs and RCDs are still not fully understood. Thus, reliable prediction of ROD/RCD in the region is still a great challenge and further investigations are necessary for realistic prediction of ROD/RCD. Other important factors during the rainy season are the frequency of dry and wet spells, the duration and length of the season. However, the scope of this thesis focuses more importantly on the RODs but will also investigate the RCDs and length of the rainy season (LOR) in West Africa. Thus, a sound understanding of both factors (ROD and RCD) is fundamental to satisfying the needs of the farmers and potentially increasing the GDP of the countries in West Africa for better socio-economic livelihoods.

Various studies investigated the factors that may influence rainfall onset and cessation (e.g Sultan and Janicot, 2003; Gu and Adler 2004; Ramel *et al.* 2006; Vizy and Cook 2006; Thorncroft *et al.* 2011; Vellinga *et al.* 2013; Nicholson 2013; Mounkaila *et al.* 2014) and found a strong link between the processes controlling the West African monsoon systems (WAMs) and the timing of the rainy season. These studies suggested that the factors that control the rainfall onset and cessation are sea-surface temperatures, vegetation and soil moisture, wind shear, the mid tropospheric African easterly jet (AEJ) and upper level tropical easterly jet (TEJ), the Inter-tropical Discontinuity (ITD), the African easterly waves (AEW), the moist static energy or potential equivalent temperature gradient and the strength and position of the Saharan heat low (SHL) which controls the southerly inflow of moist air into the West African subcontinent. Furthermore, the interactions between these mechanisms and their appropriate representation in a dynamical modeling are still not fully understood. Little is also known about the intra-seasonal, monthly and inter-annual variations of the components of the rainy seasons (onset, cessation, frequency of rain events, dry spells etc.) and how they contribute individually in the variability of rainfall amounts during the rainy season. From the foregoing, it is therefore necessary to evaluate the physical mechanisms that drive the rainfall processes by using RCMs. This will also enable the assessment of the ability of dynamical climate models in simulating the RODs and RCDs in the context of climate variability and change over the region.

1.6 CONTRIBUTIONS TO KNOWNLEDGE

The contributions to knowledge of this thesis are the following:

a) the output of this project will provide a more reliable information on the usage, ability and application of RCMs in simulating the rainfall onset and cessation over West Africa,

b) the results will also provide suitable information on the likely impacts of climate change and reforestation of the future ROD/RCD in the region to enable policy-makers to take early action for mitigating these possible future impacts over West Africa.

c) the results will give also a good insight to decision-makers and governments on how agriculturists can avoid seeds and crops failure in future and hence fight food insecurity at sub-regional to regional scale in West Africa,

CHAPTER TWO

LITERATURE REVIEW

2.1 INTRODUCTION

Before evaluating the skill of regional climate models in simulating the rainfall onset and cessation over West Africa, it is important to understand the various features of West African climate system. West Africa has a very complex climate driven by local processes, such as tropical convection and alternation of monsoons, and by remote processes for example the El Niño-Southern Oscillation of the Pacific Ocean (Gordon, 2009). Each of these processes strongly influences the intra-seasonal, seasonal, inter-annual and decadal variability of temperature and rainfall patterns in the region. As a result, understanding the interactions between these processes and the likely impact of climate change on them are crucial to mitigating the negative impacts of climate variability and change in West Africa. This chapter will review previous studies related to dynamical modeling of the rainfall onset and cessation using RCMs. In this regard, the climate system of West Africa will be introduced by focusing on the rainfall and temperature variability, followed by a brief description of RCMs applications in the region and how well these models reproduce the observed climatology of temperature and rainfall for a reliable prediction of the ROD/RCD in West Africa.

2.2 CLIMATE SYSTEM OF WEST AFRICA

Solar radiation represents the main driver of the atmospheric engine and provides the energy necessary for the various transformations in the climate system (Derek and Julis, 1987). As a result, the net radiation is responsible of the variation of the atmospheric and soil temperatures which determine the global patterns of air pressure (e.g. air mass movement) that control precipitation, evaporation and evapotranspiration over the region. Many drivers are involved in the West African climate system and many of them are not fully understood. We distinguish the air mass movement (e.g. Inter-Tropical Discontinuity (ITD) and the Inter-Tropical Convergence Zone (ITCZ)), the annual variability of the monsoon systems, the Atlantic Ocean Sea Surface Temperature (SST) variability and the land-atmosphere interaction.

2.2.1 Major Air Mass Systems of West Africa: the ITD and ITCZ

Two main air masses influence the climate of West African countries. The first is the warm, moist tropical maritime (equatorial) air mass that transports moisture inland from the Atlantic Ocean and provides West Africa with the moisture for rainfall. The northernmost position of this moist air mass is reached in July/August with northernmost latitude between 18°N and 21°N (FAO, 1985). The second is hot, dusty and dry tropical continental air mass from the Sahara of high pressure system that blows from the northeast over most West Africa countries. It is characterized by dry and hot condition over land. The southernmost position of this dry air mass is reached in January between latitudes 5° and 7°N over Guinea zone. The position where these two air masses meet is called the ITCZ if the meeting occurs over Ocean and the ITD when it occurs over land (Abiodun *et al.* 2008). Peter and Tetzlaff (1988) suggested that the ITD reaches about 7°N as its southernmost position in January over Guinea and about 22°N in August over the Sahel. This belt of air masses has a variable width and stability and follows the apparent movement of the sun in its north and south migration that determines the climate over the region (Abiodun *et al.* 2008). Among others factors, the interaction of these two air masses are responsible for the temperature and rainfall variability over West Africa.

2.2.2 Temperature Variability

The temperature over West Africa varies according to the seasons and climatic zones. The mean annual temperature is usually above 18°C for lowland climates due to high sunshine that induces high temperatures throughout the year (FAO, 1985). For instance, the mean annual temperature is about 26°C close to the equator around 10°N (e.g. Guinea zone and the southernmost parts of the Savanna area) with a range of 1.7–2.8°C. However the diurnal range varies between 5.6–8.3°C. The temperature variability is even greater between latitude 10°N and the southern part of the Sahara (e.g. northern Savanna to Sahelian zone) where the mean monthly temperatures can rise to 30°C. The diurnal range can reach between 14°C to 17°C, while the annual range is about 9°C. However, the highest temperature are observed over central Sahara, north of the Sahel zone where during the day the temperature in July can be as high as 58°C and as low as 4°C at night (FAO, 1985). In this area, the mean annual temperature range is between 10°–35°C. As a result, the Savanna and Sahel zones are characterized by cloudless skies during the day and low temperature at nights, while the areas over Guinea zone have cloudier skies during the day and higher temperature at nights (FAO, 1985).

2.2.3 Rainfall Mechanisms and Variability

2.2.3.1 Rainfall Mechanisms

The most important mechanism for rainfall occurrence is the vertical displacement of air and the adiabatic processes of cooling and condensation. For instance when air rises up, its pressure decreases and it expands and cools down. So, if there is sufficient moisture, the air becomes saturated leading to condensation of water vapor and the creation of cloud from which rains or water droplets will likely fall. However, the formation of cloud does not necessarily mean that rainfall will occur. The cloud type and intensity depend on the moisture amount and instability conditions. The types of rainfall systems frequently observed in West Africa include the monsoon rainfall system, the meso-scale convective systems and the squall lines.

2.2.3.1.1 Monsoon Rainfall

The monsoonal rainfall systems are the most dominant during the boreal summer in the region. The mechanism of the monsoon rainfall derives from a temperature gradient between the land surface and the adjacent ocean. For instance the land surface has a heat low through an intense solar radiation. Since the ocean gets heated more slowly than the land surface, the heat low and the moist low level air from the ocean warm up and rise to create convective cloud and rainfall. The monsoon rainfall is directly connected to the two air masses explained above and its northward propagation and southward retreat are given by the position of the ITD over land and the ITCZ over Ocean.

2.2.3.1.2 Meso-scale Convective Systems (MCS) and Squall Lines (SLs)

According to the Glossary of meteorology of the American Meteorological Society, an MCS can be defined as *any ensemble of thunderstorms which produce a contiguous precipitation area that can extend from 100 km or more in horizontal scale in at least one direction*. The lifetime of these systems varies from 1 to 2 hours and is highly variable from one region to another in West Africa.

The SLs are meso-scale convective systems that are very well organized and present generally a leading convective region and a trailing stratiform precipitation region (Thomas *et al.*, 2003). The width of the convective region varies from 10 to 30 km, while the stratiform region might exceed 100km (Thomas *et al.*, 2003). The SLs travel across the West African countries from east to west, many of them originate east of Niamey or east of lake Tchad (Derek and Julis, 1987) and are the most frequent convective systems in the region (Chong and Hauser, 1989; Rowell and Milford, 1993; Hodges and Thorncroft, 1997; Fink and Reiner, 2003; Schumacher and Houze, 2006; Futyan and Del Genio, 2007). These systems bring much rainfall in the region with an annual rainfall ranging 16-32% over Guinea, 50% in the Soudanian zone and up to 80% over the Sahel (Omotosho, 1985) respectively. This high variability in the convective systems constitutes a major problem in the region particularly over the Sahel where the rainy season is very short compare to the coastal regions. Thus, there is a crucial need to understand the rainfall variability in West Africa.

2.2.3.2 Rainfall Variability

2.2.3.2.1 Annual Rainfall Variability over West Africa

The annual rainfall over Guinea areas (Fig. 2.1) varies from above 3000 mm (e.g. Liberia and south-west Nigeria) to above 1500 mm (e.g. Cote d'Ivoire). The rainy season starts between February/March and ends around November or December. The monsoonal rainfall is bimodal in these zones following the movement of the ITD. Inland over Savanna zone, the annual rainfall varies from about 1500 to 800 mm in most areas from central Savanna to the West (Fig. 2.1). However, the eastern part of Savanna receives higher annual rainfall of up to 2000mm (e.g. Sierra Leone and Guinea-Bissau). The rainfall starts in the Savanna zone from May/June. Over Sahel, the annual rainfall is below 700 mm in most areas and becomes even less than 200 mm at the edge of the Sahara desert (e.g. Agadez ~18°N in Niger where rainfall is about 175 mm/year for a period of only two months). Most of the Savanna and Sahel zones are characterized by a single rainy season (July-September). However the factors that produce this rainfall variability (e.g. thus the onset and cessation) at inter-annual to decadal time scale are not yet fully understood.

Figure 2.1 : Average annual rainfall over West Africa[1]

2.2.3.2.2 Factors Influencing the Rainfall Variability (i.e. the ROD and RCD)

Many studies investigated the factors influencing the rainfall variability in West Africa. Compared to the others regions in West Africa, the Sahel region has been the most vulnerable to rainfall variability due to severe droughts and famine in the last century (e.g. in the 1970s and 1980s). The factors that might affect the West African rainfall systems include the West African Monsoon (WAM) and its associated systems (e.g. the African easterly Jet (AEJ), the Tropical easterly jet (TEJ), the African Easterly Wave (AEW)…), the ITD/ITCZ, the Sea Surface Temperature (SST), the land use changes

[1]Enciclopedia Britannica available online November,11th 2014 at http://www.britannica.com/EBchecked/topic/640047/West-African-monsoon

and aerosols as well as their interactions with the atmosphere. Other factors include the land-sea thermal contrast (Carlson, 1969; Adedokun, 1978; Odekunle *et al.*, 2005) which is derived from the monsoon system. To produce reliable prediction of the rainfall onset and cessation, it is therefore crucial to understand the dynamics and mechanisms of the rainfall variability in the region.

The West African Monsoon (WAM)

The WAM plays a crucial role in the determination of onset and retreat of the rainy season as well as the rainfall variability in the region. The WAM can be defined as southwesterly regime of winds which transports moist air from the Atlantic Ocean into the continent. Omotosho and Abiodun (2007) and Djiotang *et al.* (2010) show that the WAM is the main source of moisture which has an impact on the onset, cessation, amount and variability of rainfall in West Africa. Many studies investigate the monsoon onset and retreat using various methods and models. Zeng and Lu (2004) proposed the first unified global summer monsoon onset and retreat using only global daily precipitable water data on 1^ox1^o grids. The results showed consistency of onset and retreat dates with those obtained using local precipitation data over most monsoon regions. According to Janicot (1992) the West African rainfall inter-annual variability can be described into two main zones respectively: north and south of 10^oN (i.e. from the middle of Savanna that interconnects the wet Guinea coat and the dry Sahel). Sultan and Janicot (2003), using daily rainfall data, reanalysis and outgoing long wave radiation (OLR) studied the mean circulation and characteristics of the WAM. Their results showed that the mean pre-onset date occurred 14 May where the ITD is at 15^oN and the ITCZ is at 5^oN, leading to some isolated convective systems in Sudano-Sahel. They also found that the mean date of the real monsoon onset occurrence is 24 June when the ITCZ shift from a quasi-stable position of 5^oN (May-June) to 10^oN (July-August). This leads to an increase in rainfall over the Sudano-Sahel. On the other hand, the ITD, according to Ilesanmi *et al.* (1972), Omotosho (1992), the AEJ at about 700 hPa with its associated vertical shear and the TEJ located at 250 hPa are also important factors to take into account. Grist and Nicholson (2000) found a weaker African easterly jet (AEJ) and stronger tropical easterly jet (TEJ) are linked with wet years and suggested that the latitudinal location of the AEJ with respect to the ITD is the most important characteristic rather than its strength over the Sahel. Nicholson (2008, 2009) confirmed the previous results and showed that a stronger TEJ is related to more intense rainfall over the Sahel. Pu and Cook (2010) have shown that the West African westerly jet (WAWJ) which is a low-level westerly jet located at 8^{o}–11^{o}N, plays a crucial role in the transport of moisture into the Sahel and can vary independently of the southwesterly monsoon flow. The African Easterly Waves (AEWs) which propagate westward are synoptic-scale systems that are an extremely important component of the West African monsoon (Nicholson, 2013). They originate in the middle of the troposphere of northern Africa between June and October and are associated with the TEJ. Among others factors, the rainfall variability in the region has also been linked to the ocean SST variability.

Sea Surface Temperature

Many studies have shown that the variability of the SSTs influence the variability of rainfall in West Africa (e.g. Janicot *et al.*, 1996; Fontaine *et al.*, 1998; Giannini *et al.*, 2003; Lu and Delworth, 2005; Biasutti *et al.*, 2008). These studies indicated that the ocean is getting warmer and this has resulted in changes in the atmospheric circulation and the rainfall patterns. As a result, the rainfall has shown a pronounced increase over equatorial West Africa and along the Guinea coast but a decrease is observed over Sahel (Deser *et al.*, 2010; Tokinaga and Xie, 2011).

Land Use and Aerosols

The land use surface effects, including aerosols play a non-negligible role in the climate of the region. First introduced by Charney *et al.* (1975) after the severe droughts over Sahel, the influence of land use change on the climate especially rainfall may be due to changes in surface albedo, soil moisture and evapotranspiration. Recent studies, using RCMs; instead of General Circulation Model (GCM), showed an improvement in the prediction of the hydrological processes and circulation features, and indicated a relationship between the land surface feedback and convection (Druyan *et al.*, 2004; Konare *et al.*, 2008; Wang *et al.*, 2010; Hurk *et al.*, 2010). Indeed, these studies demonstrated that convective rainfall impacted the surface fluxes of moisture and heat (Clark *et al.*, 2004) and inversely, the surface anomalies related to moisture and temperature can strongly create a new circulation that can affect the boundary layer depth and cloud development and generate convection (Adler *et al.*, 2011a,b). Therefore, there is a consensus that land use changes play an important role in the occurrence of convection in the region and vice-versa (Nicholson *et al.*, 2013). The aerosols (mainly from dust) also have an important role in the convection process because they can be used as ice nuclei and cloud condensation nuclei in the process of cloud formation over West Africa. The impact of dust in the rainfall variability comes from its effects on the atmospheric radiation budget (deMott *et al.*, 2003). The AEJ and TEJ are respectively intensified and weakened by dust (Konare *et al.*, 2008), while the AEWs play a crucial role in initializing dust. For example over Sahel, Lau *et al.* (2009) found that dust can increase the rainfall by strengthening the monsoon and may shift it northward. However, other studies indicated a decrease in rainfall when deep convection is linked with dust in the region (Kluser *et al.*, 2010; Solmon *et al.*, 2012).

2.3 DETERMINATION OF RAINFALL ONSET AND CESSATION OVER WEST AFRICA

Various studies have suggested different factors that may control the ROD and RCD. The factors include sea surface temperatures, vegetation and soil moisture, wind shear, the mid- and upper tropospheric jets (AEJ and TEJ), moist static energy or equivalent potential temperature gradient and the strength and position of the Saharan heat low. Many empirical models have used these factors in various ways in predicting the ROD. Notable among these are models based on upper atmospheric winds (Omotosho, 1990, 1992) and on sea surface temperature (Lamb and Peppler, 1992; Eltahir and Gong, 1996; Janicot *et al.*, 1998), rainfall–evapotranspiration relations (Cocheme and Fraquin, 1967) and equivalent potential temperature (Oduru 1989; Omotosho *et al.*, 2000). Other methods are based on precipitation or surface data only (Sarria-Dodd and Jolliffe, 2001; Ati *et al.*, 2002 and Omotosho *et al.*, 2000). The main problem with most of the empirical models is their low skill in simulating the ROD. This may be due to lack of sufficient data for developing the models and/or training for implementation of the models. The other problem is that empirical models are not dynamically competent since they cannot account for all the factors that control RODs. To overcome the shortcomings of empirical approaches, some studies have employed dynamic methods (use of atmosphere-ocean general circulation models (AOGCMs) in predicting RODs (e.g. Cook and Vizy, 2006; Djiotang *et al.*, 2010)). However, AOGCMs usually have coarse horizontal grid resolution (typically 2°×2° long×lat) and therefore cannot represent well the influence of meso-scale features (such as isolated reliefs, lakes, coastlines and sharp variation in vegetation, temperature and soil moisture) on RODs (e.g. Druyan *et al.*, 2010; Xue *et al.*, 2010). As a result, AOGCM simulations are usually downscaled using regional climate models (RCMs) with a higher resolution (typically 10–50 km).

2.4 CLIMATE MODELING AND DOWNSCALING IN WEST AFRICA

2.4.1 Definitions

The tern climate models can be defined as a mathematical representation of the climate system based on physical, biological and chemical principles[2]. Climate models provide numerical solution of complex equations which are discretized in space and time. Thus, climate models are crucial tools that improve our understanding of the climate behavior on seasonal, annual, decadal and centennial time scales mainly due to natural variability, human activity, or a combination of both[3]. Warner (2011) defined climate downscaling as the usage of input data from AOGCM forecasts or the global-reanalysis as boundary to force a regional climate model or as a statistical procedure to interrelate the large and small scale climate of a specific region. Downscaling techniques can be used to investigate the initial-value based inter-seasonal or longer forecast as IPCC simulations types which are radiative forcing. It exist two main techniques of climate downscaling: the dynamical and statistical one. The statistical downscaling technique consists of resolving sub grid-scale variability based on resolved

[2] http://www.climate.be/textbook/chapter3_node3.html

[3] http://www.gfdl.noaa.gov/cms-filesystem-action/model_development/climate_modeling.pdf

grid-scale value from the global data set. Some of the major disadvantages of this technique are the requirement of long and reliable observed historical data record for calibration, there is no feedbacks in the climate-system and the biases of the General Circulation Model (GCM) can cause error if the procedure used does not correct them (Warner, 2011). Therefore, this thesis uses the dynamical downscaling techniques that can take into account the physical process of the gridded output and can capture the extreme events and their variability.

2.4.2 Regional Climate Modelling over West Africa

Regional climate models are numerical models that simulate the climate of a specific region with its boundary conditions coming from either AOGCM or reanalyzes data. These models cover a fraction of the globe (e.g. limited area model) typically at a fine-scale of the order of tens of kilometers (e.g. 50x50km to 10x10km or less) grid resolution which is higher than that of the driven AOGCM. Many attempts have been made to improve upon the models through grid resolution, physical parameterizations, and data assimilation etc. (Krishna *et al.*, 2011). The physical parameterizations play an important role in the development and intensification of Meso-Scale Convective Systems (MSCs) in the model. This includes cumulus convection, surface fluxes of heat, moisture and momentum as well as vertical mixing in the planetary boundary layer (PBL). Also, the PBL parameterization schemes (PBLSs) as well as turbulent eddies in the PBL which transport moisture into the free convection levels are essential for a good numerical model prediction (Hong *et al.*, 2006). Consequently, as numerical models are not always able to resolve the small scale convective clouds, many varieties of cumulus parameterization schemes (CPSs) have also been developed and incorporated into three-dimensional mesoscale models (Kuo, 1974; Arakawa and Schubert, 1974; Anthes, 1977; Grell 1993). However, some of the above schemes were made for a specific convective environment (Grell, 1993; Kuo *et al.*, 1996). Therefore it is necessary to select the most suitable parameterizations schemes applicable to West Africa. As a result, when the best model physics is given for a specific region, more realistic rainfall regimes can be expected (Giorgi and

Marinucci, 1996; Fulakeza *et al.*, 2002; Druyan *et al.*, 2002).

Various RCMs have been used to study the West Africa climate. Most of these studies used dynamical downscaling methods to evaluate the ability of RCMs in simulating the climatology of West Africa and its variability (e.g. Vizy and Cook, 2002; Paeth *et al.*, 2005; Afiesimama *et al.*, 2006; Abiodun *et al.*, 2008; Vigaud *et al.*, 2009; Sylla *et al.*, 2009,2010; Diallo *et al.*, 2012a). For example, Afiesimama *et al.* (2006), Abiodun *et al.* (2008), Sylla *et al.* (2009) assessed the skill of the RegCM3 to simulate the monsoon system. Their results showed that RegCM3 is able to capture the inter-annual variability of WAM. Vigaud *et al.* (2009) showed also that the Weather Research and Forecasting model (WRF) can simulate well the spatio-temporal variability of rainfall regime and the atmospheric circulations in West Africa (i.e. AEJ, Sahara heat low, etc.). Other studies investigated the ability of RCMs to simulate the ROD and RCD over West Africa.

2.4.3 RCMs Simulations of ROD and RCD over West Africa

Many studies have demonstrated the capability of RCMs in simulating the intra-seasonal, inter-annual and decadal variability of rainfall, as well as the characteristic of the West African Monsoon (WAM) system (e.g. Omotosho and Abiodun, 2007; Afiesimama *et al.*, 2006; Abiodun *et al.*, 2008; Sylla *et al.*, 2009, 2010; Vigaud *et al.*, 2009; Pu and Cook, 2010). However, only few of these studies examined the ability of RCMs in simulating the ROD over West Africa (Sultan and Janicot, 2003; Zeng and Lu, 2004; Sijikumar *et al.*, 2006) but those studies focused on individual models designed for some specific purposes, making it difficult to know the general performance of RCMs in simulating ROD. Hence there is need for RCMs inter-comparison on ROD and RCD simulation over West Africa.

On the other hand, there have been some multi-RCM experiments with encouraging results over West Africa. These include the West African Monsoon Modeling and Evaluation (WAMME; e.g. Druyan *et al.*, 2010; Xue *et al.*, 2010), the Monsoon Multidisciplinary Analyses (AMMA, Linden and

Mitchell 2009; Ruti *et al.*, 2011; Hourdin *et al.*, 2010) and the ENSEMBLE-AMMA project (e.g. Paeth *et al.*, 2011; Diallo *et al.*, 2012a; Sylla *et al.*, 2013). These multi-RCM studies show different results over West Africa. For instance, Druyan *et al.* (2010) evaluated the ability of five RCMs in simulating the WAM systems and found that the RCMs skillfully represent the monsoon onset. Hourdin *et al.* (2010) used AMMA model inter-comparison to study the seasonal and intra-seasonal variations in climate over the Sahel and found many discrepancies among the RCMs in simulating rainfall and the latitudinal position of AEJ over the Sahel. They show that none of the RCMs captures all the aspects of the monsoon system. In the inter-comparison of the multi-model RCM from the ENSEMBLES and AMMA projects, Paeth *et al.* (2011) also found that RCMs exhibit systematic errors in simulating the amplitude and pattern of the West African rainfall; and they have a dry bias in sub-Saharan Africa. Meanwhile, Diallo *et al.* (2012b) and Sylla *et al.* (2013) reported RCMs that give a remarkable simulation of the inter-annual variability of rainfall, with a correlation coefficient greater than 0.5. However, most of the above studies indicated that the RCMs' ensemble mean always outperforms individual RCMs in simulating precipitation, but this is not always true for temperature. The most recent multi-RCM experiment is the Coordinated Regional Downscaling Experiment of Africa (CORDEX Africa; Nikulin *et al.*, 2012; Gbobaniyi *et al.*, 2013). One of the aims of CORDEX-Africa is to evaluate the quality of RCMs in simulating precipitation and to close the gap of data accessibility of the regions, thereby enabling the scientific community to give suitable information to decision-makers (Nikulin *et al.* 2012). Nikulin *et al.* (2012) and Gbobaniyi *et al.* (2013) found that most RCMs realistically capture the WAM and its related features over West Africa. However, no study has investigated how CORDEX-Africa RCMs perform in simulating the RODs over West Africa. One of the main goals of the present thesis is to extend the analyses of Nikulin *et al.* (2012) by focusing on RODs/RCDs and hence evaluate the performance of CORDEX-Africa RCMs in simulating the ROD/RCD over West Africa.

2.5 IMPACTS OF CLIMATE CHANGE AND REFORESTATION ON ROD AND RCD OVER WEST AFRICA

2.5.1 Climate Variability and Change in West Africa

Both climate variability and change affect tremendously the agriculture sector at different time scales in West Africa. For instance the inter-annual (year to year) variability of crop yield is affected by climate variability and the long-term term variability (e.g. 30 years) due to climate change give the difference between good and bad years of changes in crop yields.

2.5.1.1 Climate Variability

Climate variability constitutes a major problem to agriculturists in West Africa. Its variability on intra-seasonal, seasonal, inter-annual or longer scales has been a big concern at local, national and regional scales. Indeed, many countries have been affected by wet conditions in the 1930-1960, droughts conditions in the 1970-1990 and some rainfall recovery in the 1990s -2000s that indicated the vulnerability of the people in the regions (Nicholson, 2013). This high climatic variability combined with poor infrastructure and economic poverty has worsened the situation (Adger, 2006; Mertz *et al.*, 2009). Christansen *et al.* (2007) projected that extreme of high intensity rainfall events would increase by 20% in the next decade in West Africa. More importantly, the unpredictability of the ROD/RCD in the region constitutes a serious problem in the fight against food security and many countries especially those in the Sahel have food crisis every year. Therefore, the higher variability of rainfall onset and cessation dates directly impacts the production of food and cash crop in the region. Furthermore, changes in the frequency and intensity of dry spells can also lead to crop failure even if the total amount of rainfall for that year would have given a normal harvest (Yaro *et al.*, 2014).

2.5.1.2 Projections of Climate Change

The rain-fed agriculture sector in West Africa has faced tremendous challenges in water supply variability, recurring extreme events and soil degradation. Climate change is projected to intensify existing known problems in agriculture in many West African countries. According to the IPCC

(2013 AR5 and others), the impacts of climate change due to elevated GHGs under all the scenarios and representative concentration pathway (RCPs) will likely be severe in Africa, particularly over West Africa. They have projected that droughts and floods will likely be greater in frequency and will intensify in many countries. However, the occurrence and regularity of more extreme events to which the populations have to find adaptation strategies in the future will likely be uncertain. The uncertainty of climate change (and its impacts) over Africa, particularly West Africa Sahel are real because of the lack of robust agreement about the possible impacts of global temperatures increase, changes in mean rainfall, rainfall variability and associated hydrological processes at global and regional scale (Guinini, 2010). Hence, the main message of the impact of climate change in the region is that dry areas will likely become drier, while the wet areas will also become wetter (e.g. Desanker and Magadza, 2001; Thomas *et al.*, 2005, IPCC AR5, 2013). There will also be more frequent dry periods in West Africa.

2.5.2 Impacts of Climate Change and Reforestation on ROD and RCD over West Africa

Many studies have investigated the impacts of climate change in West Africa using very high resolution regional climate models (RCMs) for future climate projections and impacts studies (e.g Paeth *et al.*, 2006; Paeth and Diederich, 2010; Sylla *et al.*, 2010; Rummukainen, 2010; Patricola and Cook, 2010; Wang and Alo, 2012; Abiodun *et al.*, 2011, 2012, 2013). For example, Abiodun *et al.* (2011) used the regional climate model RegCM3, forced with the AOGCM ECHAM5 as boundary condition to investigate the effects of future climate change over West Africa the elevated greenhouse gases (GHGs) A1B scenario for the period 2031-2050. They found a likely warmer climate over West Africa throughout the year except in the rainy season (April-September). The south west monsoon flow that brings cool and moist air from the coast inland would become stronger and would induce a warmer western part of Sahel than its eastern part in the summer June, July, August period. Patricola and Cook (2010) also evaluated the future rainfall changes in West Africa by using an ensemble of future predictions by RegCM3 driven with sea surface temperature and lateral boundary conditions from nine GCMs. The results showed wetter conditions over West Africa in spring, drying in early summer. They also found that more flooding will likely occur in the late summer. Only few studies investigated the future climate ROD/RCD (e.g. Kunstmann and Jung, 2003; Biasutti and Sobel, 2009; Sarr, 2012). These studies suggested that rainfall is projected to be more variable and less reliable with a delayed ROD in the future over West Africa. More recently, IPCC (AR5, 2013) indicated that climate models show low confidence or no changes in the ROD over West Africa. However, they suggested that the RCD would be later with an intensification of rainfall at the end of the rainy season leading to an increase in the length of the rainy season.

Nevertheless, to reduce the impact of climate change over West Africa, reforestation can be used as an option according to the last IPCC assessment report (IPCC AR5, 2013). Indeed, the reforestation/ afforestation accounts for the biophysical effect on climate with carbon sequestration thereby reducing the concentration of the atmospheric GHGs (Abiodun *et al.* 2012, 2013). For example, Abiodun *et al.* (2012) investigated the potential impact of reforestation on the future climate over West Africa and found that reforestation could delay the monsoon flow (i.e. delay of onset) in transporting cool moist air over the area downwind of the reforested zone and could weaken the temperature gradient in the reforested area. Some studies (e.g. Bonan, 2010; Barbier *et al.*, 2009; Bernier *et al.*, 2011) showed that reforestation changes the albedo, the evapotranspiration and the roughness of the surface of the reforested area, while others (e.g. Bonan *et al.*, 1992; Betts, 2000; Bala *et al.*, 2007; Montenegro *et al.*, 2009; Bathiany *et al.*, 2010) suggested that reforestation in areas like West Africa will likely enhance the latent heat flux from evapotranspiration and will produce a net cooling effect. However, most of the previous studies mentioned above investigated only the impacts of climate change on some mean climate variables (e.g. temperature and rainfall) but did not take into account the rainfall onset and cessation dates. There is therefore a strong need to evaluate the potential impacts of climate change and reforestation on the future climate ROD/RCD due elevated GHGs over West Africa.

CHAPTER THREE

RESEARCH METHODOLOGY

3.1 PRESENTATION OF STUDY AREA

The study area of this research is West Africa which is located between the latitudes 4°N and 28°N and the longitudes 15°E and 16°W (Fig. 3.1). Following Omotosho and Abiodun (2007) and Abiodun *et al.* (2012), the West African domain is divided into three climatic zones: Guinea (4°N–8°N), Savanna (8°N–12°N) and Sahel (12°N–20°N). The Guinea zone represents the southern boundary to the Atlantic Ocean. This climatic zone has sub-humid climate with an average annual rainfall is between 1250mm and 1500mm. The numbers of days of growing period (DGP) varies between 180-270 days. The Savanna zone is a semi-arid zone (Sahelo-Sudan) with an average annual rainfall between 750mm and 1250mm in a season. During the monsoon jump, this zone is affected by a little dry season. The Sahel or Sahelian zone covers the northern boundary of Mauritania, Mali and Niger. It is an arid zone and has up to 750mm of rain in a single but short rainy season (June-September) with a mean GDP of 90 days. However, the topography plays an important role in the climate variability in West Africa and some of the most important Plateau are (FAO, 1985): Fouta Djallon (1537m), Guinea Highlands (1656m), Sierra Leone Mountains (1948m), Nimba Mountains (1752m), Mandara Mountains (1142m), Jos Plateau (1690m), Adamawa Highlands (2042m), the Saharan Uplands of Air (1850m) and the Plateau of Djado (1120m) in northern Niger (Fig. 3.1). The region contains five major rivers systems but the largest river is the Niger River that drains most of the countries over a distance of 4180km (FAO, 1985). Sixteen countries constitute West Africa: Benin, Burkina Faso, Cape Verde, Gambia, Ghana, Guinea, Guinea-Bissau, Ivory Coast, Liberia, Mali, Mauritania, Niger, Nigeria, Senegal, Sierra Leone and Togo with a surface area of about 6 million km^2. The climate of West Africa is very complex and consists of dry and wet seasons throughout the entire region.

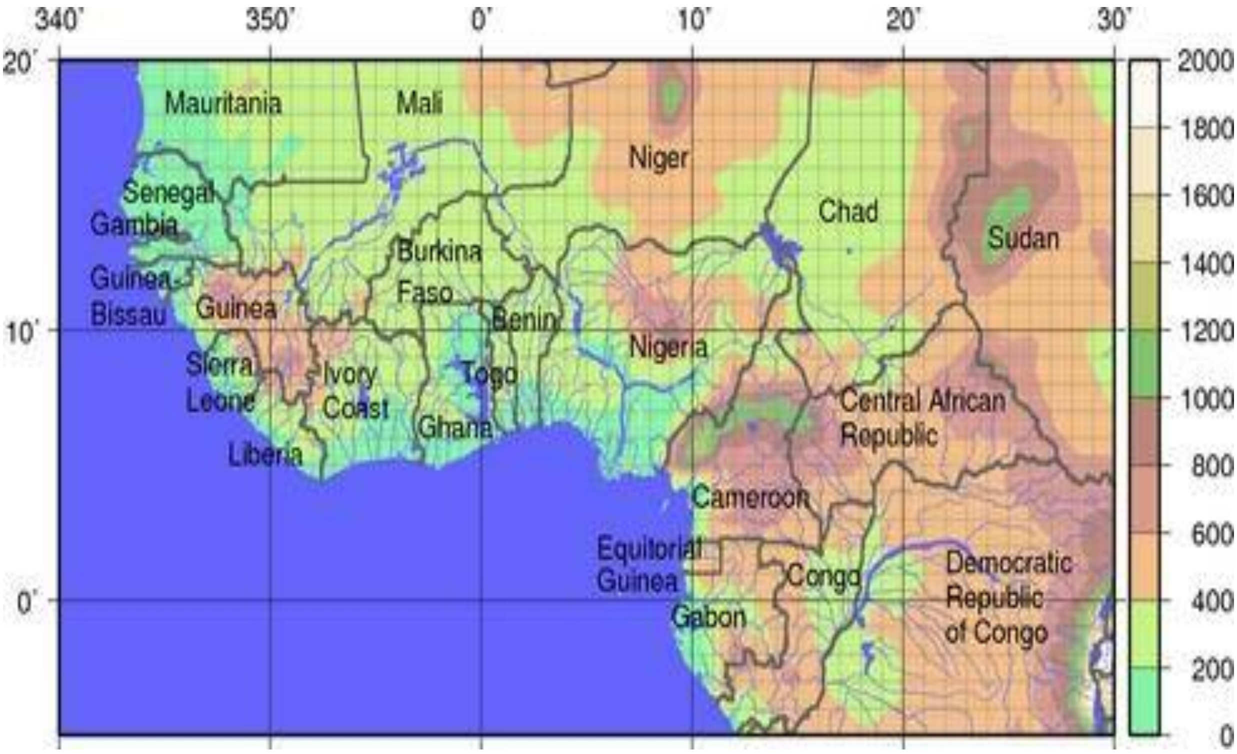

Figure 3.1: West African topography (shaded, in meters) and rivers (blue colors) taken from http://aaron.boone.free.fr/work.html

3.2 DATA

3.2.1 Observations Data

In this thesis satellite-derived datasets are used as observation data. There is a lack of high-quality observation datasets over West Africa and accessing the existing one is still a challenge in the region. In addition, the temporal and spatial resolution of the station network is very poor and this constitutes the main problem when evaluating RCMs simulations over West Africa (Nikulin *et al.*, 2012). To overcome this problem, satellite measurements have been used to ameliorate the data scarcity in the region. In this study, the Tropical Rainfall Measuring Mission (TRMM, 3B42 version 6; 1998–2010; Huffman *et al.* 2007) is used for model validation. The TRMM data sets are satellite-based precipitation products with 0.25^{o} spatial and 3-hourly temporal resolutions. TRMM precipitation averages are shifted by one and one-half hours, representing approximately the 22:30–01:30, 01:30–04:30 … 19:30–22:30 UTC intervals (Nikulin *et al.* 2012). Similarly, we used also an additional observation dataset to TRMM, the gridded observational datasets called the Global Precipitation

Climatology Project (GPCP, version 1.1; 1998–2010; Huffman *et al.* 2001). The GPCP dataset has a coarser temporal and spatial resolution (i.e. 1^o degree with daily temporal resolution) than TRMM and is a satellite–gauge combination dataset for the entire African domain (Huffman *et al.* 2001). The use of two observations datasets (GPCP and TRMM) was to account for differences in uncertainty around observed RODs (Huffman *et al.* 2009; Huffman and Bolvin 2011).

3.2.2 ERA-Interim Reanalysis Data

The reanalysis datasets used in the thesis are from the European Centre for Medium-Range Weather Forecasts (ECMWF) ERA-Interim reanalysis (hereafter ERAIN; 1989–2008; Dee *et al.* 2011). Covering the period from 1 January 1989 onwards, the ECMWF reanalysis ERAIN is the latest global atmospheric reanalysis and its primary goal was to overcome the problems of data assimilation (e.g. hydrological cycle, quality of the stratospheric circulation and consistency in time of reanalyzed geophysical fields) observed in ERA-40 (Dee *et al.* 2011). ERAIN aims also at improving the quality of the reanalysis products relating to quality control, bias correction, and performance monitoring to be consistent with observations given the estimated uncertainties (Dee *et al.* 2011).

The forecast ERAIN precipitation can be derived either with different spin-up, base time or forecast steps to produce the precipitation estimates (Dee *et al.* 2011). In the framework of the Coordinated Regional Climate Downscaling Experiment (CORDEX), Nikulin *et al.* 2012 tested the ERAIN dataset and showed that there is only minor difference to derive 3 hourly and daily precipitation when using the methods with and without spin-up and suggested to use the method without spin-up to derive precipitation estimates. It is to be noted that the base time of 0000 and 1200 and forecast steps 3, 6, 9, and 12 h are used for 3 hourly precipitation and the base times 0000 and 1200 and forecast steps of 12 h for the daily precipitation (Nikulin *et al.* 2012).

3.2.3 NUMERICAL SIMULATIONS USING CORDEX PROGRAM

3.2.3.1 CORDEX-RCMs Datasets

The simulation datasets are from ten of the RCMs that participated in the CORDEX-Africa experiment. The RCMs used are ARPEGE, RCA35, PRECIS, CRCM5, REMO, CCLM, RACMO, RegCM3, HIRHAM and WRF. In this thesis, HIRHAM has been excluded in the analyses. The CORDEX simulation domain (Fig. 3.2) is much wider than our study domain (West Africa; 18°W–25°E and 0°N–18°N). All the simulations were initialized and driven at the lateral boundaries by the ERAIN datasets (1989-2008) at 50 km grid spatial resolution. All the RCMs used the same sea surface temperature (SST) from ERAIN as ocean boundary condition, except that RegCM3 used the National Oceanic Atmospheric Administration (NOAA) weekly optimum-interpolated SST (Reynolds *et al.* 2007), and the Canadian Regional Climate Model (CRCM) used the Atmospheric Model Inter-comparison Project, phase 2 (AMIP2) SST (Nikulin *et al.* 2012). The dynamics and physical parameterizations used in the RCMs for the simulations are given in Tables (3.1) and (3.2). The CORDEX-Africa simulations were obtained at the Climate Systems Analysis Group (CSAG), University of Cape Town, South Africa.

3.2.3.2 Presentation CORDEX Program

Sponsored by the World Climate Research Program (WRCP), the CORDEX program is an international coordinated framework that has mainly two-fold purposes in its first phase. Firstly, the framework of model evaluation to evaluate and benchmark the performance of the model, and secondly the framework of climate projection to produce some design set of experiments to provide an improved information on the regional climate change projections for impact and adaption studies world-wide (Giorgi *et al.*, 2009). For broader scientific community use, ~50 km (or 0.5 degrees) has been selected to be the standard horizontal resolution for the first phase CORDEX simulations in order to produce an ensemble of multiple regional climate dynamical and statistical downscaling models which will be initially forced by the latest ECMWF ERA-Interim reanalysis for the first framework and then with forcing data based on the set of new global model simulations from the fifth phase of the Coupled Model Inter-comparison Projects (CMIP5) GCM models used in the IPCC AR5 for the 21 century in the second framework for the following order of priority 1981-2010, 2041-2070, 2011-2040, 2071-2100, 1951-1980 were based on the so-called reference concentration pathways (RCPs) 4.5 and 8.5 (Giorgi *et al.*, 2009). The detail of the first phase of CORDEX is given in Figure (3.2).

Table 3.1: The CORDEX-Africa RCMs and their details (taken from Nikulin *et al.* 2012)

RCMs	**CNRM ARPEGE5.1**	**ICTP RegCM3**	**CLMcom CCLM4.8**	**KNMI RACMO2.2b**	**MPI REMO**
Institute	Centre National de Recherches Meteorologiques, France	Abdus Salam International Centre for Theoretical Physics, Italy	Climate Limited-Area Modelling Community (www.clm-community.eu)	Koninklijk Nederlands Meteorologisch Instituut, Netherlands	Max Planck Institute, Germany
Short name	**ARPEGE**	**RegCM3**	**CCLM**	**RACMO**	**REMO**
Projection resolution	Polar, stretching factor 2 (TL179)	Mercator 50 km	Rotated pole 0.44	Rotated pole 0.44	Rotated pole 0.44
Vertical coordinate/levels	Hybrid/31	Sigma/18	Terrain following/35	Hybrid/40	Hybrid/27
Advection	Semi-Lagrangian	Eulerian	Fifth-order upwind; Baldauf (2008)	Semi-Lagrangian	Semi-Lagrangian
Time step (s)	1200	100	240	720	240
Convective scheme	Bougeault (1985)	Grell (1993) Fritsch and Chappell (1980)	Tiedtke (1989)	Tiedtke (1989)	Tiedtke (1989)
Radiation scheme	Morcrette (1990)	Kiehl *et al.* (1996)	Ritter and Geleyn (1992)	Fouquart and Bonnel (1980)	Morcrette *et al.* (1986); Giorgetta and Wild (1995)
Turbulence vertical diffusion	Mellor and Yamada (1982)	Holtslag *et al.* (1990)	Herzog *et al.* (2002); Buzzi *et al.* (2011)	Eddy-diffusivity (first-order K) mass flux approach	Louis (1979)
Cloud microphysics scheme	Ricard and Royer (1993)	SUBEX; Pal *et al.* (2000)	Herzog *et al.* (2002); Buzzi *et al.* (2011)	Tiedtke (1993)	Lohmann and Roeckner (1996);
Land surface scheme	ISBA; Douville *et al.* (2000)	BATS1E; Dickinson *Et al.* (1993)	TERRA-ML; Doms *et al.* (2011)	TESSEL; ECMWF (2007)	Hagemann (2002);Rechid *et al.* (2009)
Latest reference and comments	Deque (2010)	Pal *et al.* (2007)	Rockel *et al.* (2008); Baldauf *et al.* (2011)	van Meijgaard *et al.* (2008); based on ECMWF cycle 31r1; ECMWF (2007)	Jacob (2001); Jacob *et al.* (2007)

Table 3.2: The CORDEX-Africa RCMs and their details (taken from Nikulin *et al.* 2012)

RCMs	**SMHI RCA35**	**UCT PRECIS**	**UC WRF3.1.1**	**UQAM CRCM5**	**DMI HIRHAM5**
Institute	Sveriges Meteorologiska och Hydrologiska Institut, Sweden	University of Cape Town, South Africa	Universidad de Cantabria, Spain	Universite du Quebec, Montreal, Canada	Danmarks Meteorologiske Institut, Denmark
Short name	**RCA**	**PRECIS**	**WRF**	**CRCM**	**HIRHAM**
Projection resolution	Rotated pole 0.44	Rotated pole 0.44	Mercator 50 km	Rotated pole 0.44	Rotated pole 0.44
Vertical coordinate/levels	Hybrid/40	Hybrid/19	Terrain-following ETA/28	Hybrid/56	Hybrid/31
Advection	Semi-Lagrangian	Eulerian	Eulerian	Semi-Lagrangian	Semi-Lagrangian
Time step (s)	1200	300	240	1200	600
Convective scheme	Kain and Fritsch (1990, 1993)	Gregory and Rowntree (1990); Gregory and Allen (1991)	Kain (2004)	Kain and Fritsch (1990); Kuo (1965)	Tiedtke (1989)
Radiation scheme	Savijarvi (1990); Sass *et al.* (1994)	Edwards and Slingo (1996)	Dudhia (1989); Mlawer *et al.* (1997)	Li and Barker (2005)	Fouquart and Bonnel (1980); Mlawer et al(1997)
Turbulence vertical diffusion	Cuxart *et al.* (2000)	Wilson (1992)	Hong *et al.* (2006)	Benoit *et al.* (1989); Delage (1997)	Louis (1979)
Cloud microphysics scheme	Rasch and Kris tjansson (1998)	Smith (1990)	WSM5; Hong *et al.* (2004)	Sundqvist *et al.* (1989)	Tiedtke (1989); Tompkins (2002
Land surface scheme	Samuelsson *et al.* (2006	MOSES2; Essery *et al.* (2003)	Smirnova *et al.* (2000)	CLASS 3.5 Verseghy (2000)	Schulz *et al.* (1998); Hagemann (2002)
Latest reference and comments	Samuelsson *et al.* (2011)	Jones *et al.* (2004)	Skamarock *et al.* (2008)	Zadra *et al.* (2008)	Christensen *et al.* (2006)

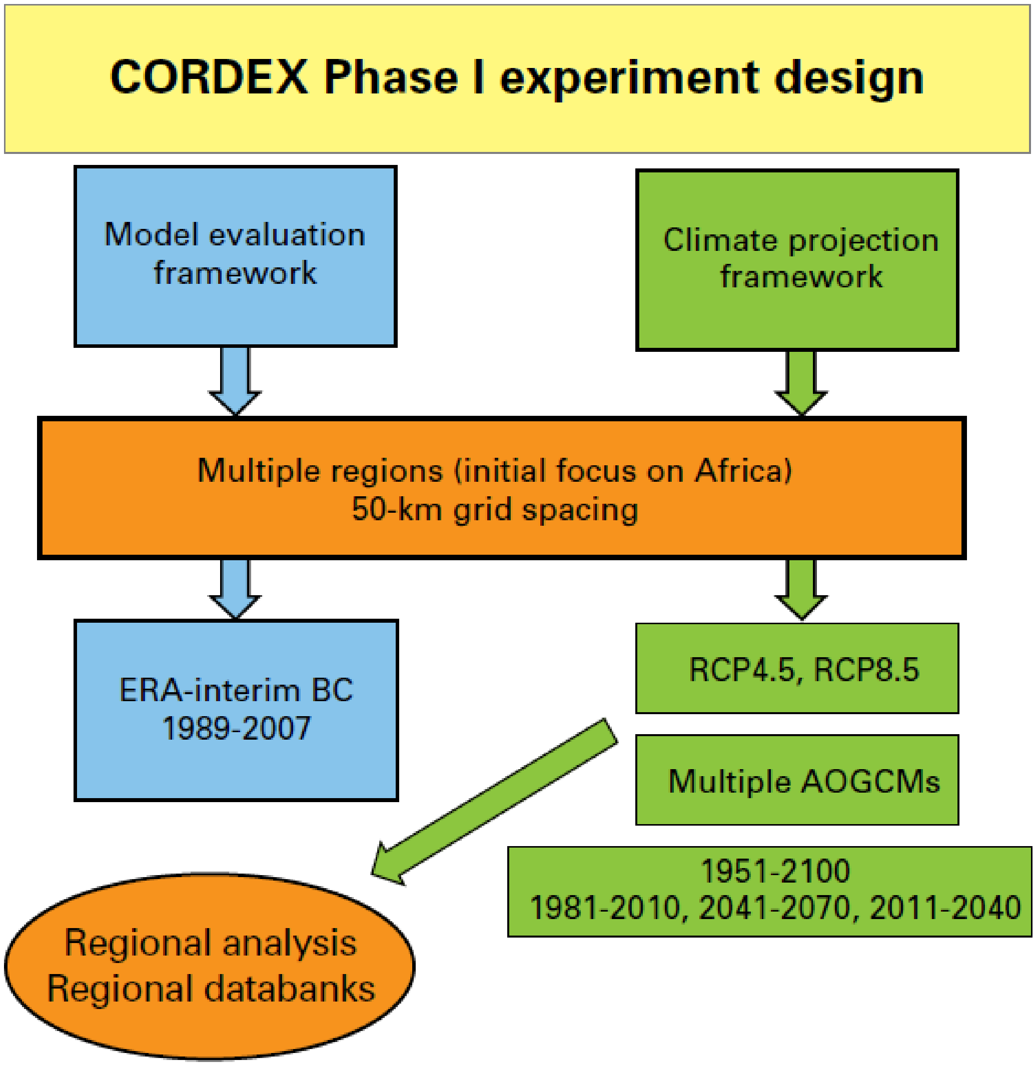

Figure 3.2: First phase of CORDEX experiment set up (Adopted from Giorgi et al., 2009)

The domain of CORDEX covers the entire world and is divided into five sub-domains covering the entire African, Australian, South American, North American and European continents. The African continent was the initial focus of CORDEX to enable assessment of the strengths and weaknesses of model framework before its application world-wide. Figure (3.3) shows the African domain (about 25°W–60°E and 44°S–42°N) used in the CORDEX experiment. Africa has been the first focus mainly because of, its vulnerability to climate variability and change, its low economic capacity for adaptation and its lack of data accessibility (Giorgi *et al.* 2009, Nikulin *et al.* 2012).

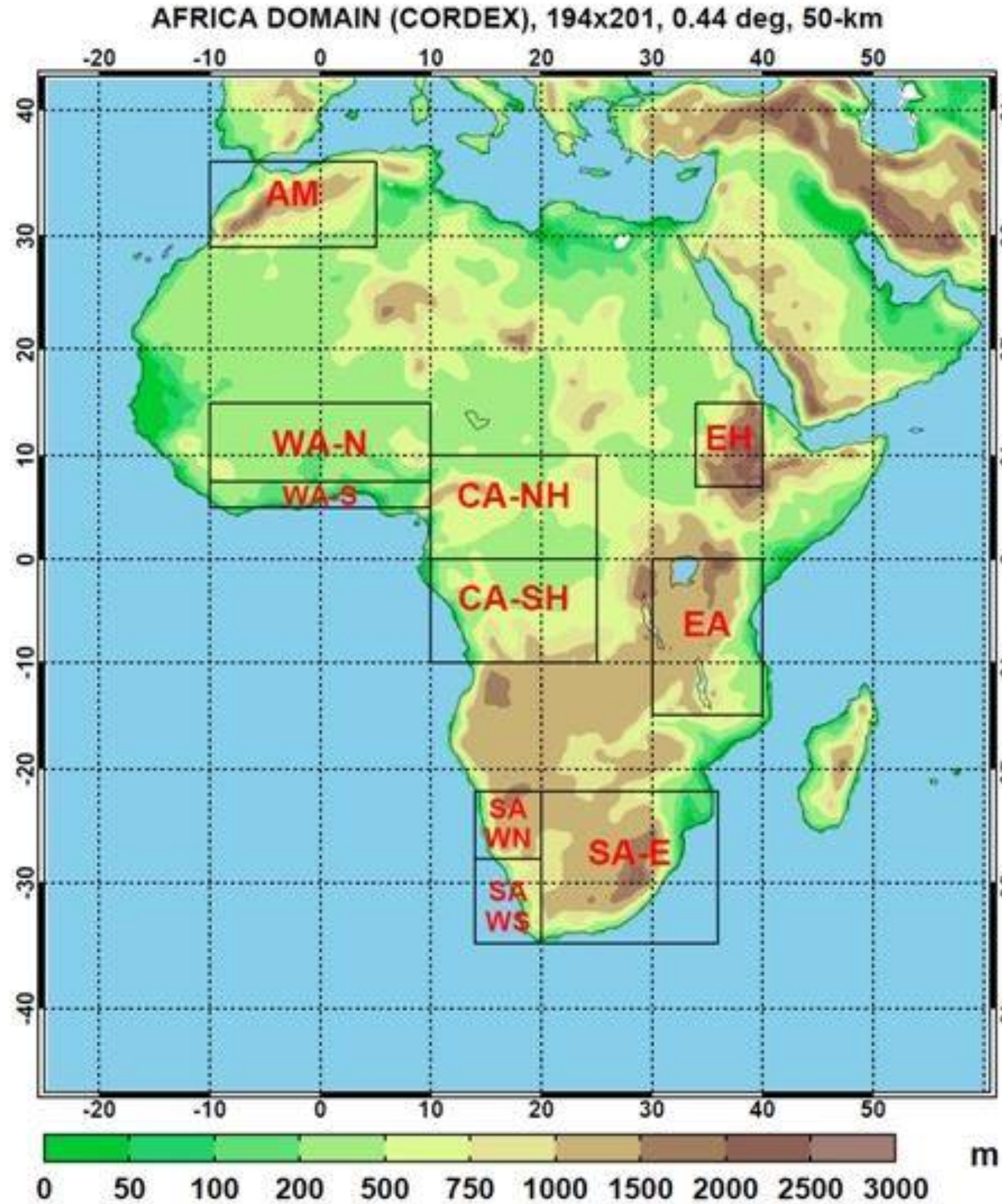

Figure 3.3: Orography (in meter) of the CORDEX Africa evaluation domain. The sub-region in the ten boxes shows the evaluation zones in Africa (e.g. East Africa (EA), Central Africa (CA), West Africa (WA) and South Africa (SA)) taken from *https://www.imk-tro.kit.edu/english/4659.php*

3.2.4 Regional Climate Modeling using RegCM and WRF

3.2.4.1 Description of RegCM Model

The study used the latest version of the community regional climate model of the International Centre for Theoretical Physics (ICTP, RegCM, version 4, hereafter RegCM) as described by Giorgi *et al.*

(2012). RegCM and its predecessors (RegCM3 and others) use the same model dynamics and the details of the available options are given in Table 3.3.

Table 3.3: Options available in the new RegCM (from Giorgi *et al.* 2012). The configurations of RegCM used in the present study are given in bold.

Model aspects	**Options available in RegCM4**
Dynamics	- Hydrostatic, σ-vertical coordinate (Giorgi *et al.* 1993a)
Radiative transfer	- Modified CCM3 (Kiehl *et al.* 1996)
Planetary Boundary Layer (PBL)	- **Modified Holtslag (Holtslag *et al.* 1990)** - UW-PBL (Bretherton *et al.* 2004)
Cumulus convection	- Simplified Kuo (Anthes *et al.* 1987) - Grell (Grell 1993) - **MIT (Emanuel & Zivkovic-Rothman 1999)** - Tiedtke (Tiedtke 1989)
Resolved scale precipitation	- SUBEX (Pal *et al.* 2000)
Land surface	- **BATS (Dickinson *et al.* 1993)** - Sub-grid BATS (Giorgi *et al.* 2003) - CLM (Steiner *et al.* 2009)
Ocean fluxes	- BATS (Dickinson *et al.* 1993) - **Zeng (Zeng *et al.* 1998)** - Diurnal sea surface temperature (Zeng & Beljaars 2005)
Interactive aerosols	- Organic and black carbon, SO4 (Solmon *et al.* 2006) - Dust (Zakey *et al.* 2006) - Sea salt (Zakey *et al.* 2008)
Interactive lake	- 1D diffusion/convection (Hostetler *et al.* 1993)
Tropical band	- Coppola *et al.* (2012)
Coupled ocean (not in public version)	- MIT (Artale *et al.* 2010) - ROMS (Ratnam *et al.* 2009)

RegCM is therefore hydrostatic, compressible, sigma-p vertical coordinate model over an Arakawa B-grid (Giorgi *et al.* 2012). The RegCM4 model physics used in the present thesis are the following:

Radiative transfer: The modified community climate model (version 3, CCM3) from the National Center for Atmospheric Research (NCAR) as described by Kiehl *et al.* (1996) is used to calculate the radiative transfer scheme in RegCM. This calculation takes into account the short-wave and infrared parts of the spectrum, aerosols and atmospheric gases (e.g. including GHGs). The delta-Eddington formulation (Briegleb, 1992) is used for solar radiative processes contributions where the aerosol optical properties determine the solar radiation scattering and absorption (Giorgi *et al.* 2012). Moreover, the optical properties of the solar spectrum (such as the cloud liquid water path, the cloud fractional cover, and the effective cloud droplet radius) are included in the calculations of cloud radiation. Concerning the aerosol transfer scheme, RegCM has added the infrared spectrum contributions to the shortwave scattering and absorption spectrum of RegCM3 (Solmon *et al.*, 2008) to take into account the relatively large dust and sea salt particles (Giorgi *et al.* 2012).

Planetary boundary layer (PBL): Two PBLs schemes are available in RegCM (see Table 3.3). We used the modified PBL from Holtslag *et al.* (1990) with the lateral boundary conditions scheme that used a relaxation, exponential technique. To calculate the PBL height, this scheme implemented an iteration technique based on a formulation of bulk critical Richardson number. Then the PBL height indicates the heat, moisture and momentum's vertical profile eddy diffusivity which is a function of the friction velocity, height, Monin-Obhukov length (Giorgi *et al.* 2012). Many modifications of this scheme have resulted in solving some major problems (e.g. excessive vertical transfer of moisture, heat, and momentum leading to surface inversion problem or to a warmer winter in northern hemisphere) in the model (Giorgi *et al.* 2012). Corrections have been made for these problems in the scheme so that RegCM4 captures the vertical transfer of moisture between the surface and the top of PBL as well as a consistent reduction of the warm bias in the high latitude regions.

Land surface processes: The Biosphere-Atmosphere Transfer Scheme (BATS) as described by

Dickinson *et al.* (1993) is used for land surface processes. The explicit moisture as described in Pal *et al.* (2000) is also used as moisture scheme (SUBEX) for sub-grid processes. The BATS scheme consists of many layers (i.e. 1-layer vegetation module, 1-layer snow module, a force-restore model for soil temperatures, 3-layer soil scheme, and a simple surface runoff), 20 types of surfaces, 12 types of coloured soil and soil texture (Giorgi *et al.* 2012). Recently, BATS has incorporated urban and suburban types of land use to improve the model grid and sub-grid processes. These new land use types play an important role in the properties of the land surface processes such as the surface energy balance, runoff and evapotranspiration. Therefore, the BATS package includes maximum vegetation cover, roughness length, albedo, and soil characteristics (Giorgi *et al.* 2012).

Cumulus convection: Four cumulus convective schemes are available in RegCM (Table 3.3). However, in this study, the cumulus convective scheme used is the Emanuel (1991) with the Arakawa and Schubert (1974) closure. In this scheme, convection is given by the level of cloud base buoyancy. Therefore, the model sub-cloud-scale updrafts and downdrafts produced convective fluxes with an in-homogenous and episodic cloud mixing. This scheme also used a simplified ice processes during the auto-conversion of cloud water into rain water (Giorgi *et al.* 2012). Although the scheme is complex it has the advantage of applications to different climate regimes.

Ocean fluxes: The Zeng *et al.* (1998) ocean flux scheme is used for processes over the ocean. Introduced in RegCM3 for the first time by Pal *et al.* (2007), this scheme is based on the representation of Monin-Obhukov turbulence and has been implemented to improve some problems in BATS option regarding excessive evaporation in tropical warm oceans (Giorgi *et al.* 2012).

Other model physics includes the coupling of RegCM to other components of the climate system such as lakes and oceans, aerosol and chemistry. More details of the model description in given by Giorgi *et al.* (2012).

The model domain extends from about 28°S to 28°N and 38°W to 32°E, with horizontal grid resolution of 40 km (Fig. 3.4). This study uses the same horizontal and vertical resolutions as in Abiodun *et al.* (2012, 2013) but it differs in the PBL and convection schemes. The model uses 18 vertical levels from the surface to 50 hPa. The model domain extends up to South America, thus it is large enough to bring more moisture which enable better investigation of the West African monsoon systems and its dynamisms. The model RegCM is forced by the general circulation model (GCM) HadGEM as lateral and boundary conditions in the present study.

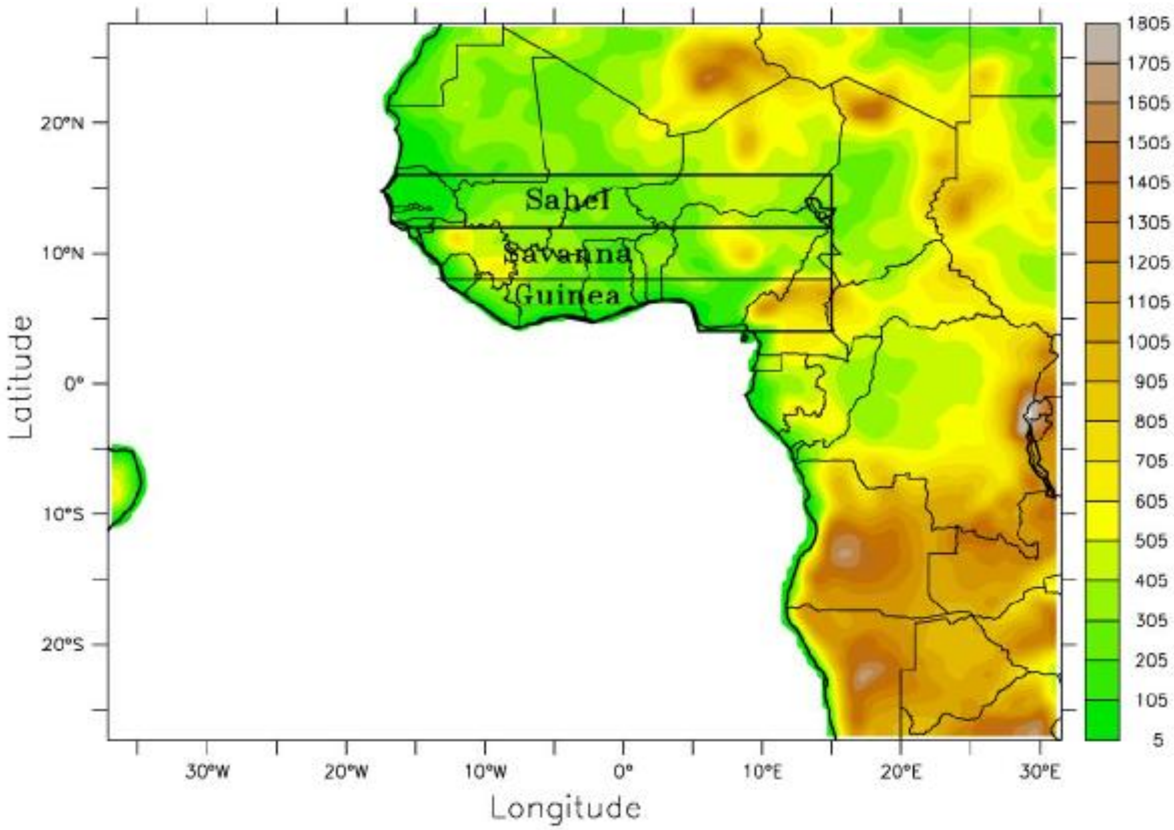

Figure 3.4: RegCM4 model domain showing the topography and the study zones.

3.2.4.2 The Forcing GCM of RegCM

The United Kingdom Meteorological Office Hadley Centre Earth System Model (HadGEM2-ES hereafter HadGEM, Collins *et al.* (2008)) of the CMIP5 models that participated in the IPCC AR5 has been used as the forcing GCM of RegCM. The HadGEM model has a horizontal spatial grid resolution of 1.875°x1.25° (~140km) at middle latitudes in the atmosphere; over the ocean it is about 1°x1° spatial resolution. However, the ocean latitudinal resolution varies and even increases at the equator (e.g. Jones *et al.* 2011, Dike *et al.* 2014). In addition, the HadGEM model has 38 hybrid height levels in the vertical. This extends from the surface to 40 km height and 40 z-levels in the ocean including 5km from the sea surface downward into the sea. It is an upgrade of the previous version HadGEM1. The HadGEM model takes into account many forcing (such as aerosols, GHGs emissions, solar irradiance, ozone) and its configuration components included atmosphere, land surface and hydrology, aerosols, ocean and sea ice, terrestrial carbon cycle, atmospheric chemistry, and ocean biogeochemistry (Jones *et al.* 2011). The simulations period of this model followed the centennial CMIP5 experiments. Therefore the historical simulations (present day) stand from the period 1950 to 2005, while the future projections are from 2006 to 2100 under the RCPs emission scenarios.

The RegCM model used the HadGEM model simulations as initial and lateral boundary condition data for all the experiments. HadGEM gives 6 hourly sea surface temperature data for present-day (1970-2004) and future (2030-2064). The first The performance of HadGEM model in simulating the West African climatology and its comparison with RegCM present and future projections are given in Chapter4.

3.2.4.3 Description of WRF Model

The Weather Regional Forecast model (WRF, version 3.5.1) as described by Shamarock *et al.* (2008) and developed at the National Center for Atmospheric Research (NCAR) was also used in this study. The WRF model is driven by the GCM ECHAM6 of the Max Plank Institute as lateral and boundary conditions. The WRF model offers many options for dynamical downscaling. It presents several planetary boundary layer schemes, an internal land surface model (LSM) coupling for a good representation of land-atmosphere interaction and uses sigma vertical coordinate system in the layers of lower troposphere (Krishna et al 2011). The physical parameterization schemes set for WRF in this study are: the WSM 5-class scheme (Hong *et al.*, 2004) as the microphysics scheme, the land surface processes (Chen and Dudhia, 2001) from the Unified NOAA scheme, the Yonsei University scheme for the PBL (Hong *et al.*, 2006), the rapid radiative transfer model (RRTM) scheme for long waves (Mlawer *et al.*, 1997), the Dudhia scheme for short waves (Dudhia, 1989) and the Kain-Fritsch Cumulus parameterization schemes (Kain, 2004). These physical schemes are used because they give consistent results over West Africa (e.g. Vigaud *et al.*, 2009; Flaounas *et al.*, 2010). The WRF model was run for the period 1970-2004 for historical simulations and 2030-2064 for future projection, at a spatial horizontal grid resolution of 40 km.

3.2.4.4 The Forcing GCM of WRF

The sixth generation of the atmospheric general circulation model ECHAM (ECHAM6) developed at the Max Planck Institute for Meteorology (MPI-M) is used as lateral boundary conditions for the WRF model in the present study. ECHAM6 (hereafter ECHAM) has been part of the CMIP5 GCM models used for assessing the Earth's state regarding climate variability and change in the IPCC AR5. ECHAM is a major component of the new coupled system of the MPI Earth System Model (MPI-ESM) as described in Giorgetta *et al.*, (2012). The MPI-ESM includes also the land vegetation model JSBACH, the ocean GCM MPIOM and the ocean biogeochemistry model HAMOCC. In addition, the state of information exchanges and fluxes between the ocean and the atmosphere is controlled by the OASIS coupler (Giorgetta *et al.*, 2012). ECHAM and its predecessor ECHAM5 have been developed on the same basis as described in Roeckner *et al.* (2003, 2006). ECHAM differs significantly from ECHAM5 on the land processes, radiation schemes, surface albedo computation, and convection occurrence condition. However there are minor changes between the two models for some parameters such as moist convection, optical properties of cloud, orographic drag at sub-grid scale and gravity wave drag of the atmosphere (Giorgetta *et al.*, 2012). Therefore, ECHAM integrated the JSBACH land vegetation model (i.e. physical parameterizations of exchanges of heat and water storage with the atmosphere as well as the hydrological discharge, and carbon cycle land-based processes) for land surface processes. For radiative forcing, ECHAM used the newly implemented RRTMG-SW scheme (from Atmospheric and Environmental Research (AER) of Lexington Massachusetts) as described in Giorgetta *et al.* (2012). Moreover, ECHAM has been developed with three types of resolutions, namely T63L47, T63L95 and T127L95. For coupled simulations, ECHAM used T63L47 resolution at 1.5 degrees ocean resolution in MPI-ESM-LR. The T63L95 resolution is used with a higher resolved ocean grid of 0.4 degree in MPI-ESM-MR. The last available resolution is prescribed for atmosphere only simulations at 0.95 degree spatial grid resolution. In the present study, the coupled simulations spatial resolution has been used (i.e. 1.5^o grid spatial resolution). Note that all the resolutions resolve the troposphere and the stratosphere (Giorgetta *et al.*, 2012).

3.3 METHODOLOGY

3.3.1 Definitions of Rainfall Onset and Cessation

There are different definitions for determining ROD and RCD in West Africa (Omotosho, 1990; Odekunle, 2004, 2005, 2006; Laux *et al.*, 2008). However, these methods do sometimes produce different ROD/RCD, even when applied to the same observation dataset. For this study, we select and compare four prominent ROD definitions and also use one RCD definition to evaluate the performances of regional climate models over West Africa (Table 3.4). The ROD definitions (hereafter DEF1, DEF2, DEF3 and DEF4) and RCD definition are given in Table (3.4).

The definitions of ROD/RCD are computed using the two observations and RCMs datasets over each zone in West Africa. The results are compared in order to select the ROD definition that produced the least statistical discrepancy between the results of the datasets.

Table 3.4 : Definitions of ROD and RCD over West Africa (from Mounkaila *et al.*, 2014)

Methods	Definitions	References
DEF1	The first 'dekad' (10days) with at least 25 mm of rains, followed by two decades of at least 20 mm of rains.	AGRHYMET, 1996
DEF2	The total of at least 25 mm of rainfall within five (5) days. The starting day and at least two other days in this 5 days period must be wet (at least 0.1 mm rainfall recorded), followed by no dry period of seven or more consecutive days occurring in the following 30 days.	Stern *et al.*, 1981
DEF3	Any date after January 1st (instead of May 1st) totaling at least 20 mm of rainfall observed within three consecutive days without a dry period in the next 30 days that exceeds seven (7) days.	Sivakumar *et al.*, 1988
DEF4	The first two rains totaling 20 mm or more within 7 days, followed by two to three weeks each with at least 50% of the weekly crop–water requirement and without a dry spell within two to three weeks	Omotosho *et al.*, 2000
RCD	Any day from 1 September after which there are 21 or more consecutive days of rainfall less than 50% of the crop–water requirement.	Omotosho *et al.*, 2000

3.3.2 Experimental Set Up for RCMs Climate Projections

Three numerical experiments were performed. The first experiment simulated the present-day climate for the period 1970-2004 (denoted PRS). The second experiment simulated the future climate without reforestation for the period 2030-2064 (denoted NOREF). The first and second experiments used the same vegetation type from the United States Geological Survey (USGS) Global Land Cover

Characterization (GLCC) version 2 data as land cover. The third experiment simulated the future climate with reforestation (denoted REF) for the same period as in the NOREF experiment (2030-2064) but with deciduous broad leaf trees used as vegetation type over the Savanna in West Africa (Fig. 3.5). The third experiment is an assumption made with static vegetation to evaluate the potential impacts of reforestation on the Savanna zone and how this will influence the onset over Sahel and Guinea.

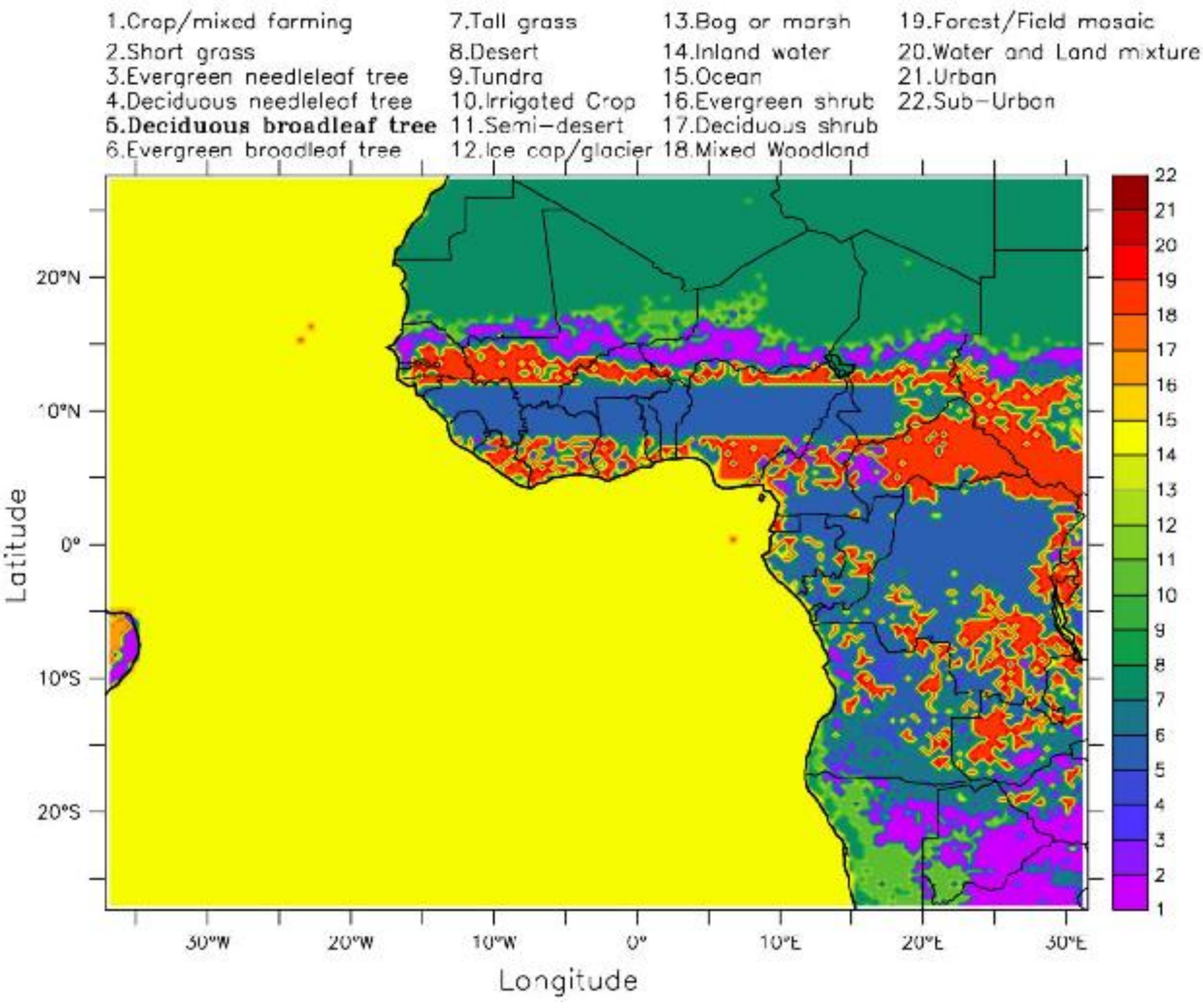

Figure 3.5: Reforestation experiment over Savana (8^{o}N-12^{o}N) with deciduous broadleaf trees as land use categories, as defined in BATS1E in RegCM.

This zone is critical because it constitutes a frontier between the coastal zone and the Sahel. The so-called monsoon jump (e.g. Le Barbe *et al.*, 2002; Abiodun *et al.*, 2011, 2012) that marks the beginning of the rainy season over Sahel occurs over this zone as well. Thereafter, we computed the rainfall onset for each experiment based on the definitions of onset used in Mounkaila *et al.* (2014). The difference in the results of future without reforestation (NOREF) and present-day (PRS) provides the impacts of GHG on future climate change over West Africa based on the increasing GHG concentration levels (rcp45). Likewise, the difference in the results of the future with reforestation (REF) and the future without reforestation (NOREF) provides the impacts of reforestation on the projected future climate change over West Africa under the rcp45 concentration levels. The GCMs (HadGEM and ECHAM) data were interpolated to the grid point of RegCM and WRF and the simulations were run for 35 years for all the experiments (present-day and future). However, the first simulated year was discarded for spin-up.

CHAPTER FOUR

RESULTS AND DISCUSSION

4.1 THE CAPABILITY OF REGIONAL CLIMATE MODEL IN SIMULATING THE ROD AND RCD OVER WEST AFRICA

This section discusses the results of the first objective of the thesis. The differences and similarities between the definitions are compared as well as their sensitivity to changes with respect to the observed rainfall datasets (GPCP and TRMM). Then, the simulated ROD and RCD of the CORDEX-RCMs are investigated to evaluate how well these RCMs simulate the ROD and RCD as compared to observations and ERAIN reanalyzes. This includes the spatial distribution of the mean, standard deviation, trend, correlation, and inter-annual variability of the ROD and RCD as well as the relationship between the ROD/RCD and the WAM and its features.

4.1.1 Comparison of Rainfall Onset Dates (RODs) Definitions

We compare four definitions (DEF1, DEF2, DEF3, and DEF4) of RODs to evaluate their similarities and differences in producing the ROD for two observation datasets (GPCP and TRMM) over West Africa. Figure 4.1 gives the inter-annual variability of the simulated ROD for each definition over the three climatic zones of our study area. The results show that the four definitions produce different rainfall onset dates (RODs) over each zone in West Africa (Fig. 4.1, Table 5). Over Sahel, both observations show similar patterns for the inter-annual variability of RODs (Fig. 4.1a, b) regardless the definitions used, though the RODs are different for each year. For instance, the difference between the RODs is up to 30 days in 2002 but all the definitions agree that Sahel experienced the latest ROD in the year. Similarly, the spread in the RODs in 2003 is more than 30 days but the definitions agree that the earliest RODs occur in the year. Among the definitions, DEF1 consistently produces the earliest ROD (i.e. earliest date), while DEF4 gives the most delayed (i.e. latest) ROD. In most years, DEF2 and DEF3 produce the RODs, which fall within those of DEF1 and DEF4. The maximum difference between DEF2 and DEF3 is less than 5 days. This strong agreement between DEF2 and DEF3 may be because the two definitions use the same criteria for identifying false ROD (Stern *et al.*, 1981). Nevertheless, with each definition, there are substantial differences between ROD obtained using GPCP and TRMM dataset. For DEF1, DEF2 and DEF3 the differences are about 11-15 days over Guinea and Savanna. Hence the differences between the ROD of DEF2 (or DEF3) and DEF1 are smaller using TRMM dataset. The characteristics of the RODs over Savanna are similar to that of Sahel (Fig. 4.1b), except the RODs occur earlier over Savanna than over Sahel. On the other, the characteristics of RODs over Guinea differ from that of Sahel or Savanna. All the definitions agree on early RODs in 1999 and 2006 and later RODs in 2001 and 2007. The difference between the RODs is up to 15, 10 days and 15 days respectively for the early and later RODs. Apart from producing earlier RODs over Guinea, the RODs pattern position differs in each definition in Guinea compared to Savanna and Sahel. Thus, the definitions are more sensitive to the climatic zones (Guinea, Savanna and Sahel respectively, Fig. 4.1).

Tables 5 and 6 present the mean and standard deviation of the RODs for each definition. In general, the mean RODs fall within February-March in Guinea, April-May in Savanna, and May-June in Sahel. However, DEF1 consistently produces the earliest RODs in each zone and shows large differences in RODs from the two datasets (11, 11, and 4 days over Guinea, Savanna, and Sahel, respectively). DEF1 also gives a smaller difference in standard deviation. However, DEF2 and DEF3 produce the largest differences among the four definitions in the mean RODs and standard deviation from GPCP and TRMM (15, 15, 9 days and 12, 12, 7 days respectively over Guinea, Savanna and Sahel in DEF2 and DEF3 for the mean, 4, 2 days in DEF2 over Guinea and Savanna, while DEF3 and DEF4 show no difference in standard deviation over Savanna. Moreover, DEF4 gives the lowest difference in the RODs from the datasets (6, 1, and 2 days respectively over Guinea, Savanna and Sahel) and produces the least differences in the RODs standard deviation from the datasets (Table 5&6). However, it is difficult to conclude that DEF4 gives the best ROD among the four definitions.

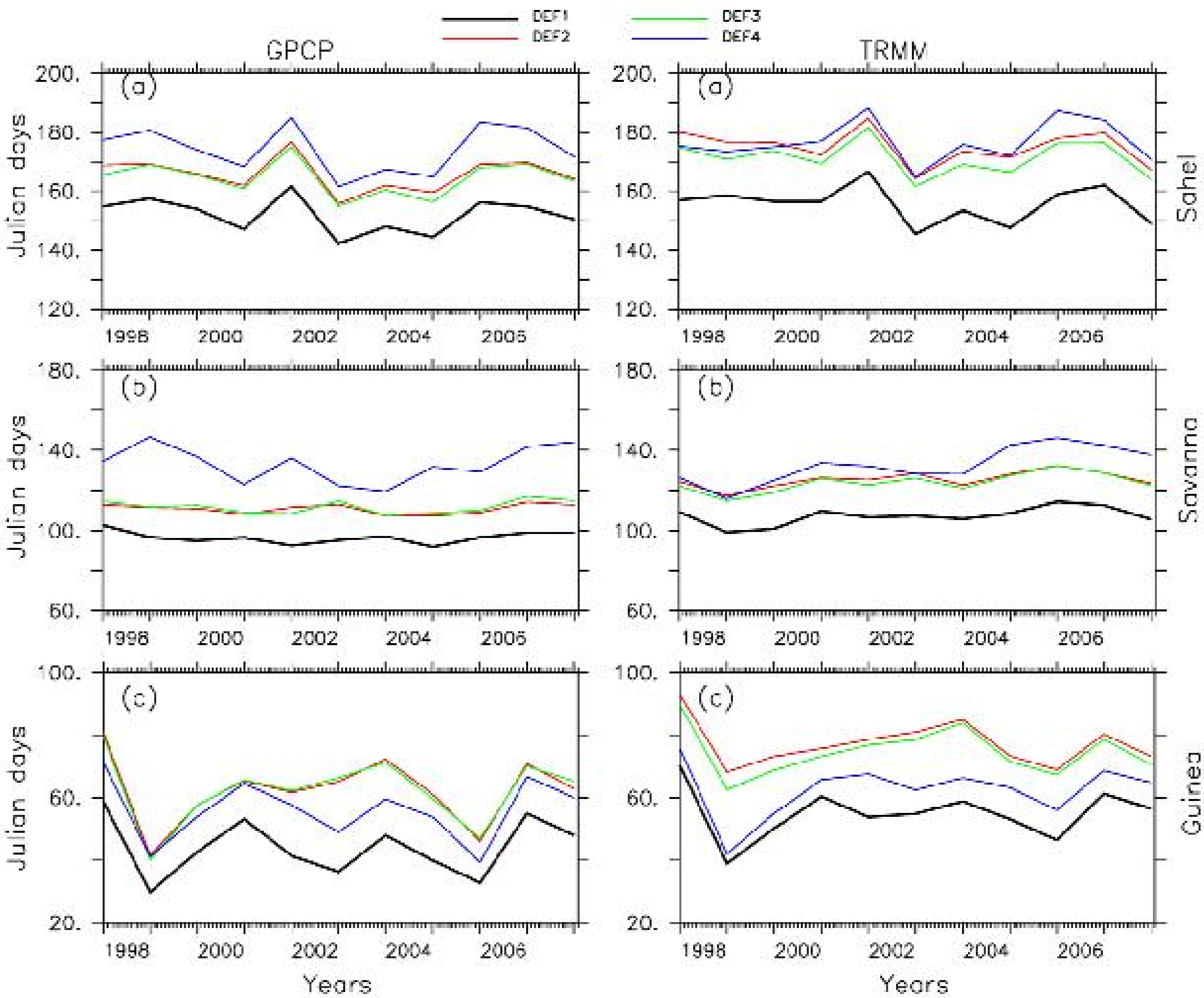

Figure 4.1 : The inter-annual variation of rainfall onset dates calculated with the four definitions using observed datasets (GPCP, left panels; TRMM, right panels) for 1998 – 2008 over Guinea (bottom panels), Savanna (middle panels) and Sahel (top panels).

Table 4.1: The mean RODs over West Africa for the period 1998-2008, obtained from four onsets definitions using GPCP and TRIMM datasets. Δ (in days) is the difference between the mean RODs from the two datasets.

Definitions	Guinea			Savanna			Sahel		
	GPCP	TRMM	Δ	GPCP	TRMM	Δ	GPCP	TRMM	Δ
DEF1	13-Feb	24-Feb	11	05-Apr	16-Apr	11	31-May	03-Jun	4
DEF2	02-Mar	17-Mar	15	19-Apr	04-May	15	13-Jun	22-Jun	9
DEF3	02-Mar	14-Mar	12	20-Apr	02-May	12	12-Jun	19-Jun	7
DEF4	25-Feb	02-Mar	6	12-May	11-May	1	22-Jun	24-Jun	2

Table 4.2: The standard deviation of RODs over West Africa for the period 1998-2008, obtained from four onsets definitions using GPCP and TRIMM datasets. Δ (in days) is the difference between the RODs standard deviation from the two datasets.

Definitions	Guinea			Savanna			Sahel		
	GPCP	TRMM	Δ	GPCP	TRMM	Δ	GPCP	TRMM	Δ
DEF1	9	8	1	3	4	1	6	6	0
DEF2	11	7	4	2	4	2	6	6	0
DEF3	11	7	4	3	5	0	6	6	0
DEF4	10	8	2	9	9	0	8	7	1

4.1.2 Spatial Distribution of ROD over West Africa

This part evaluates the performance of the RCMs in simulating the spatial distribution of the mean, standard deviation, trend and correlation of the ROD and RCD as compared with observations (GPCP and TRMM) and the forcing reanalyses (ERAIN) of the RCMs. The performance of the models is based on how well the RCMs capture the observed pattern and also if they perform better than ERAIN.

4.1.2.1 Spatial Distribution of simulated ROD mean over West Africa

4.1.2.1.1 Distribution for DEF1

Figure 4.2 compares the spatial distribution of the stimulated mean ROD over West Africa with observation (GPCP and TRMM) using DEF1. The observed ROD (Fig. 4.2a & b) is generally zonal and the dates increase inland from the coast. This is associated with the northward progression of the monsoon rainfall system behind the Intercontinental Discontinuity (ITD) over West Africa. The Rainfall starts along the Guinea coast in February-March, progresses inland (northward) and reaches the Sahel in May-June. ERAIN, ARPEGE, RACMO and WRF do not capture the spatial distribution of the ROD as observed in GPCP and TRMM. With DEF1, they produce earlier RODs (than observed) south of 8^{o}N. Most other RCMs show remarkable improvements over the ERAIN in simulating the RODs (Fig. 4.2). However, the simulated RODs produced by CRCM5, RCA35, REMO, and RegCM3 show improvement over that of ERAIN when compared with observations. CCLM fails to reproduce the observed zonal distribution south of 10oN; instead it produces a local maximum over Cote d'Ivoire and Ghana.

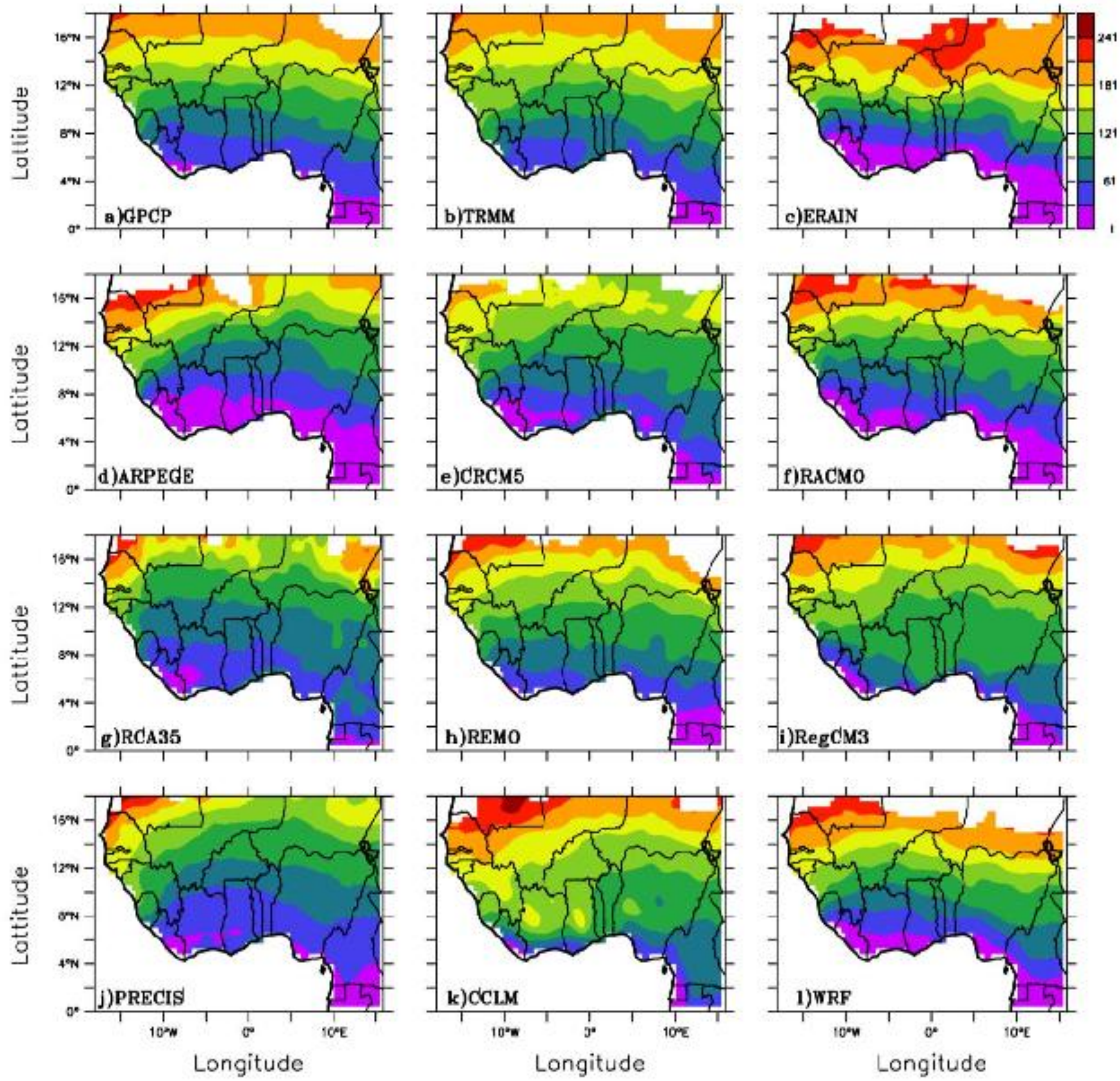

Figure 4.2 : Mean onset dates (in Julian days) as observed (GPCP/TRMM) and simulated (CORDEX-RCMs) from DEF1 for the period of 1998–2008

4.1.2.1.2 Distribution for DEF2 and DEF3

Figures 4.3 and 4.4 compare the spatial distribution of the simulated ROD with observations (GPCP and TRMM) using DEF2 and DEF3. As noted above, the observed ROD is generally zonal and the results using DEF2 and DEF3 are similar to each other and to that of DEF1. Again, ERAIN fails to capture the observed spatial distribution north of 12^{o}N over Sahel in both definitions as it consistently overestimates the ROD when compared to observation.

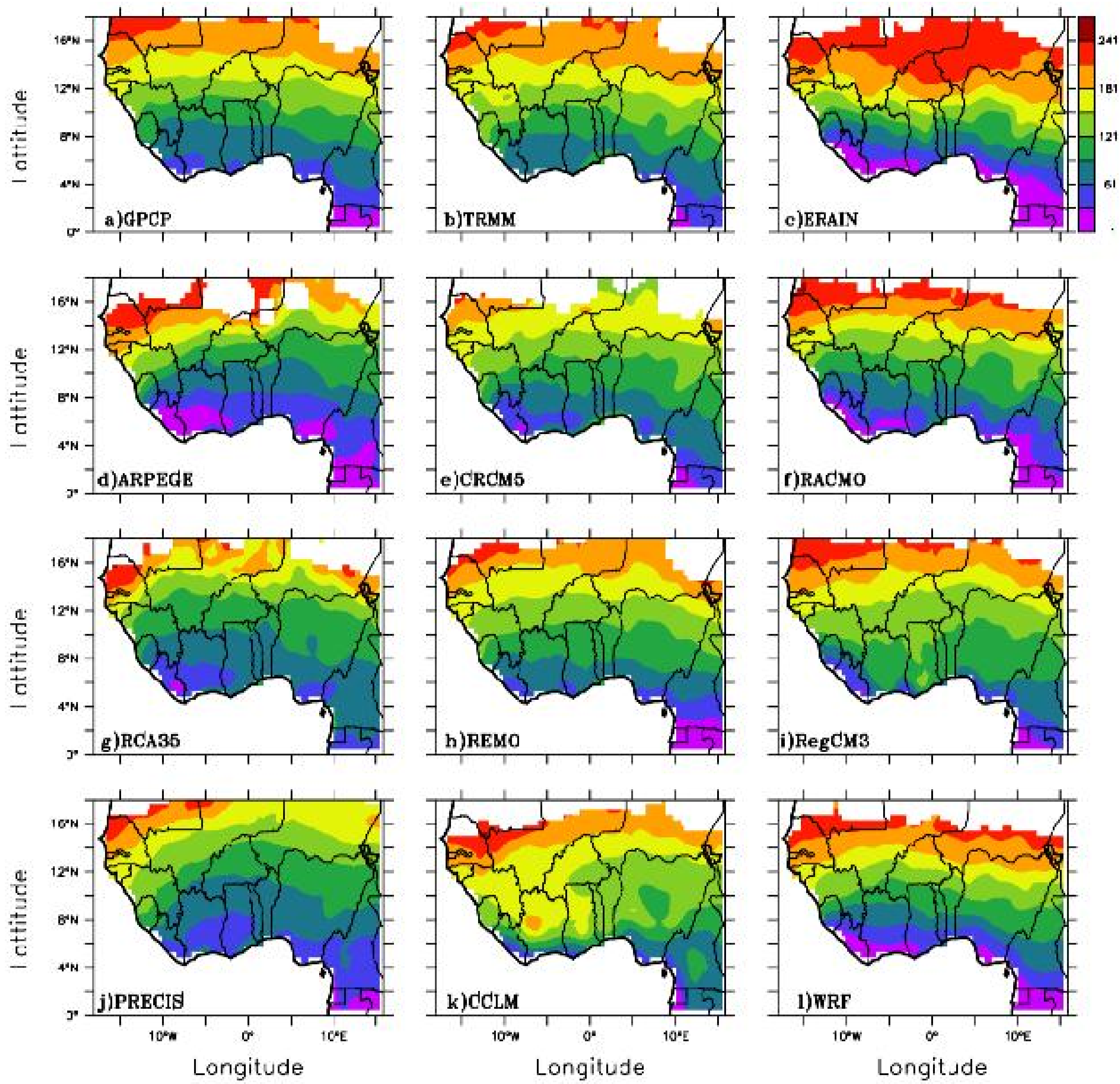

Figure 4.3 : Mean onset dates (in Julian days) as observed (GPCP/TRMM) and simulated (CORDEX-RCMs) with DEF2 over West Africa for the period of 1998–2008

However, it performs better over Guinea and Savanna zones than in DEF1. Most of the RCMs results are in agreement with the observed. All other RCMs show improvement over ERAIN. Again CCLM did not perform well for DEF2 and DEF3 just as in DEF1. It overestimates the ROD between 6^{o}N-

12°N producing a local maximum over Cote d'Ivoire and thus not capturing the zonal distribution of the ROD. Thus, ERAIN outperforms CCLM in simulating the spatial distribution of the ROD over Guinea and Savanna.

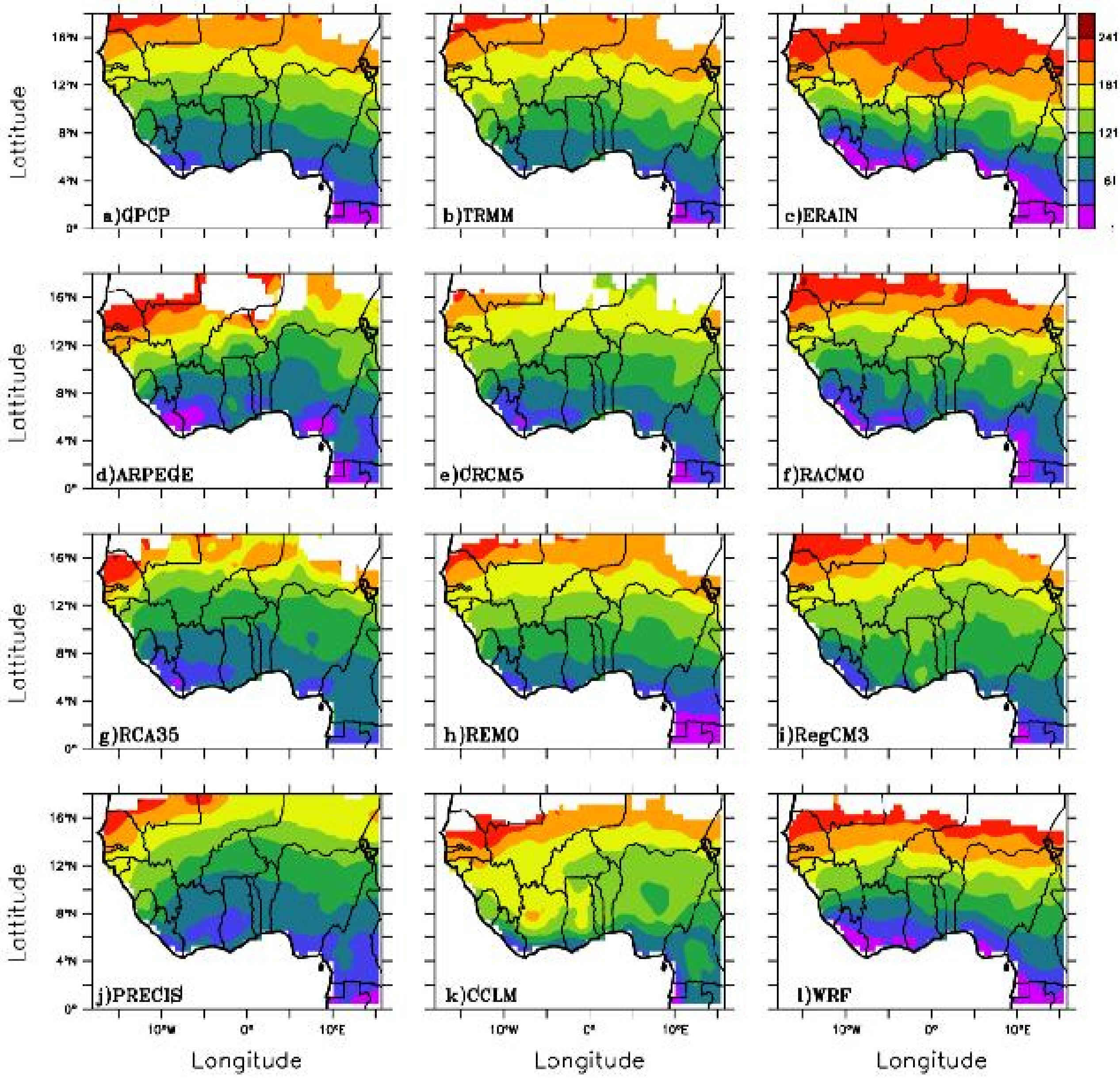

Figure 4.4 : Mean onset dates (in Julian days) as observed (GPCP/TRMM) and simulated (CORDEX-RCMs) with DEF3 for the period of 1998–2008

4.1.2.1.3 Distribution for DEF4

Figure 4.5 compares the spatial distribution of the stimulated ROD over West Africa with the observations (GPCP and TRMM) using DEF4. ERAIN, ARPEGE and RACMO do not capture the spatial distribution of the ROD as observed in GPCP and TRMM. They overestimate RODs over most areas especially north of 8°N and also fail to meet the DEF4 ROD criteria north of 12°N.

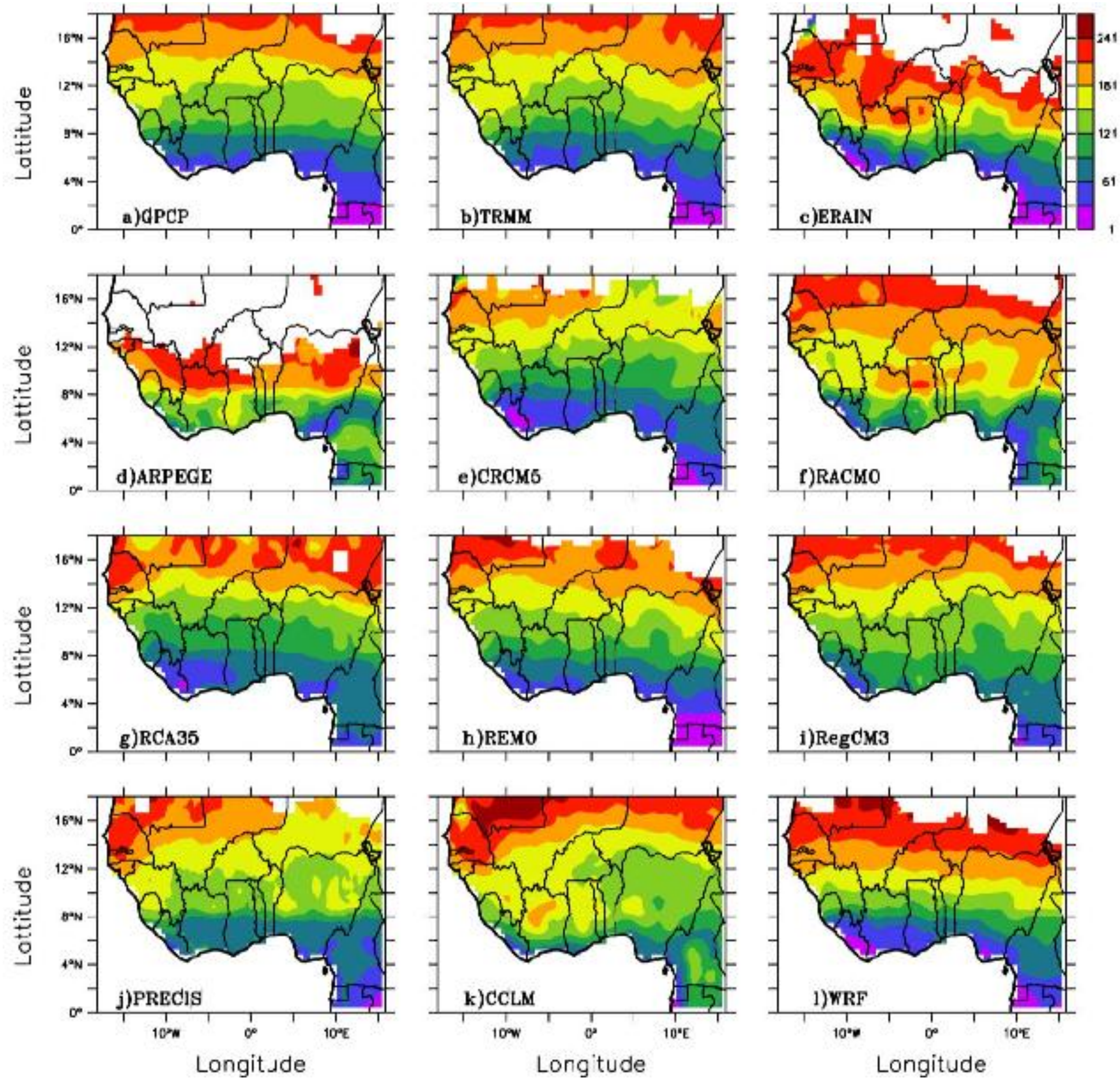

Figure 4.5 : Mean onset dates (in Julian days) as observed (GPCP/TRMM) and simulated (CORDEX-RCMs) for DEF4 for the period of 1998–2008

The reason for the shortcoming of ERAIN may be due to its low resolution dataset. Four RCMs (RCA35, REMO, RegCM3, WRF, and PRECIS) are remarkably better than ERAIN and show comparable ROD distributions with the observation. ARPEGE overestimates the ROD north of 8^oN and fails to meet the DEF4 criteria north of 10^oN. RACMO fails to reproduce the zonal pattern of ROD between 8^oN-12^oN, producing a local ROD maximum in northern part of Ghana. CCLM again fails to reproduce the observed zonal distribution south of 12^oN, instead it produces a local maximum over Republic of Guinea.

4.1.2.2 Spatial Distribution of ROD standard deviation over West Africa

4.1.2.2.1 Distribution for DEF1

Here, the simulated ROD standard deviations (σ) are compared with the observed (GPCP and TRMM) for DEF1 (Fig. 4.6). Sigma (σ) indicates the spread of RODs around the mean, hence it is a measure of the inter-annual variability of the ROD. High σ indicates high inter-annual, while low σ indicates low inter-annul variability. For DEF1, both observations show similar pattern of σ over Guinea and Savanna, except that TRMM shows generally higher deviations and also a local maximum in western part of Savanna (over Republic of Guinean). ERAIN does not capture the distribution of σ as in the observation (GPCP or TRMM) with DEF1 and generally overestimates the ROD standard deviation by 10-20 days over most part of West Africa.

AS for the RCMs, most of them except REMO and WRF do not capture well the distribution of σ, especially over northern part of Sahel, while CCLM produces high overestimate values of σ over most of the Guinea, making it worst with this definition DEF1. Some of the RCMs perform better than ERAIN with this definition (e.g. REMO, RCA35, RegCM3 and WRF). However, ERAIN performs better than CCLM especially over the coastal area between 6^oN-8^oN.

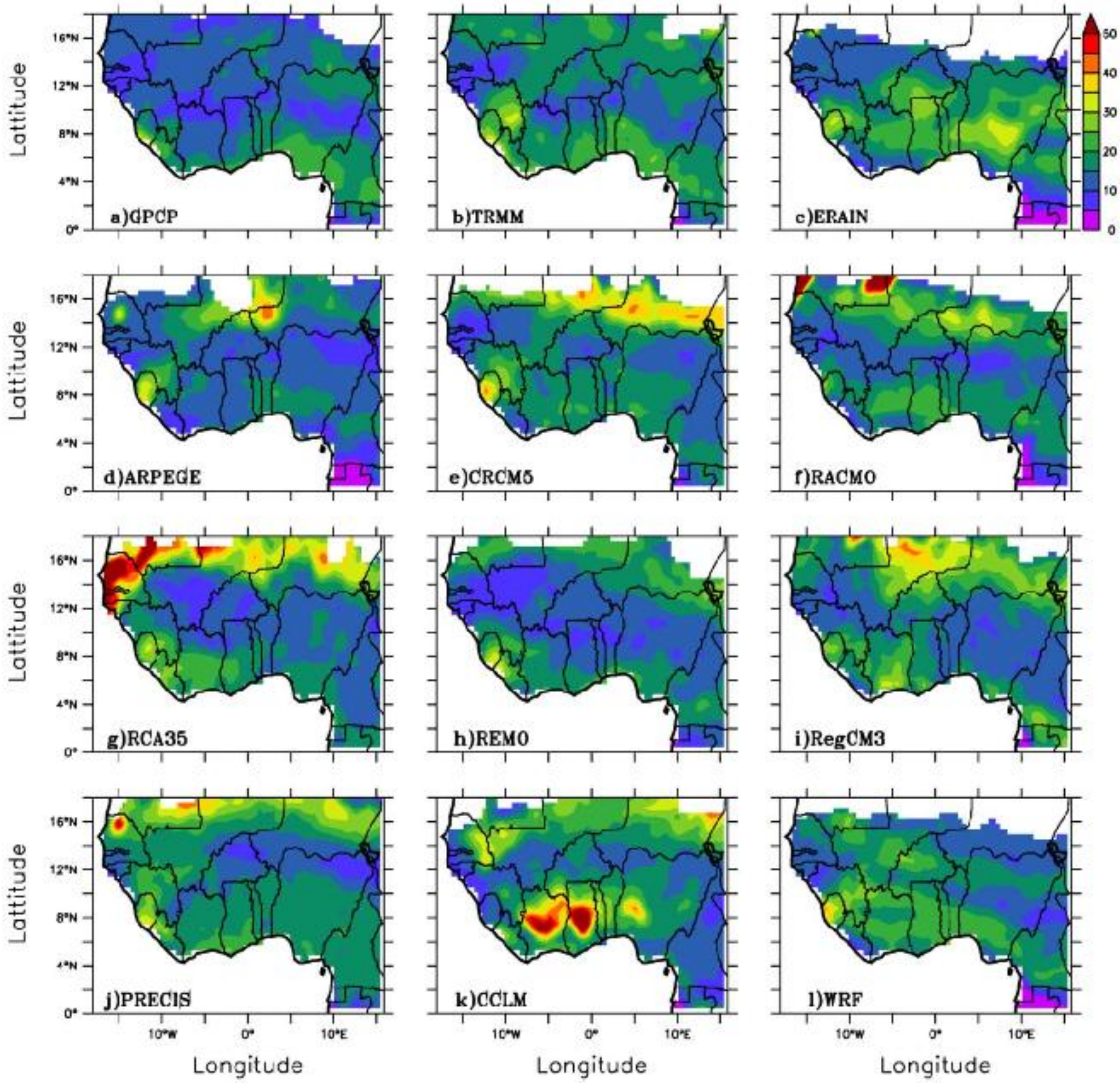

Figure 4.6 : Standard deviation of onset dates (in days) as observed (GPCP/TRMM) and simulated (CORDEX-RCMs) in DEF1 for the period of 1998 – 2008.

4.1.2.2.2 Distribution for DEF2 and DEF3

Comparison of the simulated ROD standard deviation (σ) with the observed (GPCP and TRMM) for DEF2 and DEF3 is given in Figures 4.7 and 4.8 respectively. The results for DEF2 and DEF3 are similar to those of DEF1. The GPCP and TRMM indicate similar patterns of σ with both definitions although

TRMM has generally higher σ and also overestimates over the Republic of Guinea. The overestimation of TRMM is higher in DEF3 than DEF2 and DEF1. As already noted in DEF1, ERAIN does not capture well the distribution of σ as in the observation (GPCP or TRMM) with DEF2 and DEF3.

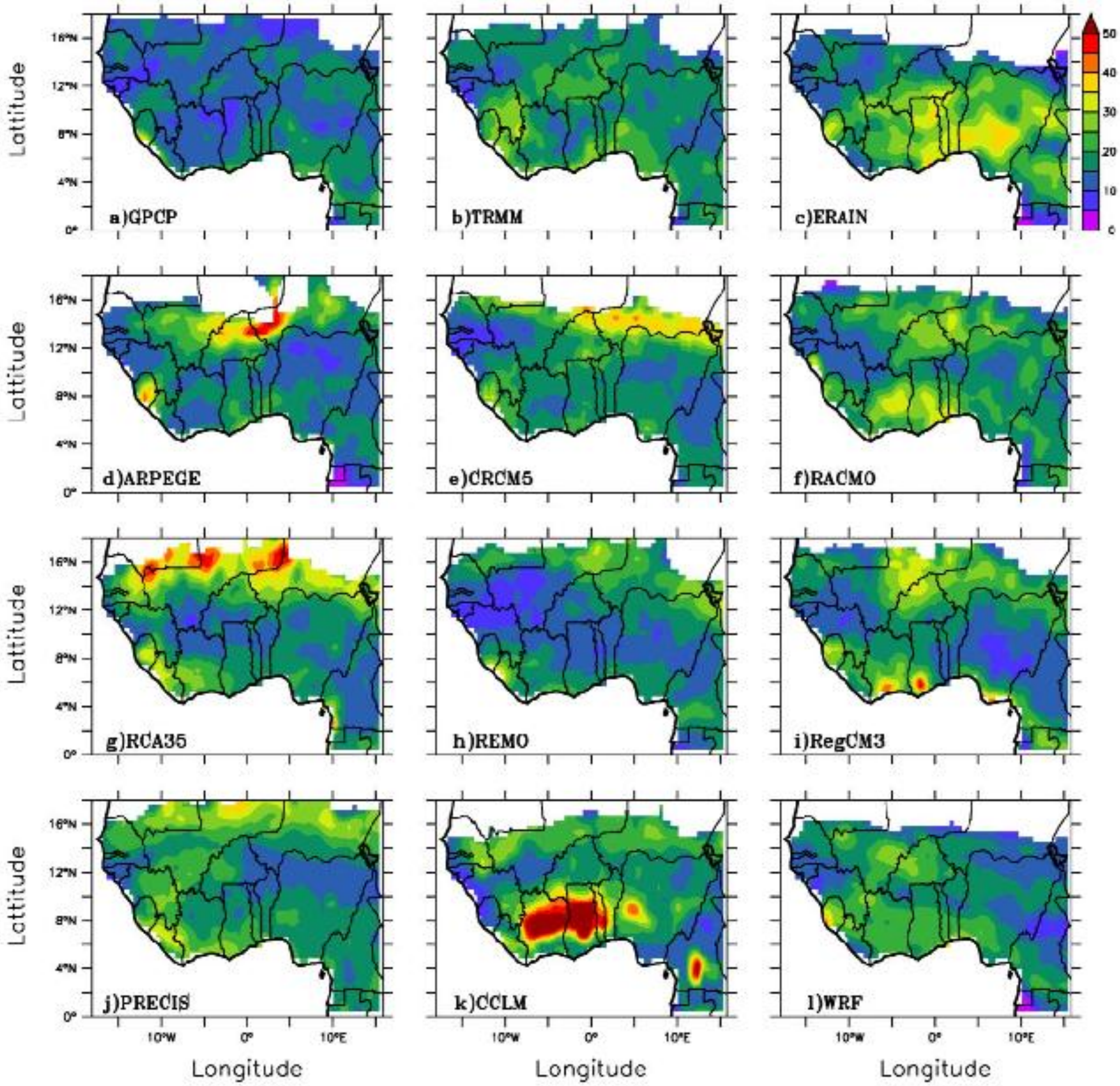

Figure 4.7 : Standard deviation of onset dates (in days) as observed (GPCP/TRMM) and simulated (CORDEX-RCMs) in DEF2 for the period of 1998 – 2008.

It overestimates the standard deviation of the ROD over central Savanna and most parts of Guinea coast, with values more than 20 days in DEF2 and DEF3. The results for the performances of the RCMs as compared to ERAIN are similar to that of DEF1 except that the magnitude is higher in DEF2 and DEF3 than in DEF1. ARPEGE and CCLM distributions are worse than that of ERAIN. Therefore the same RCMs as in DEF1 perform better than ERAIN in DEF2&3 and the same for RCMs that perform worse than ERAIN (Fig. 4.7 and 4.8).

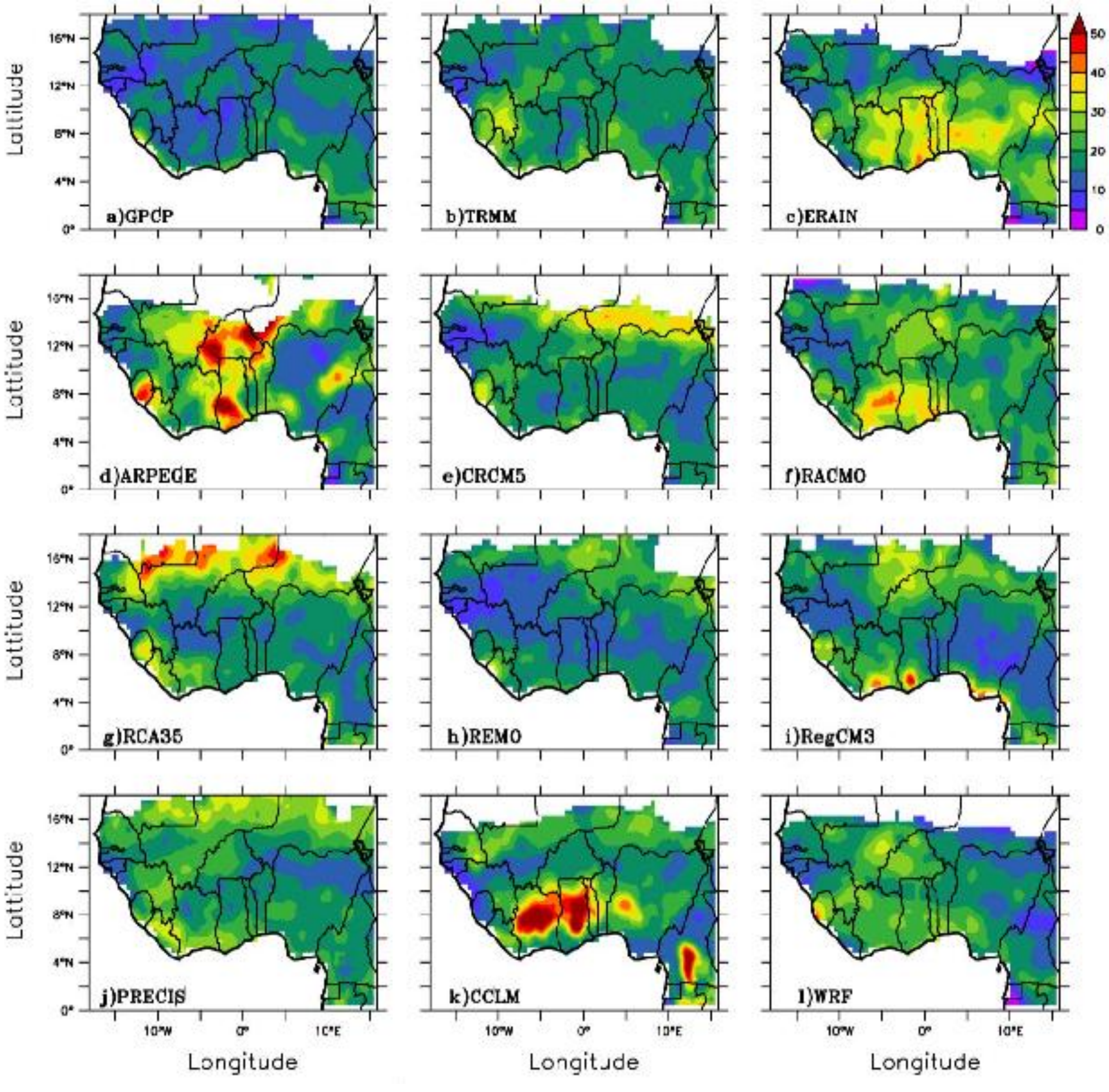

Figure 4.8 : Standard deviation of onset dates (in days) as observed (GPCP/TRMM) and simulated (CORDEX-RCMs) in DEF3 for the period of 1998 – 2008.

4.1.2.2.3 Distribution for DEF4

In Figure 4.9, we compare the simulated ROD standard deviation (σ) with the observed (GPCP and

TRMM) for DEF4. The results of DEF4 show that the magnitude of σ are consistently higher than that of the three others definitions. However, all the three zones (Guinea, Savanna and Sahel) indicate similar pattern of σ in DEF4 for both GPCP and TRMM except that TRMM produces a local maximum of σ over Republic of Guinean which is higher in DEF4 than with DEF1, DEF2 and DEF3.

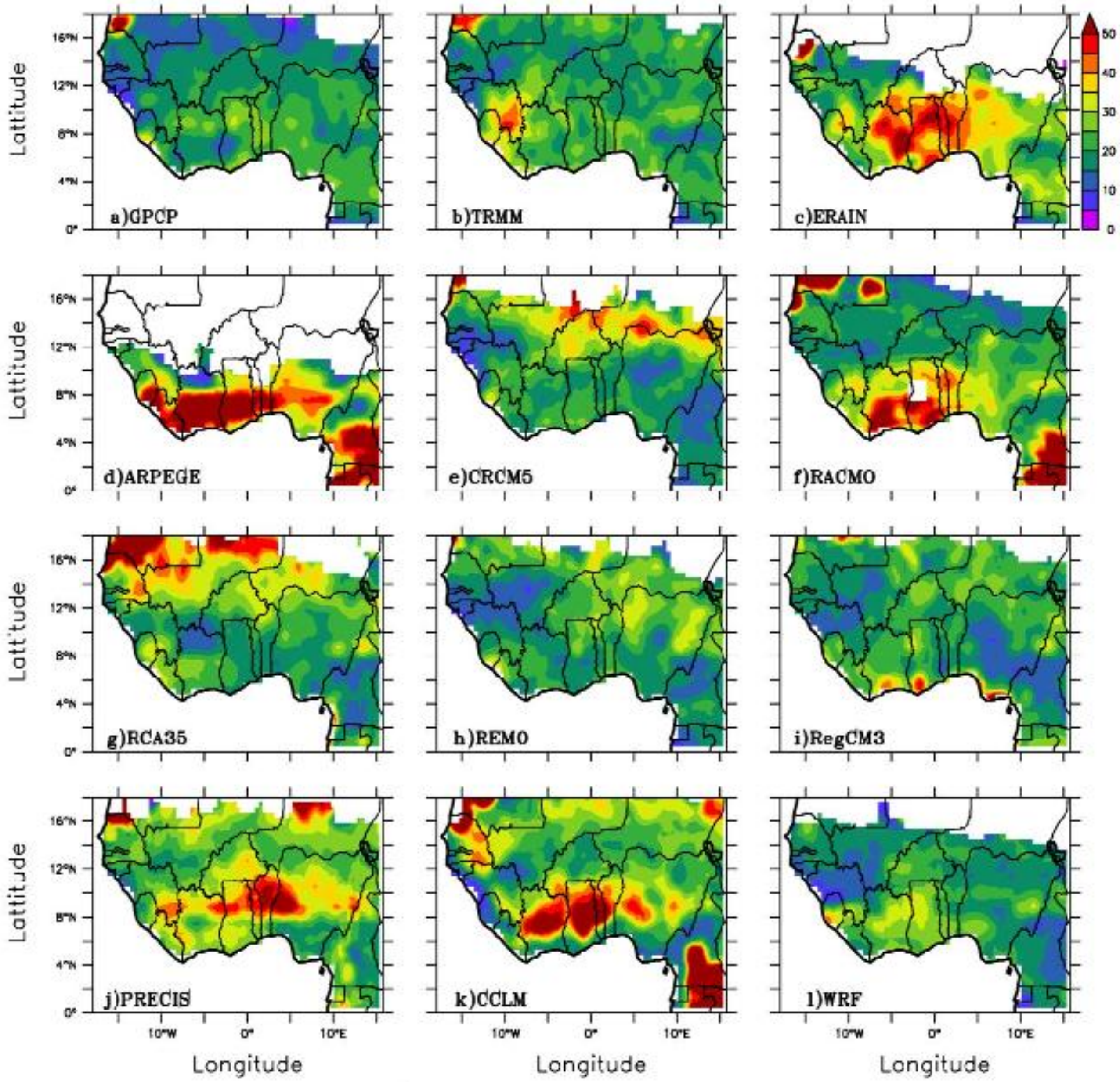

Figure 4.9 : Standard deviation of onset dates (in days) as observed (GPCP/TRMM) and simulated (CORDEX-RCMs) for DEF4 for the period of 1998 – 2008.

Also again, ERAIN does not capture the distribution of σ as in the observation (GPCP or TRMM) with

DEF4 and overestimates the ROD standard with a local maximum over central Savanna and some parts of the coastal area. In addition, ERAIN fails to reproduce σ north of 14^{o}N using any of the definitions because the reanalysis does not meet the criteria for obtaining ROD.

Among all the RCMs, only REMO, RegCM3 and WRF adequately capture the distribution of σ in this fourth definition. The others do not as they highly overestimate the deviations especially over Savanna and part of Guinea. Therefore, ERAIN outperforms the RCMs (ARPEGE, CCLM, PRECIS, RACMO and RCA35) in simulating the ROD standard deviation distribution for DEF4. This result is similar to that of the others definitions.

4.1.2.3 Spatial Distribution of ROD trend over West Africa

4.1.2.3.1 Distribution for DEF1

The spatial distribution of the simulated trend ROD in West Africa compared with observations (GPCP and TRMM) for the DEF1 is given in Figure 4.10. The trend of the ROD is defined as the possible tendency (pattern) of the RODs around the mean. Hence, it is a measure of the variability of the ROD: positive trend indicates late RODs occurrence, while negative trend indicates early RODs occurrence. The observations GPCP and TRMM simulate similar ROD trends over the coast (south 8^{o}N) and northern part of Sahel (north of 12^{o}N) for DEF1. However, TRMM fails to capture the observed ROD trend over Savanna. It shows early onset date with a local maximum across the Savanna between 8^{o} and 12^{o}N (that is earliest onset dates). In the case of ERAIN, the pattern of the ROD trend for DEF1 shows early onset almost everywhere with a local maximum over southern Mali/Burkina Faso and north Nigeria. ERAIN also fails to simulate the pattern ROD trend north of 14^{o}N.

Most of the RCMs simulate negatively the ROD trend (late onset dates) compared to the GPCP and TRMM. Others RCMs (ARPEGE, CRCM5, REMO, RACMO RegCM3, and WRF) remarkably outperform ERAIN in most area generally except that some of them largely underestimate the spatial distribution of the ROD trend that it is indicating later onset dates. Moreover, the RCMs (PRECIS, RCA35 and CCLM) perform almost as ERAIN over central Savanna and eastern part of Sahel respectively.

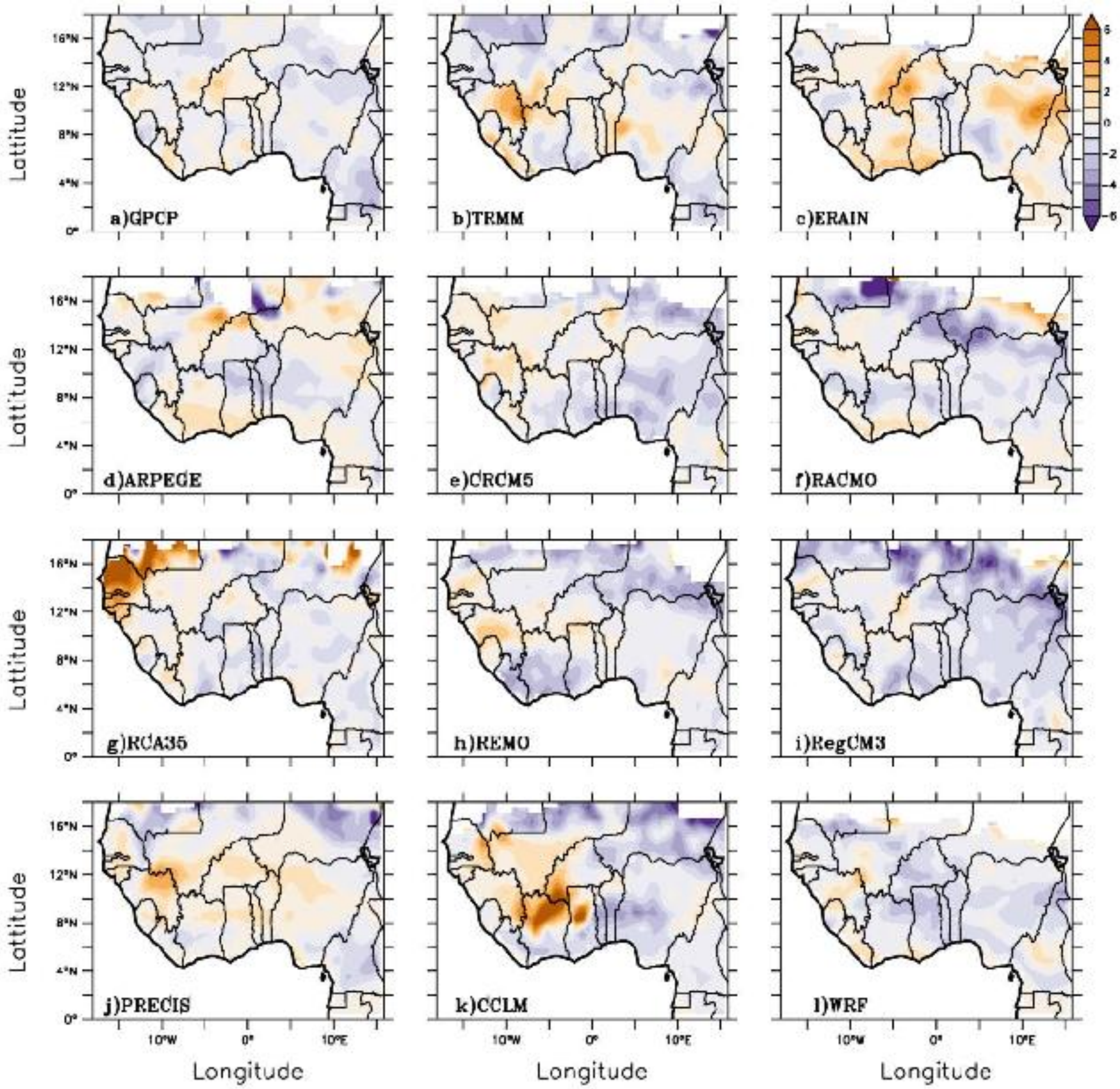

Figure 4.10: Trend of onset dates as observed (GPCP/TRMM) and simulated (CORDEX-RCMs) for DEF1 for the period of 1998–2008.

4.1.2.3.2 Distribution for DEF2 and DEF3

Figures 4.11 and 4.12 compare the spatial distribution of the simulated ROD trend in West Africa with observations (GPCP and TRMM) for DEF2 and DEF3 respectively. Both observations (GPCP and TRMM) show similar result except that TRMM indicates a local maximum (earlier onset dates) west of 10^{o}N over central Savanna.

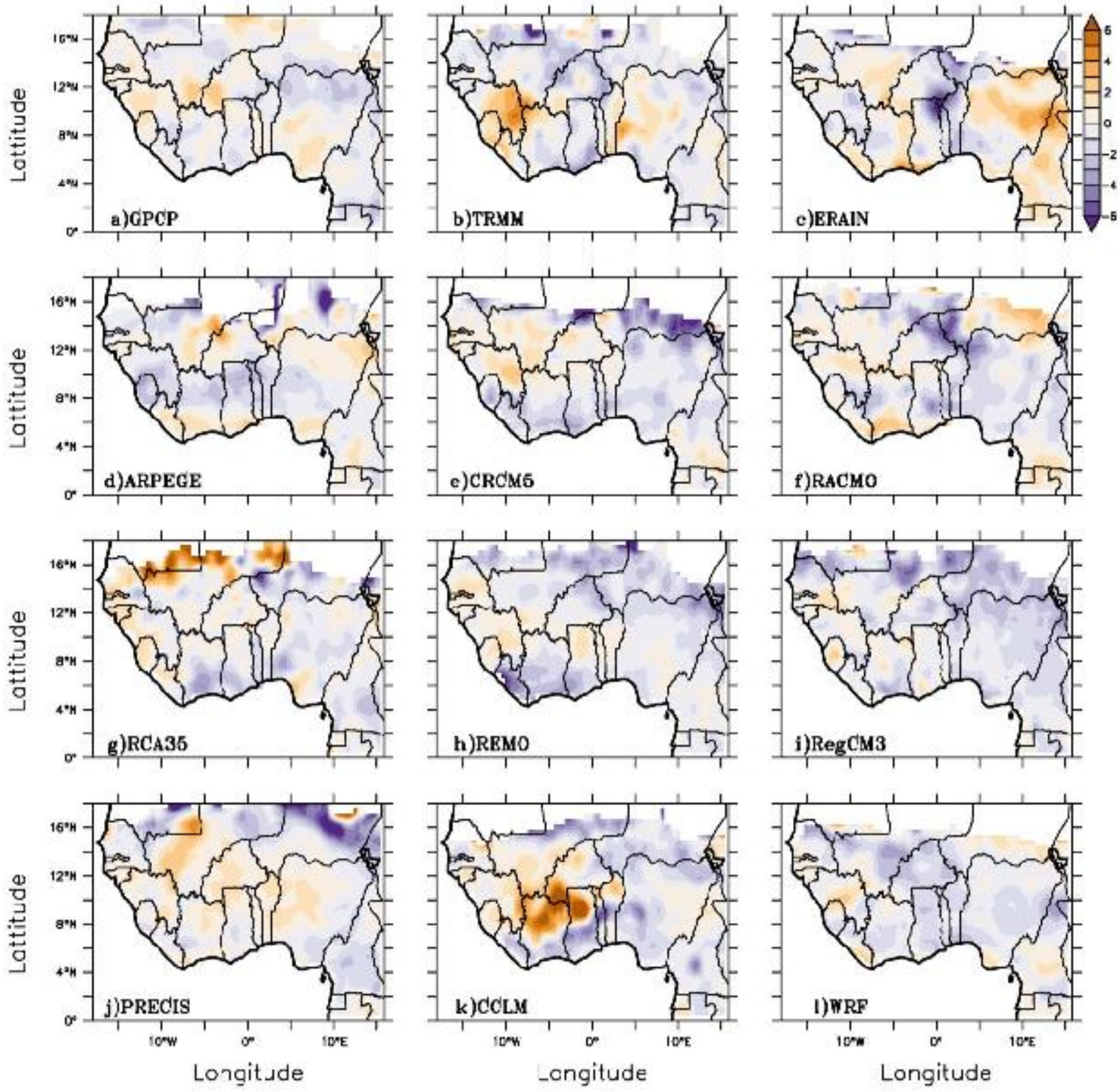

Figure 4.11 : Trend of onset dates as observed (GPCP/TRMM) and simulated (CORDEX-RCMs) for DEF2 for the period of 1998–2008.

The results for DEF2 and DEF3 are very similar to that of DEF1 except those for ERAIN which present a local maximum (earlier onset) over eastern part of Savanna (particularly central Nigeria) and a local minimum (late onset) over central Savanna (i.e. south-east Burkina Faso, north-east Ghana and Benin).

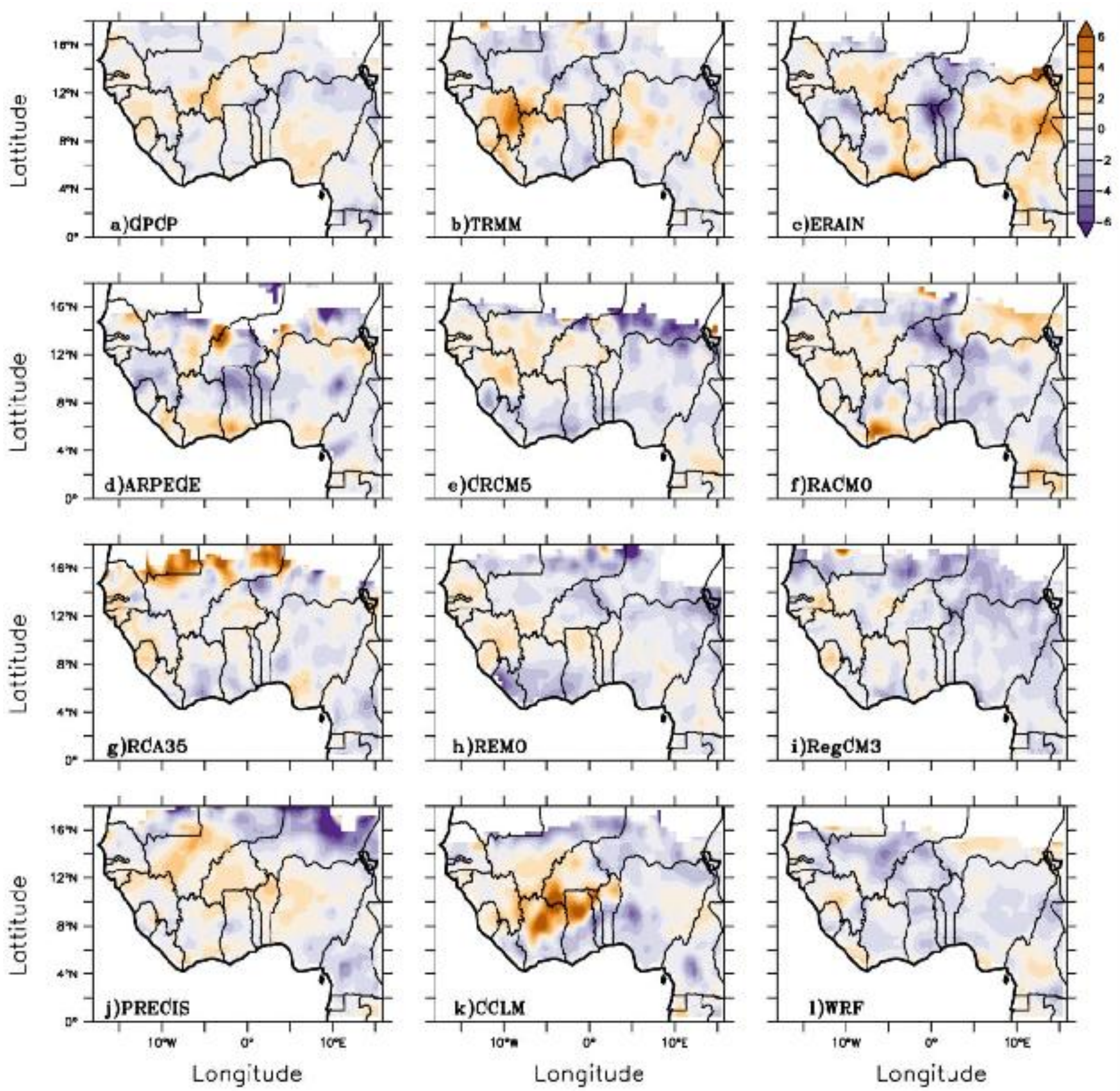

Figure 4.12 : Trend of onset dates as observed (GPCP/TRMM) and simulated (CORDEX-RCMs) for DEF3 for the period of 1998–2008.

As observed for DEF1, most of the RCMs again outperform ERAIN in all the areas for DEF2 and DEF3 also except for CCLM which produces a local maximum ROD trend (earlier onset) over central Savanna.

However, CCLM performs better than ERAIN in the areas outside central Savanna. Despite the earlier onset given by some RCMs (PRECIS, RCA35) and underestimations (later onset dates by) others (RACMO, RegCM3), most of the RCMs capture the spatial distribution of the ROD trend over West Africa well when DEF2 and DEF3 are used.

4.1.2.3.4 Distribution for DEF4

For DEF4, Figure 4.13 compares the spatial distribution of the simulated ROD trend with observations (GPCP and TRMM). The comparison of observations show that TRMM fails to capture the ROD trend as observed in GPCP over Guinea and Savanna areas. It produces a local maximum over western part of Savanna, from south-western Guinea Republic across to central Nigeria. But it simulates well the ROD trend over Sahel (north of 12^{o}N). Just as for DEF1, DEF2 and DEF3, ERAIN again does not capture the ROD trend for DEF4. It produces a local maximum (earlier onset) and minimum (late onset) values of ROD trend respectively over the Guinea zone (i.e. south of Cote d'Ivoire and Ghana; and east of Nigeria) and over central Savanna (Burkina Faso Ghana, Togo and Benin). ERAIN fails again to simulate the ROD trend distribution criteria north of 12^{o}N in DEF4. Out of the RCMs only CRCM5, REMO, RegCM3 and WRF gave reasonable ROD trend and perform better than ERAIN although they also produce later/earlier RODs than GPCP.

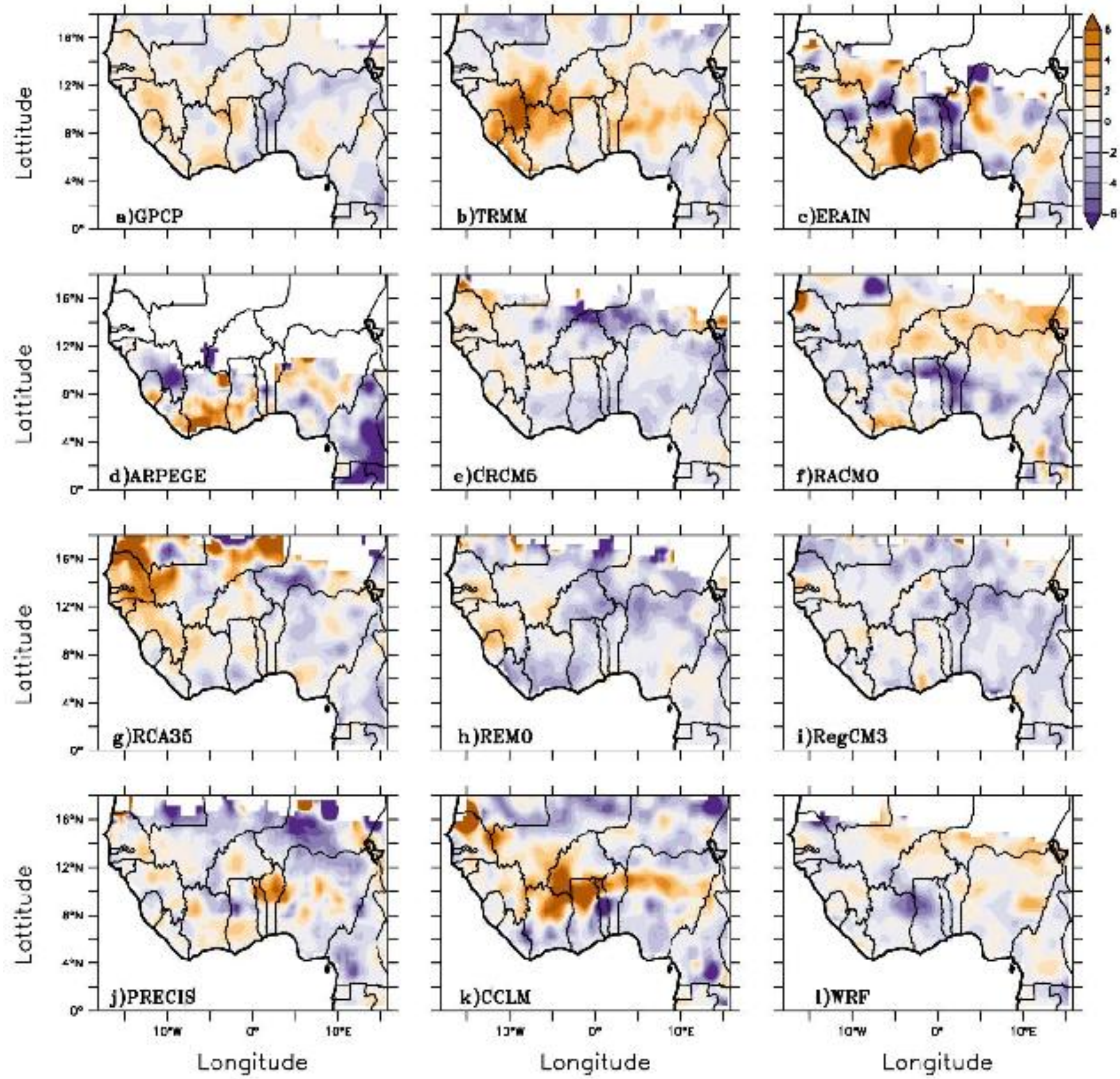

Figure 4.13 : Trend of onset dates as observed (GPCP/TRMM) and simulated (CORDEX-RCMs) for DEF4 for the period of 1998–2008.

4.1.2.4 Spatial Distribution of ROD correlation over West Africa

4.1.2.4.1 Distribution for DEF1

We evaluate the spatial distribution of the correlation between observation (GPCP) and RCMs. The spatial correlation (r) between TRMM and GPCP over West Africa is higher and uniform over most of the region. TRMM indicates the highest correlation value for DEF1 (Fig. 4.14a), with maximum values (r≈0.9) over northern Sahel and close to the coast.

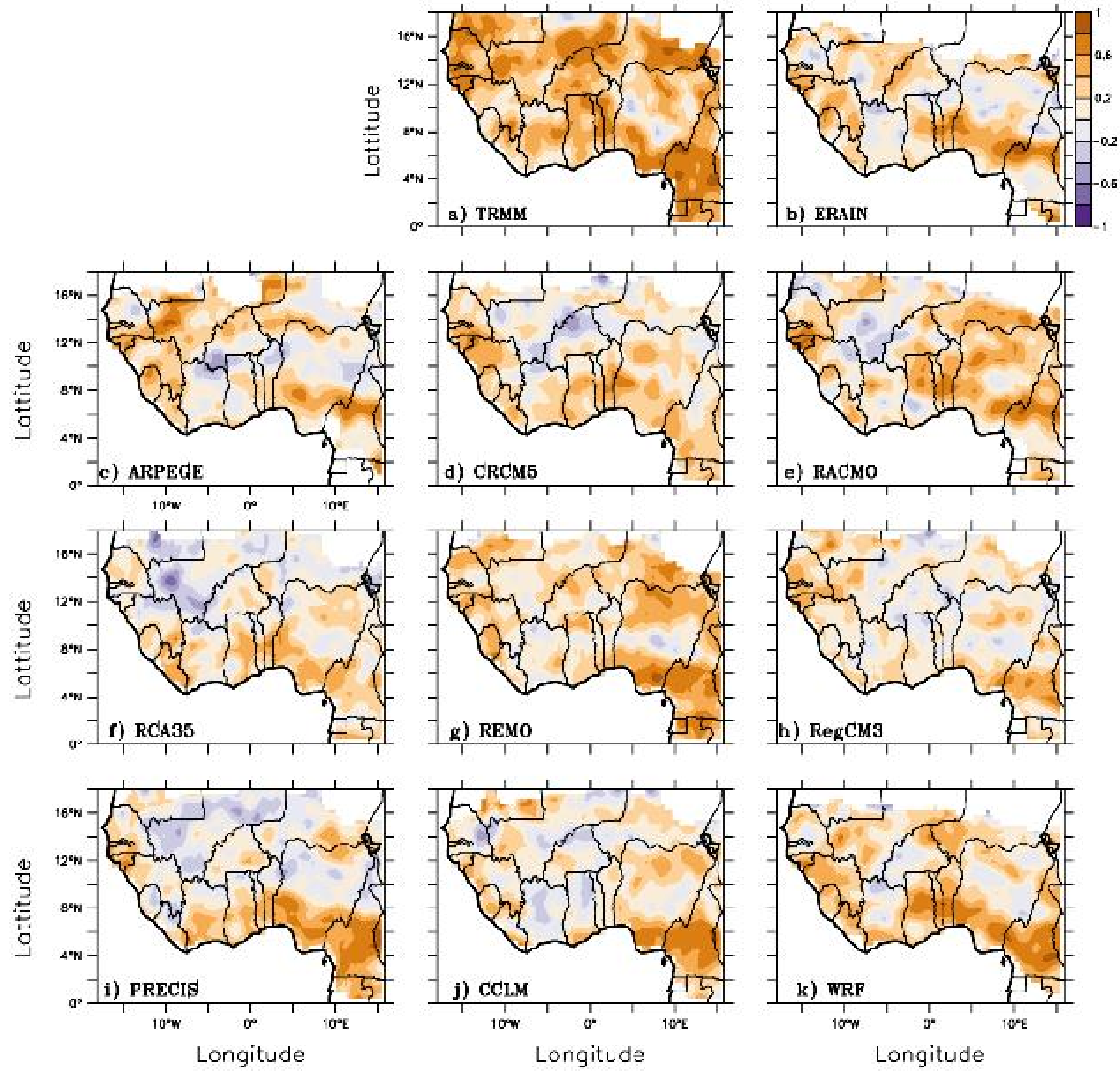

Figure 4.14 : Correlation of onset dates with respect to observed (GPCP) and simulated (CORDEX-RCMs) for DEF1 for the period of 1998–2008.

Maximum positive correlation between TRMM and ERAIN are observed in many areas particularly over central parts of Ghana, Togo, Benin and Nigeria but the correlation is low elsewhere especially Cote d'Ivoire, central Ghana and northern Nigeria (Fig. 4.14a, b). As for the RCMs most of them simulate positive r along the coast of Guinea, western Sahel and some over northern Sahel. However, RegCM3 generally has the lowest correlation with GPCP, while RCA35 and PRECIS have low to negative correlation over areas north of about 11°N.

4.1.2.4.2 Distribution for DEF2 and DEF3

In Figures 4.15 and 4.16, we compute the spatial correlations between GPCP and the RCMs for DEF2 and DEF3.

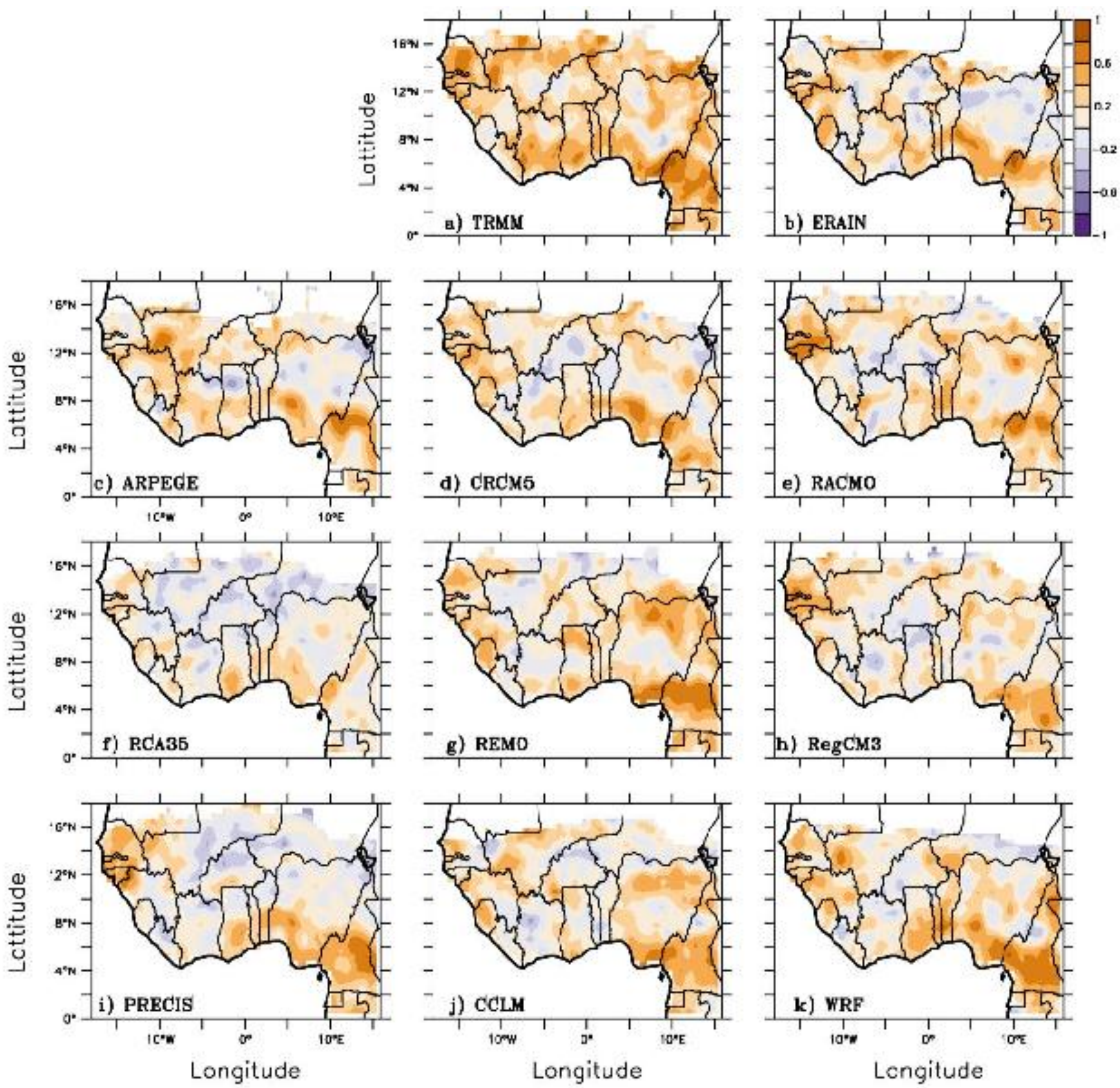

Figure 4.15 : Correlation of onset dates with respect to observed (GPCP) and simulated (CORDEX-RCMs) for DEF2 for the period of 1998–2008.

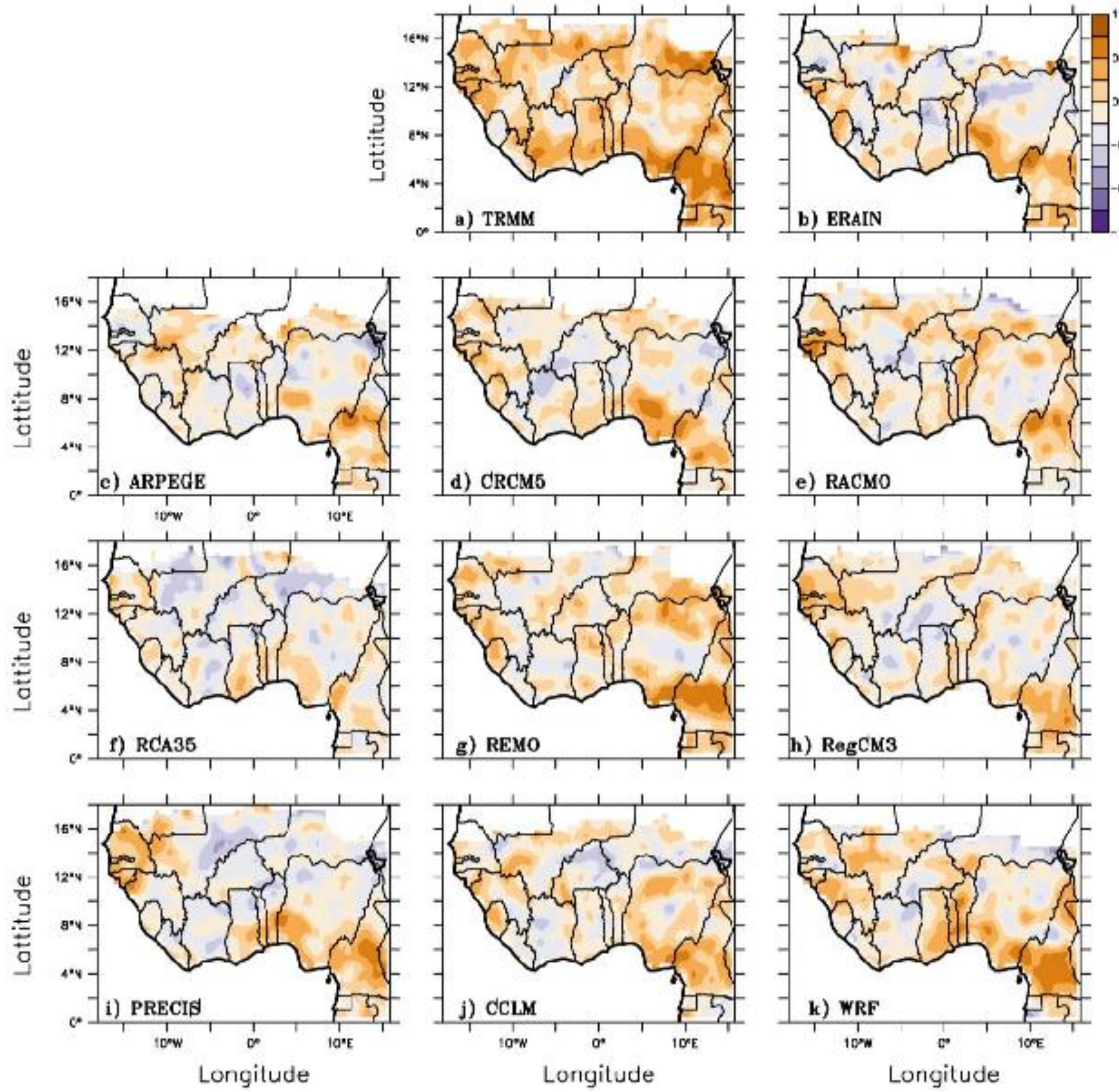

Figure 4.16 : Correlation of onset dates with respect to observed (GPCP) and simulated (CORDEX-RCMs) for DEF3 for the period of 1998–2008.

For both definitions, the spatial correlation (r) between TRMM and GPCP shows the highest value, as for DEF1. The inter-comparison between TRMM and ERAIN spatial distribution of the correlation indicates similar results for DEF2 and DEF3, and also for DEF1 but the values are lower for DEF2 and DEF3. However, the magnitude of the correlation r is higher in DEF2 than in DEF3. For both DEF2 and DEF3, the RCMs patterns of the correlation are similar although with slightly higher values for DEF2.

Despite their generally poor agreement with TRMM, the RCMs performance is not much different from that of ERAIN for DEF2 and DEF3.

4.1.2.4.3 Distribution for DEF4

Figure 4.17 gives the spatial distribution of the ROD correlation between observation (GPCP) and the RCMs.

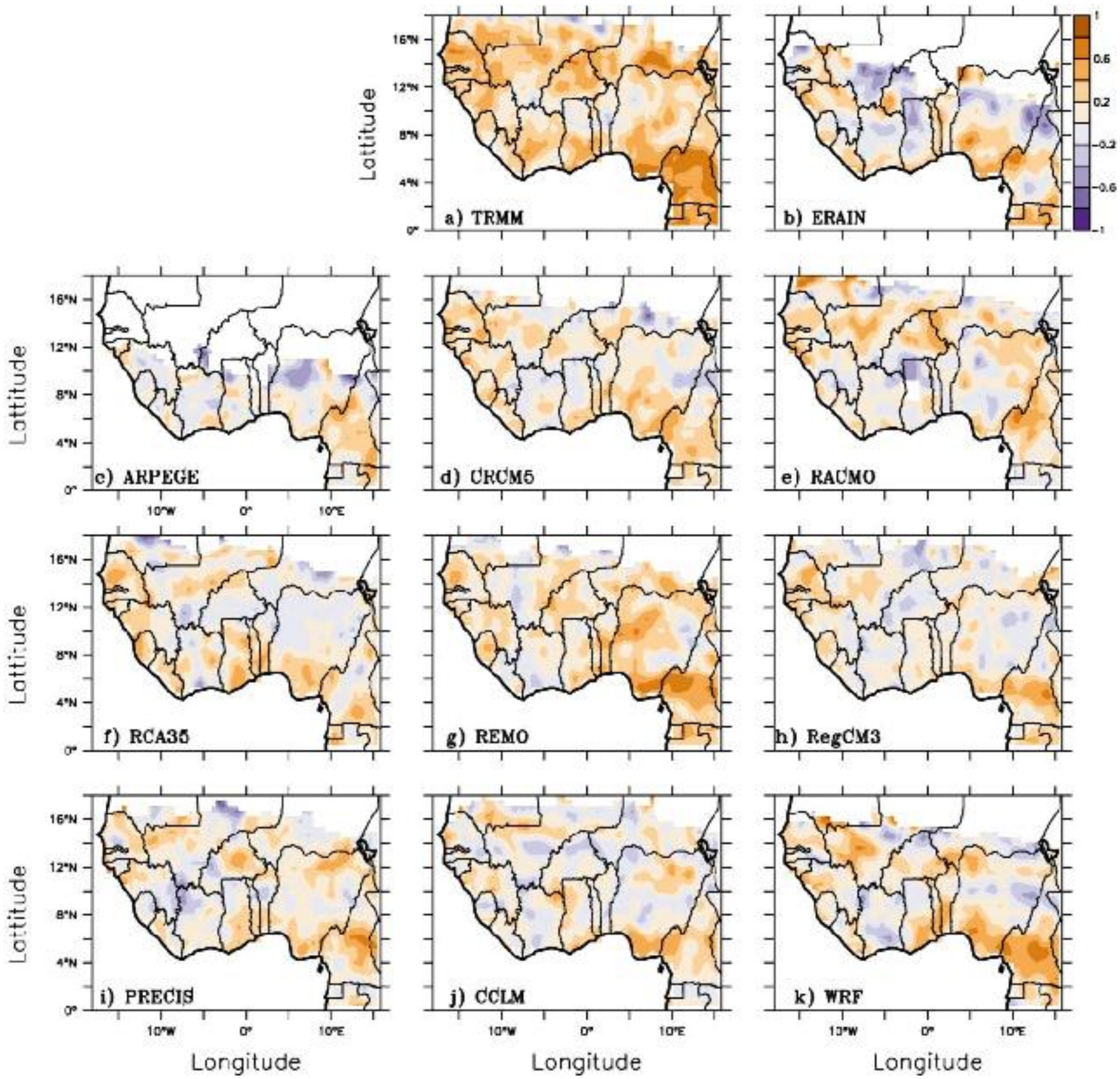

Figure 4.17 : Correlation of onset dates with respect to observed (GPCP) and simulated (CORDEX-RCMs) for DEF4 for the period of 1998–2008.

The correlation of TRMM as compared to GPCP shows good agreement over most areas of West Africa with lower values over the Savanna. Comparison of ERAIN distribution pattern of the correlation with TRMM in this DEF4 is similar to that of the three other definitions but the values for DEF4 are more negative over the Savanna and Sahel and less positive elsewhere when compared to those for DEF1, DEF2 and DEF3.

For the RCMs, the distribution of r is higher in DEF1, DEF2 and DEF3 than DEF4. Regardless the definitions used, most of the RCMs simulate positive r (Figs 4.14 to 4.17). Therefore most the RCMs outperform ERAIN in simulating the distribution of r as observed in TRMM except ARPEGE that fails to satisfy the DEF4 criteria north 10^{o}N and performs worse than ERAIN.

From the section 4.1.2.4, we can summarize that most RCMs show high (positive) correlations with observation over Guinea and Sahel, but weak (positive and negative) correlations with observation over Savanna. These results are in agreement with those of Nikulin *et al.* 2012 who found that most of the models present skillful simulation of the bimodal form of rainfall over Guinea as well as the northward monsoon jump from Guinea to the Sahel. However, the RCMs correlation outperform ERAIN regardless the definitions used except along the coast at 5^{o}N over southern Nigeria where it produces higher correlation.

From the above discussion it is clear that the performance of the RCMs in simulating the characteristic of ROD varies across West Africa. Regardless of definition used, some RCMs (i.e. CRCM5, RCA35, REMO, RegCM3 and WRF) perform better than ERAIN in simulating the ROD, while some perform worse. The performance of others depend on the definition used, and in general, using DEF1 (DEF2 or DEF3) enhances the performance of the models better than using DEF4.

4.1.2.5 Spatial Distribution of Multi-RCMs ROD Ensemble over West Africa

Figure 4.18 shows the spatial distribution of the RCMs ensemble average for the ROD mean, standard deviation and correlation for each definition. The results of the RCMs ensemble average for the RODs mean are similar to those of observations (GPCP and TRMM). The ROD characteristics of the RCMs ensemble average vary from February to April for DEF2, DEF3 and DEF4 over Guinea, while it varies from February to March in DEF1. Over the Savanna, the multi-RCMs ensemble mean for DEF1 gives the earliest ROD but the latest RODs for DEF4 (from April to May). Similarly, the results for the standard deviation and correlation show better distribution of the RCMs ensemble average variability of standard deviation and correlation as observed in GPCP and TRMM in most areas for all the definitions.

From the foregoing, the multi-RCMs ensemble average improves the simulated ROD mean, standard deviation and correlation in most parts of West Africa. For instance, the multi-RCMs for the ROD mean show agreement results over Guinea, Savanna and southern part of the Sahel in all the definitions. However, the results are different over northern part of Sahel in all the definitions. As a result, in DEF4, the RCMs mean fails to simulate ROD over central and eastern part of Sahel (over northern Mali, Burkina Faso and Niger). On the other hand, the multi-RCMs standard deviation mean outperforms individual RCMs regardless of the definition used in all the regions. The multi-RCMs correlation mean (r) shows positive and negative correlation depending on the definition used. For instance, DEF1, DEF2 and DEF3 indicate negative r over central Savanna (i.e. Burkina Faso, northern Cote d'Ivoire and north Nigeria) and for DEF4, over Cote d'Ivoire, east Nigeria and northern Sahel. All the definitions show positive r over Guinea, east of 5^{o}W and, western part of Savanna and Sahel. The improvement of the multi-RCMs mean over individual RCM results found in this study is consistent with previous studies (e.g. Paeth *et al.*, 2011, Diallo *et al.* 2012, Sylla *et al.*, 2013, Mounkaila et al, 2014) that attribute the improvement to the cancelling of individual RCM errors in the multi-RCMs mean.

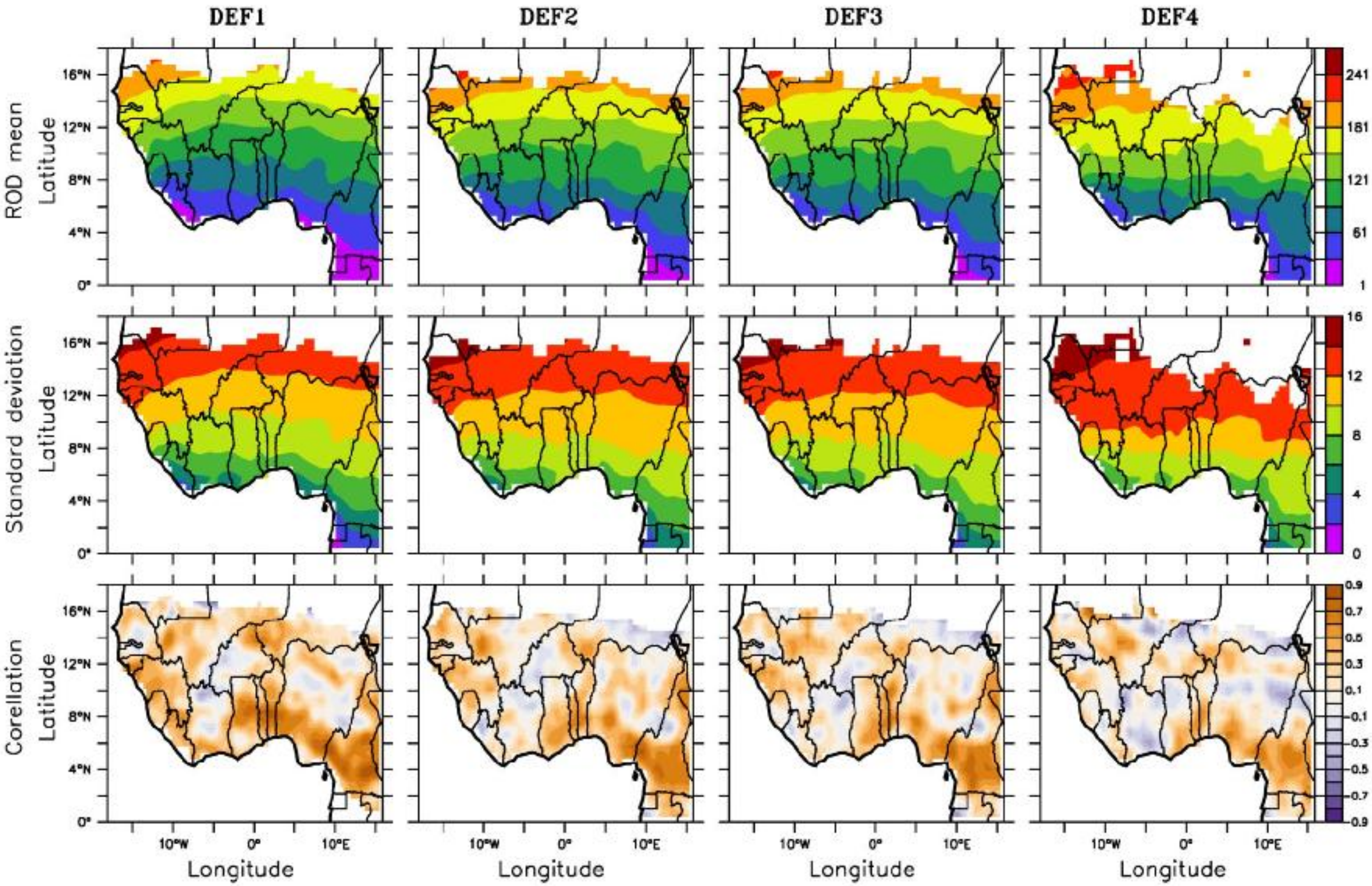

Figure 4.18 : CORDEX- Multi-RCMs ensemble average for the ROD mean, standard deviation and correlation over West Africa for the period of 1998–2008.

4.1.3 Spatial Distribution of RCD over West Africa

4.1.3.1 Distribution of mean RCD

The spatial distribution of the mean rainfall cessation dates (RCD) as observed (GPCP and TRMM) and simulated (CORDEX-RCMs) are shown in Figure 4.19.

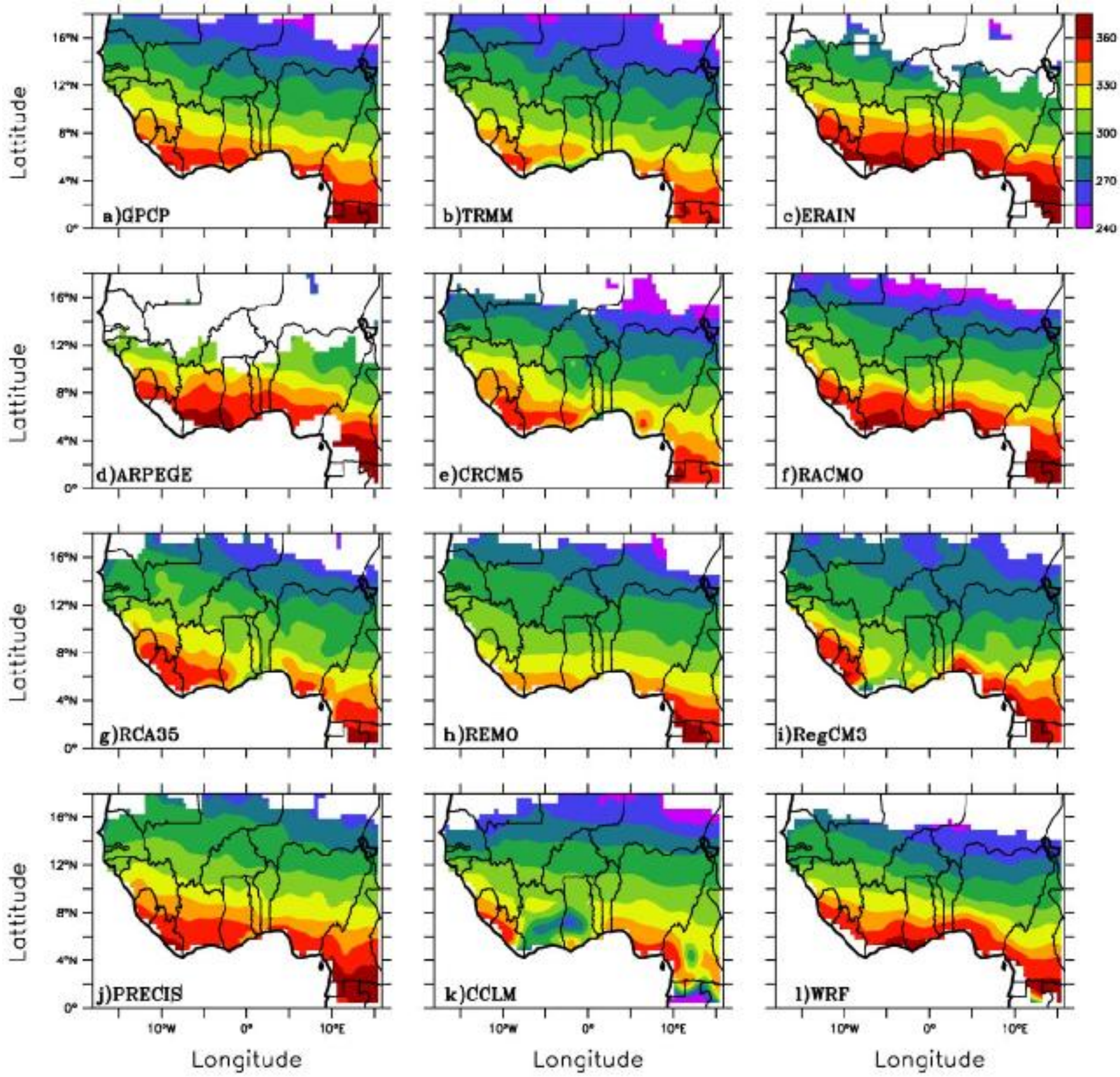

Figure 4.19 : Mean rainfall cessation dates (RCDs) as observed (GPCP/TRMM) and simulated (CORDEX-RCMs) for the period of 1998-2008.

The observations (GPCP and TRMM) show that the RCDs occur in September-October over Sahel, October-November over Savanna and November-December over Guinea. This corresponds to the southward movement of the ITD and the monsoon systems (i.e. Le Barbe *et al.* 2002, Abiodun *et al.* 2011). Both observations simulate RCD over West Africa, except over southern part of Cote d'Ivoire and Ghana where TRMM underestimates the RCDs. ERAIN simulates well the RCDs over Savanna but overestimates it over Guinea zones and fails to produce the RCD over Sahel north of 14^{o}N.

All the RCMs except ARPEGE simulate the RCDs well as observed and perform better than ERAIN, although WRF and RACMO fail to simulate the RCD over coastal area of Sierra Leone. ARPEGE fails to simulate the RCD over Savanna and parts of Guinea and does not satisfy the criteria of the RCD definition north 10^{o}N. CCLM and RegCM3 largely underestimate the RCDs over some part of Guinea. In general these RCMs adequately simulate the RCDs as well as ERAIN but ARPEGE and CCLM are not as good over Savanna and Sahel.

4.1.3.2 Distribution of RCD standard deviation

Figure 4.20 shows the spatial distribution of the simulated RCD standard deviation as observed (GPCP and TRMM) and for CORDEX-RCMs over West Africa. Both observations generally show similar results except over south-east of Guinea coast (i.e. Cote d'Ivoire and Ghana) where TRMM show an overestimation of the RCD standard deviation. ERAIN underestimates RCD standard deviation almost everywhere, and also fails to simulate the RCD standard deviation north of 12^{o}N.

Most of the RCMs except ARPEGE perform better than ERAIN in simulating the RCD standard deviation over West Africa. However, CCLM gives high overestimates of the deviation over Cote d'Ivoire and Ghana, while RegCM3 and PRECIS produce underestimates over northern Cote d'Ivoire and, for PRECIS over central Benin and Nigeria. Among the RCMs, ARPEGE performs worse than ERAIN in simulating the RCD standard deviation, especially over Guinea and north of 12^{o}N where it also fails to satisfy the criteria of RCD definition.

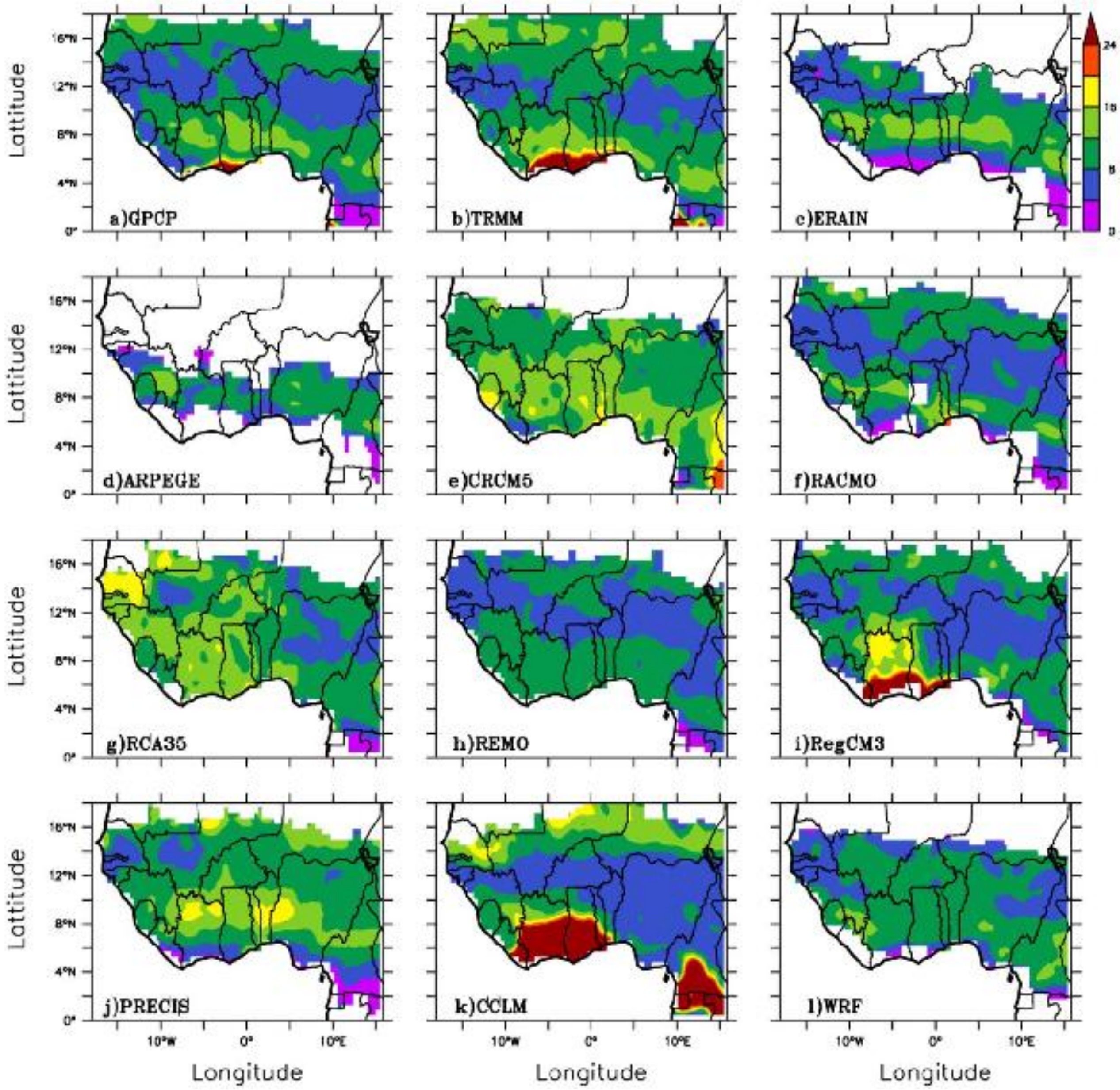

Figure 4.20 : Standard deviation of cessation dates as observed (GPCP/TRMM) and simulated (CORDEX-RCMs) for the period of 1998-2008.

4.1.3.3 Distribution of RCD correlation

The evaluation of the spatial distribution of the RCD correlation (r) between observation (GPCP) and RCMs is shown on Figure 4.21. The correlation r of TRMM with respect to GPCP shows positive and highest values of r over entire West Africa with local maxima over most parts of Sahel and central

Savanna. ERAIN produces similar results as TRMM over western part of Savanna and Guinea but fails over the eastern part of northern Savanna (north Nigeria) and south-east Guinea (i.e. south Nigeria). ERAIN fails again to evaluate the r north of 14^{o}N.

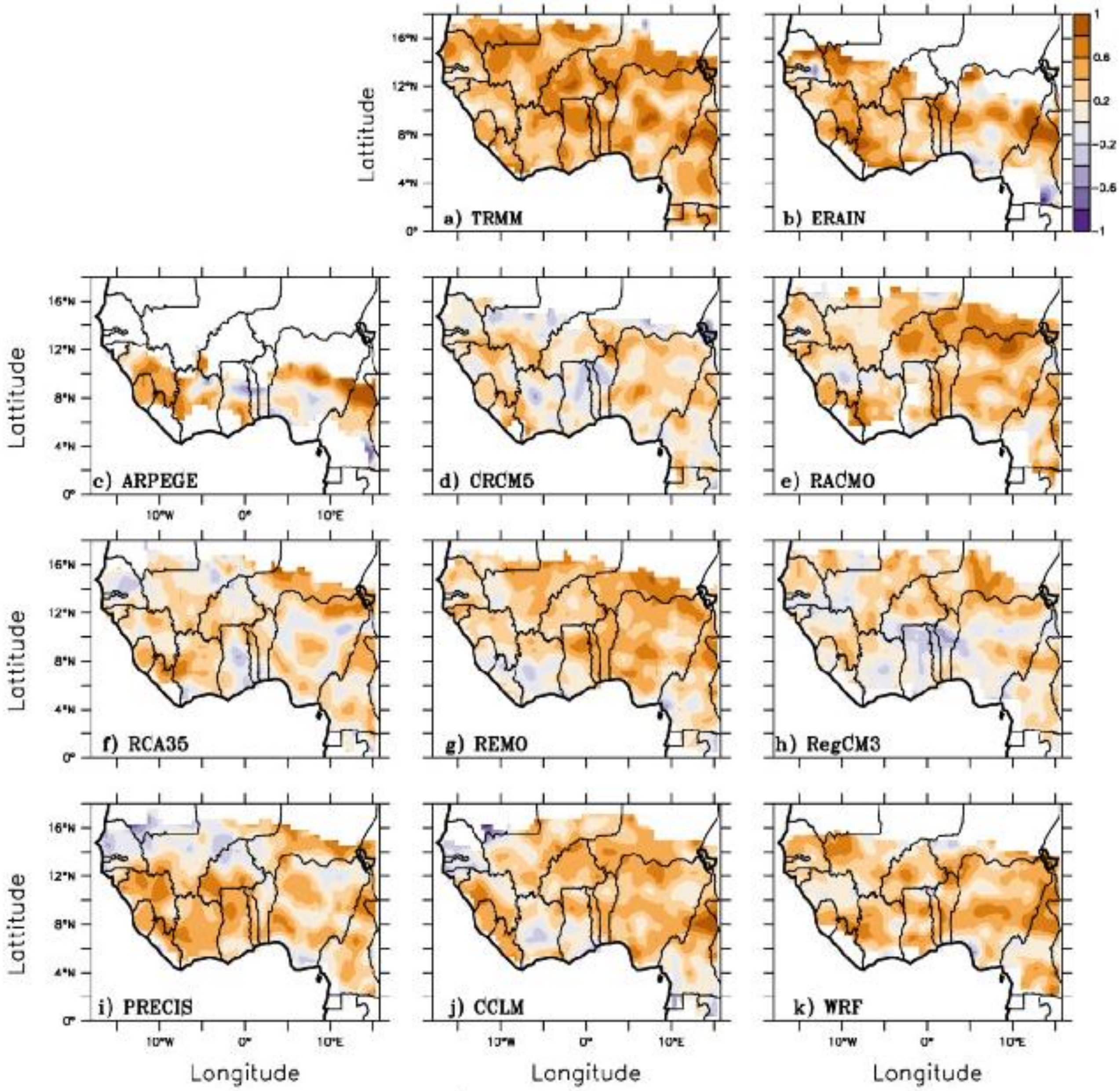

Figure 4.21: Correlation of cessation dates as observed (GPCP/TRMM) and simulated (CORDEX-RCMs) for the period of 1998 – 2008.

In the case of the RCMs, ARPEGE has been the case so far that does not capture the correlation distribution pattern as observed in TRMM north 10^{o}N. In fact it produces the worst performance.

However, some of the RCMs perform better than ERAIN, while others (CRCM5, RCA35, and CCLM) produce negative values of r over Guinea and over northern Ghana, Togo and Benin.

4.1.4 The ROD/RCD and West African Monsoon System (WAMS)

The monsoon is associated with atmospheric features like the Saharan Heat Low (SHL), the dry north-easterly Harmattan flow, the Inter-tropical Discontinuity (ITD), the African Easterly Waves (AEW), the AEJ, TEJ (e.g. Omotosho and Abiodun 2007, Abiodun *et al.* 2011, 2012). Hence, there is strong link between the ROD and the northward progression of the WAMS. Since the complex interactions of the features dictate the onset, intensity and location of the monsoon, it is of interest to see how the RCMs link the ROD with these features. Unfortunately, the first evaluation of CORDEX output available for the present study did not archive data needed to analyse all these features. Therefore with the available datasets, we discuss the relationship between the RODs and the temperature maximum, moist south-westerly monsoon flow, ITD and the associated rainfall. The observations (GPCP and TRMM; Fig 4.22a & b) show that WAMS can be categorized into three different phases: the onset, the peak and the cessation of rainfall, as in previous studies (e.g. Le Barbe *et al.*, 2002; Abiodun *et al.*, 2011, 2012; Sylla *et al.*, 2013). The onset of rainfall corresponds to the northward progression of the rain belt from the coast (about 6^{o}N) to 16^{o}N and it is also associated with the position of ITD (Sultan and Janicot 2003, Omotosho and Abiodun 2007). As can be seen in Fig. 4.22a&b both observations (GPCP and TRMM) agree that the monsoon rainfall starts over the Guinea coast (5^{o}N) in February-March and progresses inland (northward) to reach its northernmost position over the Sahel (about 18^{o}N) in August. The cessation corresponds to the southward retreat of the ITD to the coast and occurs from September to December in observations and RCMs (as well as in ERAIN). This is in agreement with the results of Abiodun *et al.* (2011). In ERAIN (Fig. 4.22c), the onset of rainfall starts earlier (in January) than observed and the northward progression is slower, reaching the northward position of only 14^{o}N.

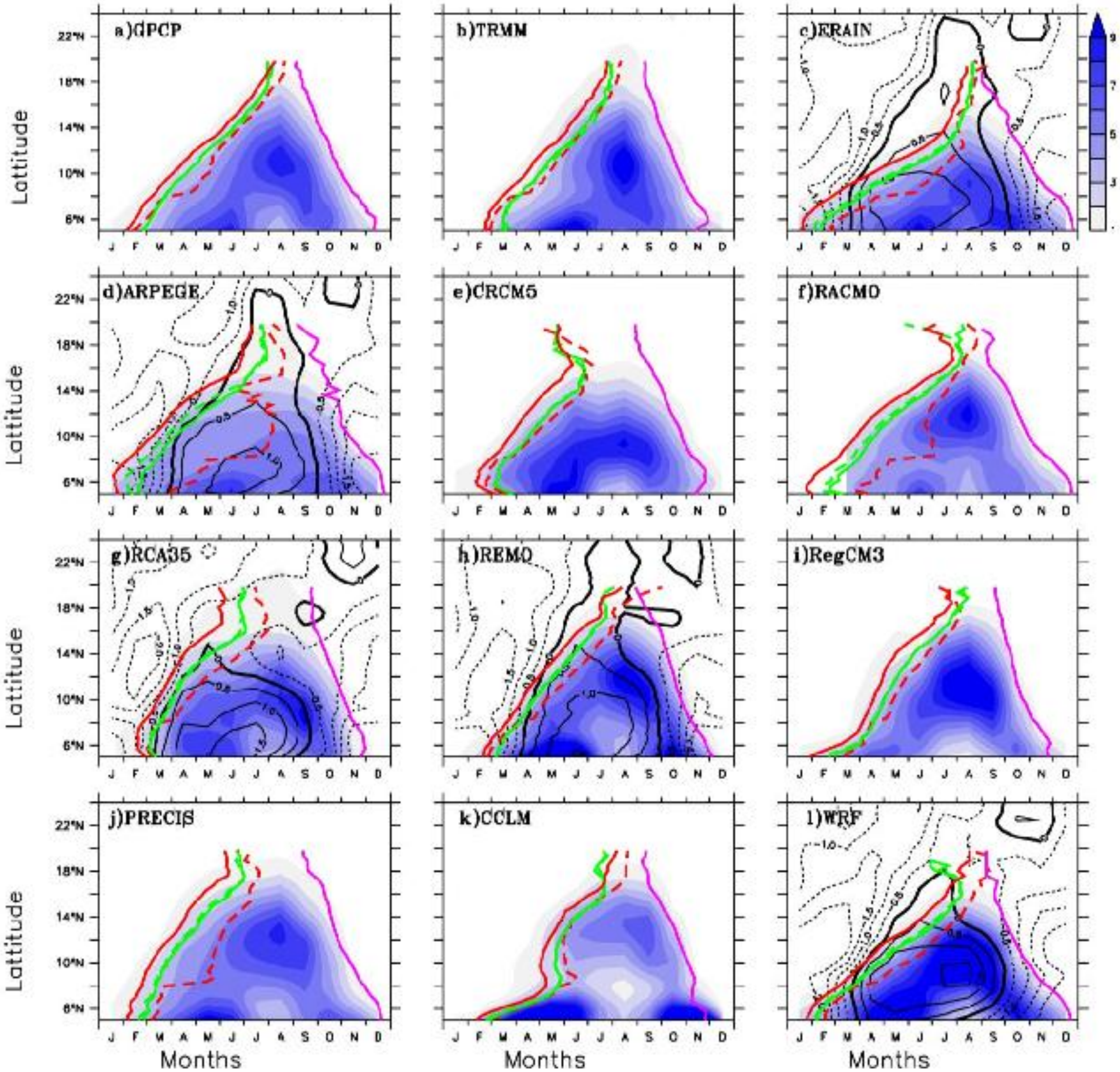

Figure 4.22: Time-latitude cross section of monthly rainfall (mm/day; shaded) and onset of monsoon rainfall (green and red thick/dashed lines), averaged over 10°W-10°E for observations (GPCP, TRMM) and CORDEX RCMs over West Africa for the period of 1998–2008. The corresponding zonal winds (dashed contours) are shown in the background. Panels (a), (b), (e), (f), (i), (j) and (k) have no wind data.

Hence in ERAIN, the northernmost position of the monsoon rainfall is at least 4° latitudes south of the observed position. This possibly explains why it fails to satisfy the ROD criteria north of 14°N in DEF4, while DEF1, DEF2 and DEF3 are not sensitive to that. Most RCMs (i.e. RACMO, REMO, RegCM3, and PRECIS) produce the start and inland penetration of the monsoon rainfall better than ERAIN does, but for CRCM5, RCA35 and WRF the northernmost position is between 14^{o}-15^{o}N. For the cessation dates, most RCMs have similar sharper cessation slope (e.g. Adejokun, 1966) as GPCP and TRMM, while ERAIN and ARPEGE have a gentler slope.

A notable feature in the northward progression of the monsoon rainfall is the so-called ‘monsoon jump’ (e.g. Le Barbe *et al.*, 2002; Abiodun *et al.* 2011, 2012), which signifies a break in the peak of monsoon rainfall during the northward progression. Both observations (GPCP and TRMM) show that the monsoon-jump occurs over Savanna (8^{o} -10^{o}N, in June – July), with a local rainfall peak over Guinea (6^{o}N, in May-June) and another over Sahel (11^{o}N, August). ERAIN poorly represents the monsoon-jump; in ERAIN, the location is south of the observed and the values are higher than observed, while the August rainfall peak is located over Savanna (9^{o}N) instead of over the Sahel (11^{o}N). ARPEGE simulated a worse monsoon-jump than ERAIN does, while some RCMs (i.e. REMO, RegCM3) simulate the monsoon-jump better than ERAIN does. However, Figure 4.22 shows that the ROD definitions are sensitive to the rain-jump and in this regard, DEF4 seems to be the most sensitive definition. For the above reason, the section 4.2.3 will evaluate the potential impact of the reforestation of Savanna in order to investigate how reforestation will affect the monsoon jump and the ROD over Sahel.

An important feature of West Africa rainfall climatology is the little dry season (LDS) that occurs in July/August over areas south 9^{o}N (e.g. Hamilton and Archbold, 1945; Adejokun, 1966). Capturing this phenomenon is a good reality test of all the models and satellite-derived rainfall patterns. The observation GPCP is the only one that captures the LDS; TRMM does not. ERAIN also does not capture it. Among the RCMs, only ARPEGE fails to capture it well, while CCLM produces a very intense LDS over the Savanna.

Despite the huge discrepancies in the monsoon rainfall produced by the RCMs (and ERAIN), there is a good agreement between their monsoon flows (Fig 4.22 and 4.23).

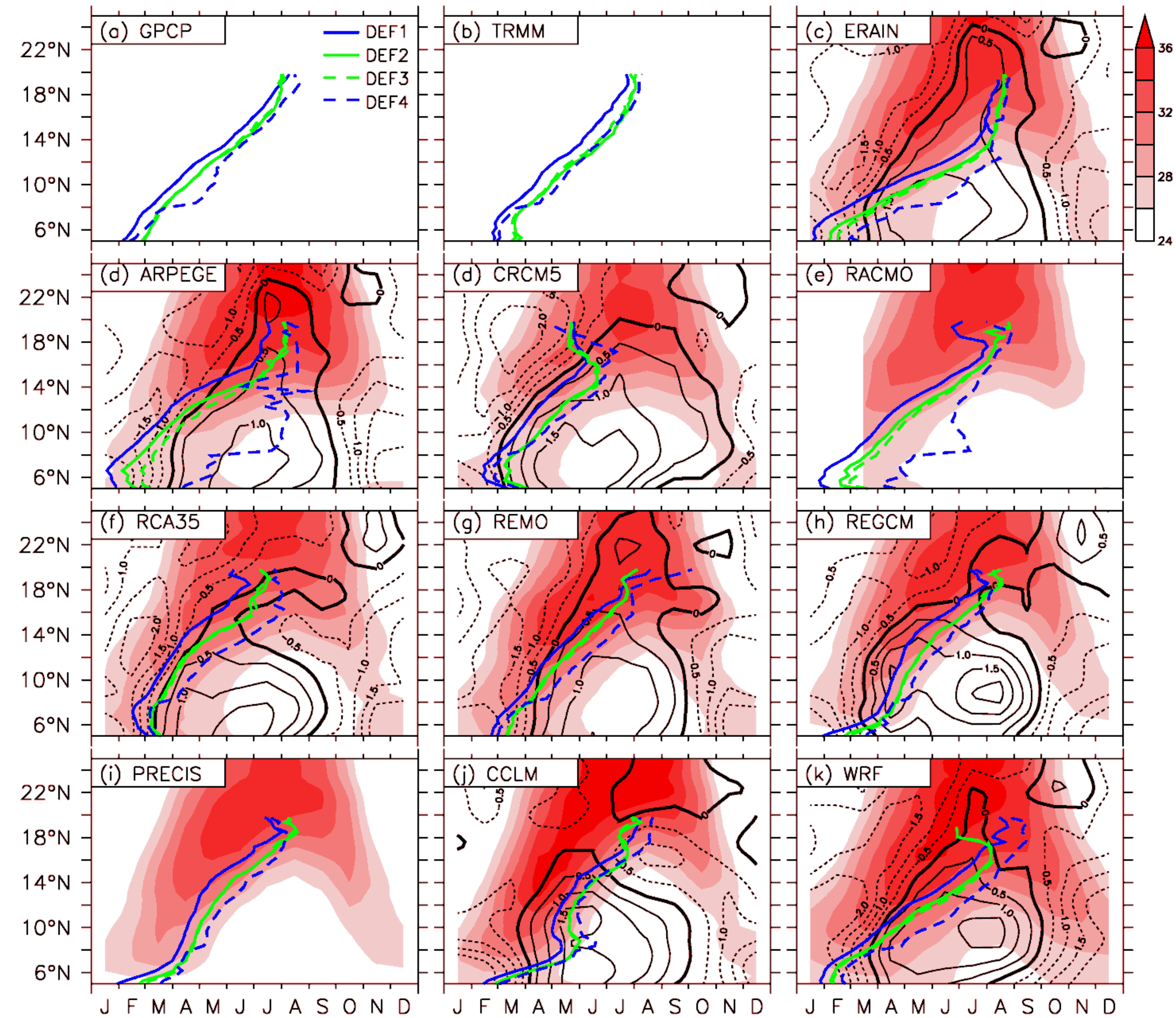

Figure 4.23 : Time-latitude cross section of monthly temperature (^{o}C; shaded) and onset of monsoon rainfall (green and blue thick lines), averaged over $10^{o}W$-$10^{o}E$ for observations (GPCP, TRMM) and CORDEX RCMs over West Africa for the period of 1998–2008. The corresponding zonal winds (contours) are shown in the background. Panels (a), (b), (e), and (i) have no wind data.

Figure 4.23 links the monsoon flow with the temperature fields that drive them. In all RCMs (and ERAIN), the temperature maximum starts from Guinea in January-February (but less intense in ARPEGE, CRCM5, and RACMO) and progresses northward (with higher values) to reach the northernmost position between 20^{o}-22^{o}N (with a value of about 36^{o}C). The location of ITD, which indicates the northward boundary of the moist south-west monsoon flow, roughly lies over the temperature maximum, and the strength of the flow decreases northward but with a maximum value (about 1-2 ms-1) over Savanna in July-august. Even ARPEGE, WRF and CRCM5 that have the highest disagreement in monsoon rainfall pattern (and RODs) still show a very good agreement in the monsoon flow. This suggests that the main source of discrepancy among the RCMs in simulating the RODs is in their representation of processes that convert the monsoon moisture to rainfall (i.e. rainfall or convection parameterization schemes), the soil moisture, and the atmospheric feedback in the models, surface albedo, cloudiness, advection of temperature, energy fluxes (Sylla *et al.*, 2012; Gbobaniyi *et al.*, 2013). Various studies have indentified convection scheme as a major bottleneck in simulating monsoon flow (e.g. Giorgi and Marinucci, 1996; Fulakeza *et al.*, 2002; Krishna *et al.*, 2011). Therefore, applying empirical method/definition (e.g. Drobinski *et al.*, 2005; Fontaine *et al.*, 2008) to compute ROD directly from RCMs dynamical and thermo-dynamical fields (wind, temperature, and moisture) as in Omotosho (1990, 1992) and Omotosho *et al.* (2000), instead of rainfall, may produce better and more consistent RODs from the RCMs. However, this is beyond the scope of present thesis.

4.1.4 The Inter-annual variation and Taylor diagrams of ROD and RCD

4.1.4.1 The Inter-annual variation and Taylor diagrams of ROD

Figure 4.24 shows the spread among the RCMs in simulating the inter-annual variation of ROD over the three climatic zones (Guinea, Savanna, and Sahel) of West Africa. The spread among the RCMs characterize the uncertainty due to physical parameterization errors in the models. Over Guinea, most RCMs show that the earliest ROD occurs in 1999 and 2006, but the spread among the simulated ROD is more than 50 days using any of the definitions. ARPEGE shows early ROD over Guinea with the first three definitions; in agreement with Nikulin *et al.* (2012) who also show that ARPEGE underestimates the rainfall over Guinea. Nevertheless, ARPEGE also shows the latest ROD with DEF4. CCLM consistently shows the latest ROD in DEF1, DEF2 and DEF3. Over Savanna, the spread among the RCMs is widest with DEF4 (about 100 days). However, with the first three definitions, CCLM consistently shows the latest ROD, while PRECIS shows the earliest ROD. With DEF4, ARPEGE produces the latest ROD, while RCA35 produces the earliest. Over Sahel, the spread among the RCMs is narrowest with DEF4. PRECIS and RCA35 consistently show the earliest ROD in the first three definitions, while WRF shows the latest ROD in all the definitions over the Sahel. In most cases (except with DEF4 over Guinea), the observed ROD (GPCP) falls within the spread of the simulated RODs. Hence, the RCMs ensemble ROD shows a lower bias than that of individual RCM. The ensemble ROD has the lowest bias (less than 5 days) with DEF2 and DEF3 over Savanna and the highest bias (about 20 days) with DEF4 over Guinea.

The Taylor diagrams (Fig. 4.25) are plots of the correlations (r) between the simulated and observed RODs against the normalized standard deviations (σ') and show the different patterns over the three climatic zones. Over Guinea zone, all RCMs and reanalysis cluster around a point ($r \approx 0.85$, $\sigma' \approx 0.90$) with all definitions. This implies that the RCMs and reanalysis show very good and similar capability in simulating the inter-annual variability and standard deviation of ROD, though with different biases (Tables 4.3, 4.4, 4.5, and 4.6). The correlation of the ensemble ROD is about 0.9 with DEF1 and DEF4, but about 0.8 with DEF2 and DEF3. Over Savanna, the Taylor diagrams show a scatter pattern, except with DEF4 where most RCMs aligned on $r \approx 0.35$; REMO produces the highest correlation (r=0.6) and the best standard deviation ($\sigma' = 1$). This indicates that most RCMs perform poorly and differently in simulating the inter-annual variability and standard deviation of ROD over Savanna. For the ensemble ROD, $r = 0.6$ with the first three definitions, but $r = 0.30$ with DEF4; $\sigma' \approx 1.5$, 1.5, 1.0 and 0.2 with DEF1, DEF2, DEF3 and DEF4, respectively. Over Sahel, the results are similar to that of Guinea, except that the RCMs aligned on $\sigma' \approx 1.5$ with r varying from 0.0 to 0.7, except with DEF4 where models cluster around a point ($r \approx 0.6$, $\sigma' \approx 0.70$). The correlation for the ensemble ROD is about 0.4 with the first three definitions and 0.8 with DEF4 but the standard deviation of the ensemble ROD is lower than that of any RCM. Hence, the best performance of the RCMs in simulating the inter-annual variability of ROD (i.e. correlation, standard deviation, and root mean square errors) is over Guinea and their worst performance is over the Savanna.

The inter-annul variability of the ROD indicates that the RCMs are sensitive to the climatic zones and the definitions used. The RCMs produce similar pattern in the first three definitions over Guinea and Savanna than over Sahel. Among the four definitions, DEF4 gives the highest spread among the RCMs RODs. The RCMs give higher correlation over Guinea and Sahel than over Savanna. In both cases, the ensemble ROD simulates better inter-annual variability and correlation than any RCM, when compared with observation. These results are consistent with those of previous studies (e.g. Druyan *et al.*, 2010; Nikulin *et al.*, 2012; Diallo *et al.*, 2012a, b).

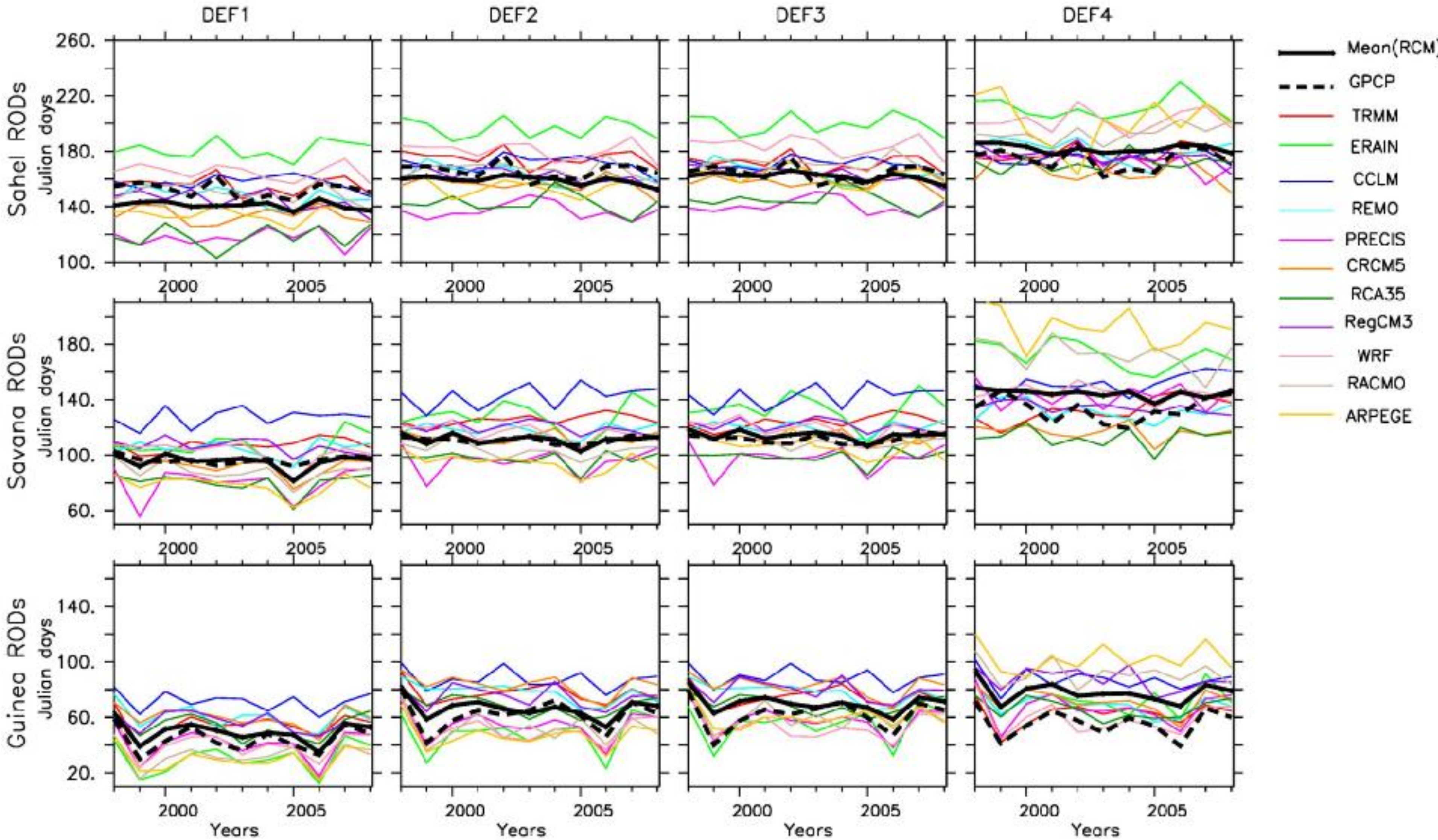

Figure 4.24 : Inter-annual variability of onset dates as observed (GPCP/TRMM dash lines) and simulated (CORDEX-RCM, lines) in DEF1-4 for the period 1998-2008 over Guinea, Savanna and Sahel zones.

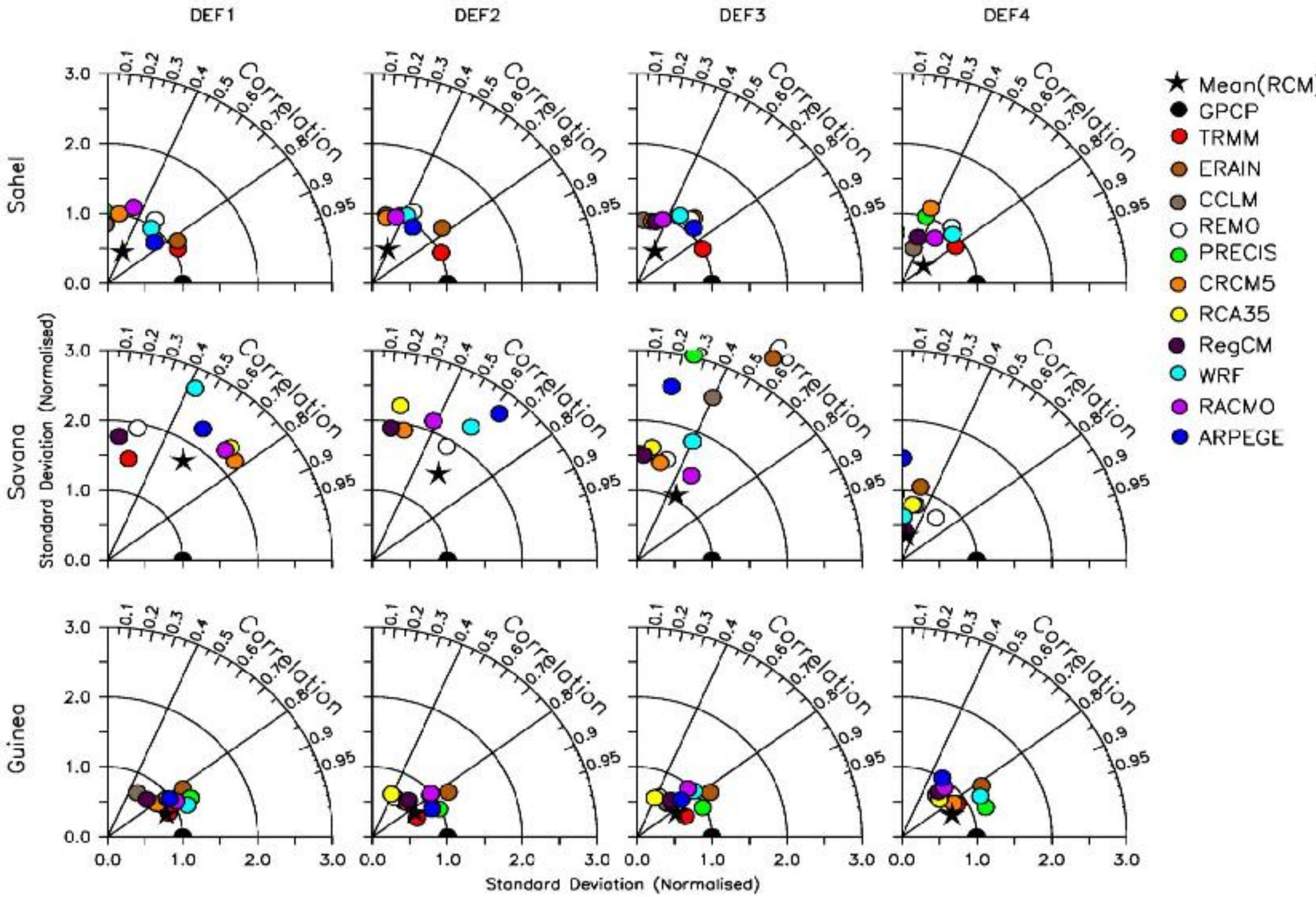

Figure 4.25 : Taylor diagram of ROD with respect to observed (GPCP) for simulated (CORDEX-RCMs) in DEF1-4 for the period of 1998–2008 over Guinea, Savanna and Sahel zones.

Table 4.3: Comparison of simulated and observed RODs over Guinea, Savanna and Sahel, showing the mean, the bias in the mean (ΔM) and root mean square error (using GPCP as reference) in DEF1 for the period 1998–2008.

	Guinea			Savanna			Sahel		
Models	Mean	ΔM	rmse	Mean	ΔM	rmse	Mean	ΔM	rmse
GPCP	13-Feb			5-Apr			31May		
TRMM	30-Jan	14	5	18-Mar	18	6	15May	16	4
ERAIN	22-Feb	9	5	20-Mar	16	5	28-Apr	33	11
ARPEGE	9-Feb	4	5	20-Mar	16	10	27-Apr	34	8
RCA35	24-Feb	11	3	16-Apr	11	5	3-Jun	3	3
PRECIS	28-Feb	16	5	1-Apr	5	5	13-May	18	7
CRCM5	29-Feb	17	5	13-Apr	8	6	24-May	7	6
REMO	11-Mar	28	8	6-May	31	8	6-Jun	6	8
CCLM	30-Jan	14	6	13-Apr	31	10	1-Jul	31	3
RACMO	31-Jan	12	5	28-Mar	8	5	29-May	2	7
RegCM3	25-Feb	12	6	15-Apr	10	6	24-May	7	9
WRF	9-Feb	4	4	10-Apr	5	7	12-Jun	12	5
RCMs(mean)	18-Feb	5	5	04-Apr	1	6	20-May	11	7

Table 4.4: Comparison of simulated and observed RODs over Guinea, Savanna and Sahel, showing the mean, the bias in the mean (ΔM) and root mean square error (using GPCP as reference) in DEF2 for the period 1998–2008.

	Guinea			Savanna			Sahel		
Models	Mean	ΔM	rmse	Mean	ΔM	rmse	Mean	ΔM	rmse
GPCP	02-Mar			19-Apr			13-Jun		
TRMM	17-Mar	15	5	04-May	14	5	20-Jun	07	3
ERAIN	17-Feb	13	7	06-May	17	9	16-Jun	33	4
ARPEGE	16-Feb	15	5	03-Apr	16	5	03-Jun	10	5
RCA35	08-Mar	06	10	06-Apr	14	5	22-May	22	10
PRECIS	23-Feb	08	4	04-Apr	15	9	16-May	28	9
CRCM5	23-Mar	21	8	21-Apr	01	5	31-May	14	7
REMO	17-Mar	15	9	27-Apr	07	4	08-Jun	05	6
CCLM	27-Mar	26	8	21-May	32	8	18-Jun	05	7
RACMO	21-Feb	10	8	12-Apr	07	5	14-Jun	01	7
RegCM3	14-Mar	13	9	28-Apr	09	5	11-Jun	02	6
WRF	21-Feb	10	8	25-Apr	06	5	27-Jun	14	6
RCMs(mean)	06-Mar	04	8	20-Apr	1	5	06-Jun	07	7

Table 4.5: Comparison of simulated and observed RODs over Guinea, Savanna and Sahel, showing the mean, the bias in the mean (ΔM) and root mean square error (using GPCP as reference) in DEF3 for the period 1998–2008.

	Guinea			Savanna			Sahel		
Models	Mean	ΔM	rmse	Mean	ΔM	rmse	Mean	ΔM	rmse
GPCP	02-Mar			20-Apr			11-Jun		
TRMM	14-Mar	12	5	02-May	12	5	17-Jun	6	3
ERAIN	24-Feb	7	7	12-May	21	9	22-Jun	41	6
ARPEGE	29-Feb	2	7	15-Apr	5	8	15-Jun	4	5
RCA35	09-Mar	7	10	07-Apr	13	5	29-May	14	10
PRECIS	27-Feb	4	5	07-Apr	14	9	19-May	23	9
CRCM5	22-Mar	21	8	21-Apr	1	5	09-Jun	3	7
REMO	17-Mar	16	10	28-Apr	8	5	14-Jun	3	5
CCLM	29-Mar	27	8	21-May	31	7	21-Jun	10	7
RACMO	29-Feb	1	8	19-Apr	2	4	9-Jun	7	6
RegCM3	19-Mar	17	8	30-Apr	9	5	14-Jun	1	7
WRF	23-Feb	8	7	28-Apr	7	5	21-Jun	24	6
RCMs(mean)	10-Mar	8	8	23-Apr	2	6	09-Jun	1	7

Table 4.6: Comparison of simulated and observed RODs over Guinea, Savanna and Sahel, showing the mean, the bias in the mean (ΔM) and root mean square error (using GPCP as reference) in DEF4 for the period 1998–2008.

	Guinea			Savanna			Sahel		
Models	Mean	ΔM	rmse	Mean	ΔM	rmse	Mean	ΔM	rmse
GPCP	25-Feb			12-May			22-Jun		
TRMM	2-Mar	6	5	11-May	1	13	24-Jun	3	5
ERAIN	11-Mar	15	7	20-Jun	39	11	29-Jul	37	6
ARPEGE	11-Apr	46	9	11-Jul	60	15	21-Jul	29	20
RCA35	6-Mar	10	7	21-Apr	20	10	19-Jun	3	10
PRECIS	7-Mar	11	4	21-May	10	13	20-Jun	2	9
CRCM5	11-Mar	16	5	25-Apr	17	11	12-Jun	9	9
REMO	9-Mar	13	6	10-May	2	7	28-Jun	6	7
CCLM	27-Mar	31	8	30-May	19	10	23-Jun	1	8
RACMO	31-Mar	35	8	20-Jun	39	15	11-Jul	19	7
RegCM3	27-Mar	31	8	13-May	1	9	23-Jun	2	8
WRF	28-Feb	3	6	23-May	11	10	19-Jul	28	6
RCMs(mean)	18-Mar	21	7	23-May	11	11	29-Jun	7	9

4.1.4.2 The Inter-annual variation and Taylor diagrams of RCD

The inter-annual variability between observations and RCMs shows the spread between the models depends on the climatic zone (Fig. 4.26). Over Sahel (Fig. 4.26a), reanalysis ERAIN and RCMs (ARPEGE and PRECIS) produce the latest RCDs, while TRMM gives the earliest. All the RCMs agree that in the year 2000 cessation was delayed in this zone and the spread among the RCM is about 10 days. In contrast, the RCMs also indicate that an early RCD occurs in this region in 2001, 2004 and 2007 with spread less than 10 days. The ensemble mean of the RCMs show agreement result with observation with spread less than 5 days.

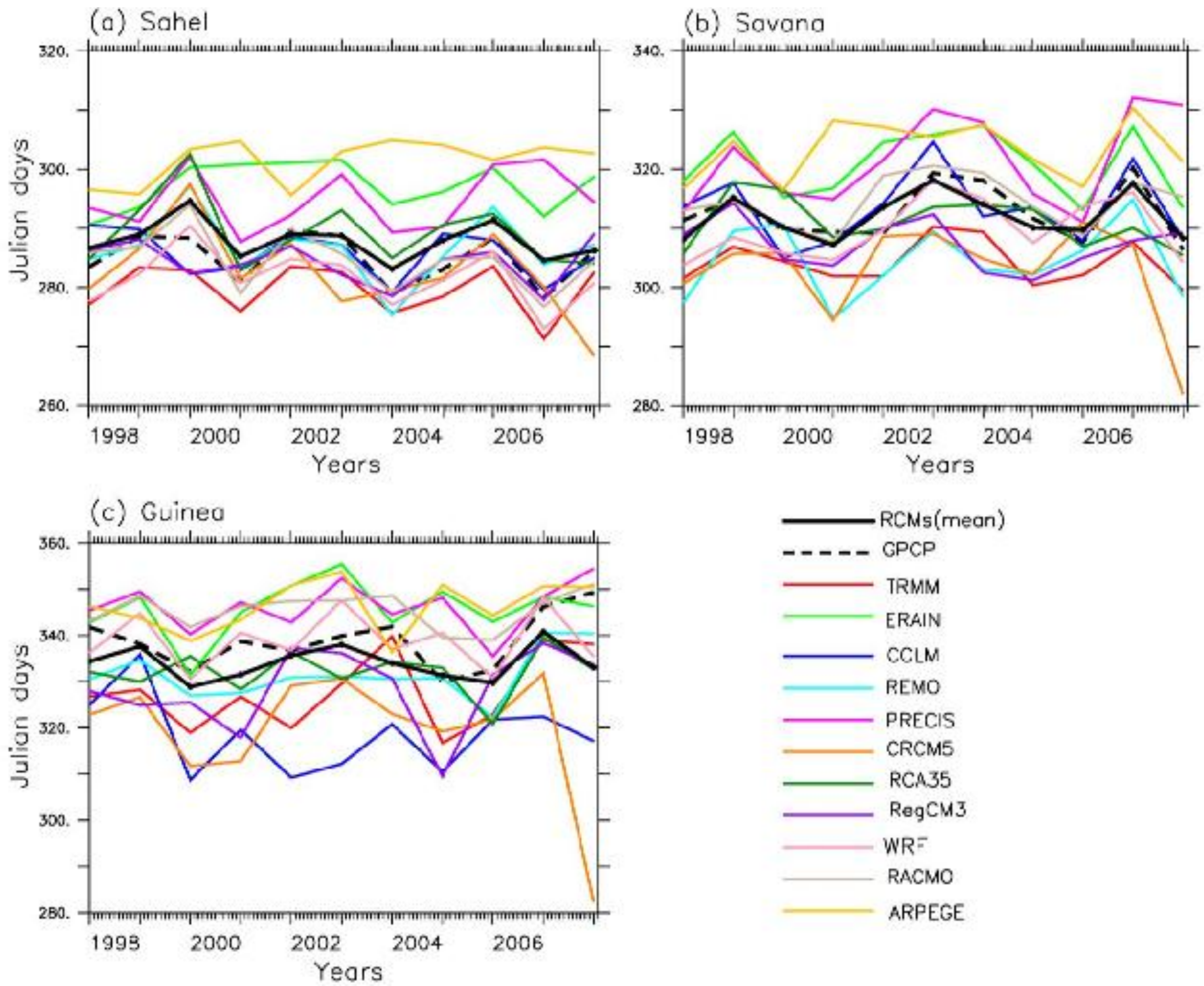

Figure 4.26 : Inter-annual variability of rainfall cessation dates as observed (GPCP, dash lines) and simulated (CORDEX-RCMs, thick lines) for the period 1998-2008 over Guinea, Savanna and Sahel.

Over the Savanna, the RCMs and observations indicate similar patterns as over Sahel except that the spread among the models is higher. ARPEGE and PRECIS and reanalysis ERAIN give the latest RCD in this zone, while CRCM5 and REMO produce the earliest RCD (Fig. 4.26b). The RCMs ensemble captures better the observed GPCP pattern than over Sahel, though with higher spread in the models (more than 10 days). Over Guinea (Fig. 4.26c), the inter-annual variability indicates scattered patterns between observation and RCMs. The spread among the RCMs is higher than in Savanna and Sahel (more than 20 days). CCLM consistently produces the earliest RCD in this zone, while ARPEGE, PRECIS and RACMO give the latest RCD. The ensemble mean of the RCMs RCD shows agreement result with observation (GPCP) and produces lower spread over Sahel and Savanna than over Guinea. The RCMs ensemble gives better results than all the RCMs with a spread of about 10 days.

The correlation (r) between the simulated and observed RCDs against the normalized standard deviations (σ') is given in Figure 4.27. The results show scatter patterns over the three climatic zones. Over the Sahel (Fig. 4.27a), the RCMs correlation varies between r=0.4 to 0.8 and σ'=0.5 to 1.2. RACMO and WRF have the best r and σ' among the RCMs over this zone (r=0.8 and σ'=1, r=0.81 and σ'=1.1 respectively). PRECIS and CRCM5 gives the worst r and σ' respectively 0.3 and 1.7. The RCMs ensemble show r=0.8 and σ'=0.6. This indicates that the RCMs are able to capture the inter-annual variability over Sahel. Over Savanna, the results are similar to that of Sahel and the RCMs ensemble show r =0.83and σ'=0.6. Over Guinea, the correlation are more scattered than over Savanna and Sahel. The RCMs (ARPEGE, RCA35, CCLM, and WRF) show the lowest r (between 0.2-0.4) and CCLM gives the highest σ' of 1.5. RACMO and REMO simulate the best r and σ' over Guinea(r=0.8 and σ'=0.5, r=0.8 and σ'=0.7 respectively).The RCMs ensemble indicate that r=0.6 and σ'=0.4.

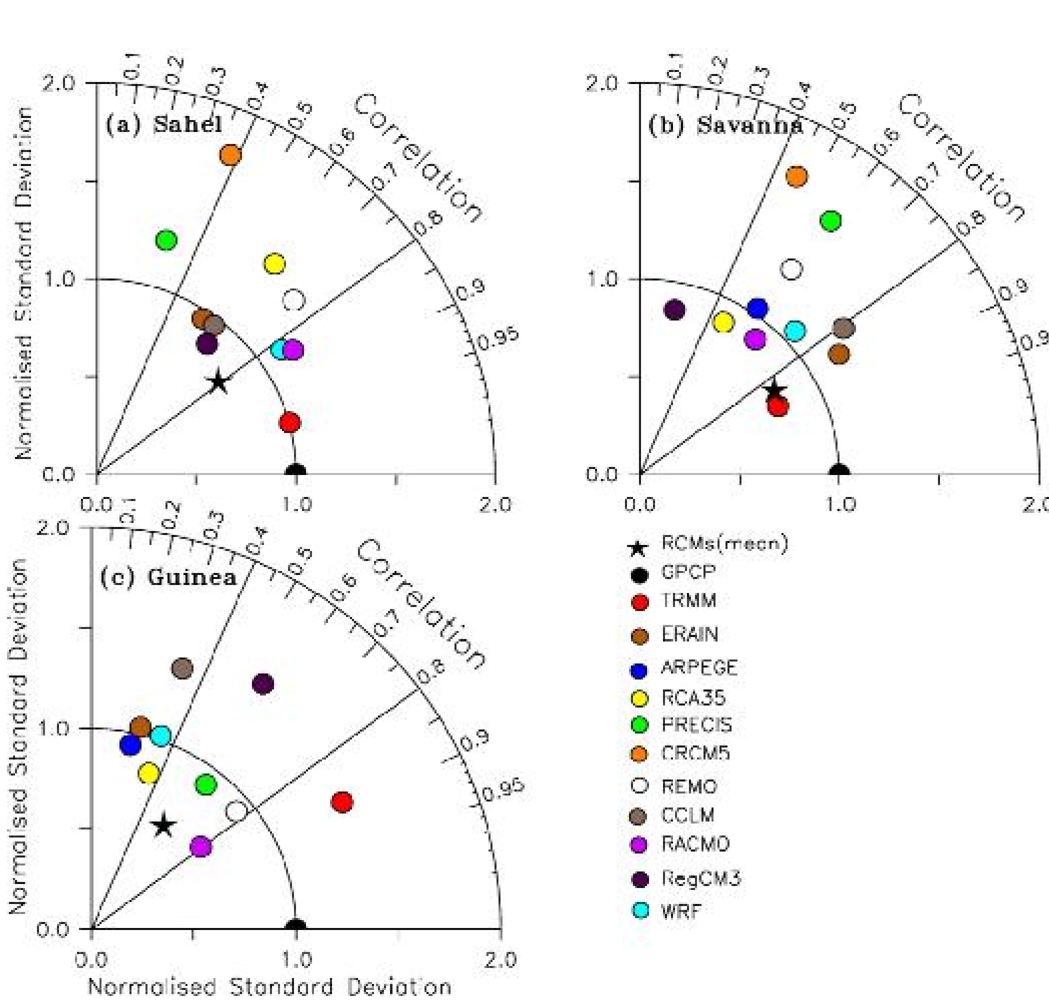

Figure 4.27 : Taylor diagram of RCD with respect to observed (GPCP) for simulated (CORDEX-RCMs) over Guinea, Savanna and Sahel for the period of 1998–2008.

Table 4. 7: Comparison of simulated and observed RCDs over Guinea, Savanna and Sahel, showing the mean, the bias in the mean (ΔM) and root mean square error (using GPCP as reference) for the period 1998–2008.

	Guinea			Savanna			Sahel		
Models	Mean	ΔM	rmse	Mean	ΔM	rmse	Mean	ΔM	rmse
GPCP	03-Dec			07-Nov			10-Oct		
TRMM	22-Nov	11	4	30-Oct	-8	2	05-Oct	5	1
ERAIN	12-Dec	9	7	15-Nov	8	3	22-Oct	12	4
ARPEGE	12-Dec	9	7	18-Nov	11	4	27-Oct	17	7
RCA35	27-Nov	7	6	6-Nov	2	4	15-Oct	5	4
PRECIS	11-Dec	8	5	16-Nov	9	6	20-Oct	10	5
CRCM5	17-Nov	16	5	30-Oct	8	7	08-Oct	2	7
REMO	26-Nov	4	6	30-Oct	8	5	12-Oct	2	4
CCLM	13-Nov	8	8	08-Nov	1	3	11-Oct	1	3
RACMO	10-Dec	3	8	09-Nov	2	4	10-Oct	0	3
RegCM3	24-Nov	7	8	02-Nov	5	5	10-Oct	0	3
WRF	04-Dec	7	6	04-Nov	3	4	07-Oct	3	3
RCMs(mean)	29-Nov	7	7	07-Nov	0	5	13-Oct	3	4

4.1.5 The length of the rainy season over the zones

The length of the rainy season (LOR) is an important factor that helps to determine the types of crop to use. Table 12 gives the LR of the observed GPCP and TRMM and simulated CORDEX-RCMs over West Africa for a given RCD definition. The LR depends on the definitions and the RCMs used. Both observations indicate that the LOR varies between 8 to 10 months over Guinea, 6 to 7.5 months over Savanna and 3.5 to 4.8 months over Sahel regardless the definitions used. TRMM underestimates the observed LOR of GPCP at about 24 days in DEF2 and DEF3, about 18 days in DEF4 over Guinea; at about 21days in DEF2and DEF3, about 9 days in DEF4 over Savanna; at about 9 days in DEF3 and DEF4, about 12 days in DEF2 over Sahel. In DEF1, TRMM always overestimates of the observed LOR of GPCP at about 3, 9, and 12 days respectively over Guinea, Savanna and Sahel. ERAIN capture the observed GPCP LR in DEF1 over Guinea but overestimates it over Guinea (i.e. DEF2 (21days), DEF3 (15days)), over Savanna (i.e. DEF1 (24days)) and Sahel (i.e. DEF1 (45days), DEF2 (9days), and DEF3 (3days)) and underestimates the LR in DEF4 (27days) in all the climatic zones.

Table 4.8 : Length of the rainy season (LOR, in months) calculated for the CORDEX-RCMs using the RODs and RCD definitions for the period 1998–2008.

	Guinea				Savanna				Sahel			
Models	DEF1	DEF2	DEF3	DEF4	DEF1	DEF2	DEF3	DEF4	DEF1	DEF2	DEF3	DEF4
GPCP	9.8	9.2	9.2	9.4	7.2	6.7	6.7	6.0	4.4	4.0	4.0	3.7
TRMM	9.9	8.3	8.4	8.8	7.5	6.0	6.0	5.7	4.8	3.6	3.7	3.4
ERAIN	9.8	9.9	9.7	9.2	8.0	6.4	6.2	4.9	5.9	4.3	4.1	2.8
ARPEGE	10.2	10.0	9.6	8.2	8.1	7.6	7.2	4.3	6.1	4.9	4.5	3.3
RCA35	9.2	8.8	8.8	8.9	6.8	7.1	7.1	6.6	4.5	4.9	4.6	3.9
PRECIS	9.5	9.7	9.6	9.3	7.6	7.5	7.4	6.0	5.3	5.2	5.1	4.1
CRCM5	8.7	8.0	8.0	8.4	6.7	6.4	6.4	6.3	4.6	4.3	4.0	3.9
REMO	8.7	8.5	8.5	8.7	5.9	6.2	6.2	5.8	4.3	4.2	4.0	3.5
CCLM	9.6	7.7	7.6	7.7	7.0	5.7	5.7	5.4	3.4	3.8	3.7	3.7
RACMO	10.4	9.7	9.5	8.5	7.5	7.0	6.8	4.7	4.5	3.9	4.1	3.0
RegCM3	9.1	8.5	8.3	8.1	6.7	6.3	6.2	5.8	4.6	4.0	3.9	3.6
WRF	9.9	9.5	9.5	9.3	6.9	6.4	6.3	5.5	3.9	3.4	3.6	2.7
RCMs(mean)	9.5	8.9	8.8	8.5	7.2	6.7	6.6	5.6	4.9	4.3	4.2	3.5

Similarly, most RCMs overestimates the LOR as observed in GPCP respectively ARPEGE, RACMO (in DEF1, DEF2 and DEF3), PRECIS and WRF (in DEF2 and DEF3) over Guinea; ARPEGE PRECIS RACMO (in DEF1, DEF2, and DEF3) RCA35 (in DEF2 and DEF3) over Savanna; ARPEGE, RCA35, PRECIS, CRCM5, and RegCM3 (in DEF1, DEF2, DEF3, and DEF4) over Sahel. The other RCMs underestimate the LOR depending of the definitions used. The RCMs ensemble mean produce better results over Savanna than over Guinea and Sahel.

In the next section the RCMs (RegCM and WRF) will be used to evaluate the potential impacts of climate change and reforestation on ROD and RCD over West Africa. Among the CORDEX-RCMs only RegCM and WRF were available when this study was conducted and they are also the most commonly used RCMs in the region.

4.2 MODEL VALIDATION FOR THE PRESENT DAY SIMULATIONS FOR THE RCMs REGCM AND WRF OVER WEST AFRICA

This section examines the second objective of the thesis. In this section, the model validation for the present day (1970-2004) is evaluated. The validation consists at examining the performance of the RCMs (RegCM and WRF) in simulating the WAM and it features.

4.2.1 West African Monsoons System

The RCMs (forced with GCMs) reliably simulate the West African monsoon (WAM) and its dynamical features as well as the ITD that controls the northward penetration and or southward retreat of the WAM. Figures 4.28 and 4.29 present the seasonal cycle of the WAM system and its associated temperature and rainfall patterns as simulated by RegCM and WRF models respectively. The WAM annual cycle is characterized by the onset of rainfall, the peak of the onset and the retreat of rainfall (Fig. 4.28&4.29). The onset of rainfall corresponds to the northward progression of the rain belt from the Guinea coast (about 6°N) to about 16°N over Sahel. It is also associated with the position of ITD (Sultan and Janicot, 2003; Omotosho and Abiodun, 2007; Mounkaila *et al.*, 2014). Both observations (GPCP and TRMM) produce similar results and agree that the monsoon rainfall starts over the Guinea coast (5°N) in February–March and progresses inland (northward) to reach its northernmost position of about 18°N in August. This is in agreement with the results of Mounkaila *et al.* (2014). HadGEM and ECHAM fail to reproduce the rainfall patterns as given in GPCP and TRMM. The monsoonal rainfall starts between March-May (i.e. late onset date) and March-April over the coast (about 5^{o}N) respectively, in HadGEM and ECHAM, and reaches its northernmost position of only about 12^{o}N over Savanna in HadGEM (i.e. August, Fig.4.28d) and only about 14^{o}N over Sahel in ECHAM (in August, Fig. 4.29d).

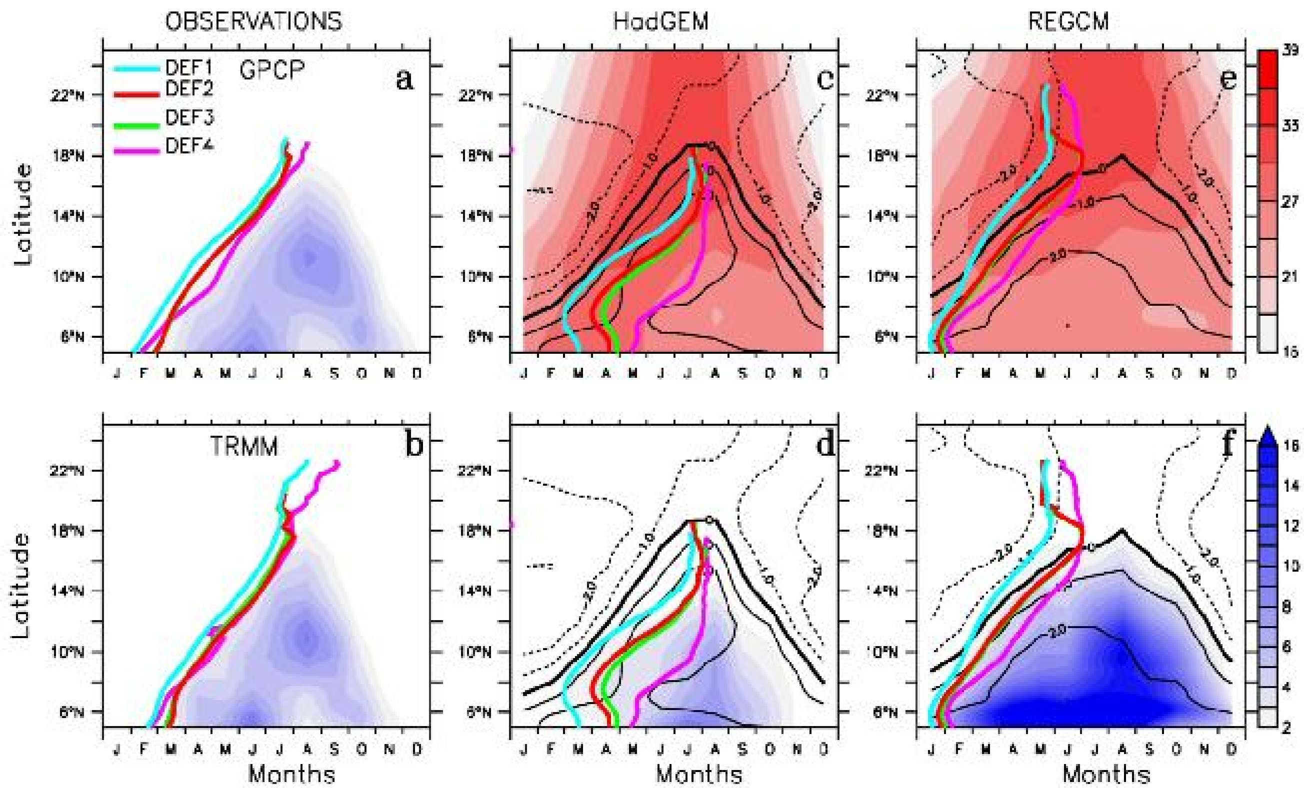

Figure 4.28 : Time-latitude cross section of monthly temperature (^{o}C, shaded in red, c: from HadGEM and e: from RegCM), rainfall (mm/day, shaded in blue) and onset of monsoon rainfall (colored thick lines), averaged over 8^{o}W-8^{o}E for observations (a: GPCP (1997-2004), b: TRMM (1998-2004)), c: from HadGEM (1971-2004) and e: from RegCM4 (1971-2004) over West Africa. The dashed contours lines are the zonal wind.

RegCM and WRF highly overestimate the rainfall patterns observed in GPCP and TRMM and they produce rainfall pattern that reaches about the same northernmost latitudes as GPCP and TRMM. However, WRF simulates the onset period better than ECHAM. RegCM also produces an early onset which varies between January-February, while HadGEM produces later onset between April-May (Fig. 4.28f). Furthermore, the peak of the onset corresponds to the northernmost position of the rain-band in its inland penetration (about north 16^{o}-18^{o}N) and refers to the beginning of the rainy season over Sahel. This peak of onset occurs after a sudden break of the monsoon flow the so called “monsoon jump” (Sultan and Janicot, 2003). The observations (GPCP and TRMM) show that the monsoon abrupt shift occurs over Savanna (about 7^{o}N to 12^{o}N in June-July). HadGEM and ECHAM do not simulate the monsoon jump.

Their inland monsoon penetrations stop at about 12^{o}N over Savanna (in HadGEM) and 14^{o}N over Sahel (in ECHAM). Similarly RegCM and WRF fail to reproduce the monsoon jump but they simulate the peak of onset better than their driver models. In general, both RCMs overestimate the monsoonal rainfall but capture well the monsoon penetration inland. These overestimations of the RCMs may be due to the difference in physical parameterizations schemes and internal errors of each individual model.

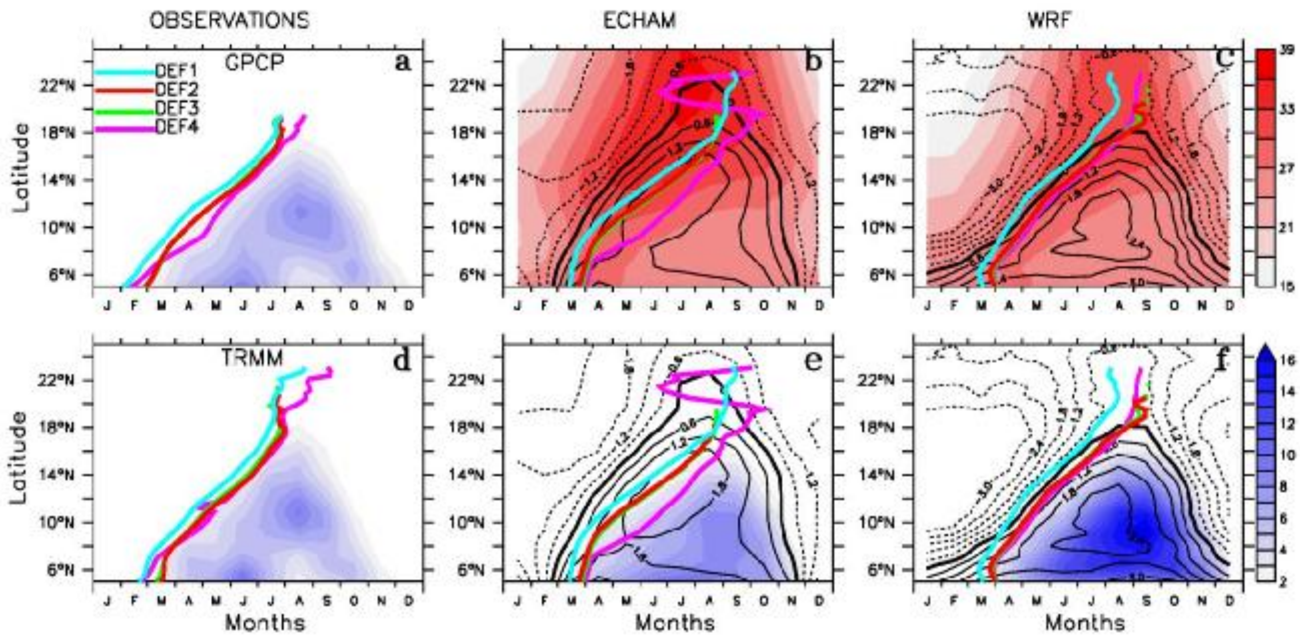

Figure 4.29 : Time-latitude cross section of monthly temperature (^{o}C, shaded in red, b: from ECHAM and c: from WRF), rainfall (mm/day; shaded in blue) and onset of monsoon rainfall (colored thick lines), averaged over 8^{o}W-8^{o}E for observations (a: GPCP (1997-2004), d: TRMM (1998-2004)), e: from HadGEM (1971-2004) and f: from WRF (1971-2004) over West Africa. The dashed contours lines are the zonal wind.

The WAM associated temperature features shows that the RCMs and their driven AOGCMs (RegCM and HadGEM, WRF and ECHAM) produce consistent simulations of the temperature patterns. However, while RegCM overestimates the temperature north 16^{o}N as observed in HadGEM, WRF underestimates it when compared to ECHAM. In all the models, the meridional wind decreases northward before reaching the position of the Inter Tropical Discontinuity (ITD) which is given by the zero value of the wind contours. This position corresponds to the northerly boundary of the southwest moist monsoon flow (Abiodun *et al.*, 2011).

4.2.2 Spatial Distribution of ROD for the Present Day

Figures 4.30 and 4.31 show the spatial distribution of the mean onset dates (RODs) as simulated by the two RCMs (RegCM and WRF) and their driven GCMs (HadGEM and ECHAM) and the observed (GPCP and TRMM) using the four RODs definitions. The RODs increase northward in all the definitions from the coast to inland. The observed (GPCP) shows that DEF2 and DEF3 give similar results of RODs and produce a later ROD than DEF1. It is seen that DEF4 produces the latest RODs among the definitions, while DEF1 gives the earliest ROD. Both observations (GPCP and TRMM) are in good agreement in simulating the RODs for all the definitions. The mean RODs of both observations (GPCP and TRMM) vary between February-March over Guinea, March-May over Savanna and May-July over Sahel. These results are in agreement with Mounkaila *et al.* (2014). Both HadGEM and ECHAM fail to simulate the spatial distribution of ROD over West Africa as in the observed (GPCP and TRMM) over Guinea in all the definitions except in DEF1 for HadGEM. They consistently give late mean ROD south 8^oN (Fig. 4.30&4.31). Moreover, HadGEM fails to simulate the distribution of ROD over Savanna and Sahel regardless for all the definitions, while ECHAM does so well except over northern Sahel. In addition, HadGEM fails to satisfy the criteria in all the definitions north 15^oN. The reason could be its failure to reproduce the monsoon flow northward as observed previously in section 4.2.1.

Furthermore, while WRF shows similar results as that produced by its driven AOGCM, RegCM produces patterns different from its driven GCM HadGEM regardless of the definitions used. RegCM produces early ROD almost everywhere. In contrast, WRF captures the distribution of the ROD over Savanna and Sahel in all the definitions but fails over Guinea where it produces late ROD.

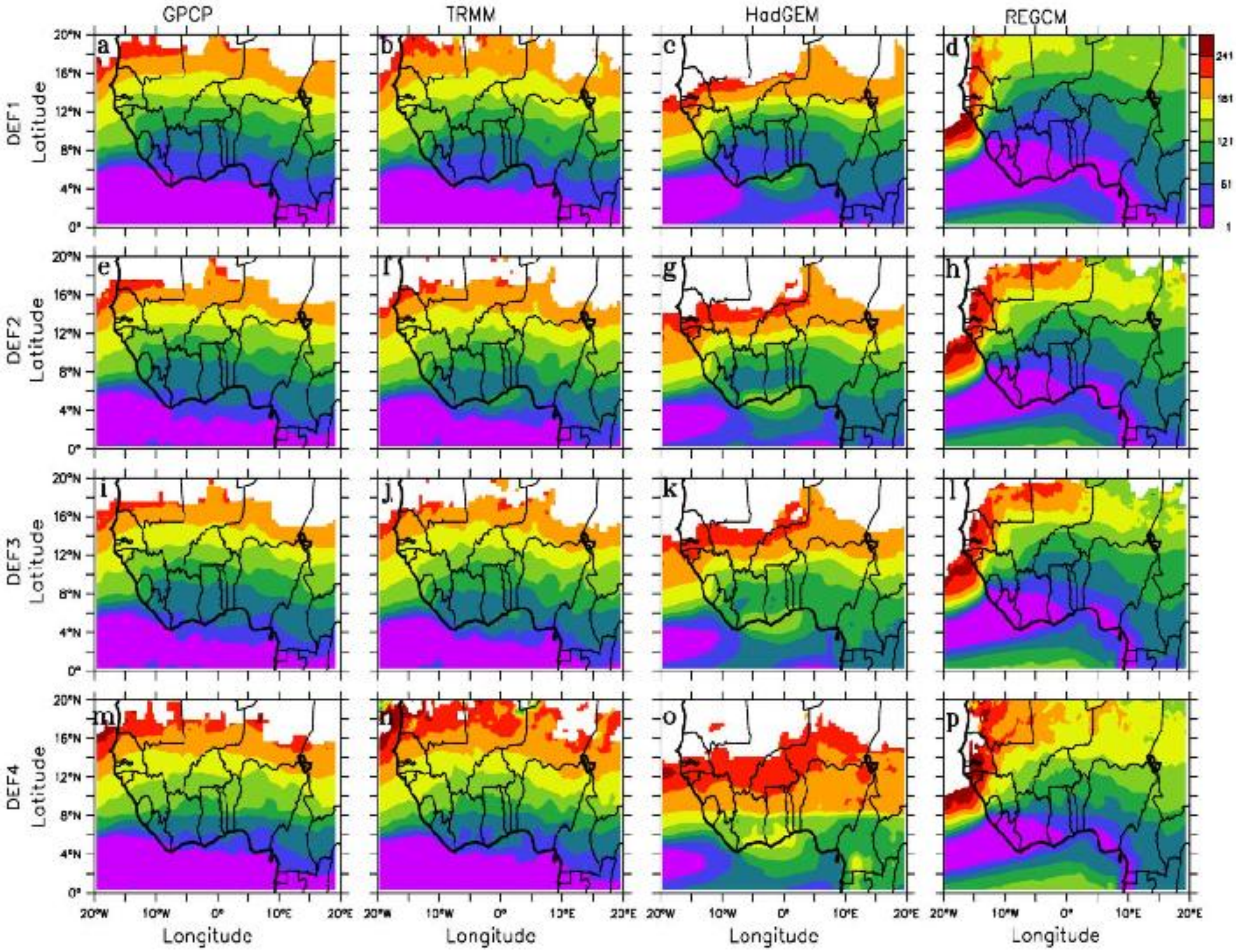

Figure 4.30 : Mean onset dates from four definitions (DEF1, DEF2, DEF3 and DEF4) as observed (GPCP (1997-2004) & TRMM (1998-2004)), HadGEM (1971-2004) and as simulated by RegCM4 (1971-2004).

In summary RegCM and WRF outperform HadGEM and ECHAM respectively in simulating the ROD spatial distribution over West Africa regardless of the definitions used. The reasons of the models failure over Guinea and Sahel are not yet known but require more analyses which is beyond the scope of this study.

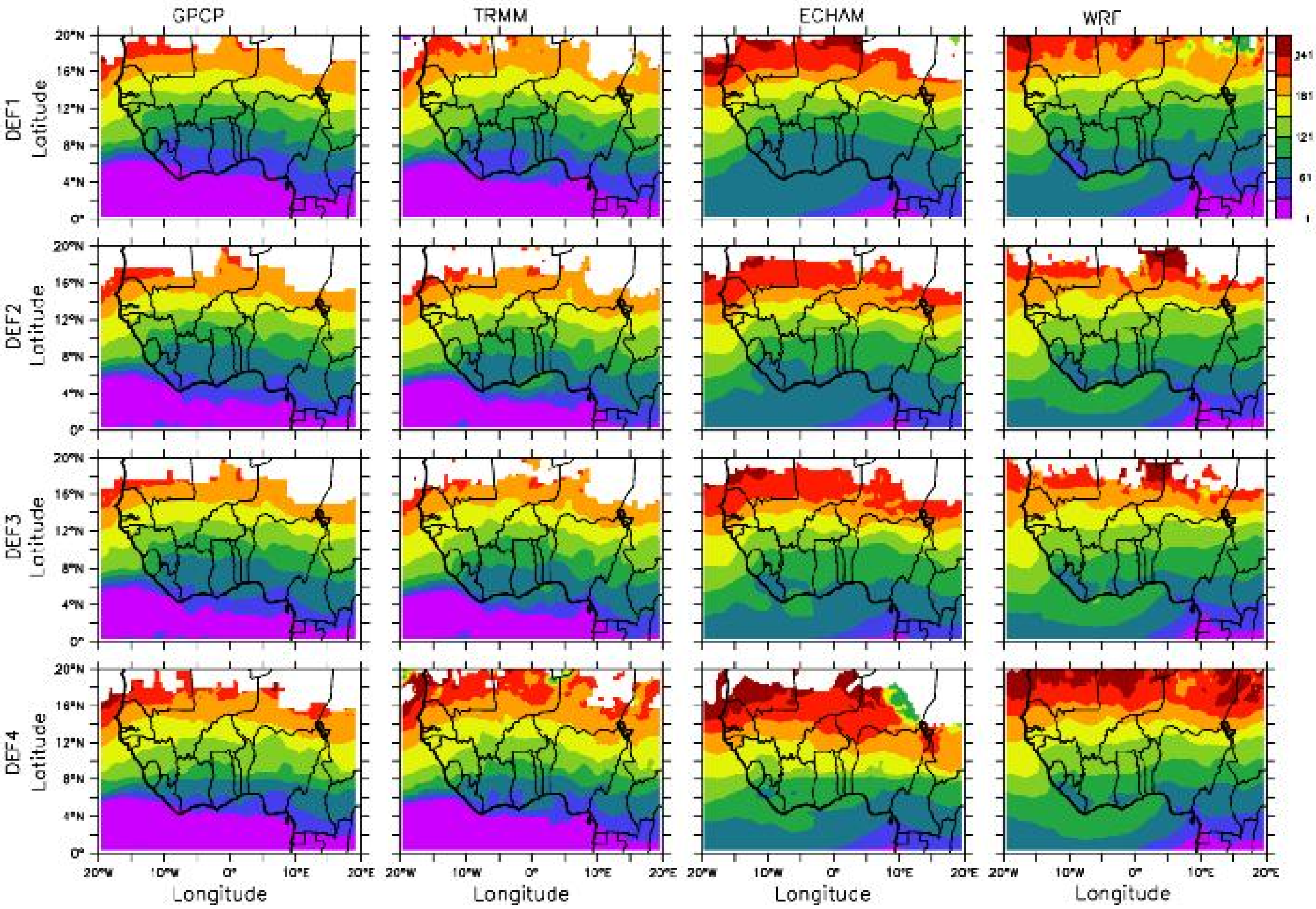

Figure 4.31 : Mean onset dates from four definitions (DEF1, DEF2, DEF3 and DEF4) as observed (GPCP (1997-2004) & TRMM (1998-2004)), ECHAM (1971-2004) and as simulated by WRF (19971-2004).

4.2.3 Inter-annual variability of ROD for the RCMs and AOGCMs

The inter-annual variability of the mean ROD for RegCM and WRF are shown in Figures 4.32 and 4.33. It characterizes the spread between the models due to uncertainty. Because of data constraint, the observed datasets have a shorter time period (8, 9 years respectively for TRMM and GPCP). Generally, the observed data show similar pattern in each zone of West Africa (Guinea, Savanna and Sahel respectively) regardless the definitions used except in DEF4 over Savanna and less so over Guinea too. It can also be seen that HadGEM and RegCM and also ECHAM and WRF produce similar patterns as in observed (GPCP and TRMM) except that over Guinea where the observed give earlier onset dates.

However, HadGEM and ECHAM generally give later ROD variability for all the definitions. Also RegCM always gives earlier ROD inter-annual variability for all definitions and over all zones but WRF gives results in agreement for all the definitions over Savanna and Sahel but overestimates the ROD inter-annual variability over Guinea for all the definitions.

Figures 4.32 and 4.33 give also the standard deviation and correlation between the AOGCMs and RCMs. HadGEM and RegCM produce very low correlation (r) for all the definitions and over the Sahel and Savanna but has higher correlation over Guinea. The correlation is much higher for ECHAM and WRF over all the zones and for all the definitions. Furthermore, HadGEM and RegCM give lower value of the ROD standard deviation (σ) over Guinea and higher value over Savanna and Sahel. This can be explained by the higher spread of the ROD inter-annual variability between HadGEM and RegCM. Moreover, ECHAM and WRF produce similar results in all the definitions and climatic zones except over Savanna in DEF4. Their standard deviation (σ) and correlation (r) indicate that both models produce higher r in DEF1 and DEF4 than the others two definitions in all the zones. The ROD values of σ are lower over Guinea regardless the definitions used but produce higher values of Savanna and Sahel in the definitions.

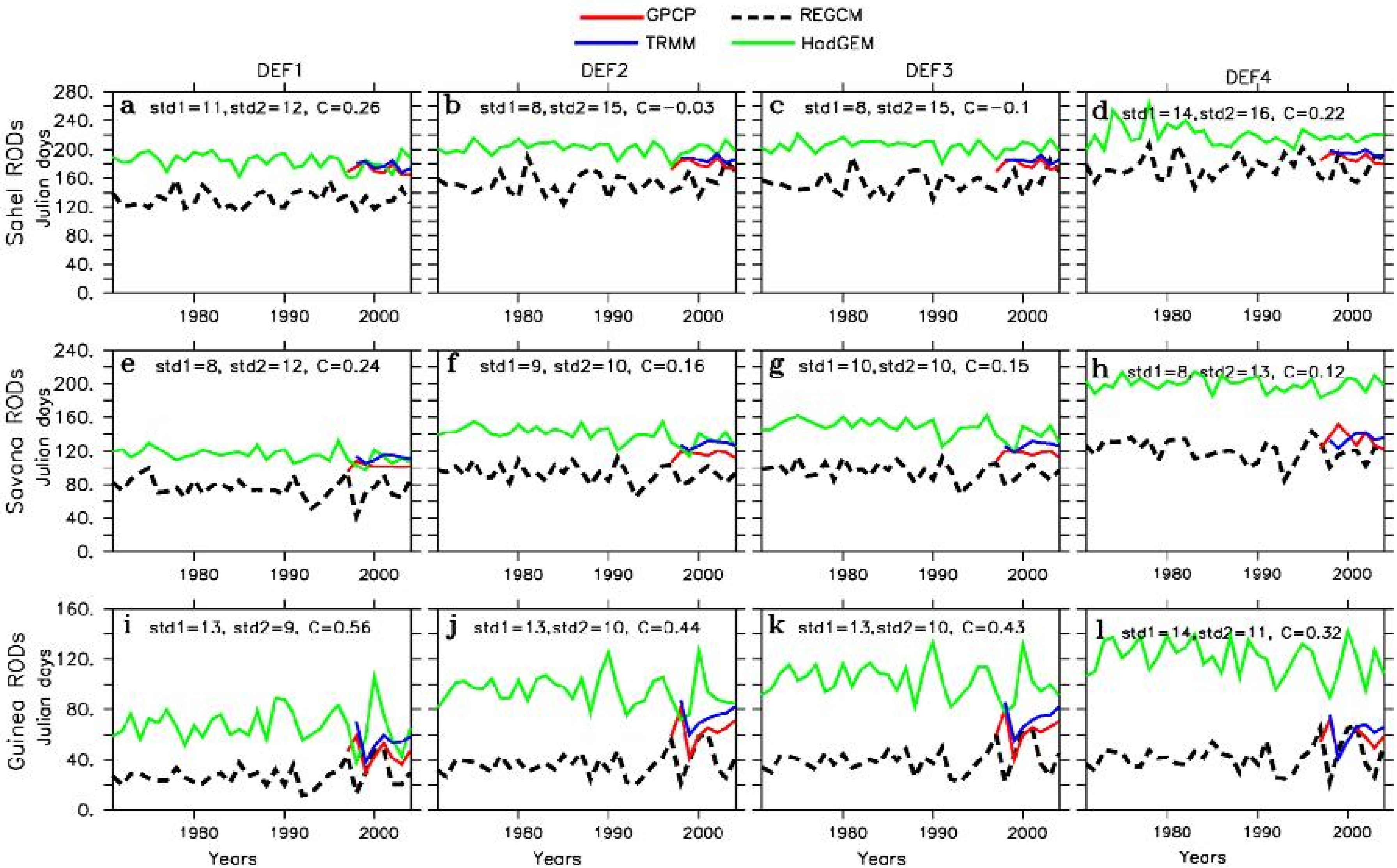

Figure 4.32 : Inter-annual variability of onset dates from four definitions (DEF1, DEF2, DEF3 and DEF4) as observed (GPCP (1997-2004), TRMM (1998-2004) red, blue lines respectively), HadGEM (1971-2004) green line and simulated RegCM (1971-2004) dash line over West Africa. The standard deviation (std) and correlation (c) between HadGEM and RegCM are also indicated.

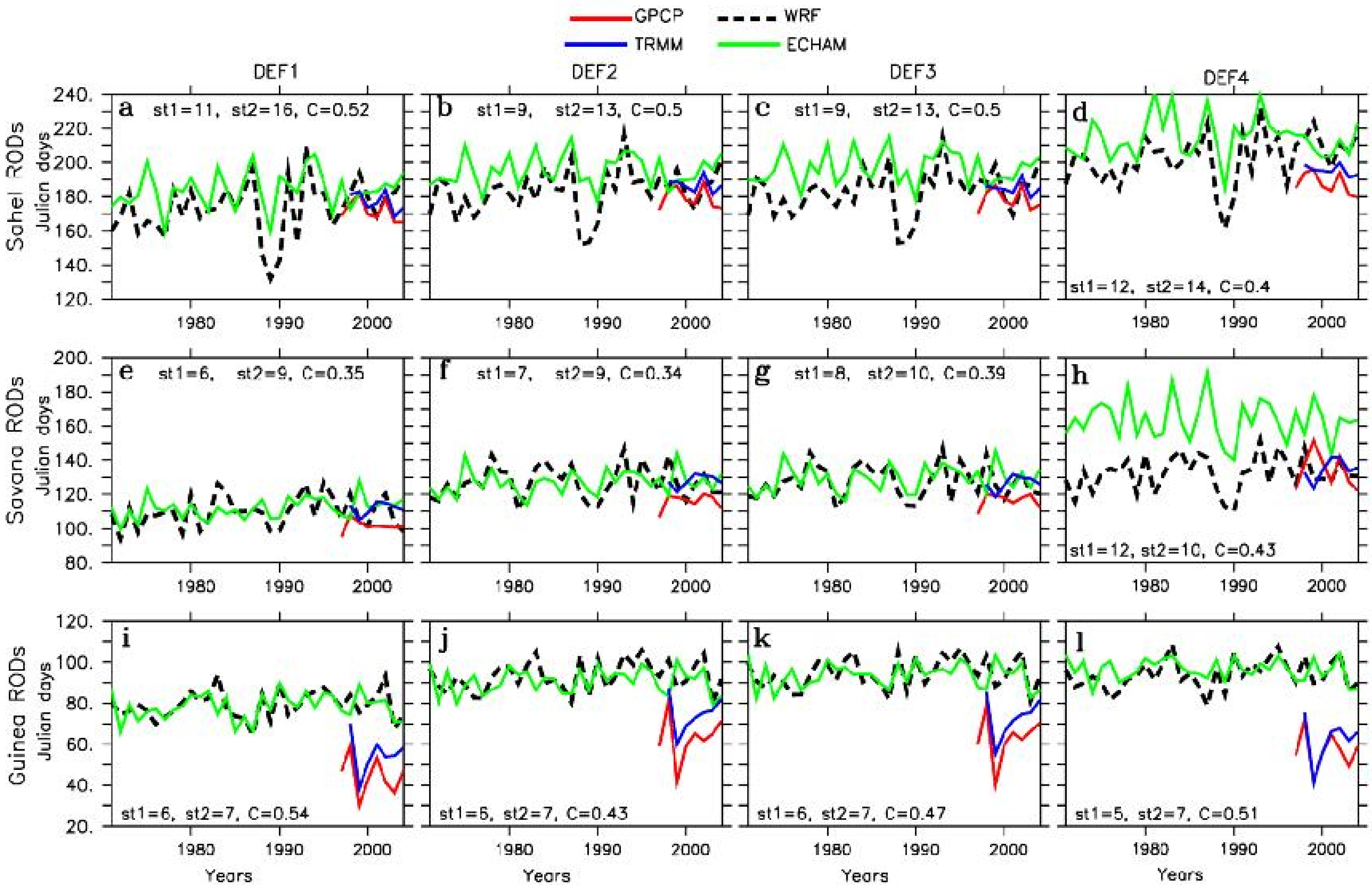

Figure 4.33 : Inter-annual variability of onset dates in four definitions (DEF1, DEF2, DEF3 and DEF4) as observed (GPCP (1997-2004), TRMM (1998-2004) red, blue lines respectively), ECHAM (1971-2004) green line and simulated WRF (1971-2004) dash line over West Africa. The standard deviation (std) and correlation (c) between of ECHAM and WRF are also indicated.

4.2.4 Comparison of RCMs Driven by ERAIN and RCMs Driven by GCMs

Here we compare the results of the RCMs (RegCM and WRF) driven by ERAIN (i.e. from the CORDEX simulations) and those of RegCM and WRF driven by HadGEM and ECHAM respectively. The performances of the RCMs driven by ERAIN as compared to those driven GCMs indicate that RegCM produces early RODs when forced by GCMs and later RODs when forced by ERAIN. By contrast, WRF produces early RODs when forced by ERAIN and later RODs when forced by GCMs.

4.2.5 Spatial Distribution of RCD For The Present Day Over West Africa

The RCDs spatial distribution for the present day simulations (1971-2004) for the RCMs (RegCM and WRF) and their driven GCMs (HadGEM and ECHAM) are given in Figure 4.34. The comparison between the observations (GPCP and TRMM) is the same as in section 4.1 and therefore not described again here. RegCM and HadGEM simulate late RCDs, especially over Guinea and northern Sahel, giving RCD in December over Guinea, between October-December over Savanna and between September-October over Sahel. RegCM does not simulate the RCD along the coast line over Liberia, Cote d'Ivoire, Ghana and Nigeria. This may be due to excess of precipitation in the model over these zones. However, HadGEM simulates better the RCD than RegCM over Guinea but fails to satisfy the RCD criteria north 14^{o}N. Thus, RegCM simulates better the RCD than HadGEM over Sahel. In spite of this deficiency, both RegCM and HadGEM produce results that are in agreement with the observed (GPCP and TRMM) over the Savanna and Sahel south of 16^{o}N. In the case of WRF and ECHAM, they both simulate much earlier RCDs over the three zones (Guinea, Savanna and Sahel). As a result, WRF and ECHAM largely underestimate as observed (GPCP and TRMM).

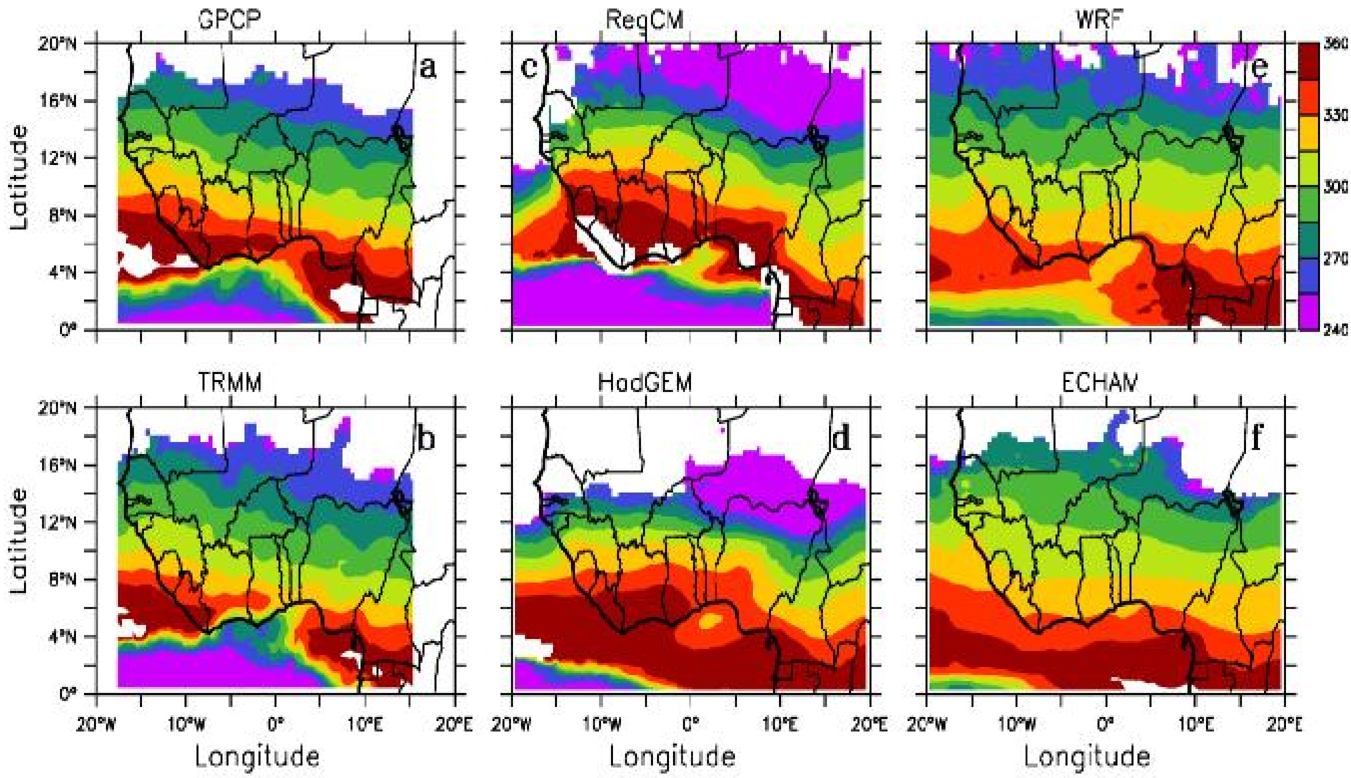

Figure 4.34 : Mean cessation dates () as observed by GPCP (1997-2004), TRMM (1998-2004), and simulated by HadGEM, RegCM, ECHAM and WRF (1971-2004).

4.3 POTENTIAL IMPACT OF CLIMATE CHANGE AND REFORESTATION ON ROD AND RCD OVER WEST AFRICA

This section examines also the second objective of the thesis. It is divided in two parts. The first part examines the potential impacts of climate change on future ROD and RCD due to elevated GHGs under the RCP4.5 scenario. The second part evaluates the potential impacts of reforestation on future ROD and RCD. The negative and positive effects of reforestation on the reforested area as well as the surrounding countries are also evaluated.

4.3.1 Projected Impacts of Greenhouses Gas (GHGs) on ROD over West Africa

In this section, the potential impacts of climate change due to elevated greenhouse gases (GHGs) on future climate is investigated using the IPCC climate scenario rcp45.

4.3.1.1 Impacts of GHGs on Surface Temperature and Rainfall

The impacts of GHGs on the future climate (under rcp45, 2031-2064) with the models HadGEM and

RegCM (Fig. 4.34), ECHAM and WRF (Fig. 4.35) indicate warmer climate throughout the years with a maximum north of 16^{o}N between June-September (Fig. 4.35&4.36 a, c) over the Sahel. These results are in agreement with the studies of Abiodun *et al.* (2012). RegCM alternately simulates the temperature changes as in HadGEM. However, the maximum is slightly more pronounced in HadGEM than in RegCM (Fig. 4.35a, c). As for WRF, it underestimates the expected changes of temperature as given in ECHAM but it shows similar results north of 12^{o}N between June-August (Fig. 4.36a, c).

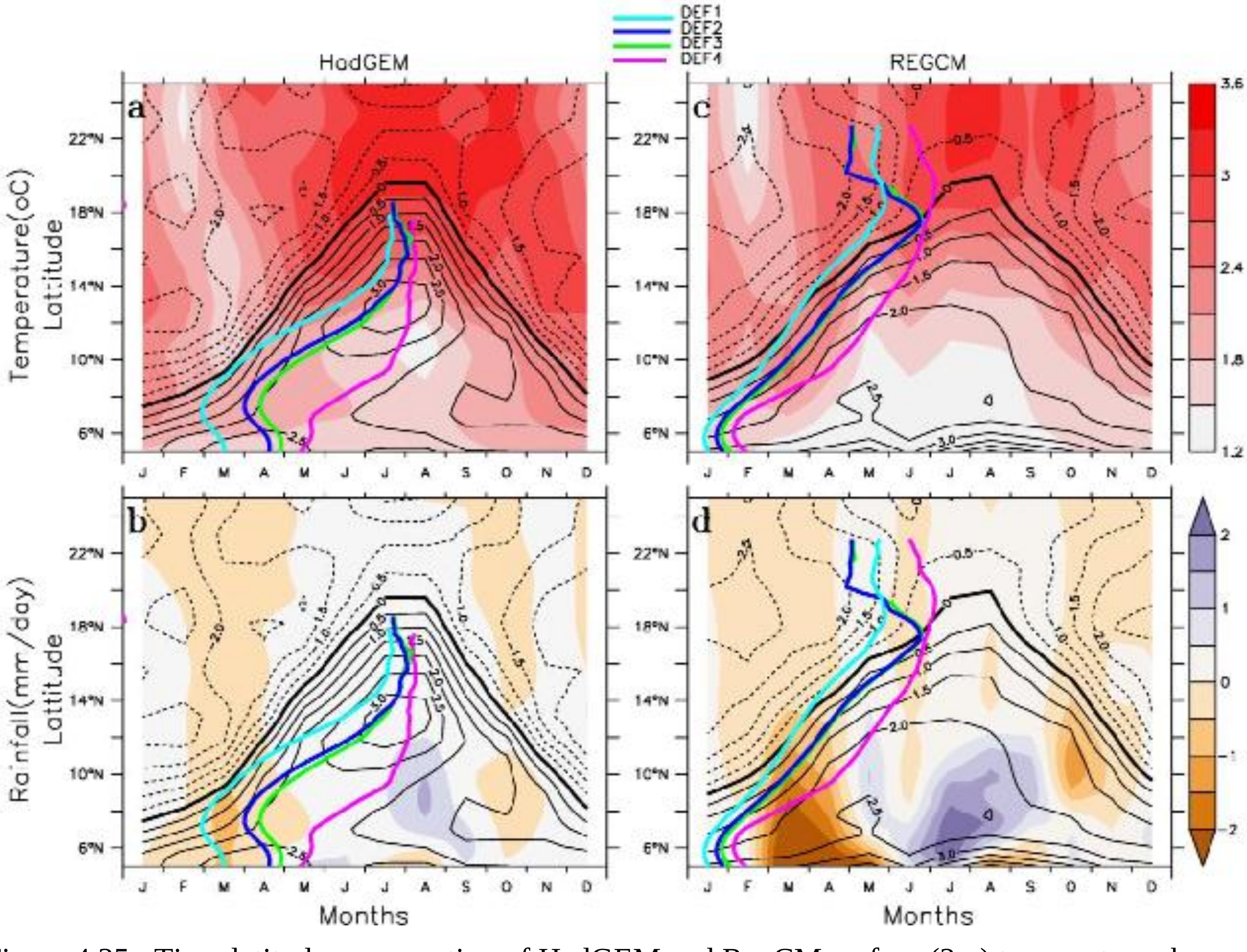

Figure 4.35 : Time-latitude cross section of HadGEM and RegCM surface (2m) temperature changes (^{o}C) top panels and rainfall changes (mmm/day) bottom panels, due to the increased GHGs (2031–2064; rcp45). The future locations of ITD (thick continuous lines), the future rainfall onset dates from four definitions (DEF1, DEF2, DEF3 and DEF4 thick colored lines) are shown. The contours are zonal wind (8°E and 8°W) averages over West Africa.

The changes in rainfall pattern due to increased GHGs show generally a decrease in rainfall in all the AOGCMs and RCMs. The decreases of rainfall are observed between February-April and October-

November in HadGEM, January-May and October-November in RegCM, north of 10°N in ECHAM in May-November and the entire year for WRF with its maximum decrease south of 14°N between May-December. In contrast, HadGEM and RegCM show that the rainfall would increase in July-September with a maximum changes at 7°N (Fig. 4.35d), while ECHAM shows a small increase between 6-10°N from June-September (Fig. 4.36b). These finding of rainfall decreases are in agreement with Abiodun *et al.* (2012) but the increases are in disagreement with the results of Abiodun *et al.* (2012) who found a decrease in rainfall between July-August and a small increase in February-March.

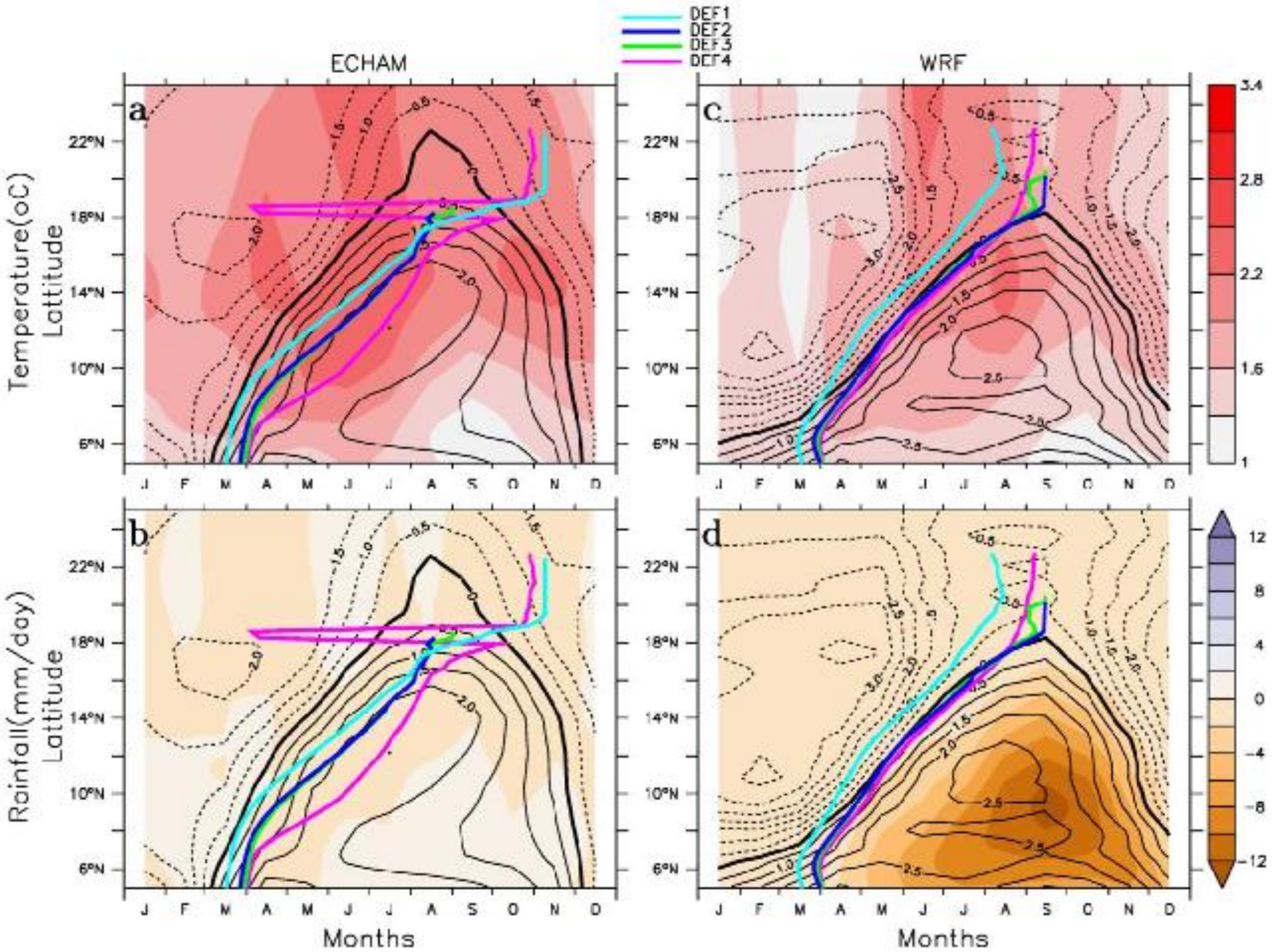

Figure 4.36 : Time-latitude cross section of ECHAM and WRF surface (2m) temperature changes (°C) top panels and rainfall changes (mmm/day) bottom panels, due to the increased GHGs (2031–2064; rcp45). The future locations of ITD (thick continuous lines), the future rainfall onset dates from four definitions (DEF1, DEF2, DEF3 and DEF4 thick colored lines) are shown. The contours are zonal wind (8°E and 8°W) averages over West Africa.

4.3.1.2 Impacts of Climate Change on JJA Temperature and Rainfall

Figures 4.37 and 4.38 indicate the spatial distribution of the changes in temperature and rainfall for June, July and August (JJA) due to increased GHGs for RegCM and WRF and their driven GCMs (HadGEM and ECHAM respectively). The projections of future climate during the JJA period shows that the RCMs RegCM and WRF produce agreement results with their corresponding AOGCMs in simulating the JJA temperature (Fig. 4.37&4.38 a, b) in all the zone except the south-eastern part of Guinea zone where RegCM underestimates the temperature as observed in HadGEM. Projections in JJA would produce a warning over West Africa with the temperature that increases from the coast to inland. The highest warming would occur over Sahel area north 14^{o}N (i.e. > +2.5^{o}C) in HadGEM and RegCM (Fig. 4.37a, b), and at about north of 12^{o}N (i.e. > +2^{o}C) in ECHAM and WRF (Fig. 4.38a, b).

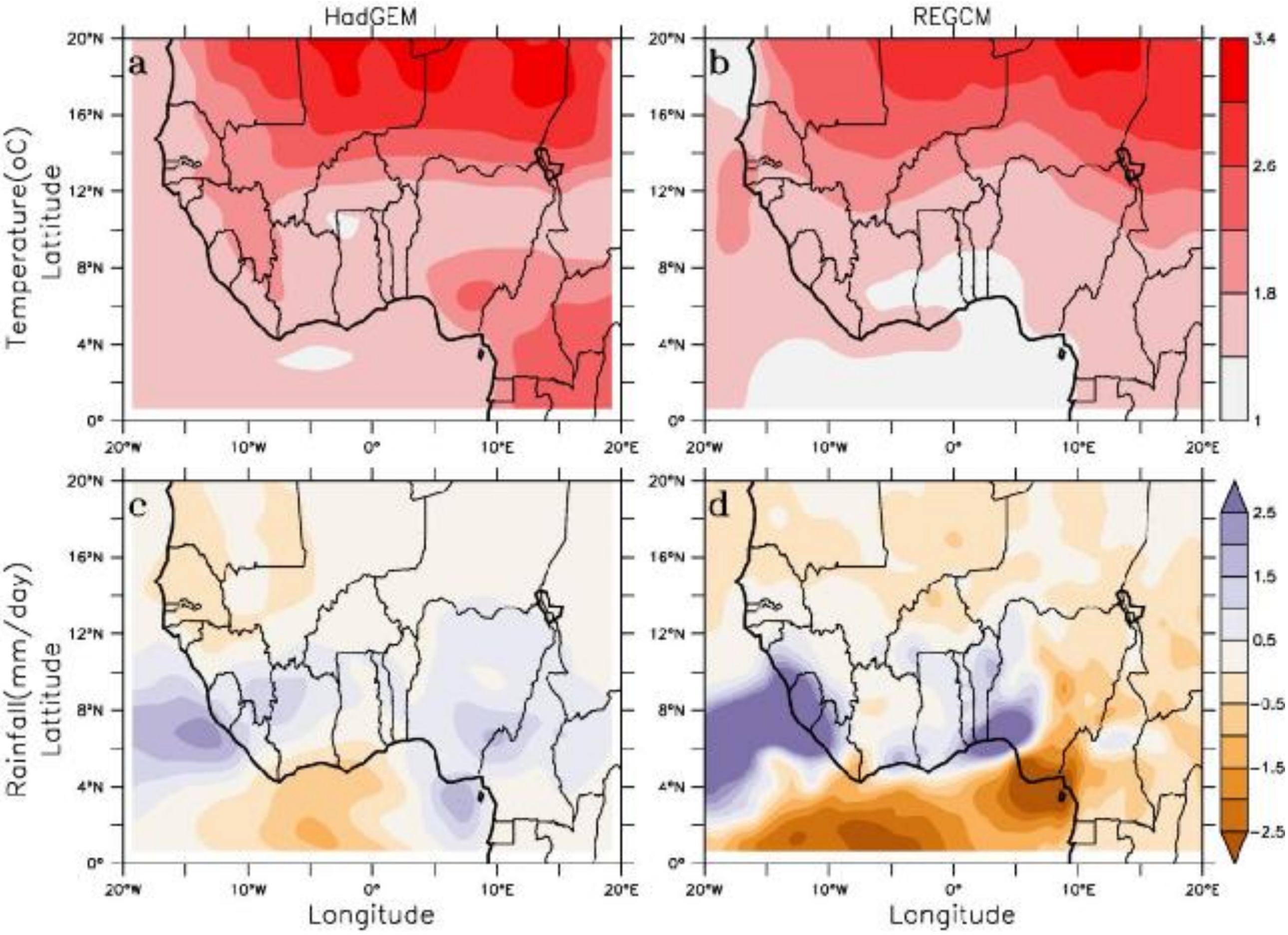

Figure 4.37: Impacts of GHGs on JJA temperature (^{o}C) and rainfall (mm/day) for HadGEM (left panels) and RegCM (right panels) under the rcp45 conditions over West Africa.

The lowest warning would occur over Guinea region south 8^{o}N (<+1.5^{o}C) in RegCM and HadGEM, and south 6^{o}N (<+1.2^{o}C) in WRF and ECHAM. The warning of the Sahel can be explained by the Sahara heat low and its associated features. This is in agreement with the results of Abiodun *et al.* (2012) and Sylla *et al.* (2010).

The changes in rainfall (Fig. 4.37c, d) show that RegCM and HadGEM produce similar results over central Guinea and Savanna but the changes are higher in RegCM than HadGEM. Both models produce also divergent results over East Guinea and over central Sahel. The highest changes in rainfall would occur in RegCM over south east Nigeria (i.e. > 3mm/day), south west Nigeria (> -3 mm/day), and over Liberia, Sierra Leone (>3 mm/day). The lowest changes would occur over Sahel in HadGEM (0.5mm/day) and RegCM (-0.5mm/day). In the other, WRF completely fails to simulate the changes in JJA rainfall as observed in ECHAM (Fig. 4.38c, d).

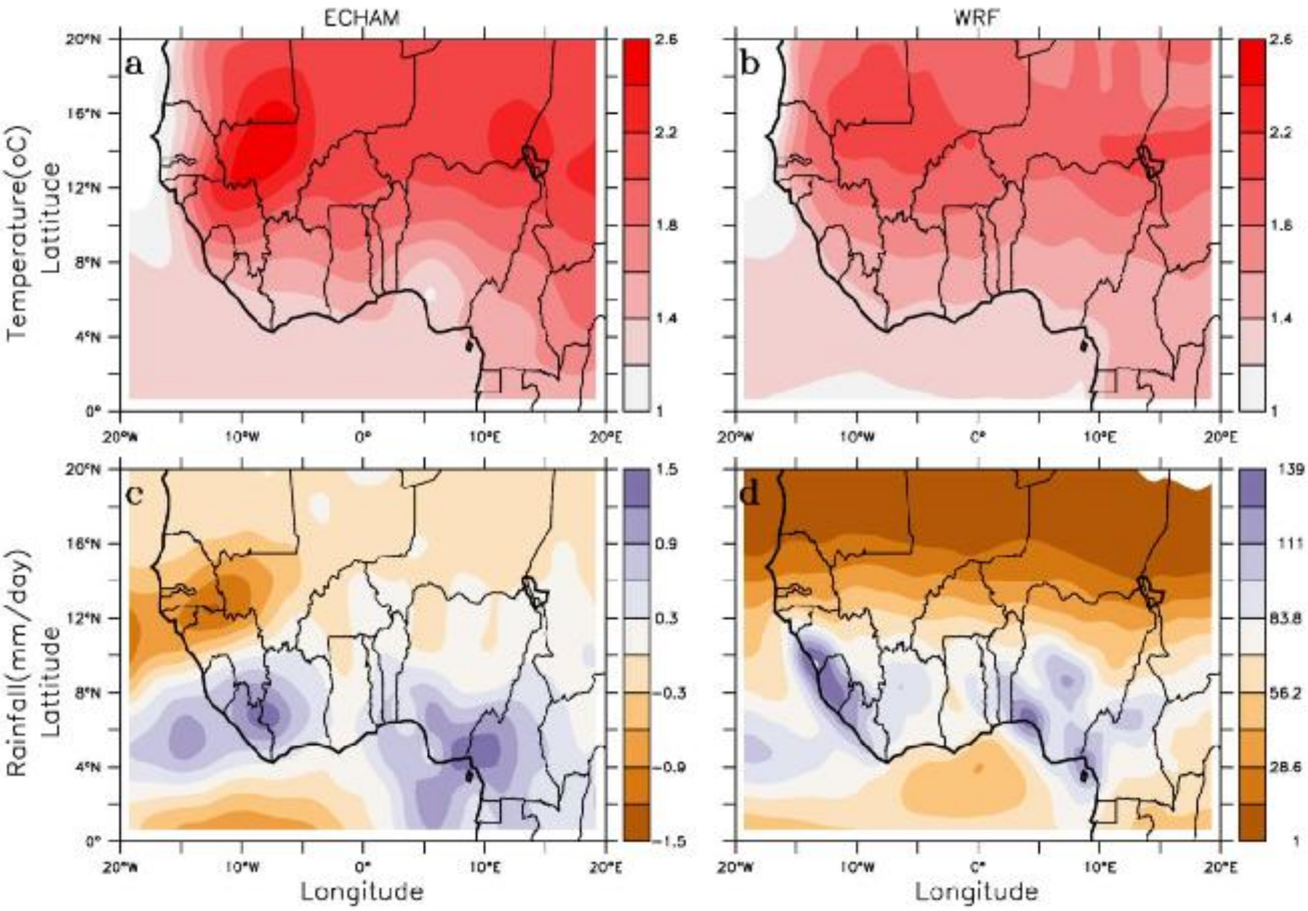

Figure 4.38 : Impacts of GHGs on JJA temperature (^{o}C) and rainfall (mm/day) for ECHAM (left panels) and WRF (right panels) under the rcp45 conditions over West Africa.

WRF indicates positive changes (increase) in rainfall in JJA over Sahel, while ECHAM produces negative changes (decrease). Over Guinea and southern part of Savanna, these models show similar results but WRF overestimates worst the changes in these zones. The highest changes would occur over south east Nigeria (i.e. > 1.5mm/day), over south Liberia and south-west Cote d' Ivoire, and western part of Sahel (> -1.5 mm/day) for the case of ECHAM and over south east and south west Nigeria (i.e. > 100mm/day), and over Liberia, Sierra Leone (> 100 mm/day) for WRF.

4.3.1.3 Impacts of Climate Change on Future ROD

From RegCM simulations (Fig. 4.39) the impact of GHGs on the future climate ROD (under rcp45 2030-2064) indicates that, regardless of the definition used central and east Savanna areas would be the most affected by delay in ROD. Similar results are obtained when WRF model is used (Fig. 4.40).

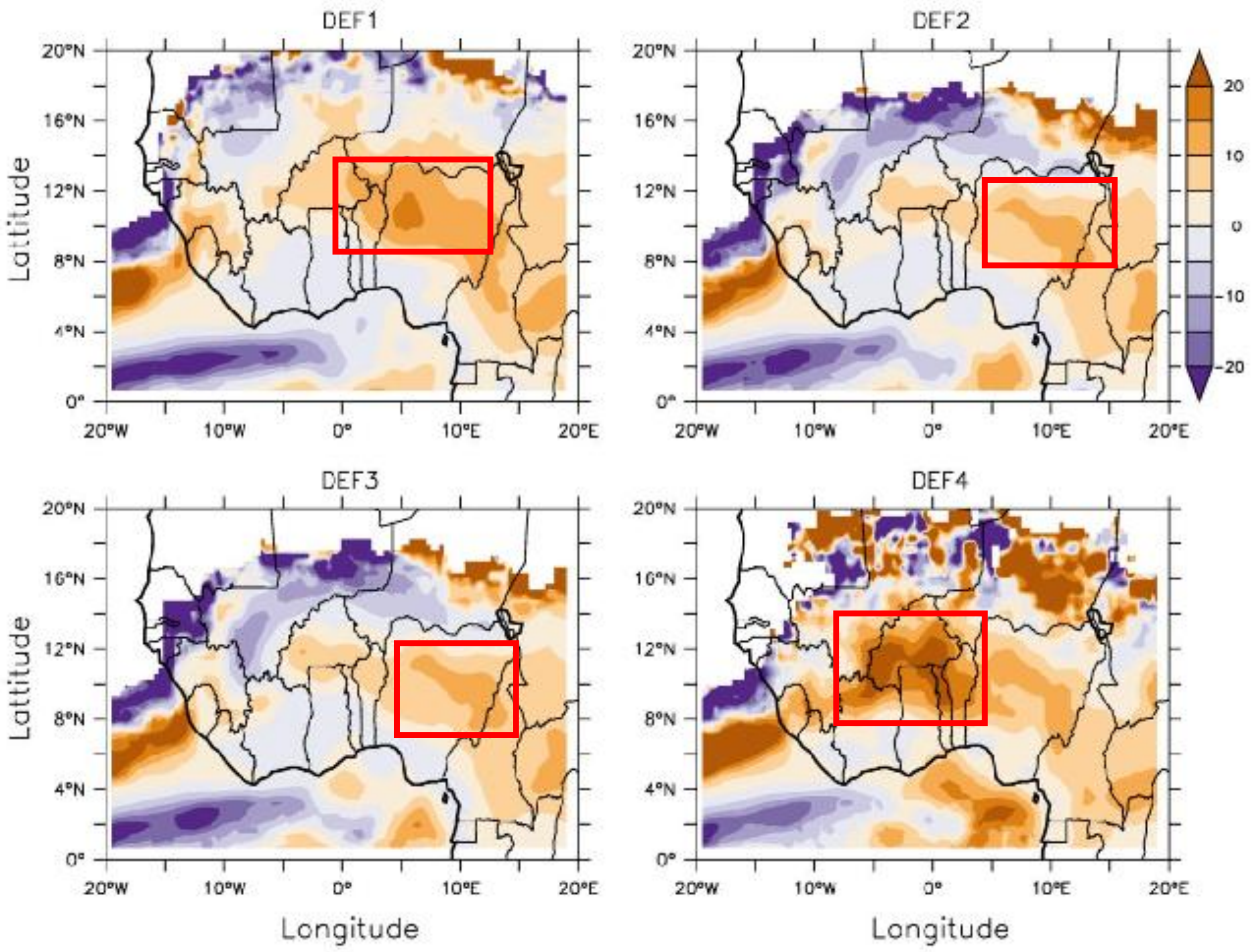

Figure 4.39 : Simulated impacts of climate change on the ROD for RegCM from four definitions (DEF1, DEF2, DEF3 and DEF4) under rcp45 conditions. The above panels show the spatial distribution of the changes in rainfall onset dates (future minus present) over West Africa.

Therefore, the impacts of GHGs on the RODs do not depend on the definitions and RCMs but the intensities vary. By contrast, the GHG impact over Savanna and Guinea depend on the definitions and RCMs used. WRF indicates late RODs over western Guinea for all definitions, while RegCM generally does not and in fact indicates rather early RODs. It is interesting to note that the patterns obtained for DEF2 and DEF3 are almost exactly similar everywhere. This may be due to the fact that DEF3 is derived from DEF2 (Mounkaila *et al.* 2014). The projected values by WRF appear on the very high side as it indicates late onset dates of the rainy season as large as 50-90 days over the Sahel and Guinea, in contrast to the highest value of just above 20 days indicated by RegCM.

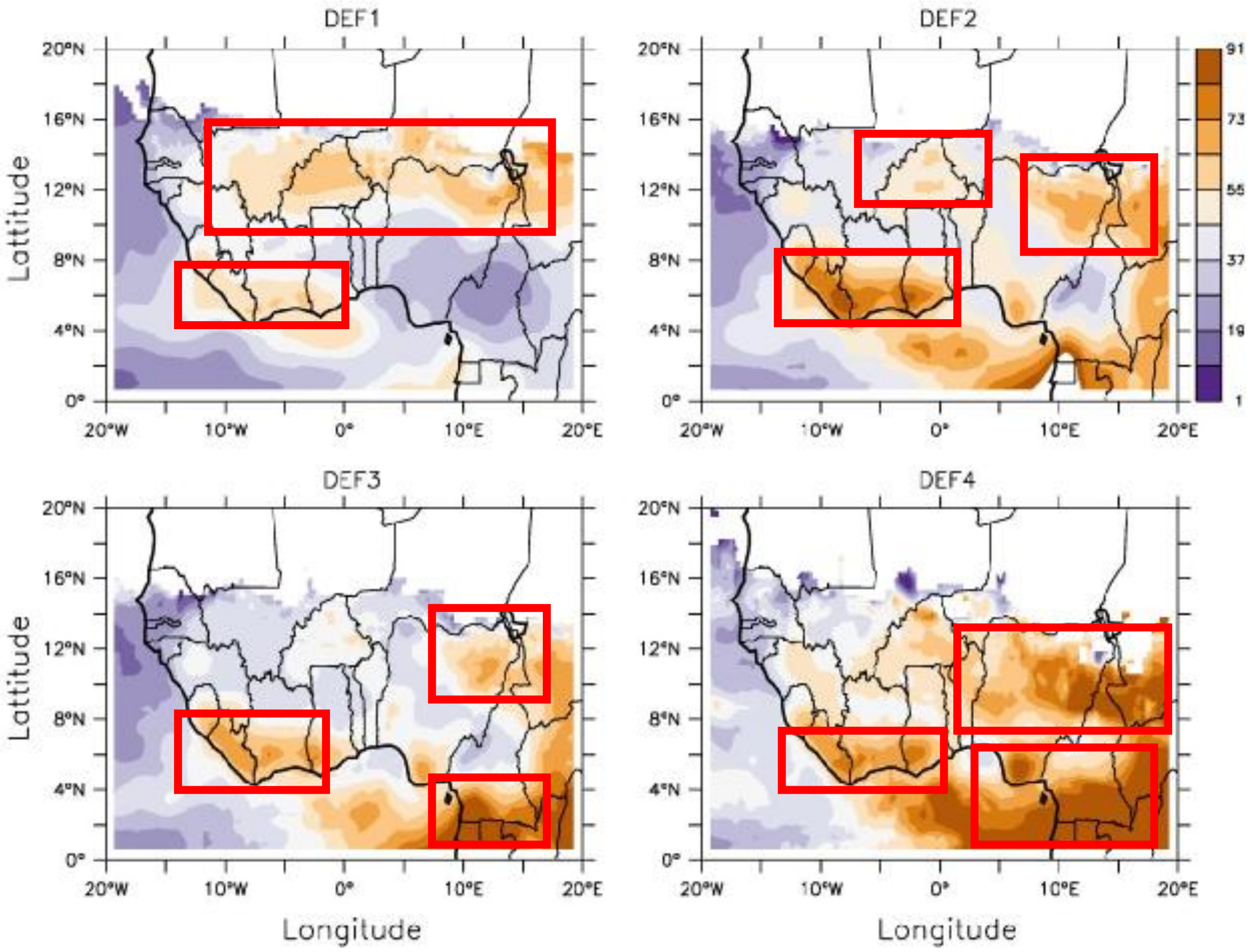

Figure 4.40 : Simulated impacts of climate change on the ROD for WRF from four definitions (DEF1, DEF2, DEF3 and DEF4) under rcp45 conditions. The above panels show the spatial distribution of the changes in rainfall onset dates (future minus present) over West Africa.

The reason of the highest impacts of ROD is not well understood. RegCM performs better than WRF in simulating ROD. Therefore, the case of the RegCM model will be investigated for two reasons.

First, it gives more realistic and consistent results in the changes of ROD compared to WRF. Secondly, WRF has shown a large bias with its corresponding AOGCM. As no significant bias has been observed with RegCM model, it will be used to analyse the highest impact of ROD observed in the definitions. For ease of reference, each definition will be assigned an area namely area1, area2, area3 and area4 (rectangles Fig. 4.38) respectively for DEF1, DEF2, DEF3, and DEF4.

4.3.1.4 Assessing the highest changes on RODs due to GHGs

To assess the highest variability of ROD observed in each area in RegCM, the projected changes in temperature, rainfall, specific humidity and equivalent potential temperature are computed to evaluate the dynamical features of the WAM around the mean RODs of the areas1-4 between the present day and future climate simulations.

4.3.1.4.1 Projected daily changes of key variables around the ROD

The simulated mean ROD for both present day (1971-2004) and future (2031-2064) in each area and the corresponding daily changes in temperature, rainfall, equivalent potential temperature and specific humidity are given in Figure 4.41. The mean RODs for present and future respectively are as follow: area1 (16 March, 28 March), area2 (27 March, 05 April), area3 (29 March, 07 April) and area4 (08 April, 24 April). Regardless the area considered, the mean ROD in the future climate is later than for the present day. Furthermore Figure 4.41 also shows that in all the areas both mean ROD (i.e. present day and future) are characterized by an increase in temperature. The warming is higher in the future than the present day in all the areas except in area4 (Fig. 4.41 blue arrow and cross) which shows cooler future). The corresponding rainfall pattern shows a decrease in rainfall of different magnitudes. Only the area1 shows higher decrease in present (-2.5 mm/day) and lower in the future (-1.4 mm/day). Areas 2, 3 and 4 show lower presently (-1.9, -2.0 mm/day) and higher in future (-2-3, -2.2 mm/day). Area4 is same pattern as for areas 2 and 3 (lower in present (-0.6 mm/day) and higher in future (-1.6 mm/day). The equivalent potential temperature gives similar results as observed with temperature, while the specific humidity confirms the decreases observed in the rainfall pattern. At the timing of the ROD, It is characterized by a decrease in all the regions except area4.

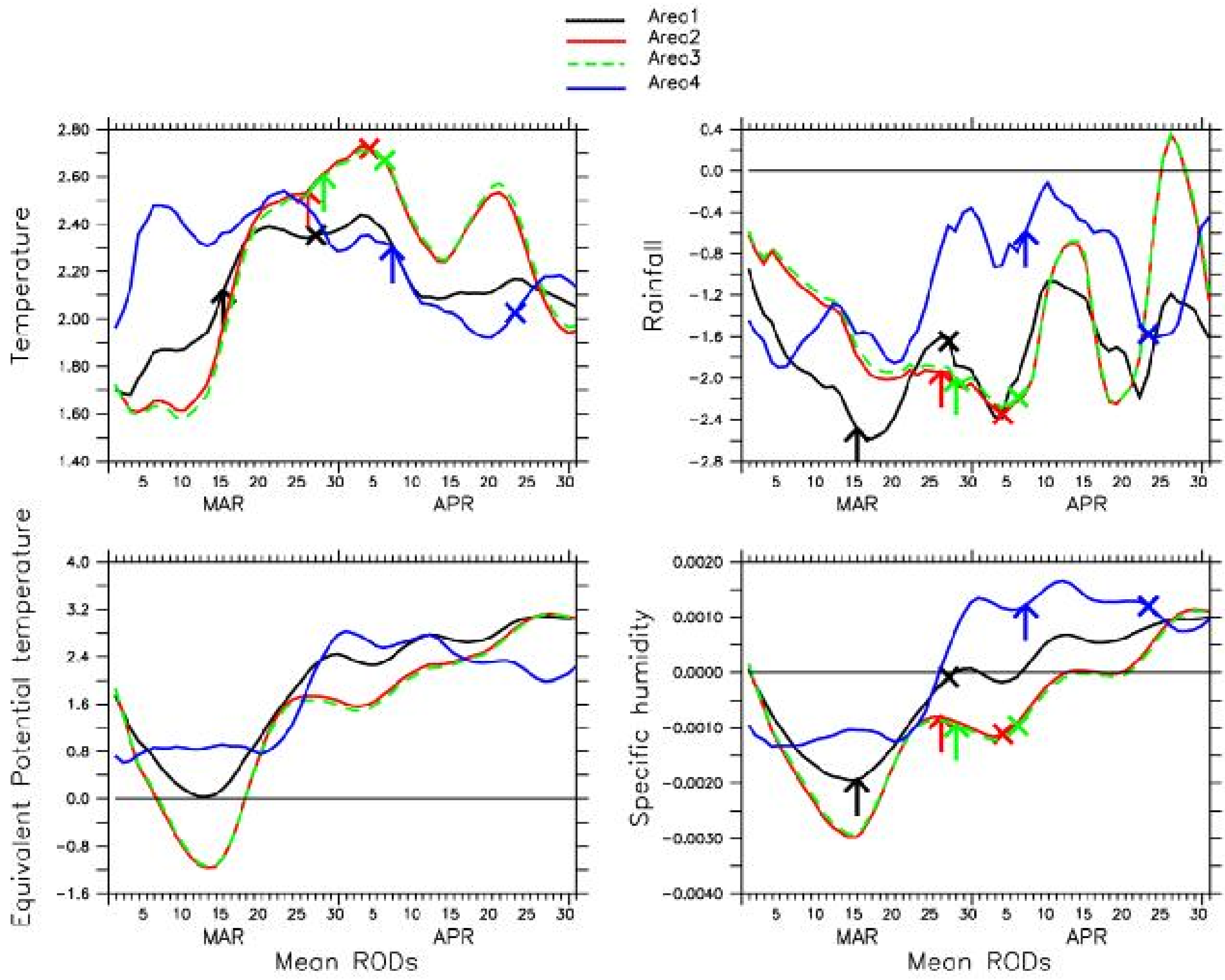

Figure 4.41: Time series of daily changes in temperature (^{o}C), rainfall (mm/day), equivalent potential temperature (^{o}C) and specific humidity (g/g) due to effects of GHGs on the projected future onset dates (2031-2064) in the four areas corresponding to the location of the highest changes in the RODs as observed with the definitions (DEF1, DEF2, DEF3 and DEF4) under rcp45 conditions over West Africa. The arrows indicate the positions of the mean ROD for present and the cross for the future.

Availability of abundant moisture is crucial for the deep convective systems which deliver about 70 percent of West African rainfall (Omotosho and Abiodun, 2007). It is therefore necessary and important to further investigate the possible future pattern of specific humidity and the potential equivalent temperature whose meridional gradient drives the monsoon that brings in the moisture over West Africa. The next two sub-sections are derived to these parameters.

4.3.1.4.2 Projected changes in specific humidity

The projected changes in specific humidity due to elevated GHGs over each area are shown in Figure 4.42. Increased specific humidity changes are expected in area1 below 900hPa over Guinea, in area2 and area3 (below 800hPa) over Guinea and Savanna and in area4 (below 700hPa) over Guinea and Savanna and southern Sahel. But regardless of the area, most of the Sahel will have little specific humidity changes and this is worse in area1 where the lowest (decreased) specific humidity is even expected. Therefore, this climatic zone (i.e. Sahel) in the future would face a warmer and drier condition due to increase in GHGs.

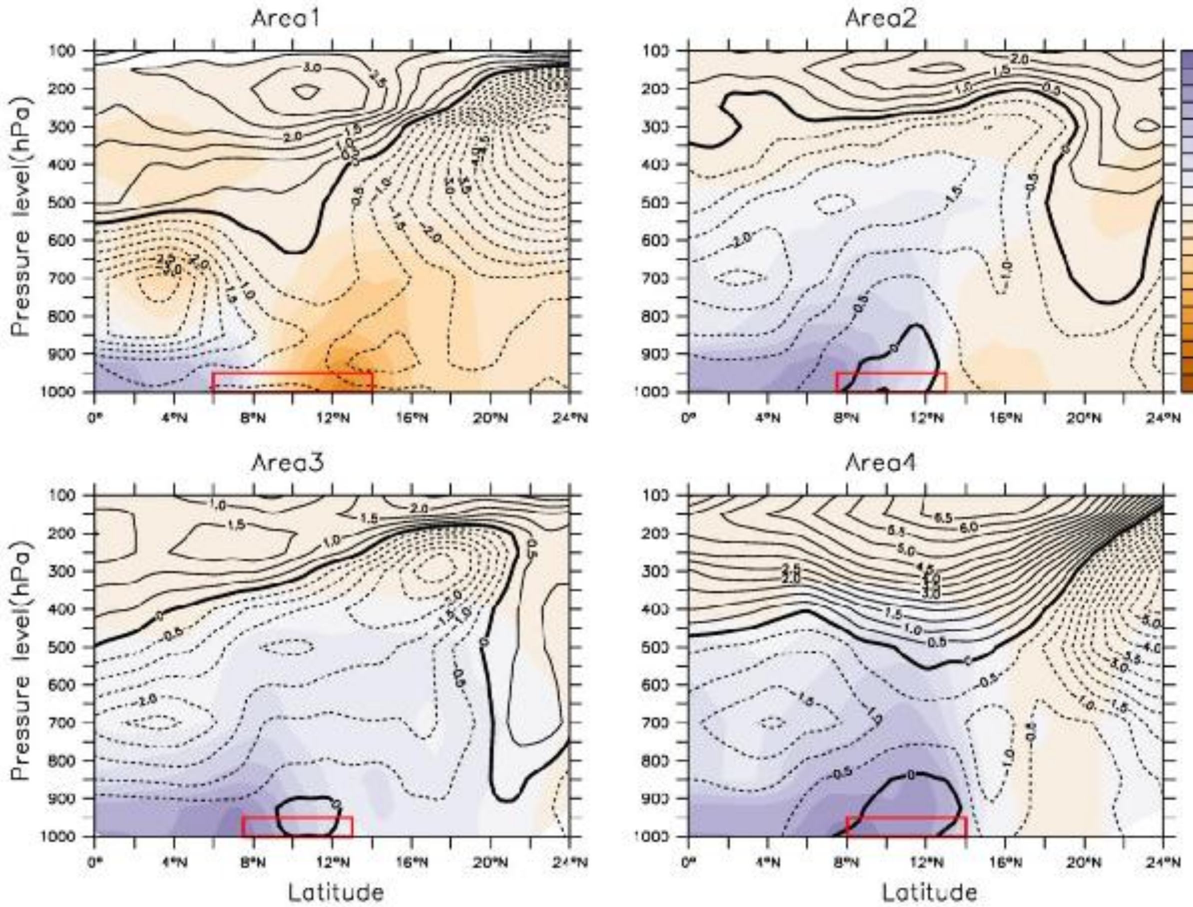

Figure 4.42 : Expected changes in specific humidity (kg/kg) due to GHGs on the projected future onset dates (2031-2064) in four areas (area1, 2, 3 and 4) identified using definitions DEF1, DEF2, DEF3 and DEF4 respectively under the rcp45 conditions over West Africa. The contours are zonal wind u(m/s). The bottom rectangles (in red) indicate the areas of interest where the latest RODs are observed.

Hence, this is why this zone would be having consistent decrease of rainfall because the monsoon flow will be ineffective due to reduced specific humidity. This is in agreement with the results of

Sylla *et al.* (2010); Abiodun *et al.* (2008, 2012) and Omotosho and Abiodun (2007). Moreover, the simulated African Easterly Jet (AEJ) at about 650-700hPa, decreases in all the areas but with different magnitudes (area1 (-3m/s), area2 (-2m/s), area3 (-2m/s), area4 (-1.5m/s). It is strongest in area1 and weaker in area4. In contrast, the Tropical Easterly Jet (TEJ) at about 200hPa, increases in all the regions and is strongest in area4 (6.5m/s) and weaker in area3 (1.5m/s).

4.3.1.4.3 Projected changes in equivalent potential temperature

The projected changes of equivalent potential temperature due to elevated GHGs shows an increase in equivalent potential temperature everywhere (Fig. 4.43) regardless of the areas but with different magnitudes.

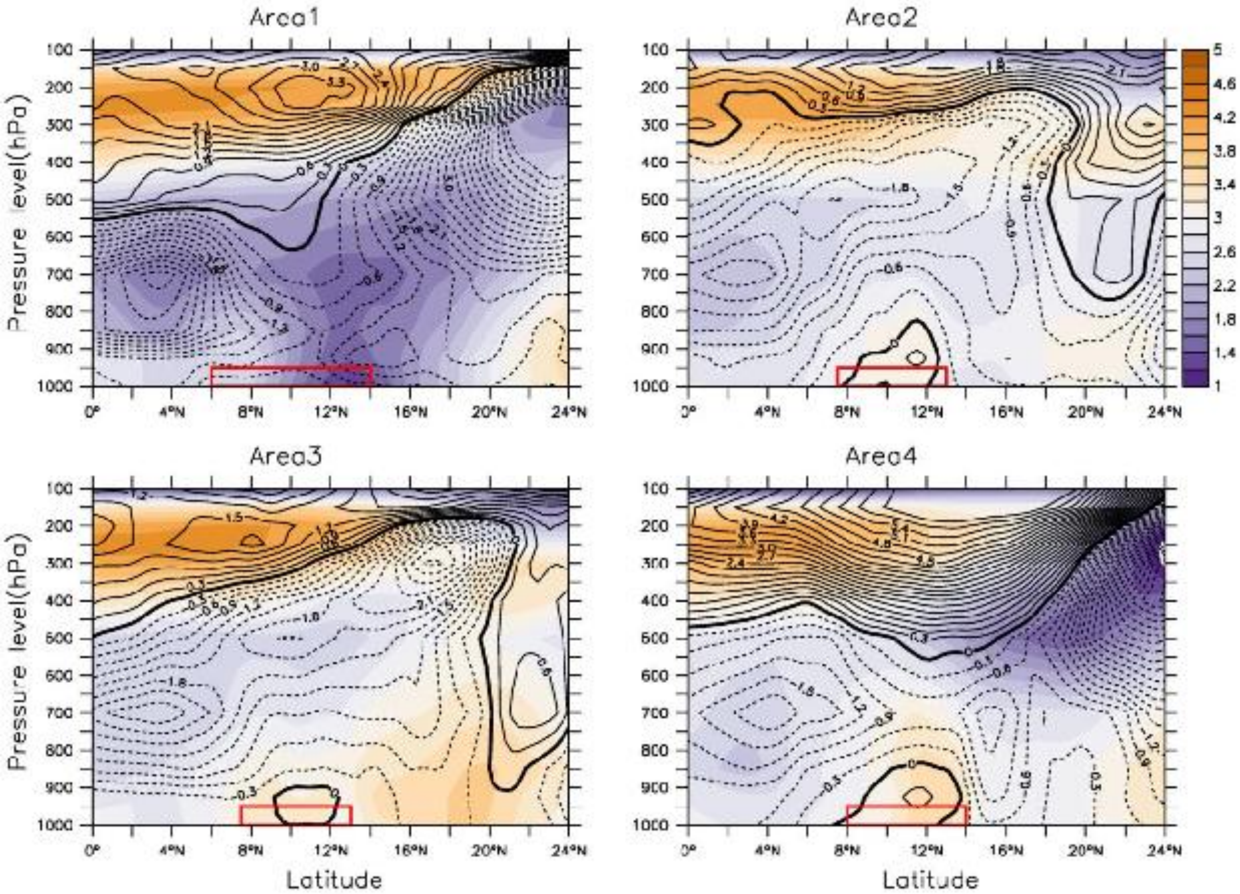

Figure 4.43 : Expected changes in equivalent potential temperature (^oC) due to GHGs on the projected future onset dates (2031-2064) in the four areas (area1, 2, 3 and 4) identified using the definitions (DEF1, DEF2, DEF3 and DEF4) under rcp45 conditions over West Africa. The contours are zonal wind u (m/s). The bottom rectangles (in red) indicate the areas of interest where the latest RODs are observed.

At the surface, the area1 produces the lowest increase (1^oC) over Savanna (about 11^oN) and Sahel (to about 16^oN), while the other three areas (area2, 3 and 4) provide the highest increase (>3^oC) over Savanna and Sahel respectively. However, in the upper troposphere (between 100hPa to 300hPa), the equivalent temperature is at its maximum with maximum increase of (>4.5^oC) regardless of the areas considered. The characteristics of AEJ and TEJ are similar to that of the projected changes in specific humidity. Therefore, these increases of equivalent potential temperature with height from the surface would induce a stably stratified atmosphere and convective systems are not likely to occur in these conditions. Thus, the decrease in rainfall observed previously.

The results obtained here indicate a warmer and drier climate especially over Sahel due to GHGs increases and are consistent with previous studies (e.g. Abiodun *et al.*, 2012). For instance Omotosho and Abiodun (2007) have shown that for a deep convection to occur, the moisture much reach a certain limit and depth for rains to occur otherwise no rain or only little will occur.

4.3.2 Projected impact of reforestation on future rainfall onset over West Africa

In the previous section, we have studied future climate change impacts on rainfall factors RODs and RCD with increased GHGs but these were done with present forestation. In the following sections, we investigated the effects of reforestation on the projected RODs and RCDs.

4.3.2.1 Impacts of Reforestation on Surface Temperature and Rainfall

Figure 4.44 depicts the impact of reforestation on the future climate (under rcp45 2030-2064) over West Africa. The Savanna zone (8^o-12^oN) is chosen as the reforested area. It can be seen that reforestation would induce a cooling effect over the reforested area for both regional climate models RegCM and WRF. As a result, the temperature decreases over Savanna with the lowest decrease of -0.5^oC in RegCM (Fig. 4.44a) and -1.8^oC in WRF (Fig. 4.44d).

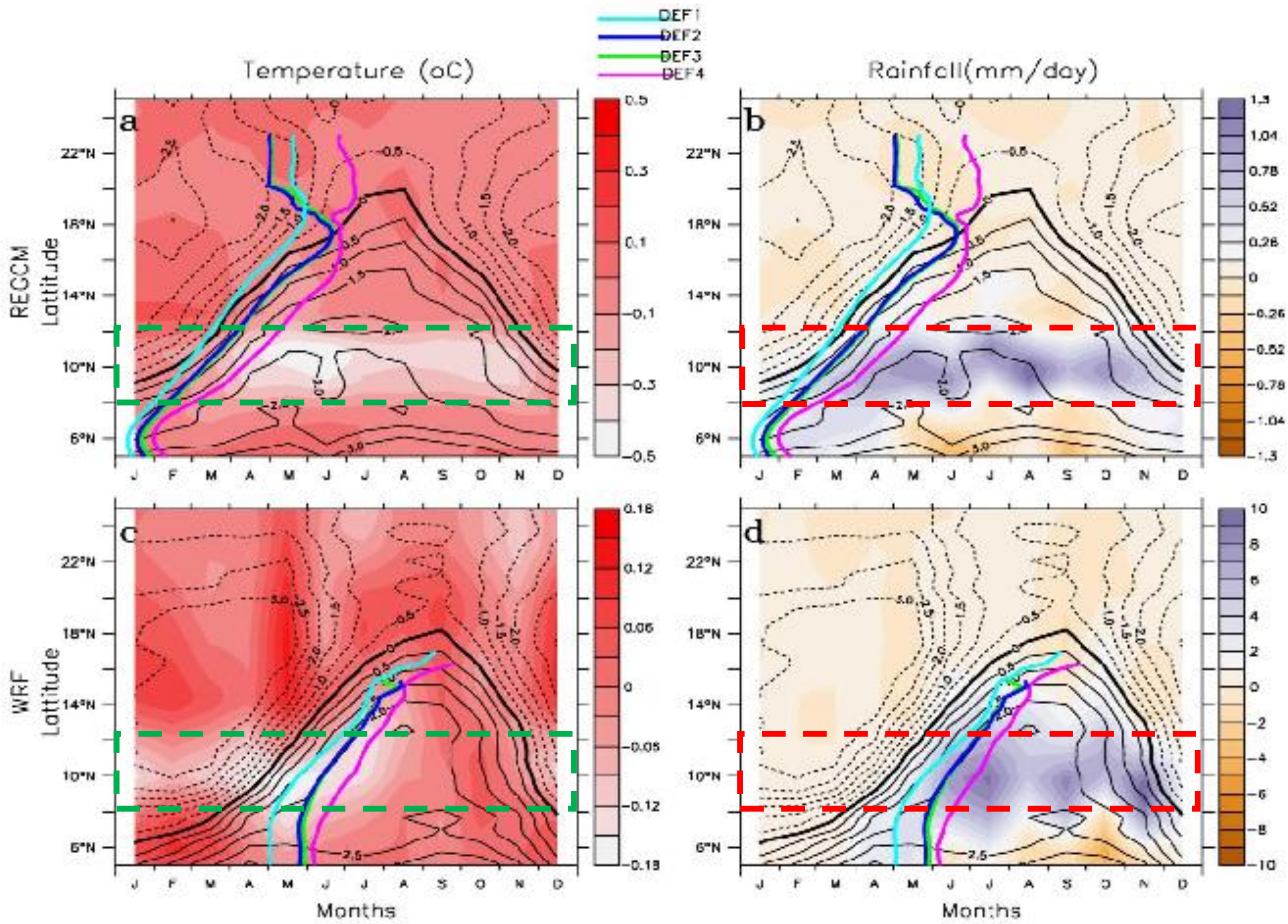

Figure 4.44 : Time-latitude cross section of changes in 2m surface temperature (°C) and rainfall (mm/day) for RegCM (top panel) and WRF (bottom panel) due to reforestion in the future (2031–2064; rcp45). The future locations of ITD (thick continuous lines), thick colored lines are the onset of rainfall from four definitions (DEF1, DEF2, DEF3 and DEF4). The contours are the zonal wind averages between 8°E and 8°W over West Africa. Reforested zone is marked by thick green dashed lines.

The decreases occur from March-November in RegCM and March-July in WRF. The cooling effect hardly extends beyond the Savanna to the surrounding areas of Guinea and Sahel, for both RCMs with induced warming over these areas. The changes in rainfall due to reforestation (Fig. 4.44 b, d) indicate significant increase in rainfall over the reforested area (Savanna) in both RegCM and WRF. The highest increase over Savanna occurs from March to October (+1.3 mm/day) in RegCM and as much as +10 mm/day from June to November in WRF. In the other hand, the changes in surface rainfall also show a decrease in rainfall over Guinea and Sahel in both RCMs. Figure 4.44 also shows that the ITD is located over the reforested area in WRF but not so in RegCM. In addition, early

RODs are observed for all the definitions from January-February over all the zones with RegCM. In contrast, WRF gives later RODs for all the definitions from April-May over Guinea and July-August over the Sahel. These results are in good agreement with previous studies (e.g. Bernier *et al.*, 2011; Abiodun *et al.*, 2012).

4.3.2.2 Projected changes of JJA temperature and rainfall due to reforestation

The spatial distribution of the JJA changes in temperature and rainfall due to reforestation (Fig. 4.45) shows that a cooling effect over the reforested area with a maximum of about -0.6^{o}C for RegCM (Fig. 4.45a) and -0.15^{o}C for WRF (Fig. 4.45c).

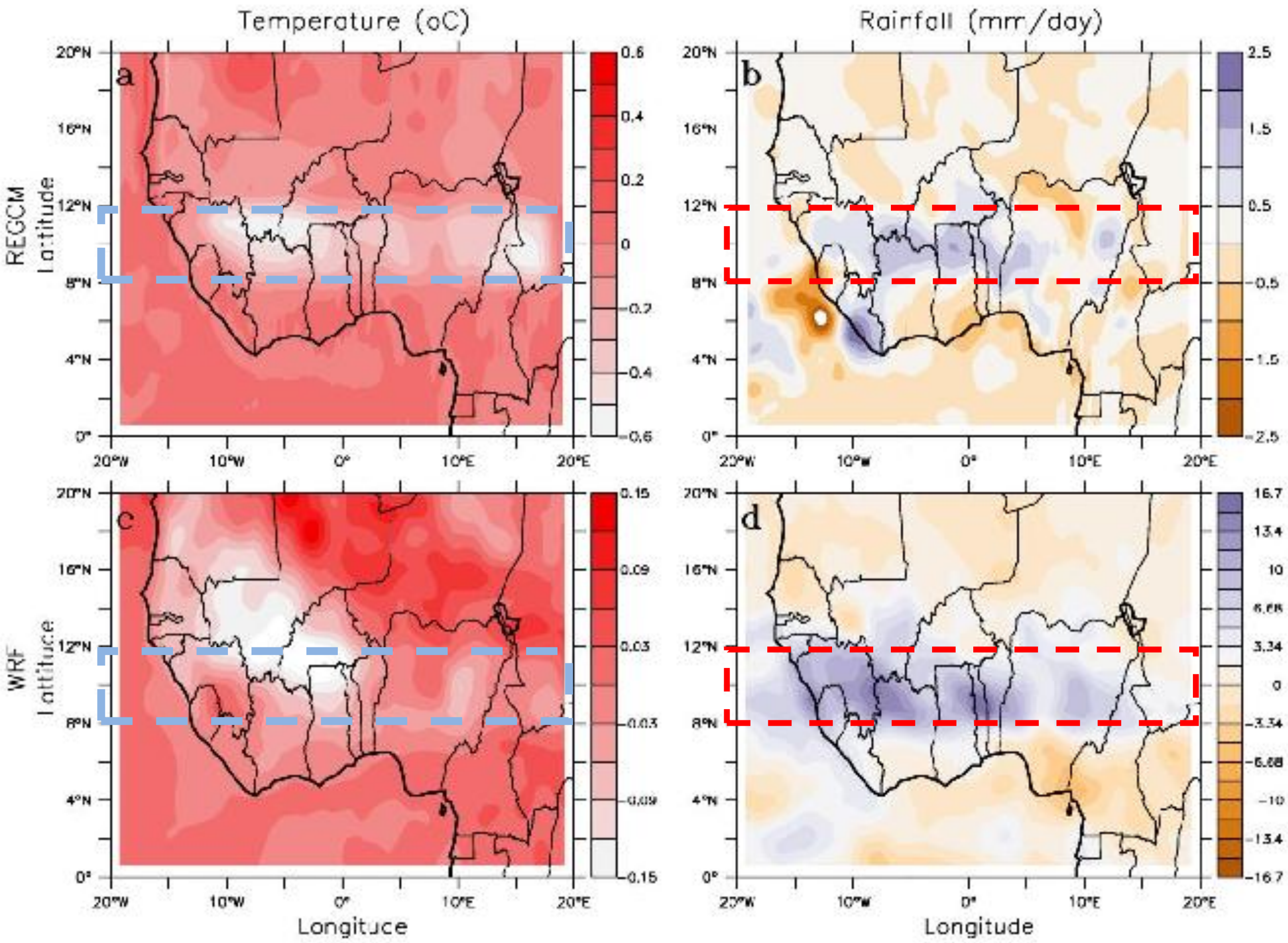

Figure 4.45 : Simulated impacts of reforestation over Savanna (8^{o}N-12^{o}N) under rcp45 conditions (2031–2064) with RegCM (top panel) and WRF (bottom panel) of the projected changes in JJA temperature (^{o}C) left panel and rainfall (mm/day) right panel.

This decrease in temperature is greater over western part of Sahel in WRF, while there is an increase in temperature over the reforested region in Nigeria in both models. Similarly, the changes in JJA rainfall due to reforestation show that most of the Savanna in both RegCM and WRF (Fig. 4.45 b, d) would experience rainfall increases but western and central Savanna would be the most affected by the increase of rainfall for the case of WRF, with increase up to 15mm/day over the reforested area. RegCM indicates also an increase of rainfall outside the reforested area over eastern part of Guinea (i.e. Liberia), while WRF shows the increase over south-west Sahel (i.e. Mali). Previous studies by Montenegro et al. (2009) and Bathiany et al. (2010) have obtained similar results. Furthermore, both RCMs simulate decrease in rainfall in most areas over Guinea and Sahel zones.

4.3.2.3 Potential Impacts of Reforestation on Future ROD

Figures 4.46 and 4.47 show the potential impacts of reforestation on the future climate onset dates (simulated future onset with reforestation minus future onset without reforestation). Comparison between the future simulations with reforestation and without reforestation are made to evaluate the impact of reforestation because this study focuses on the potential impacts of reforestation options on the future climate (2031–2064) under the rcp45 condition of GHGs, not on the present-day climate (1971–2004). Regardless the definitions used, both RCMs (RegCM and WRF) indicate that reforestation over the Savanna would induce negative changes in ROD (i.e. early ROD) over most areas of West Africa, except over north Nigeria in RegCM. However, DEF4 gives the highest ROD changes (much earlier ROD) among the definitions for RegCM and the spatial distribution of the changes are more uniform in RegCM than WRF.

Very significantly, Figures 4.46 and 4.47 also indicate that the areas where the maximum ROD changes occur are different from the reforested zone in the case of increase GHGs. Therefore, we select again the areas of highest ROD impact for each RCM (boxes in Fig. 4.46&4.47) in order to understand the reasons for the higher variability. Thus, as in section 4.2.2, four areas (area1, 2, 3 and

4 for DEF1, DEF2, DEF3, and DEF4 respectively) are chosen for the RegCM only to investigate the reasons for the potential impacts of reforestation.

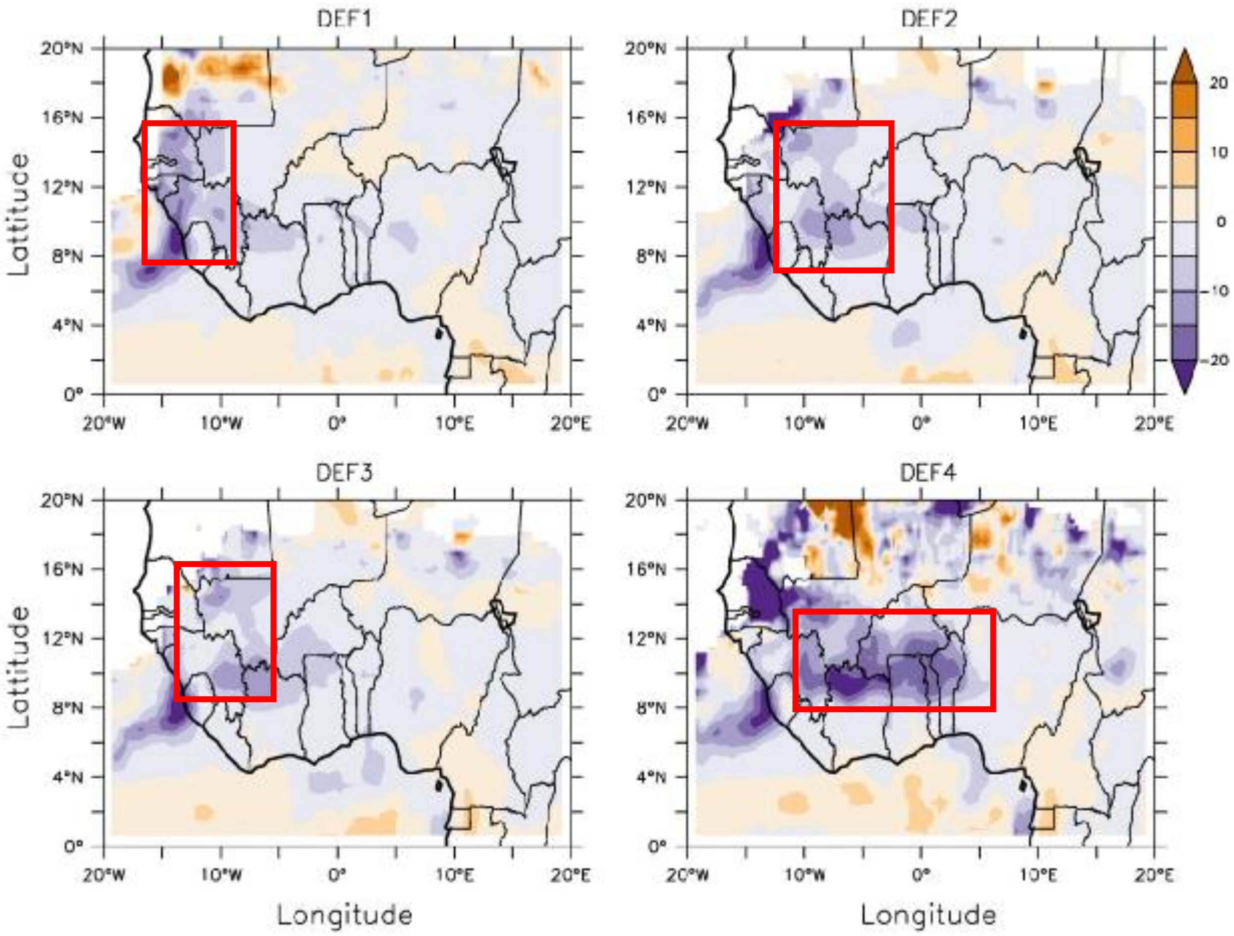

Figure 4.46 : Simulated impacts of reforestation on the projected future mean onset dates (2031-2064) from four definitions (DEF1, DEF2, DEF3 and DEF4) under rcp45 conditions using RegCM. The panels represent the changes in onset dates (future onset with reforestation minus future onset without reforestation) over West Africa. The boxes show the areas of highest impact on ROD.

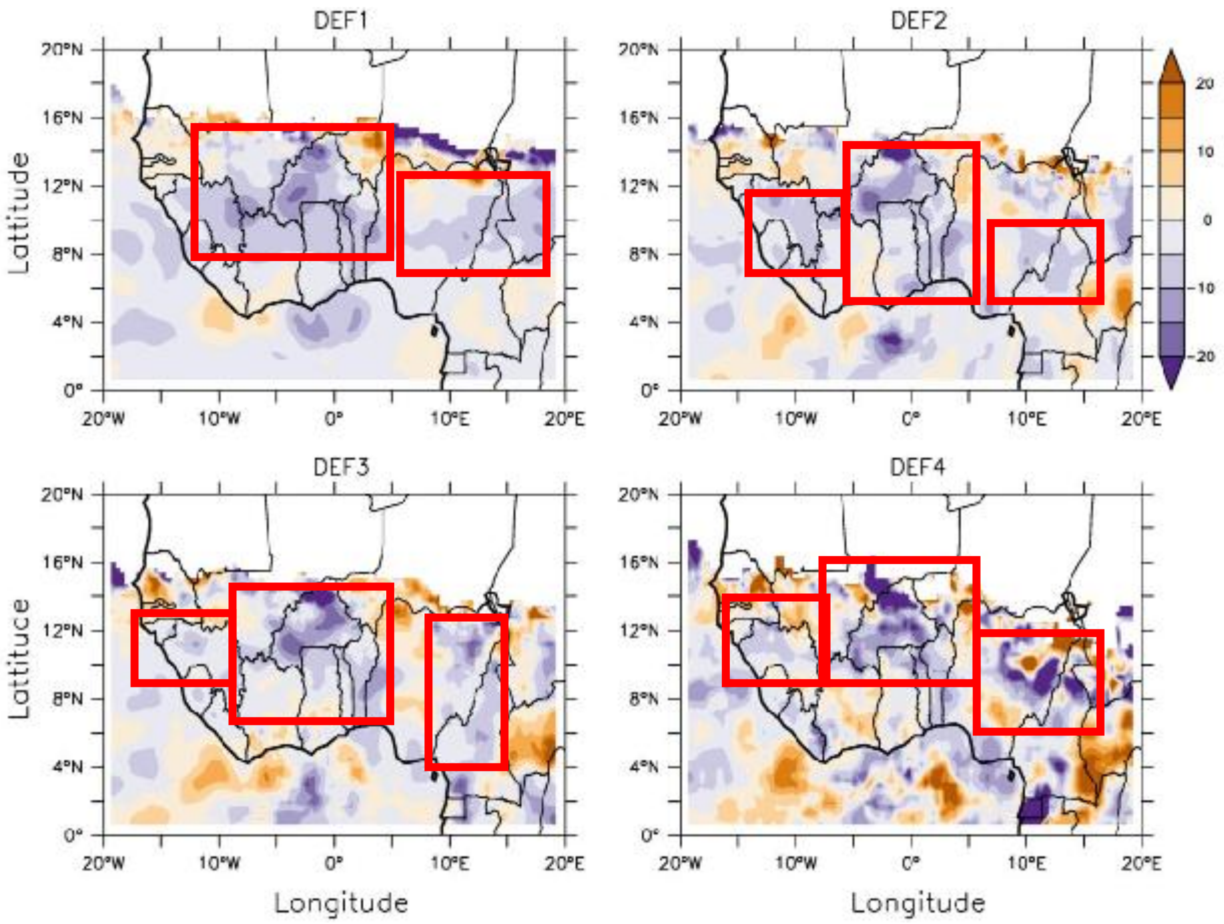

Figure 4.47 : Simulated impacts of reforestation on the projected future mean onset dates (2031-2064) from four definitions (DEF1, DEF2, DEF3 and DEF4) under rcp45 conditions using WRF. The panels represent the changes in onset dates (future onset with reforestation minus future onset without reforestation) over West Africa. The boxes show the areas of highest impact on ROD.

4.3.2.4 Assessing the highest changes on RODs due reforestation

The simulated mean ROD for both future without reforestation and future with reforestation (2031-2064) in the areas of highest changes on ROD (Fig. 4.46) are calculated and the results are given as follows: area1 (25 February, 18 February), area2 (07 March, 28 February), area3 (01 April, 24 March) and area4 (19 April, 05 April). Hence, regardless of the areas considered, the future mean ROD with reforestation is earlier than the mean ROD without reforestation. In this section, we investigate the reasons of the potential impacts of reforestation on these areas.

4.3.2.4.1 Projected daily changes of key variables around the mean ROD

Figure 4.48 gives the daily of the changes in temperature, rainfall, specific humidity and potential equivalent temperature around the mean ROD for the four areas. It shows that the temperature decreases because of reforestation in all the areas but the cooling is higher in areas1, 2, and 3 than area4. Previous studies also obtained decrease in temperature due to reforestation (e.g. Bernier *et al.*, 2011; Abiodun *et al.*, 2012). The corresponding changes in rainfall pattern due to reforestation shows an increase in rainfall in all the areas. The other variables at the surface (i.e. specific humidity and equivalent potential temperature) produce general decrease in temperature due to reforestation but area4 has an increase in specific humidity.

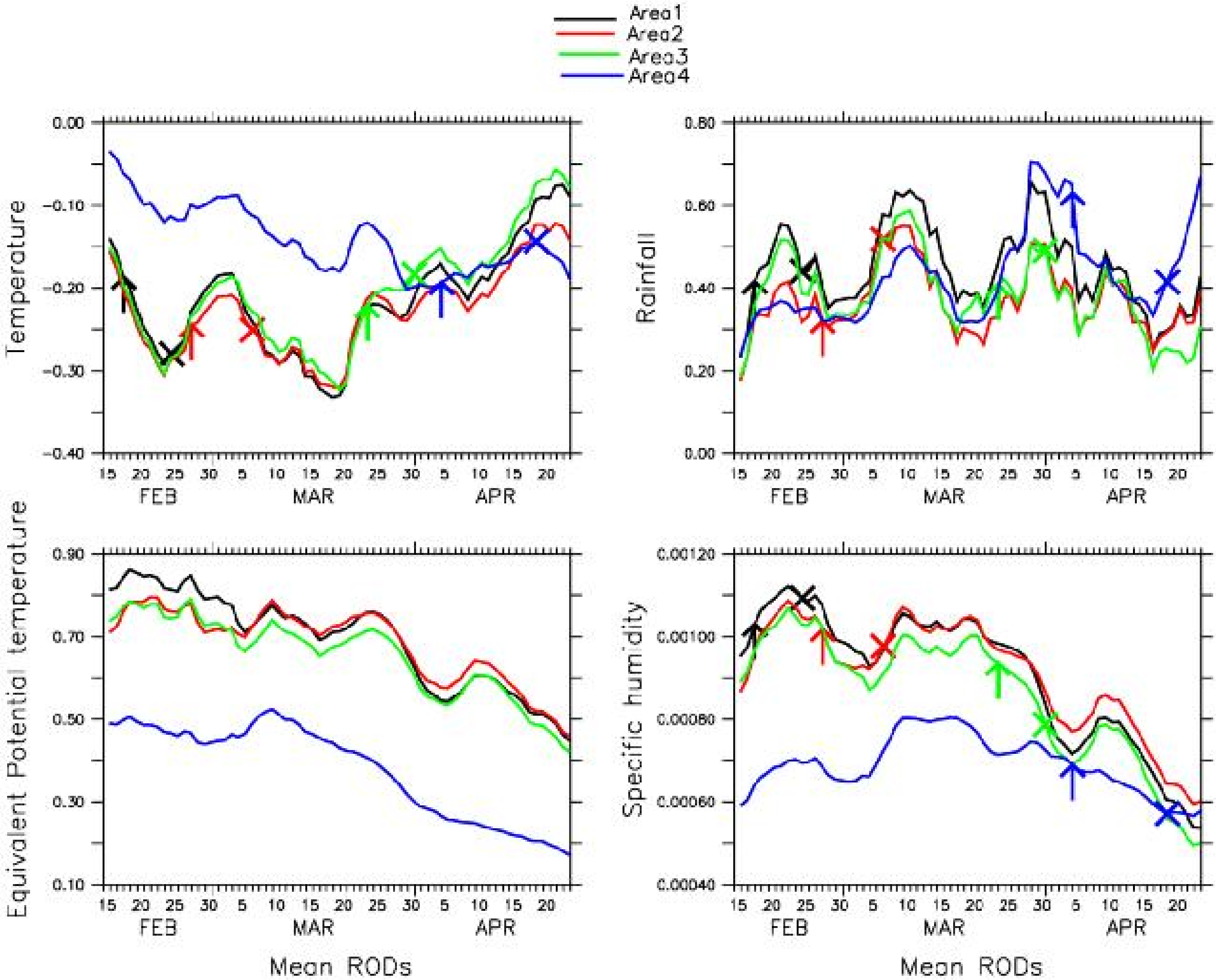

Figure 4.48 : Time series of daily of changes in temperature (^oC), rainfall (mm/day), equivalent potential temperature (^oC) and specific humidity (g/g) due to effects of reforestation on the projected future onset dates (2031-2064) in the four areas under the rcp45 conditions over West Africa. Arrows indicate the mean ROD positions for future with reforestation and the cross future mean ROD without reforestation.

4.3.2.4.2 Projected changes in specific humidity

To understand the monsoonal rainfall processes during the mean ROD period, the vertical structure of the monsoon system was computed in each area. The changes of specific humidity due to reforestation (Fig. 4.49) indicate an increase in monsoon moisture over the reforested zone over all the four areas. The projected changes in specific humidity show stronger monsoon flow everywhere over the reforested area (Fig. 4.49) particularly below 900hPa but it is stronger in area1, 2, and 3 than in area4. Therefore, this climatic zone (i.e. Savanna) in the future would face a warner and more humid condition due to reforestation.

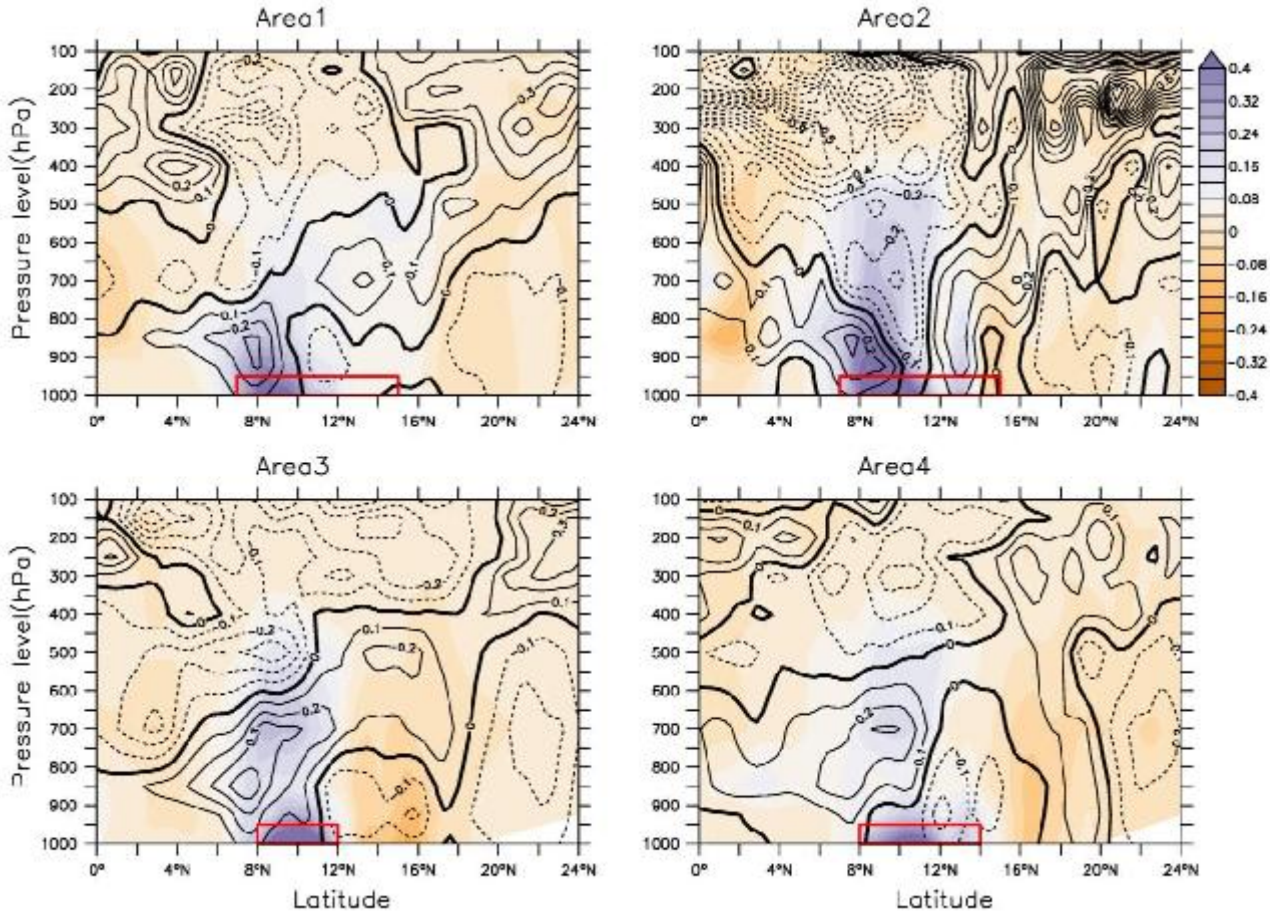

Figure 4.49 : Changes in specific humidity (kg/kg) due to reforestation on the projected future onset dates (2031-2064) in the four areas under the rcp45 conditions over West Africa. Contours are zonal wind (m/s). Red boxes indicate the areas where the earliest RODs are observed.

This is in agreement with Abiodun *et al.* (2012) who showed that the increase of rainfall over the forested area can be explained by an increase in evapotranspiration and moisture flux convergence over the forests area. Figure 4.49 also shows that the monsoon flow is weaker outside the reforested area and becomes weakest over the Sahel over the area2, 3 and 4. The simulated African Easterly Jet

(AEJ, 650-700hPa) increases in the areas2 and 3 over the reforested area but will be weaker except in area1 and 4. The changes are strongest in area2 and area3 but weakest in area1 and area4. For the Tropical Easterly Jet (TEJ, about 200hPa), it increases everywhere over the forested area and the surrounding regions.

4.3.2.4.3 Projected changes in equivalent potential temperature

The projected changes of equivalent potential temperature due to reforestation are depicted in Figure 4.50. It can be seen that the equivalent potential temperature increases over the reforested area everywhere just as the specific humidity (Fig. 4.50).

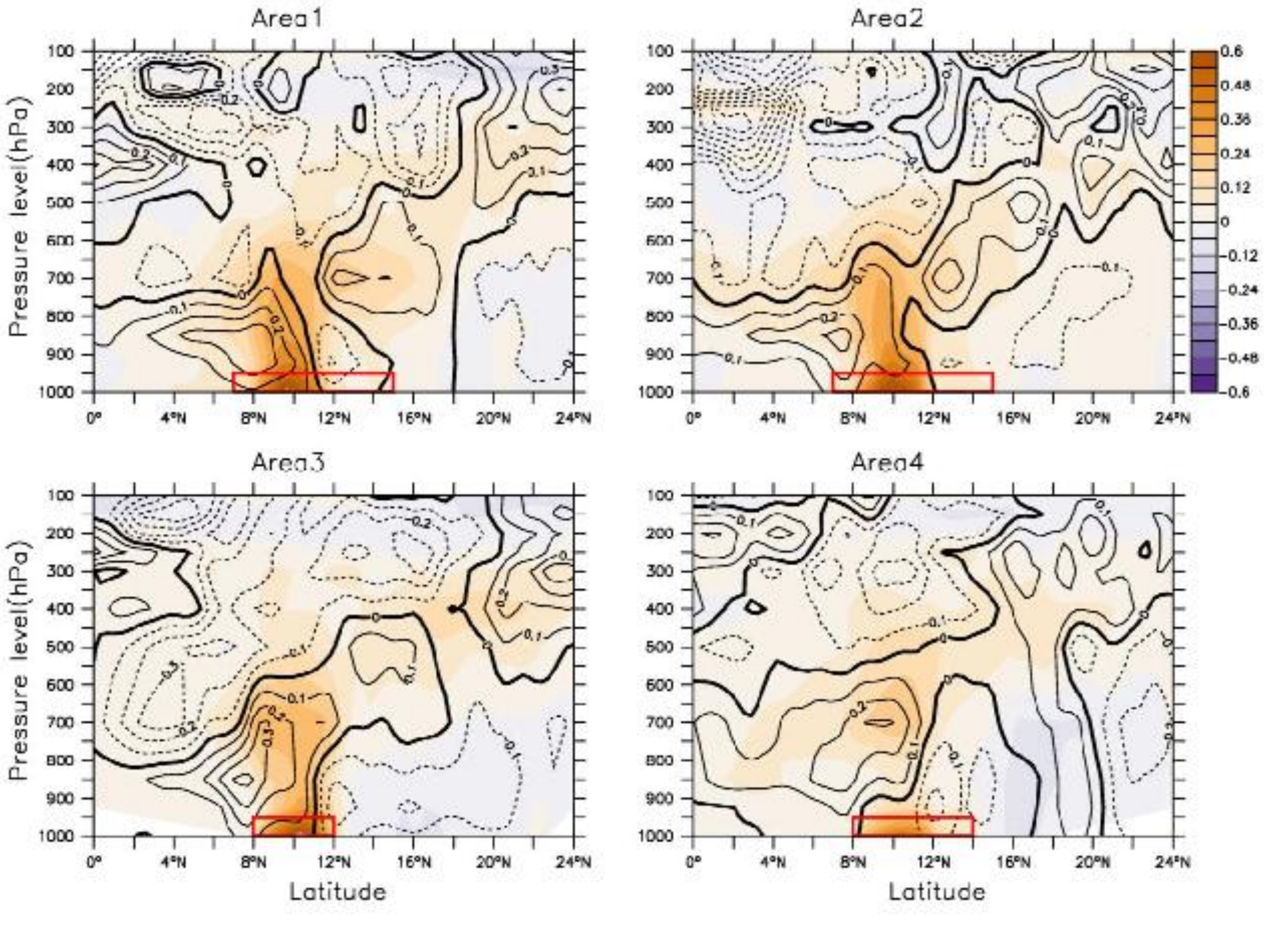

Figure 4.50 : Changes in equivalent potential temperature (^oC) due to reforestation on the projected future onset dates (2031-2064) in the four areas under the rcp45 conditions over West Africa. Contours are zonal wind (m/s). Red boxes indicate the areas where the earliest RODs are observed.

The increases reach up to about 600 hPa but are stronger over the Savanna, especially in areas 1 and 2. There are only very small increases outside the reforested area. The characteristics of AEJ and TEJ with the equivalent potential temperature are essentially similar to that of the projected changes in specific humidity. The above temperature conditions due to reforestation would induce an unstable atmosphere which will lead to more convective systems over the reforested area (Abiodun *et al.*, 2012). This is consistent with the increase in rainfall observed over the Savanna zone. However, the monsoon flow decreases outside the reforested area especially over the Sahel. This will produce a delay in ROD over Sahel because the depth of the monsoon flow will be shallower. This is consistent with previous results (e.g. Abiodun *et al.* 2012).

4.3.3 Impact of climate change and reforestation on the RCDs over West Africa

In the following two sections, the impacts of climate change and reforestation on the rainy season cessation dates (RCDs) are investigated as any change in RCDs will also affect the length of the rainy season and consequently the cropping systems.

4.3.3.1 Impact of climate change on the RCD over West Africa

The projected impacts of GHGs on the future RCD under the rcp45 (Fig. 4.51) show markedly different results between RegCM and WRF. RegCM indicates that later RCDs would likely be observed over central Sahel (i.e. central part of Mali and western part of Niger) and central part of Ghana and Togo with early RCDs over central Savanna (Burkina Faso and south Mali). RegCM did not capture any changes in RCD along the coast line as it failed to do in Fig. 4.34. In complete contrast, WRF indicates that the entire West African countries would likely observe earlier RCDs in the future due to GHGs, with the earliest over Sahel. This means that the future simulations of the RCD with WRF under the rcp45 produce very early RCDs as compared to the present day simulations. The reason of this very contrasting result is not understood but may be due to the difference in physical parameterizations of convective schemes. WRF also shows no changes in the RCDs north 15^{o}N over Sahel in spite of any elevated GHGs. The complete disagreement of the two models (RegCM and WRF) results is not fully understood but is beyond the scope of this study.

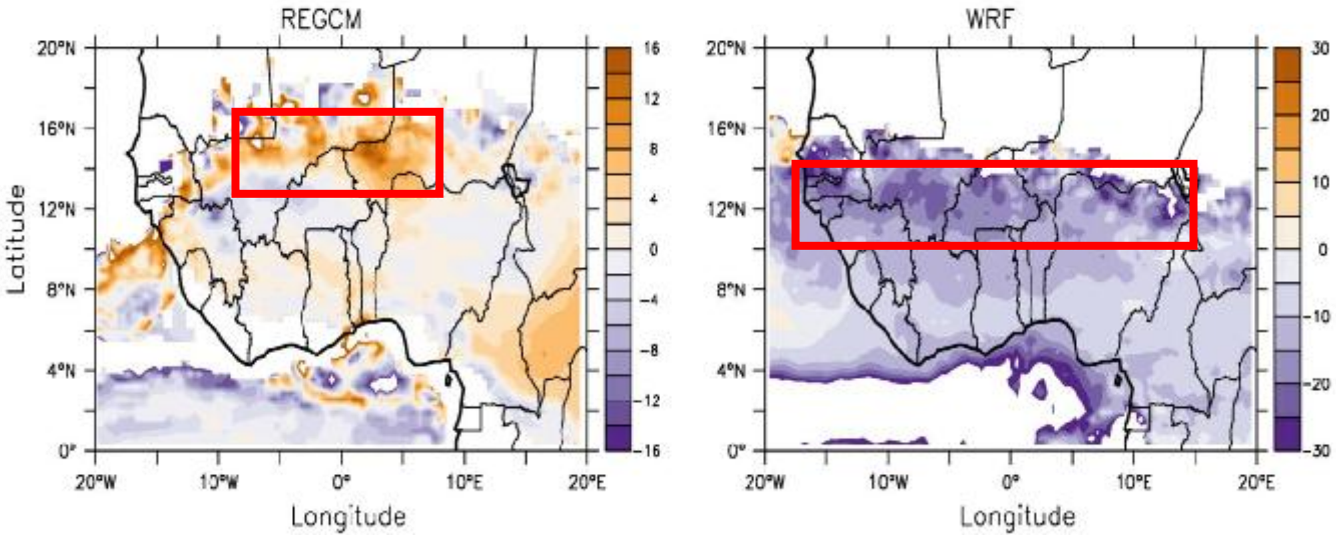

Figure 4.51 : Simulated impacts of GHGs on the projected future mean rainfall cessation dates (RCDs) under rcp45 conditions for the period 2031-2064 using RegCM and WRF. The above panels show the changes in RCDs (present day RCD minus projected future RCD.

4.3.3.2 Impacts of reforestation on the RCD over West Africa

The impacts of reforestation on the projected future RCDs (Fig. 4.52) under the rcp45 condition show that reforestation would induce both later and early RCDs in the RCMs but over different locations.

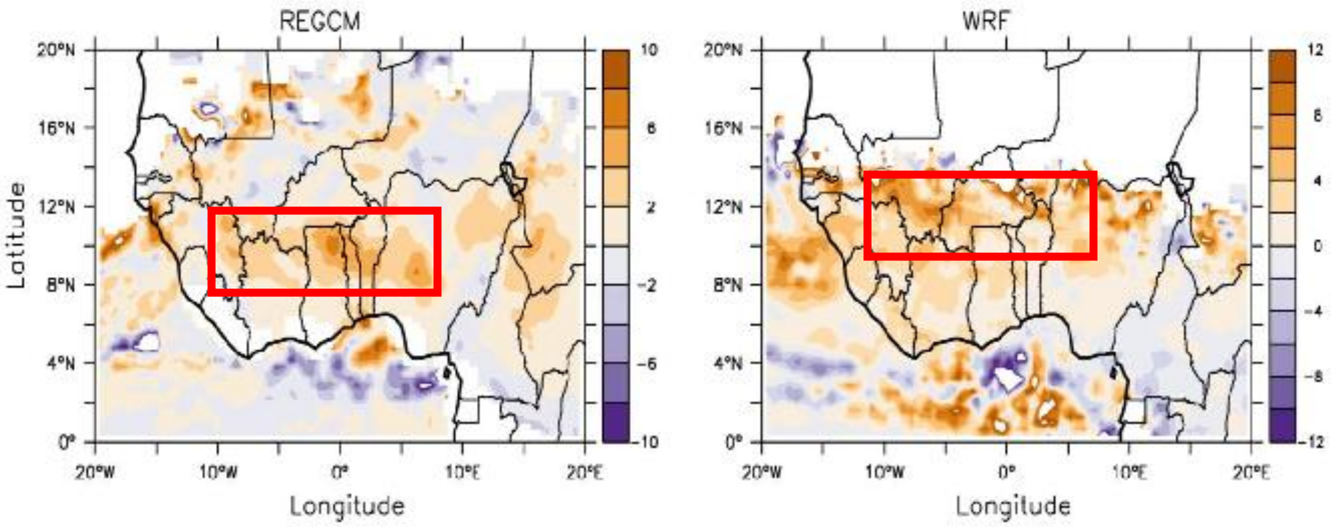

Figure 4.52 : Simulated impacts of reforestation on the projected future mean rainfall cessation dates (RCDs) under rcp45 conditions for the period 2031-2064 using RegCM and WRF. The above panels show the changes in RCDs (projected future with reforestation RCD minus projected future without reforestation RCD).

RegCM shows that the reforested area would induce later RCDs over the Savanna as well as some part of Guinea zone but that the Sahel zone would likely be dominated by a little early RCD, especially over eastern part of Mali, northern Niger and northwestern Nigeria. In the case of WRF, later RCDs would likely dominate the entire West Africa, especially over Sahel where the maximum would occur. WRF also shows that no changes are observed in the RCDs north 14^{o}N.

The potential impact of climate change and reforestation on the RCDs shows that elevated GHGs and reforestation would likely induce later and early RCDs over West Africa. There is no agreement at all between the models (RegCM and WRF) about the impacts of elevated GHGs on the RCDs. RegCM produces delayed RCDs over Sahel due to elevated GHGs, while WRF in contrast produces earlier RCDs over all West Africa. However, there is good agreement in the results of the two models with regards to the impact of reforestation as they both delayed cessation dates in most parts of West Africa.

CHAPTER FIVE

CONCLUSION AND RECOMMENDATIONS

5.1 CONCLUSION

The objectives of this thesis are twofold. The first objective consists of evaluating the ability of the Coordinated Regional Climate Downscaling Experiment (CORDEX) of Africa (hereafter CORDEX-Africa) regional climate models (RCMs) in simulating the rainfall onset and cessation dates (RODs and RCDs) over West Africa. The observations data used for the performance evaluations of the RCMs are the GPCP and TRMM. ERA-Interim (ERAIN) which has been used as lateral and boundary conditions for all the RCMs is also included in the RCMs performance evaluation. In pursuing the objective, four definitions of RODs and one definition of RCDs have been used and compared to evaluate the capability of CORDEX-Africa regional climate models (RCMs) in simulating the characteristics of ROD/RCD over West Africa. The evaluation focused on how well the CORDEX-Africa RCMs simulate the mean, standard deviation and inter-annual variability of RODs/RCDs as observed in GPCP and TRMM for the period 1998-2008. Both observations (GPCP and TRMM) are applied to the RODs/RCDs definitions, and then ERAIN is compared to them to see its ability to capture the observed pattern. Next the RCMs were compared to both observations and ERAIN to identify the models that best simulate the RODs/RCDs over West Africa for each definition. The results obtained show that:

(i) Using the four definitions with observed datasets (GPCP and TRMM), DEF1 consistently produces the earliest ROD, while DEF4 gives latest ROD. DEF2 and DEF3 produce the RODs which fall within those of DEF1 and DEF4.

(ii) The spatial distribution of the observed mean ROD is generally zonal and the values increase inland from the coast, but the ROD distribution is generally more zonal in DEF1 than in DEF4. DEF2 and DEF3 give similar ROD distribution to that of DEF1. The RODs are earlier north of 8^{o}N in DEF1 than in DEF4, with rainfall reaching its northernmost position over

Sahel (about 18^{o}N) in August. However, ERAIN produces earlier onset dates (i.e. January) which reaches only 14^{o}N in contrast to the RCMs. Some of the RCMs produce the start and inland penetration of the monsoon rainfall better than ERAIN which also does not capture the spatial distribution of the RODs as observed in GPCP and TRMM regardless of the ROD definitions used.

(iii) The spatial distribution of the standard deviation, trend and correlation are similar to the spatial distribution of the mean ROD. The results derived from the ability of the reanalysis (ERAIN) and the RCMs to capture the mean ROD distribution show that ERAIN does not capture the distribution of the standard deviation, trend and correlation as observed in GPCP and TRMM regardless the definitions used. However, the results between the RCMs depend on the climatic zone and definition used but most RCMs perform better than ERAIN.

(iv) The spatial distribution of the observed mean RCD is generally zonal, decreasing from the coast inland. The observations (GPCP and TRMM) indicate that the RCDs occur in September-October over Sahel, October-November over Savanna and November-December over Guinea. ERAIN also captures well the observed RCDs over Savanna but overestimates it over Guinea zone and fails to produce the RCD over Sahel north of 14^{o}N. The RCMs remarkably simulate the mean RCDs distribution as observed and perform better than ERAIN but ARPEGE and CCLM fail to simulate the RCD well.

(v) The good agreement among the RCMs and ERAIN in simulating the temperature fields and monsoon flows over West Africa suggests that the main source of discrepancy among the RCMs in simulating the RODs is due to the difference in their representation of rainfall processes. In simulating the inter-annual variability of ROD/RCD, the RCMs perform best over Guinea and worst over the Savanna for the ROD and best over Savanna and worst of Guinea for the RCDs.

(vi) The RCMs ensemble mean perform much better than individual RCMs and ERAIN in simulating the mean and inter-annual variability of RODs/RCDS over West Africa regardless of the definition used.

The second objective evaluates the potential impact of climate change and reforestation on future climate rainfall onset and cessation over West Africa. In investigating the potential impact of climate change and reforestation on the ROD/RCD for rain-fed agriculture in West Africa, three different experiments were carried out using the regional climate models RegCM and WRF which were driven by HadGEM and ECHAM respectively. These models are the ones available for us among the 10 RCMs of CORDEX which give encouraging results when driven by the reanalyses ERAIN in most areas in West Africa. The experiments consist of simulations for the present day for the period 1970-2004, simulations for future projections without reforestation for the period 2030-2064 and simulations for future projections with reforestation for the same period. The future projections are under the rcp45 conditions and the projected changes are conducted under elevated GHGs and with reforestation over Savanna. The reason of choosing the Savanna zone is because of the WAM abrupt shift which occurs there prior to the onset over Sahel. After validating the models ability in simulating the climate of West Africa, the projected impact of climate change and reforestation on the ROD/RCD were evaluated. The results obtained are summarized as follow:

(a) The simulation of the WAM with RegCM and WRF show that the models simulate the West African climate realistically when compared with observations, though they overestimate the rainfall in some areas but produce temperature results in agreement with observations. The RCMs perform better than their driven GCMs (HagGEM and ECHAM, respectively) in simulating the main features of the WAM. The results of the RCMs are in agreement with previous studies (e.g. Afiesimama *et al.*, 2006; Omotosho and Abiodun, 2007; Abiodun *et al.*, 2012; Mounkaila *et al.*, 2014). Both HadGEM and ECHAM did not simulate well the spatial distribution of ROD over West Africa as observed by GPCP and TRMM over Guinea with all the definitions. In general both RegCM and WRF perform better than HadGEM and ECHAM, respectively, in simulating the ROD spatial distribution in most areas of West Africa regardless of the definitions used.

(b) The projected impact of climate change due to elevated GHGs under the rcp45 conditions (2031-2064) shows that temperature would likely increase over West Africa in the simulations of both the RCMs (RegCM and WRF) and AOGCMs (HadGEM and ECHAM). However this increase is more consistent over Sahel than over Guinea.

(c) The changes in rainfall pattern due to elevated GHGs indicate a general decrease in rainfall in both the AOGCMs and the RCMs. These decreases are more consistent over Sahel than over Guinea. However, some increases are observed by HadGEM and RegCM in July-August (about 6^{o}N) which are not in agreement with the results of Abiodun *et al.* (2012) who found a decrease in rainfall in July-August.

(d) The potential impact of increases in GHGs on the future rainfall onset dates suggests that regardless of the definitions used, central and east Savanna areas would be the most affected by a delay in ROD with RegCM model, with up to 30 days or more using DEF1 and DEF4. The changes are more consistent with DEF4 than in DEF1. The impacts on future onset over Guinea and Sahel indicate earlier ROD with Guinea having the earliest ROD when all the definitions are used. All definitions agree that northern Nigeria would be the most affected by the impact of elevated GHGs in the future climate ROD. Both RegCM and WRF project delayed ROD over the entire West Africa. In addition, regardless of the definitions used WRF fails to simulate the future climate ROD north 16^{o}N.

(e) The vertical structure of the monsoon dynamics in the areas where the highest impacts of climate change (i.e. delayed ROD) are observed for each definition show that the elevated GHGs in the future under rcp45 condition would induce a shallower monsoon flow, especially over the Sahel.

(f) There was no agreement between the RCMs on the potential impact of climate change on the RCDs shows due to elevated GHGs. RegCM produces delayed RCDs over Sahel and early RCDs over Savanna, while WRF produces early RCDs everywhere.

(g) For the projected impact of reforestation under the rcp45 condition both RCMs (RegCM and WRF) suggest that West Africa would have cooler climate in most areas with more rainfall during the rainy season especially over the reforested zone. The cooling effect is consistent and higher over Savanna but reforestation would induce a warming over surrounding areas.

(h) Regardless of the definitions used, the reforestation over Savanna area would induce earlier ROD over most areas of West Africa as simulated by both RCMs RegCM and WRF, except north of Nigeria, with the highest impact of ROD (i.e. earliest ROD) over western and central Savanna and western Sahel. Reforestation (under rcp45) would affect the monsoon flow by reducing its progression over the Sahel leading to later RODs.

(i) The potential impact of reforestation on the RCDs (under rcp45 conditions) produces divergent results by the RCMs. WRF produces delayed RCDs over all the climatic zones, while RegCM indicates delayed RCDs over the reforested area and early RCDs over Sahel.

5.2 LIMITATIONS AND RECOMMENDATIONS

In this study, the performances of the RCMs in simulating the ROD and RCD are evaluated and they depend on the definitions used. Some of the RCMs simulate the ROD and RCD well as in observations, while others perform poorly and always overestimate the ROD and RCD in most of the climatic zones. However, The RCMs ensemble mean produced the best results of the ROD and RCD simulations over the region. On the other hand, the RCMs used for future projections to evaluate the potential impact of climate change and reforestation showed clear disagreement in the model results of projected impacts of climate change on the RCDs.

5.2.1 LIMITATIONS OF THE STUDY

The major limitation of this study is the failure of some of the RCMs in simulating the ROD/RCD. The reasons for these failures may be due to the definitions used which are based only on rainfall thresholds. These might derive from the physical parameterization schemes, the internal errors of the individual RCMs and the downscaling errors of the models and those from the forcing GCMs.

5.2.2 RECOMMENDATIONS

For future work, the following recommendations are made: first the performance of RCMs may be improved by using ROD and RCD definitions that use the simulated dynamical and thermodynamical fields (e.g. wind, temperature, and moisture) rather than just rainfall data only. Secondly, for robust predictions of the ROD and RCD over West Africa, the use of RCMs ensemble mean is highly recommended. Thirdly, for the future projections, some sensitivity tests on the convective schemes of the RCMs (RegCM and WRF) should be conducted to identify the suitable schemes over the study area. Fourth, multi-RCMs ensemble mean (for future projections) should be used applied to obtain better results for impacts studies with the new dynamical and thermodynamical definitions of ROD/RCD.

REFERENCES

Abiodun B.J., Pal J.S., Afiesimama E.A., Gutowski W.J., Adedoyin A. (2008): Simulation of West African monsoon using RegCM3 part II: impacts of deforestation and desertification. Theor Appl Climatol **93**: 245–261. doi:10.1007/s00704-007-0333-1

Abiodun B.J., Gutowski W., Abatan A.A., Prusa J.M. (2011): CAM-EULAG: a non hydrostatic atmospheric climate model with grid stretching. Acta Geophys **59** (6):1158–1167

Abiodun B.J., Adeyewa Z.D., Oguntunde P.G., Salami A.T., Ajayi V.O. (2012): Modelling the impacts of reforestation on future climate in West Africa. Theor Appl Climatol. doi:10.1007/s00704-012-0614-1

Abiodun B.J., Ayobami T.S., Olaniran J.M. and Sola O. (2013): Potential impacts of afforestation on climate change and extreme events in Nigeria. Clim Dyn **41**:277–293. DOI 10.1007/s00382-012-1523-9

Adedokun J.A. (1978): West African precipitation and dominant atmospheric mechanism. Arch. Met Geoph. Biokl. Ser A., **27**,289–310

Adejokun J.A. (1966): The Three-Dimensional Structure Of The Inter-Tropical Discontinuity". Nigeria Met. Serv; Lagos. Note **39**.

Adger W.N. (2006): Vulnerability. Global Environmental Change **16**,268–281

Adler B., Kalthoff N., and Gantner L. (2011a): Initiation of deep convection caused by land-surface inhomogeneities in West Africa: a modelled case study. Meteorology and Atmospheric Physics, vol. **112**, no. 1-2, pp. 15–27.

Adler B., Kalthoff N., and Gantner L. (2011b): The impact of soil moisture inhomogeneities on the modification of a mesoscale convective system: an idealised model study. Atmospheric Research, vol. **101**, no. 1-2, pp. 354–372.

Afiesimama E.A., Pal J.S., Abiodun B.J., Gutowski W.J., Adedoyin A. (2006): Simulation of West African monsoon using the RegCM3. Part I: model validation and interannual variability. Theor. Appl. Climatol **86**:23–37

AGRHYMET (1996) : Méthodologie de suivi des zones à risque. AGRHYMET FLASH, Bulletin de Suivi de la Campagne Agricole au Sahel 0/96, Vol. **2**, 2 pp. [Available at Centre Regional AGRHYMET, B.P. 11011, Niamey, Niger.]

Anthes R.A. (1977): Hurricane model experiments with a new cumulus parameterization scheme. Mon Weather Rev., 105; 287–300

Arakawa A. And Schubert W.H. (1974): Interaction of a cumulus cloud ensemble with the largescale environment. Part I. J. Atmos. Sci., **31**;674–701

Ati F.O., Stitger C.J., Oladipo E.O. (2002): A comparison of methods to determine the onset of the growing season in northern Nigeria. Int J Climatol **22**:731–742

Bala G., Caldeira K., Wickett M., Phillips T. J., Lobell D. B., Delire C., and Mirin A. (2007): Combined climate and carbon-cycle effects of large-scale deforestation, P. Natl. Acad. Sci. USA, **104**, 6550–6555.

Barbier B., Yacouba H., Karambiri H., Zoromé M., Somé B. (2009) : Human vulnerability to climate variability in the Sahel: Farmer’s adaptation strategies in Northern Burkina Faso. J. Environ. Manage. **43**, 790–803.

Bathiany S., Claussen M., Brovkin V., Raddatz T., and Gayler V. (2010): Combined biogeophysical and biogeochemical effects of large-scale forest cover changes in the MPI earth system model. Biogeosciences, **7**, 1383–1399, doi:10.5194/bg-7-1383-2010

Bernier P. Y., Desjardins R. L., Karimi-Zindashty Y., Worth D. E., Beaudoin A., Luo Y., and Wang S., (2011): Boreal lichen woodlands: A possible negative feedback to climate change in Eastern North America. Agr. Forest Meteorol., **151**, 521–528.

Betts R. A. (2000): Offset of the potential carbon sink from boreal forestation by decreases in surface albedo, Nature, **408**, 187–190.

Biasutti M., Held I. M, Sobel A. H. and Giannini, A. (2008): SST forcings and Sahel rainfall variability in simulations of the twentieth and twenty first centuries. Journal of Climate , **21**, 3471-3486.

Biasutti M. and Sobel A.H. (2009): Delayed Sahel rainfall and global seasonal cycle in a warmer climate Geophys. Res. Lett. **36** L23707

Bonan G. B., Pollard D. and Thompson S. L. (1992): Effects of boreal forest vegetation on global climate, Nature, **359**, 716–718.

Bonan G. B., and S. Levis (2010): Quantifying carbon-nitrogen feedbacks in the Community Land Model (CLM4). Geophys. Res. Lett., **37**, L07401.

Briegleb B.P. (1992): Delta-Eddington approximation for solar radiation in the NCAR Community Climate Model. J Geophys Res **97**: 7603–7612

Carlson T. N. (1969): Some remarks on African disturbances and their progress over the tropical Atlantic. Monthly Weather Review vol. **97**, no. 10, udc 551.515.5: 551.589.1: 551.507.362.2:551.576 (0.1) (66) "1968.323"

Charney J.G. (1975): The dynamics of deserts and droughts. Quarterly Journal of the Royal Meteorological Society, vol. **101**, pp. 193–202.

Chen F. and Dudhia J. (2001): Coupling an advanced land-surface hydrology model with the Penn State-NCAR MM5 modeling system. Part I: model implementation and sensitivity. Mon Weather Rev **129**:569–585

Chong M. and Hauser D. (1989): A tropical squall line observed during the COPT 81 experiment in West Africa. Part II: Water budget. Mon. Wea. Rev., **117**, 728–744

Christensen J. H. *et al.* (2007): Regional climate projections. In: Climate Change 2007: The Physical Science Basis. Contribution of Working Group I to the Fourth Assessment Report of the Intergovernmental Panel on Climate Change

Clark D. B., Taylor C. M., and Thorpe A. J. (2004): Feedback between the land surface and rainfall at convective length scales. Journal Hydrometeor, vol. **5**, pp. 625–639.

Cocheme J., Franquin P. (1967): An agro-climatology survey of a semi-arid area in Africa, South of Sahara, FAO/WMO Technical Bulletin **86**

Collins W.J. *et al.* (2008): Evaluation of the HadGEM2 model. Met Office Hadley Centre Technical Note No. HCTN **74**, Met Office, Exeter, UK.

Cook K.H. and Vizy E.K. (2006): Coupled model simulations of the West African monsoon system: twentieth- and twenty-first-century simulations. J. Clim. **19**:3681–3703

Dee D. P. *et al.* (2011): The ERA-Interim reanalysis: configuration and performance of the data assimilation system. Q. J. R. Meteorol. Soc. **137**: 553–597. DOI:10.1002/qj.828

deMott P. J., Sassen K., Poellot M. R. *et al.* (2003): African dust aerosols as atmospheric ice nuclei. Geophysical Research Letters, vol. **30**, article 1732.

Derek HAYWARD and Julius OGUNTOYINGO (1987): Climatology of West Africa. Google books available online November 10th, 2014 at http://tinyurl.com/n9ogdfm

Desanker P. and Magadza C. (2001): Impacts, adaptation and vulnerability. Contribution of working group II to the third assessment report of the intergovernmental panel climate change. Cambridge University Press, Cambridge and New York, NY, 1032 pp

Deser C., Tomas R., Alexander M., and Lawrence D. (2010): The seasonal atmospheric response to projected Arctic sea ice loss in the late twenty-first century, J. Clim., **23**, 333–351

Diallo I., Sylla M.B., Giorgi F., Gaye A.T., Camara M. (2012a): Multi-model GCM-RCM ensemble-based projections of temperature and precipitation over West Africa for the early 21st century. Int. J. Geophys, Article ID 972896

Diallo I., Sylla M.B., Camara M., Gaye A.T. (2012b): Inter-annual variability of rainfall and circulation features over the Sahel based on multiple regional climate models simulations. Theor. Appl. Climatol. doi:10.1007/s00704-012-0791-y

Dickinson R.E., Henderson-Sellers A., Kennedy P. (1993): Biosphere–atmosphere transfer scheme (BATS) version 1e as coupled to the NCAR community climate model. Tech. Rep., National Center for Atmospheric Research Tech Note NCAR.TN-387+STR, NCAR, Boulder, CO

Dike V. *et al.* (2014): Modelling present and future African climate using CMIP5 scenarios in HadGEM2-ES. Int. J. Climatol. DOI: 10.1002/joc.4084

Djiotang Tchotchou L.A., Kamga F., Mkankam (2010): Sensitivity of the simulated African monsoon of summers 1993 and 1999 to convective parameterization schemes in RegCM3, Theor. Appl. Climatol., **100**, 207–220

Drobinski P., Sultan B., Janicot S. (2005): Role of the Hoggar massif in the West African monsoon onset. Geophys. Res. Lett. **32**, L01705. doi:10. 1029/2004GL020710

Druyan L., Fulakeza M., Lonergan P. (2002): Dynamic downscaling of seasonal climate predictions over Brazil. J. Climate, **15**, 3411–3426

Druyan L. M., Fulakeza M., and Lonergan P. (2004): Land surface influences on the West African summer monsoon: implications for synoptic disturbances. Meteorology and Atmospheric Physics, vol. **86**, no. 3-4, pp. 261–273.

Druyan L.M., Feng J., Cook K.H., Xue Y., Fulakeza M., Hagos S.M., Konare A., Moufouma-okia W., Rowell D.P., Vizy E.K., Ibrah S.S. (2010): The WAMME regionalmodel intercomparison study. Clim. Dyn. **35**:175–192

Dudhia J. (1989): Numerical study of convection observed during the winter monsoon experiment using a mesoscale two-dimensional model. J. Atmos. Sci. **46**:3077–3107

Eltahir E., Gong C. (1996): Dynamics of wet and dry years inWest Africa. J. Clim. **9**:1030–1042

Emanuel K.A. (1991): A scheme for representing cumulus convection in large-scale models. J. Atmos. Sci. **48**: 2313–2335

FAO (1985): Integrating crops and livestock in West Africa. Agriculture and Consumer Protection. Available online 19/08/2014 : http://www.fao.org/docrep/004/x6543e/X6543E01.htm#ch1

Fink A. H. and Reiner A. (2003): Spatio-temporal variability of the relation between African Easterly Waves and West African Squall Lines in 1998 and 1999. J. Geophys. Res., **108**, 4332, doi:10.1029/2002JD002816.

Flaounas Emmanouil, Sophie Bastin, Serge Janic (2010): Regional climate modelling of the 2006 West African monsoon: sensitivity to convection and planetary boundary layer parameterisation using WRF. Clim. Dyn. **36**:1083–1105. DOI 10.1007/s00382-010-0785-3

Fontaine B., Trazaska S. and Janicot S. (1998): Evolution of the relationship between near and global and Atlantic SST modes and the rainy season in West Africa: Statistical analyses and sensitivity experiments. Clim. Dyn. **14**, 353-368.

Fontaine B., Louvet S., Roucou P. (2008): Definition and predictability of an OLR-based West African monsoon onset. Int. J. Climatol. **28**: 1787–1798

Fulakeza M., Druyan L. and Krishnamurti T. (2002): A simple soil moisture scheme for climate simulations in the tropics. Met. Atmos. Phys., **79**, 105–126

Futyan J. and Del Genio A. (2007): Deep convective system evolution over Africa and the tropical Atlantic. J. Climate, **20**, 5041–5060

Gbobaniyi E., Sarr A., Sylla M.B., Diallo I., Lennard C., Dosio A., Dhiédiou A., Kamga A., Klutse N.A.B., Hewitson B., Nikulin G., Lamptey B. (2013): Climatology, annual cycle and interannual variability of precipitation and temperature in CORDEX simulations over West Africa. Int. J. Climatol. doi:10.1002/joc.3834

Giannini A., Saravanan R. and Chang P. (2003): Oceanic forcing of Sahel rainfall on interannual to interdecadal time scales. Science **302**, 1027-1030, doi:10.1126/science.1089357.

Giannini A. (2010): Mechanisms of climate change in the semi-arid African Sahel: the local view J. Clim. **23** 743–56

Giorgi F., Marinucci M. (1996): An investigation of the sensitivity of simulated precipitation to model resolution and its implication for climate studies. Mon. Weather Rev., **124**, 148–166

Giorgi Filippo, Colin Jones and Ghassem R. Asrar (2009): Addressing climate information needs at the regional level: the CORDEX framework. WMO Bulletin **58** (3).

Giorgi F. *et al.* (2012): RegCM4: model description and preliminary tests over multiple CORDEX domains. Clim. Res. Vol. **52**: 7–29, 2012, doi: 10.3354/cr01018

Giorgetta M.A. *et al.* (2012): The atmospheric general circulation model ECHAM6, Model description Reports on Earth System. Science, **135**, 2013, ISSN 1614-1199

Gordon Conway (2009): The science of climate change in Africa: impacts and adaptation. Grantham Institute for Climate Change, Discussion paper No 1, October 2009

Graham R.J., Yun W.T., Kumar A., Jones D., Bettio L., Gagnon N., Kolli R.K., Smith D. (2011): Long-range forecasting and the Global Framework for Climate Services. Clim. Res. **47**:47–55. doi:10.3354/cr00963

Grell G.A. (1993): Prognostic evaluation of assumptions used by cumulus parameterizations. Mon. Weather Rev., **121**, 764–787

Grist J. P. and Nicholson S. E. (2000): A Study of the Dynamic Factors Influencing the Rainfall Variability in the West African Sahel. J. Climate, Vol. **14** p1337-1359

Gu G. and Adler R.F. (2004): Seasonal evolution and variability associated with theWest African monsoon system. J. Climate **17**: 3364–3377.

Hamilton R. A. and Archbold J.W. (1945): Meteorology of Nigeria and adjacent territory. Quart. J. Meteo. Soc. **71**, 231-262.

Hodges K.I. and Thorncroft C. D. (1997): Distribution and statistics of African mesoscale convective weather systems based on the ISCCP Meteosat imagery. Mon. Wea. Rev., **125**, 2821–2837

Holtslag A., de Bruijn E., Pan H.L. (1990): A high resolution air mass transformation model for short-range weather forecasting. Mon. Weather Rev. **118**: 1561–1575

Hong S.Y., Dudhia J., Chen S.H. (2004): A revised approach to ice microphysical processes for the bulk parameterization of clouds and precipitation. Mon. Weather Rev. **132**:103–120

Hong S.Y., Noh Y. and Dudhia J. (2006): A New Vertical Diffusion Package with an Explicit Treatment of Entrainment Processes. Monthly Weather review Vol.**134** p2318-2341

Hourdin F., Mustat I., Guichard F., Ruti P.M., Favot F., Pham M.M.A., Grandpeix J.Y., Polcher J., Marquet P., Boone A., Lafore J.P., Redelsperger J.L., Dell'Aquilla A., Losada Doval T., Traore A.K., Gallee H. (2010): AMMA-Model intercomparison project. Bull Am. Meteorol. Soc.

Huffman G.J., Adler R.F., Morrissey M.M., Bolvin D.T., Curtis S., Joyce R., McGavock B., Susskind J. (2001): Global precipitation at one-degree daily resolution from multi-satellite observations. J. Hydrometeorol **2**:36–50

Huffman GJ et al (2007): The TRMM multisatellite precipitation analysis (TMPA): quasi-global, multiyear. combined-sensor precipitation estimates at fine scales. J. Hydrometeorol **8**:38–55

Huffman G.J., Adler R.F., Bolvin D.T., Gu G. (2009): Improving the global precipitation record: GPCP version 2.1. Geophys. Res. Lett. **36**, L17808, doi:10.1029/2009GL040000

Huffman G.J. and Bolvin D.T. (2011): TRMM and other data precipitation data set documentation. NASAGSFC Rep., 29 pp. ftp://precip.gsfc.nasa. gov/pub/trmmdocs/3B42_3B43_doc.pdf. Accessed 23 July 2013

Hurk *et al.* (2010): Diagnosing land-atmosphere interaction from a regional climate model simulation over West Africa. Journal of Hydrometeorology, vol. **11**, no. 2, pp. 467–481, 2010.

Ilesanmi O.O. (1972): An empirical formulation of an ITD rainfall model for the tropics: a case study of Nigeria. Journal of Applied Meteorology, **10**, 882–889.

Ingrama K. T., Roncolia M.C., Kirshenb P.H., (2002): Opportunities and constraints for farmers of West Africa to use seasonal precipitation forecasts with Burkina Faso as a case study. Agricultural Systems **74**, 331–349

IPCC (2013): Climate Change 2013: The Physical Science Basis. Contribution of Working Group I to the Fifth Assessment Report of the Intergovernmental Panel on Climate Change [Stocker, T.F., D. Qin, G.-K. Plattner, M. Tignor, S.K. Allen, J. Boschung, A. Nauels, Y. Xia, V. Bex and P.M. Midgley (eds.)]. Cambridge University Press, Cambridge, United Kingdom and New York, NY, USA, 1535 pp.

Janicot S., Harzallah A., Fontaine B. and Moron V. (1998): West African monsoon dynamics and eastern equatorial Atlantic and Pacific SST anomalies (1970–88). J. Climate, **11**, 1874–1882.

Janicot S. (1992): Spatiotemporal variability of West African rainfall. Part II: Associated surface and air mass characteristics. J. Climate, **5**, 499–511.

Janicot S., Moron V. and Fontaine B. (1996): Sahel droughts and ENSO dynamics. Geophys. Res. Lett., **23**, 515–518.

Jones *et al.* (2011): Development and evaluation of an Earth-system model – HadGEM2. Geosci. Model Dev. Discuss., **4**, 997–1062, doi:10.5194/gmdd-4-997-2011

Kain J.S. (2004): The Kain–Fritsch convective parameterization: an update. J. Appl. Meteorol. **43**:170-181

Kiehl J, Hack J, Bonan G, Boville B, Breigleb B, Williamson D, Rasch P (1996): Description of the NCAR Community Climate Model (CCM3). National Center for Atmo -spheric Research Tech Note NCAR/TN-420+STR, NCAR, Boulder, CO

Kluser L. and Holzer-Popp T. (2010): Relationships between mineral dust and cloud properties in the West African Sahel. Atmospheric Chemistry and Physics, vol. **10**, no. 14, pp. 6901–6915.

Konare A. *et al.* (2008): A regional climate modeling study of the effect of desert dust on the West African monsoon. Journal of Geophysical Research D, vol. 113, no. 12, Article ID D12206.

Krishna *et al.* (2011): Customization of WRF-ARW model with Physical parameterization schemes for the simulation of tropical cyclones over North Indian Ocean, Nat Hazards,DOI, 10.1007/s11069-011-9862-0

Kunstmann Harald and Jung Gerlinde (2003): Investigation of feedback mechanisms between soil moisture, land use and precipitation in West Africa. Water Resources Systems—Water Availability and Global Change (Proceedings of symposium HS02a held during IUGG2003 at Sapporo, July 2003). IAHS Publ. no. 280.

Kuo, H-L, (1974): Further studies of the parameterization of the influence of cumulus convection on large scale flow. J. Atmos. Sci., **31**, 1232–1240

Kuo, Y-H, Reed, RJ, Liu, Y-B, (1996): The ERICA IOP 5 storm. Part III: Mesoscale cyclogenesis and precipitation parameterization. Mon Weather Rev., **124**, 1409–1434

Lamb PJ, Peppler RA (1992) Further case studies of tropical Atlantic surface atmospheric and oceanic patterns associated with sub-Saharan drought. J. Clim. **5**:476–488

Lau K. M., Kim K. M., Sud Y. C., and Walker G. K. (2009): A GCM study of the response of the atmospheric water cycle of West Africa and the Atlantic to Saharan dust radiative forcing. Annales Geophysicae, vol. **27**, no. 10, pp. 4023–4037.

Laux P, Kunstmann H, árdossy AB (2008): Predicting the regional onset of the rainy season in West Africa. Int. J. Climatol. **28**:329–342

Lima, C. H. R., and U. Lall (2009): Hierarchical Bayesian modeling of multisite daily rainfall occurrence: Rainy season onset, peak, and end, Water Resour. Res., **45**, W07422, doi:10.1029/2008WR007485.

Linden van der, P., and J. F. B. Mitchell, Eds. (2009): ENSEMBLES: Climate change and its impacts at seasonal, decadal and centennial timescales; Summary of research and results from the ENSEMBLES project.MetOfficeHadley CentreRep., 160 pp.

Le Barbe L, Lebel T, TapsobaD (2002): Rainfall variability inWest Africa during the years 1950–1990. J. Clim **15**(2):187–202

Lu, J, and Delworth, R. (2005): Oceanic forcing of the late 20th century Sahel drought. Geophysical Research Letter **32**, L22706, doi:GL023316.

Marteau R, Sultan B,Moron V,AlhassaneA, Baron C, Traore SB (2011): The onset of the rainy season and farmers' sowing strategy for pearl millet cultivation in Southwest Niger. Agric For Meteorol **151**(10):1356–1369. doi:10.1016/j.agrformet.2011.05.018

Mertz, O., Halsnæs, K., Olesen, J.E., Rasmussen, K. (2009): Adaptation to climate change in developing countries.

Mlawer E, Taubman S, Brown P, Iacono M, Clough S (1997): Radiative transfer for inhomogeneous atmosphere: RRTM, a validated correlated-k model for the long-wave. J Geophys Res **102**:16663–16682

Montenegro, A., M. Eby, Q. Z. Mu, M. Mulligan, A. J. Weaver, E. C. Wiebe, and M. S. Zhao (2009): The net carbon drawdown of small scale afforestation from satellite observations. Global Planet. Change, **69,** 195–204.

Mounkaila S. Moussa, Babatunde J. Abiodun, J. Bayo Omotosho, (2014): Assessing the capability of CORDEX models in simulating onset of rainfall in West Africa. Theor Appl Climatol DOI 10.1007/s00704-014-1104-4

Nicholson S. E. , Some B, Kone B (2000): An analysis of recent rainfall conditions inWest Africa, including the rainy seasons of the 1997 ElNiño and the 1998 La Niña years. J Clim **13**:2628–2640

Nicholson S. E. and Grist J. P. (2003): The seasonal evolution of the atmospheric circulation over West Africa and equatorial Africa," Journal of Climate, vol. **16**, pp. 1013–1030.

Nicholson S. E. (2008): The intensity, location and structure of the tropical rainbelt over west Africa as factors in interannual variability, International Journal of Climatology, vol. **28**, no. 13, pp. 1775–1785.

Nicholson S. E. (2009): On the factors modulating the intensity of the tropical rainbelt over West Africa, International Journal of Climatology, vol. **29**, no. 5, pp. 673–689.

Nicholson S. E. (2013): The West African Sahel: A Review of Recent Studies on the Rainfall Regime and Its Interannual Variability. Hindawi Publishing Corporation ISRN Meteorology Volume 2013, Article ID 453521, 32 pages http://dx.doi.org/10.1155/2013/453521.

Nikulin G *et al.* (2012): Precipitation climatology in an ensemble of CORDEX-Africa regional climate simulations. J Clim 25:6057–6078

Odekunle T. O. (2004):Rainfall and the length of the growing season in Nigeria. Int. J. Climatol. **24**: 467–479, DOI: 10.1002/joc.1012

Odekunle T. O. , Balogun E. E. and. Ogunkoya1 O. O: (2005): On the prediction of rainfall onset and retreat dates in Nigeria, Theor. Appl. Climatol., **81**, 101–11

Odekunle T. O. (2006): Determining rainy season onset and retreat over Nigeria from precipitation amount and number of rainy days. Theor. Appl. Climatol. **83,** 193–201, DOI 10.1007/s00704-005-0166-8

Oduru AK (1989): On the mean monthly equivalent potential temperature and rainfall in West Africa. Theor Appl Climatol **39**:188–193

Omotosho , J. B. (1985): Spatial and seasonal variations of line squalls over West Africa. Archiv für Meteorologie, Geophysik und Bioklimatologie, A**33**:143-150.

Omotosho JB (1990): Onset thunderstorms and precipitation over northern Nigeria. Int J Climatol **10**:849–860

Omotosho JB (1992): Long-range prediction of the onset and end of the rainy season in the West African Sahel. Int J Climatol **12**:369–382

Omotosho JB, Balogun AA, Ogunjobi K (2000): Predicting monthly and seasonal rainfall, onset and cessation of the rainy season in West Africa using only surface data. Int J Climatol **20**:865–880

Omotosho JB, Abiodun BJ (2007): A numerical study of moisture buildup and rainfall over West Africa. Meteorol Appl **14**:209–225

Paeth, H, Born, K, Podzun, R, & Jacob, D. (2005): Regional dynamical downscaling over West Africa: model evaluation and comparison of wet and dry years. Meteorol Z , **14**(3), 349-367

Paeth H, Girmes R, Menz G, Hense A. (2006): Improving seasonal forecasting in the low latitudes. Monthly Weather Review **134**:1859–1879.

Paeth H, Capo-Chichi A, Endlicher W. (2008): Climate change and food security in tropical West Africa. Erdkunde **62**: 101–115.

Paeth H, Diederich M. (2010): Postprocessing of simulated precipitation for impact studies in west Africa-Part II:a weather generator for daily data. Climate Dynamics. DOI:10.1007/s00382-010-08-40-0.

Paeth H, Hall NMJ, Gaertner MA, Alonso MD, Moumouni S, Polcher J, Ruti PM, Fink AH, Gosset M, Lebel T, Gaye AT, Rowell DP, Moufouma-Okia W, Jacob D, Rockel B, Giorgi F, Rummukainen M (2011): Progress in regional downscaling ofWest African precipitation. Atmos Sci Lett **12**:75–82. doi:10.1002/asl.306

Pal JS, Small E, Eltahir E (2000): Simulation of regional-scale water and energy budgets: representation of subgrid cloud and precipitation processes within RegCM. J Geophys Res **105**: 29579–29594

Pal JS, Giorgi F, Bi X, Elguindi N and others (2007): Regional climate modeling for the developing world: the ICTP RegCM3 and RegCNET. Bull Am Meteorol Soc **88**: 1395–1409

Patricola CM, Cook KH (2010): Northern African climate at the end of the twenty-first century: An integrated application of regional and global climate models. Climate Dynamics, **35**, 193-212, DOI: 10.1007/s00382-009-0623-7.

Peter M, Tetzlaff G (1988): The structure of West African squall lines and their environmental moisture budget. Meteorol Atmos Phys **39**: 74–84

Pu B. and Cook K. H. (2010): Dynamics of the West African Westerly Jet, Journal of Climate, Vol.**23**, 6263-6276

Ramel R, Gallée H, Messager C (2006): On the northward shift of the West African monsoon. Clim Dyn Res **26**:429–440. doi:10.1007/s00382-005-0093-5

Roeckner, E. *et al.* (2003): The atmospheric general circulation model ECHAM5. Part I: Model Description. Report 349, Max-Planck-Institut für Meteorologie, Hamburg.

Roeckner, E. *et al.* (2006): Sensitivity of simulated climate to horizontal and vertical resolution in the echam5 atmosphere model. J. Climate, **19**, 3771–3791.

Roncoli C, Ingram K, Kirshen P. (2002): Reading the Rains: Local knowledge and rainfall forecasting in Burkina Faso. Society and Natural Resources **15**: 409–427.

Rowell,D. P., and J. R. Milford (1993): On the generationof African squall lines. J. Climate, **6**, 1181–1193.

Rummukainen M. (2010): State-of-the-art with regional climate models. Wiley Interdisciplinary Reviews Climate Change **1**: 82–96.

Ruti PM et al (2011): The West African climate system: a review of the AMMA model inter-comparison initiatives. Atmos Sci Lett **12**:116–122. doi:10.1002/asl.305

Sarr Benoıt (2012): Present and future climate change in the semi-arid region of West Africa: a crucial input for practical adaptation in agriculture. Atmos. Sci. Let. DOI: 10.1002/asl.368.

Sarria-Dodd DE, Jolliffe IT (2001): Early detection of the wet season in semiarid tropical climates ofwesternAfrica. Int J Climatol **21**:1251–1262

Schumacher, C., and R. A. Houze Jr. (2006): Stratiform precipitation production over sub-saharan Africa and the tropical East Atlantic as observed by TRMM. Quart. J. Roy. Meteor. Soc., **132**, 2235–2255.

Sivakumar, M.V.K. (1988): Predicting rainy season potential from the onset of rains in southern sahelian and sudanian climatic zones of West Africa. Agric. Forest Meteorol. **42**, 295–305.

Sivakumar, M.V.K. (1992): Empirical analysis of dry spells for agricultural applications in West Africa. J. Climate **5**, 532–539.

Sijikumar S, Roucou P, Fontaine B (2006): Monsoon onset over Sudan-Sahel: simulation by the regional scale model MM5. Geophys Res Lett **33**: L03814. doi:10.1029/2005GL024819

Skamarock, W. C., J. B. Klemp, J. Dudhia, D. O. Gill, D. M. Barker, W. Wang, and J. G. Powers, 2008:Adescription of the advanced research WRF version 3. NCAR Tech. Note NCAR/TN-4751STR, 113 pp.

Solmon F, Mallet M, Elguindi N, Giorgi F, Zakey A, Konaré A (2008): Dust aerosol impact on regional precipitation over western Africa, mechanisms and sensitivity to absorption properties. Geophys Res Lett **35**: L24705, doi:10.1029/2008GL035900

Solmon F., Elguindi N., and Mallet M. (2012): Radiative and climatic effects of dust over West Africa, as simulated by a regional climate model. Climate Research, vol. **52**, article 2012.

Stern RD, Dennett MD, Garbutt DJ (1981): The start of the rains in West Africa. J Clim **1**:59–68

Steward, J.I. (1991): Principles and performance of response farming. In: Ford, W., Muchow, R.C., Bellamy, Z.A. (Eds.), Climatic Risk in Crop Production. Models Management for the semi-arid Tropics and Sub-Tropics. CAB International, Wallinford.

Sultan Benjamin and Janicot Serge (2003): The West African monsoon dynamics. part II: the ‘‘preonset’’ and ‘‘onset’’ of the summer monsoon. J. Climate, vol **16** p3407-3427

Sultan B, Baron C, Dingkuhn M, Sarr B, Janicot S (2005): Agricultural impacts of large-scale variability of the West African monsoon. Agric For Meteorol **128**:93–110, doi:10.1016/j.agrformet.2004. 08.005

Sylla MB et al (2009): High-resolution simulations of West African climate using regional climate model (RegCM3) with different lateral boundary conditions. Theor Appl Climatol **98**:293–314

Sylla MB, Dell'Aquila A, Ruti PM, Giorgi F (2010): Simulation of the intraseasonal and the interannual variability of rainfall over West Africa with a RegCM3 during the monsoon period. Int J Climatol **30**:1865–1883

Sylla MB, Giorgi F, Coppola E, Mariotti L (2012): Uncertainties in daily rainfall over Africa: assessment of gridded observation products and evaluation of a regional climate model simulation. Int J Climatol

Sylla MB, Diallo I, Pal JS (2013): West African monsoon in state-of-thescience regional climate models. doi. 10.5772/55140

Thomas D., Potter, Bradley R., Colman (2003): Handbook of Weather, Climate and Water Dynamics, Climate, Physical Meteorology, Weather Systems, and Measurements Wiley Interscience

Thomas D, Knight M, Wiggs G (2005): Remobilization of southern African desert dune systems by twenty-first century global warming. Nature. 435:1218–1221

Thorncroft Chris D., Hanh Nguyen, Chidong Zhangb and Philippe Peyrill´e (2011): Annual cycle of the West Africanmonsoon: regional circulations and associated water vapour transport. Q. J. R. Meteorol. Soc. **137**: 129–147, January 2011 Part A

Tokinaga, H., and S.-P. Xie (2011): Weakening of the equatorial Atlantic cold tongue over the past six decades. Nature Geoscience, **4** (4), 222-226, doi:10.1038/ngeo1078.

Vellinga Michael, Alberto Arribas and Richard Graham (2013): Seasonal forecasts for regional onset of the West African monsoon. Clim Dyn **40**:3047–3070. DOI 10.1007/s00382-012 1520-z

Vigaud N et al (2009): WRF/ARPEGE-CLIMAT simulated climate trends over West Africa. Clim Dyn **36**:925–944. doi:10.1007/s00382-009-0707-4

Vizy, E, & Cook, K. (2002): Development and application of a mesoscale climate model for the tropics: influence of sea surface temperature anomalies on the West African monsoon. Journal of Geophysical Research **107**(D3):4023, doi: JD000686

Xue Yet al (2010): Intercomparison and analyses of the climatology of the West AfricanMonsoon in theWest African monsoon modeling and evaluation project (WAMME) first model intercomparison experiment. Clim Dyn **35**:3–27. doi:10.1007/s00382-010-0778-2

Wang Z. and R. L. Elsberry (2010): Modulation of the African easterly jet by a mesoscale convective system. Atmospheric Science Letters, vol. **11**, pp. 169–174.

Wang G., and C. A. Alo (2012), Changes in precipitation seasonality in West Africa predicted by RegCM3 and the impact of dynamic vegetation feedback, International Journal of Geophysics, Vol. 2012, Article ID 597205, 10 pages. doi:10.1155/2012/597205

Warner, Thomas T. (2011): Numerical weather and climate prediction. Published in the United States of America by Cambridge University Press, New York. ISBN 978-0-521-51389-0

Yaro Joseph Awetori, Joseph Teye and Simon Bawakyillenuo (2014): Local institutions and adaptive capacity to climate change/variability in the northern savannah of Ghana. Climate and development, doi:10.1080/17565529.2014.951018

Zeng Xubin and Er Lu (2004): Globally Unified Monsoon Onset and Retreat Indexes. Notes and Correspondence, Vol **17** p2241-2248

Zeng X, Zhao M, Dickinson RE (1998): Inter-comparison of bulk aerodynamic algorithms for the computation of seasurface fluxes using TOGA COARE and TAO data. J Clim **11**: 2628–2644.

APPENDIX

A. PUBLICATIONS FROM THE THESIS

1. Mounkaila S. Moussa, Babatunde. J. Abiodun and J. Bayo. Omotosho (2014): Assessing the capability of CORDEX Models in simulating onset of rainfall in West Africa. Theor. Appl. Climatol. DOI 10.1007/s00704-014-1104-4

2. To be submitted, Mounkaila S. Moussa, Babatunde. J. Abiodun and J. Bayo. Omotosho (2015): The potential impacts of climate change and reforestation on rainfall onset and cessation over West Africa using RegCM4 and WRF.

Assessing the capability of CORDEX models in simulating onset of rainfall in West Africa

Moussa S. Mounkaila, Babatunde J. Abiodun & J. 'Bayo Omotosho

Theoretical and Applied Climatology

ISSN 0177-798X

Theor Appl Climatol
DOI 10.1007/s00704-014-1104-4

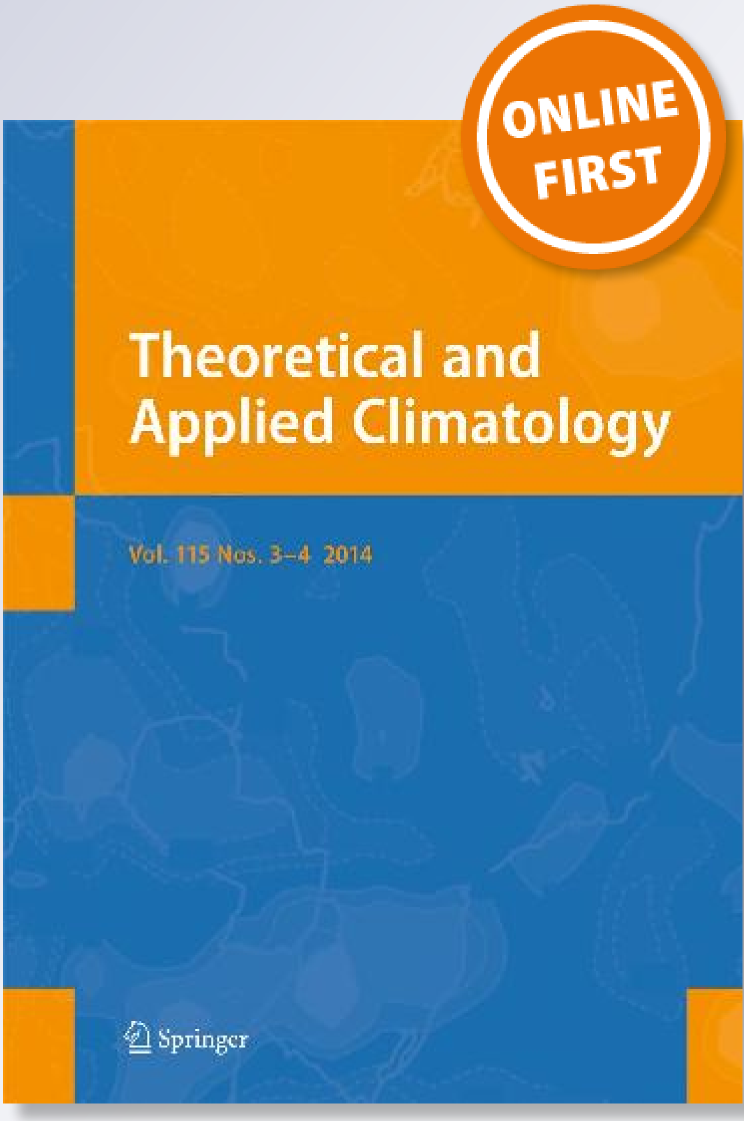

123

Theor Appl Climatol
DOI 10.1007/s00704-014-1104-4

ORIGINAL PAPER

Assessing the capability of CORDEX models in simulating onset of rainfall in West Africa

Moussa S. Mounkaila & Babatunde J. Abiodun &
J. 'Bayo Omotosho

Received: 15 August 2013 / Accepted: 23 January 2014

Abstract Reliable forecasts of rainfall-onset dates (RODs) are crucial for agricultural planning and food security in West Africa. This study evaluates the ability of nine CORDEX regional climate models (RCMs: ARPEGE, CRCM5, RACMO, RCA35, REMO, RegCM3, PRECIS, CCLM and WRF) in simulating RODs over the region. Four definitions are used to compute RODs, and two observation datasets (GPCP and TRMM) are used in the model evaluation. The evaluation considers how well the RCMs, driven by ERA-Interim reanalysis (ERAIN), simulate the observed mean, standard deviation and inter-annual variability of RODs over West Africa. It also investigates how well the models link RODs with the northward movement of the monsoon system over the region. The model performances are compared to that of the driving reanalysis—ERAIN. Observations show that the mean RODs in West Africa have a zonal distribution, and the dates increase from the Guinea coast northward. ERAIN fails to reproduce the spatial distribution of the RODs as observed. The performance of some RCMs in simulating the RODs depends on the ROD definition used. For instance, ARPEGE, RACMO, PRECIS and CCLM produce a better ROD distribution than that of ERAIN when three of the ROD definitions are used, but give a worse ROD distribution than that of ERAIN when the fourth definition is used. However, regardless of the definition used, CCRM5, RCA35, REMO, RegCM3 and WRF show a remarkable improvement over ERAIN. The study shows that the ability of the RCMs in simulating RODs over West Africa strongly depends on how well the models reproduce the northward movement of the monsoon system and the associated features. The results show that there are some differences in the RODs obtained between the two observation datasets and RCMs, and the differences are magnified by differences in the ROD definitions. However, the study shows that most CORDEX RCMs have remarkable skills in predicting the RODs in West Africa.

Electronic supplementary material The online version of this article (doi:10.1007/s00704-014-1104-4) contains supplementary material, which is available to authorized users.

M. S. Mounkaila : B. J. Abiodun (*)
Climate Systems Analysis Group, Department of Environmental and Geographical Science, University of Cape Town, Cape Town, South Africa
e-mail: babiodun@csag.uct.ac.za

M. S. Mounkaila : J. 'Bayo Omotosho
West African Science Service Center for Climate Change and Adapted Land Use (WASCAL) Graduate Research Program, Federal University of Technology Akure, Akure, Nigeria

1 Introduction

West African countries depend on rain-fed agriculture as the main source of income. As a result, the socio-economy and gross domestic products (GDPs) of these countries are strongly influenced by climate variability and change. For instance, the decrease in Sahelian rainfall in the 1970s and 1980s led to severe droughts, famines and many socio-economic problems in West Africa (Nicholson et al. 2000; Abiodun et al. 2008; Djiotang et al. 2010). Water management and agricultural practices depend not only on the amount of the annual rainfall but also on the onset and temporal distribution of the rainfall. The timing of the rainfall onset is crucial for agricultural planning. For instance, an early or late onset of rainfall may drastically reduce crop yields if the agricultural practices are not adapted to accommodate it. However, predicting the rainfall-onset date (ROD) in West Africa, particularly in the Sahel, remains a big challenge because of its great variability. Omotosho (1992) showed that the ROD variability can be as large as the length of the rainy season. The consequences of unreliable predictions of RODs include crop failure, famine and health problems. Hence, there is a keen interest in improving knowledge on predicting RODs in West Africa, as its reliable prediction will help combat famine and enhance food security.

Published online: 20 February 2014

Various studies have suggested different factors that may control the ROD. The factors include sea surface temperatures, vegetation and soil moisture, wind shear, the mid- and upper tropospheric jets (African easterly jet (AEJ) and tropical easterly jet (TEJ), respectively), moist static energy or equivalent potential temperature gradient and the strength and position of the Saharan heat low, which controls the southerly inflow of moist air into the West African subcontinent. Many empirical models have used these factors in predicting the ROD. Notable among these are models based on upper atmospheric winds (Omotosho 1990, 1992) and on sea surface temperature (Lamb and Peppler 1992; Eltahir and Gong 1996; Janicot et al. 1998), rainfall–evapotranspiration relations (Cocheme and Fraquin1967) and equivalent potential temperature (Oduru 1989; Omotosho et al. 2000). Other methods are based on precipitation or surface data only (Sarria-Dodd and Jolliffe 2001; Ati et al. 2002 and Omotosho et al. 2000). The main problem with the empirical models is their low skill in simulating the ROD. This may be owing to a lack of sufficient data in developing countries or training for implementation of the models. The other problem is that empirical models are not dynamically competent since they cannot account for all the factors that control RODs.

To overcome the shortcomings of empirical approaches, some studies have employed dynamic methods (i.e. atmosphere–ocean general circulation models, AOGCMs) in predicting RODs (e.g. Cook and Vizy 2006; Djiotang et al. 2010), but AOGCMs usually have coarse horizontal grid resolution (typically 2°×2° long×lat); therefore, they cannot represent well the influence of mesoscale features (such as isolated reliefs, lakes, coastlines and sharp variation in vegetation, temperature and soil moisture) on RODs (e.g. Druyan et al. 2010; Xue et al. 2010). As a result, AOGCM simulations are usually downscaled using regional climate models (RCMs) with a higher resolution (typically 10–50 km) than AOGCMs. Many studies have demonstrated the capability of RCMs in simulating the intra-seasonal, inter-annual and decadal variability of rainfall, as well as the characteristics of the West African monsoon system (WAMS; e.g. Omotosho and Abiodun 2007; Afiesimama et al. 2006; Sylla et al. 2009, 2010; Vigaud et al. 2009; Pu and Cook 2010; Abiodun et al. 2012). However, some studies have examined the ability of RCMs to simulate the ROD over West Africa (e.g. Ramel et al. 2006; Vanvyve et al. 2007; Sijikumar et al. 2006), but these studies focused on individual models designed for some specific purpose, making it difficult to know the general performance of RCMs in simulating RODs over West Africa. Hence, there is a need for multi-RCM inter-comparisons on ROD simulation over West Africa. The present study is in that direction.

There have been some multi-RCM experiments with encouraging results over West Africa. These include the West African Monsoon Modeling and Evaluation (WAMME; e.g. Druyan et al. 2010; Xue et al. 2010), the Monsoon Multi-disciplinary Analyses (AMMA, van der Linden and Mitchell 2009, e.g. Ruti et al. 2011; Hourdin et al. 2010) and the ENSEMBLE-AMMA project (e.g. Paeth et al. 2011; Diallo et al. 2012a; Sylla et al. 2013). These multi-RCM studies show different results over West Africa. For instance, Druyan et al. (2010) evaluate the ability of five RCMs in simulating the WAM systems and found that the RCMs skillfully represent the monsoon onset. Hourdin et al. (2010) used AMMA model inter-comparison to study the seasonal and intra-seasonal variations in climate over the Sahel and found many discrepancies among the RCMs in simulating rainfall and the latitudinal position of AEJ over the Sahel. They show that none of the RCMs captures all the aspects of the monsoon system. In the inter-comparison of the multi-model RCM from the ENSEMBLES and AMMA projects, Paeth et al. (2011) also found that RCMs exhibit systematic errors in simulating the amplitude and pattern of the West African rainfall; the RCMs have a dry bias in sub-Saharan Africa. Meanwhile, Diallo et al. (2012b) and Sylla et al. (2013) reported RCMs that give a remarkable simulation of the inter-annual variability of rainfall, with a correlation coefficient greater than 0.5. However, most of the above studies indicated that the RCMs' ensemble mean always outperforms individual RCMs in simulating precipitation, but this is not always true for temperature.

The most recent multi-RCM experiment is the Coordinated Regional Downscaling Experiment of Africa (CORDEX-Africa; Nikulin et al. 2012, Gbobaniyi et al. 2013). One of the aims of CORDEX-Africa is to evaluate the quality of RCMs in simulating precipitation and to close the gap of data accessibility of the regions, thereby enabling the scientific community to give suitable information to decision-makers (Nikulin et al. 2012). Nikulin et al. (2012) and Gbobaniyi et al. (2013) found that most RCMs realistically capture the WAM and its related features over West Africa. However, no study has investigated how CORDEX-Africa RCMs perform in simulating the RODs over West Africa. The main goal of the present study is to extend the analyses of Nikulin et al. (2012) and to focus on RODs over West Africa. Hence, the study evaluates the performance of CORDEX-Africa RCMs in simulating the ROD over West Africa. The paper is structured as follows: Section 2 describes the data and methods used in the study, Section 3 presents the results and discussions and Section 4 gives the conclusions of the study.

2 Data and methods

2.1 Data

The study used observation, reanalysis and RCMs' simulation datasets. The observation datasets, which were obtained from the Tropical Rainfall Measuring Mission (TRMM, 3B42 version 6; 0.25° spatial and 3-h resolutions; 1998–2010; Huffman

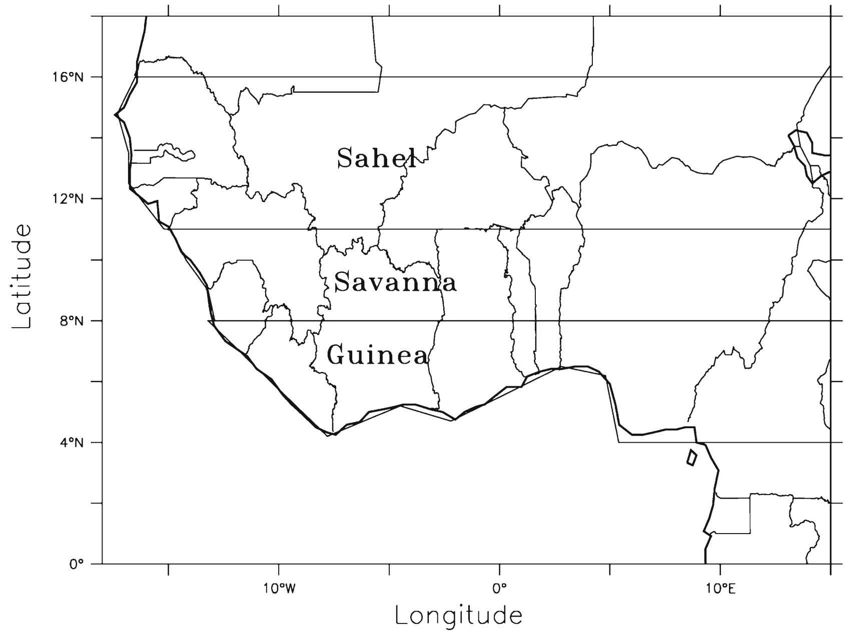

Fig. 1 West African domain divided into three climatic zones: Guinea (4°N–8°N), Savanna (8°N–11°N) and Sahel (11°N–16°N)

et al. 2007) and the Global Precipitation Climatology Project (GPCP, version 1.1; 1° spatial and daily temporal resolution; 1998–2010; Huffman et al. 2001), were used to evaluate the RCM simulations. The use of two observations datasets (GPCP and TRMM) was to account for differences in and uncertainty around observed RODs (Huffman et al. 2009; Huffman and Bolvin 2011). The reanalysis datasets are the European Centre for Medium-Range Weather Forecasts (ECMWF) Interim Re-Analysis (ERAIN; 1989–2008; Dee et al. 2011). The simulation datasets are from nine of the RCMs that participated in the CORDEX-Africa experiment. The RCMs used are ARPEGE, RCA35, PRECIS, CRCM5, REMO, CCLM, RACMO, RegCM3 and WRF. The CORDEX simulation domain (about 25°W–60°E and 44°S–42°N; Nikulin et al. 2012) is much wider than our study domain (West Africa; 18°W–25°E and 0°N–18°N). All the simulations were initialized and driven at the lateral boundaries driven by the ERAIN datasets. All the RCMs used the same sea surface temperature (SST) from ERAIN as ocean boundary condition, except that RegCM3 used the National Oceanic Atmospheric Administration (NOAA) weekly optimum-interpolated SST (Reynolds et al. 2007), and the Canadian Regional Climate Model (CRCM) used the Atmospheric Model Inter-comparison Project, phase 2 (AMIP2) SST (Nikulin et al. 2012). The dynamics and physical parameterizations used in the RCMs for the simulations are given in Nikulin et al. (2012). The CORDEX-Africa simulations were obtained at the Climate Systems Analysis Group (CSAG) at the University of Cape Town. Following Omotosho and Abiodun (2007) and Abiodun et al. (2012), this study divides West African domain into three climatic zones: Guinea (4°N–8°N), Savanna (8°N–11°N) and Sahel (11°N–16°N) as shown in Fig. 1.

2.2 Definition of ROD

There are different definitions for determining RODs in West Africa (i.e. Omotosho 1990; Odekunle 2006; Laux et al. 2008). However, these definitions do sometimes produce different RODs even when applied to the same observation dataset (e.g. Laux et al. 2008). For this study, we selected and

Table 1 Definitions of ROD over West Africa

Methods	Definition ROD	Reference
DEF1	The first decade (10 days) with at least 25 mm of rains, followed by two decades of at least 20 mm of rains	AGRHYMET (1996)
DEF2	The total of at least 25 mm of rainfall within 5 days. The starting day and at least two other days in this 5-day period must be wet (at least 0.1-mm rainfall recorded), followed by a no dry period of seven or more consecutive days occurring in the following 30 days	Stern et al. (1981)
DEF3	Any date after 1 January (instead of 1 May) totalling at least 20 mm of rainfall observed within three consecutive days without a dry period in the next 30 days that exceeds 7 days	Sivakumar (1988)
DEF4	The first two rains totalling 20 mm or more within 7 days, followed by 2 to 3 weeks each with at least 50 % of the weekly crop–water requirement and without a dry spell within 2 to 3 weeks	Omotosho et al. (2000)

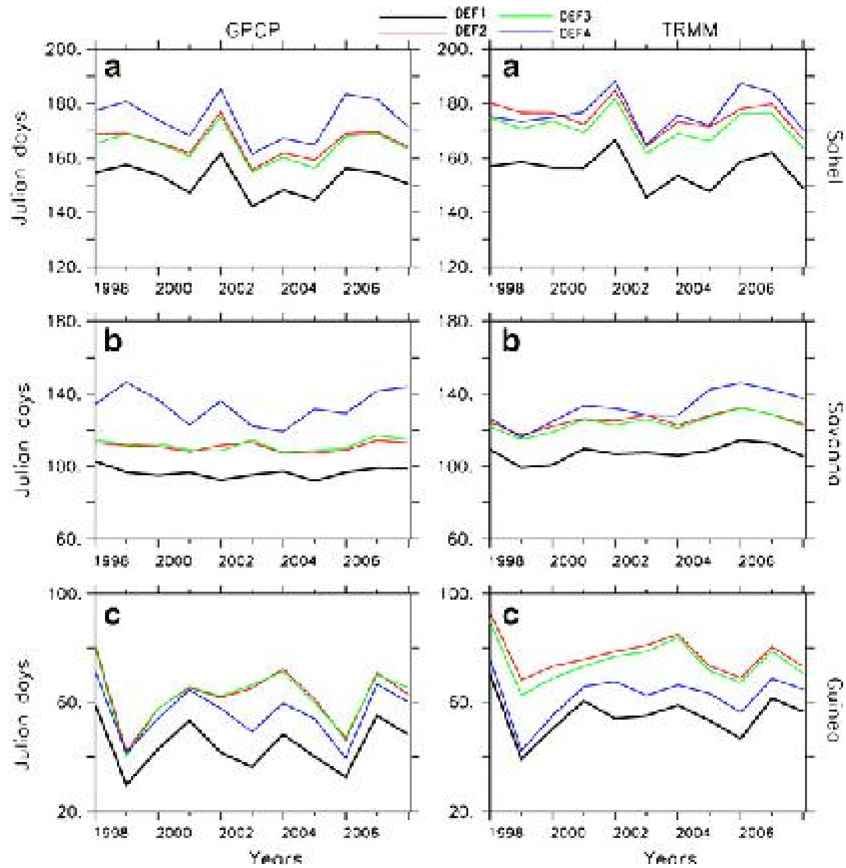

Fig. 2 The inter-annual variation of rainfall onset dates calculated with the four methods using observed datasets (GPCP, left panels; TRMM, right panels) for 1998–2008 over Guinea (bottom panels), Savanna (middle panels) and Sahel (top panels)

compared four prominent ROD definitions over West Africa. The definitions (hereafter DEF1, DEF2, DEF3 and DEF4) are given in Table 1. DEF1 is based on AGRHYMET (1996), DEF2 on Stern et al. (1981), DEF3 on Sivakumar (1988) and DEF4 on Omotosho et al. (2000). We applied the four definitions to compute ROD over each zone in West Africa using two observation datasets and compared the results.

3 Results and discussion

The results of the study are discussed in two parts. The first part examines the differences and similarities between the definitions and compares their sensitivity to changes in observed rainfall datasets (GPCP and TRMM). The second part evaluates the capability of the RCMs in simulating the ROD.

3.1 Comparison of rainfall onset definitions

The four definitions (DEF1, DEF2, DEF3 and DEF4) produce different rainfall-onset dates (RODs) over each zone in West Africa (Fig. 2, Table 2). Over the Sahel, the definitions present different RODs for each year but show similar patterns for the inter-annual variability of ROD (Fig. 2a, b). For instance, the difference between the RODs is up to 30 days in 2002, but all the definitions agree that the Sahel experienced the latest

Table 2 The mean rainfall onset dates (RODs) over West Africa for the period 1998–2008, as obtained with four onsets methods (DEF1, DEF2, DEF3 and DEF4) using GPCP and TRIMM datasets. The difference between RODs from the two dataset (Δ in days) is indicated for each definition

Methods	Guinea			Savanna			Sahel		
	GPCP	TRMM	Δ	GPCP	TRMM	Δ	GPCP	TRMM	Δ
DEF1	13 Feb	24 Feb	11	05 Apr	16 Apr	11	31 May	03 Jun	4
DEF2	02 Mar	17 Mar	15	19 Apr	04 May	15	13 Jun	22 Jun	9
DEF3	02 Mar	14 Mar	12	20 Apr	02 May	12	12 Jun	19 Jun	7
DEF4	25 Feb	02 Mar	6	12 May	11 May	1	22 Jun	24 Jun	2

Table 3 The standard deviation of rainfall onset dates (RODs) over West Africa for the period 1998–2008, as obtained with four onsets methods (DEF1, DEF2, DEF3 and DEF4) using GPCP and TRIMM datasets. The difference between the ROD standard deviation from the two datasets (Δ in days) is indicated for each method

Methods	Guinea			Savanna			Sahel		
	GPCP	TRMM	Δ	GPCP	TRMM	Δ	GPCP	TRMM	Δ
DEF1	9	8	1	3	4	1	6	6	0
DEF2	11	7	4	2	4	2	6	6	0
DEF3	11	7	4	3	5	0	6	6	0
DEF4	10	8	2	9	9	0	8	7	1

RODs in the year. Similarly, the spread in the RODs in 2003 is more than 30 days, but the definitions agree that the earliest RODs occur in the 2003. Among the definitions, DEF1 consistently produces the earliest ROD (i.e. earliest date), while DEF4 gives the latest date. In most years, DEF2 and DEF3 produce the RODs that fall within those of DEF1 and DEF2; the maximum difference between DEF2 and DEF3 is less than 5 days. The strong agreement between DEF2 and DEF3 may

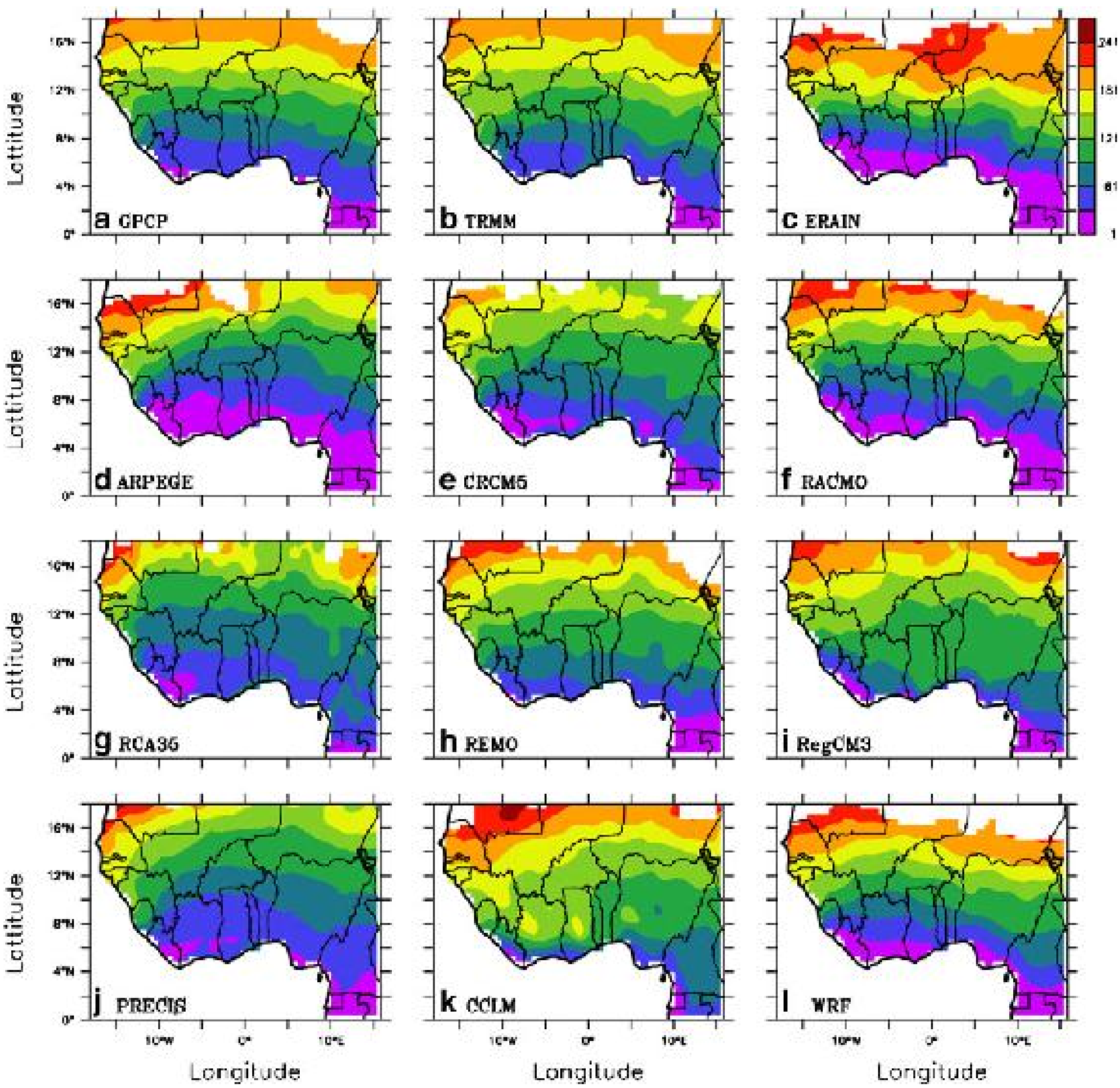

Fig. 3 Mean onset dates as observed (GPCP/TRMM) and simulated (CORDEX RCMS) in DEF1 over West Africa for the period of 1998–2008

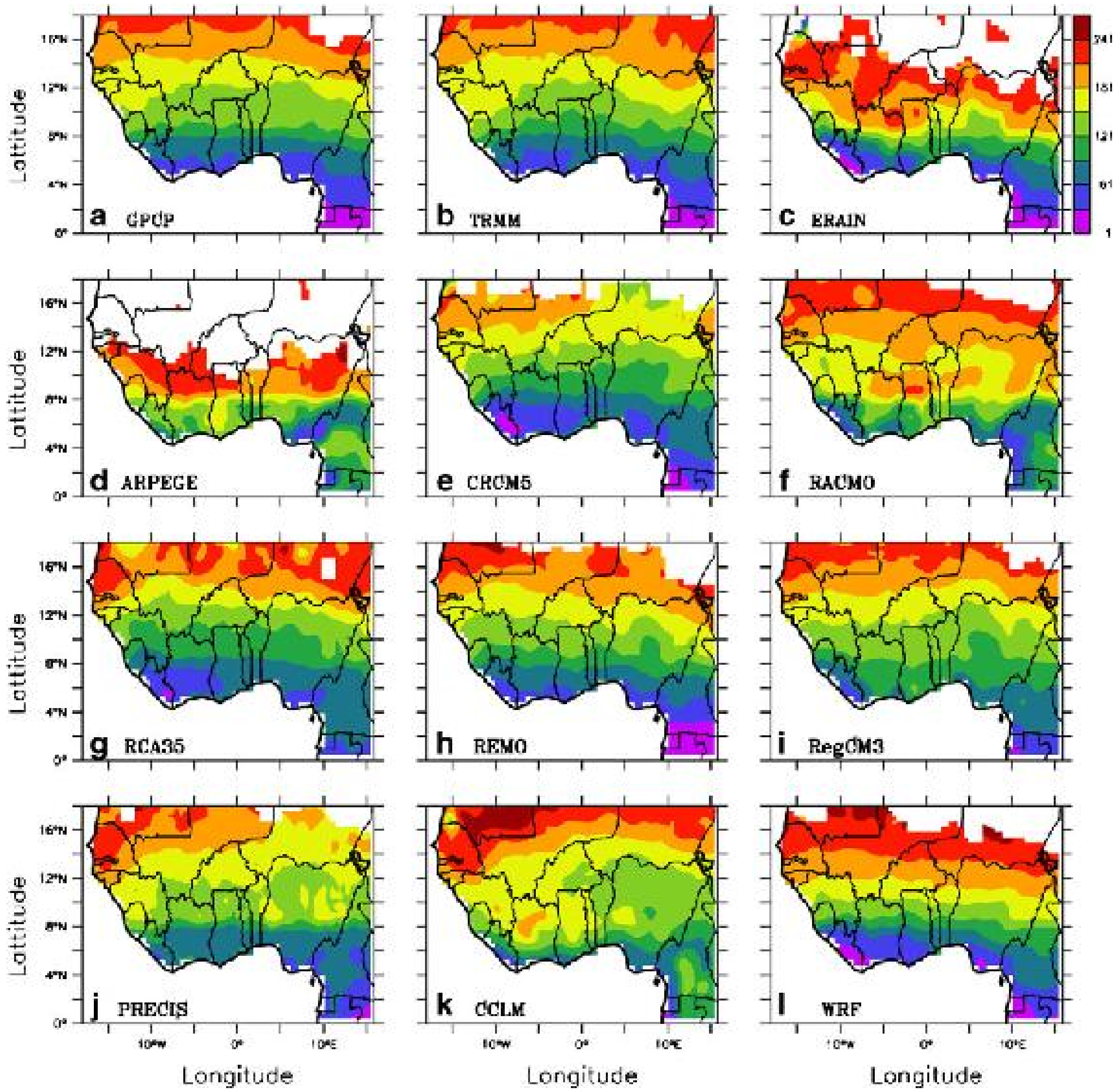

Fig. 4 Mean onset dates as observed (GPCP/TRMM) and simulated (CORDEX RCMS) in DEF4 over West Africa for the period of 1998–2008

be because the two definitions use the same criteria for identifying false ROD (Stern et al. 1981). With each definition, there are substantial differences between ROD in GPCP and TRMM datasets. For example, DEF2 and DEF3 produce later RODs in TRMM than in GPCP. The differences between the RODs with DEF2 (or DEF3) and DEF4 are smaller in the TRMM dataset than in GPCP. However, with both datasets, the characteristics of the RODs over the Savanna are similar to that over the Sahel (Fig. 2b), except that the ROD is earlier over the Savanna than over the Sahel. The characteristics of RODs over Guinea differ from that of the Sahel or the Savanna. Nevertheless, among the three zones (Guinea, Savanna and Sahel), Guinea experiences the earliest ROD and has the most pronounced difference between ROD of GPCP and TRIMM (Fig. 2c), suggesting that the zone has the highest uncertainty in the observed ROD owing to different datasets and definitions for obtaining the ROD.

Tables 2 and 3 present the mean and standard deviation of the RODs for each definition. In general, the mean RODs fall within February–March in Guinea, April–May in the Savanna and May–June in the Sahel. However, DEF1 is an outlier. It consistently produces the earliest RODs in each zone and shows large differences in RODs from the two datasets (11, 11 and 4 days over Guinea, Savanna and Sahel, respectively). The other three definitions (DEF2, DEF3 and DEF4) give comparable RODs, but DEF2 and DEF3 also produce large differences in the RODs from GPCP and TRMM. DEF4 gives the lowest difference in the RODs from the datasets and produces the least differences in the RODs' standard deviation from the datasets (Tables 2 and 3). However, it is difficult to conclude that DEF4 gives the best RODs among the four definitions.

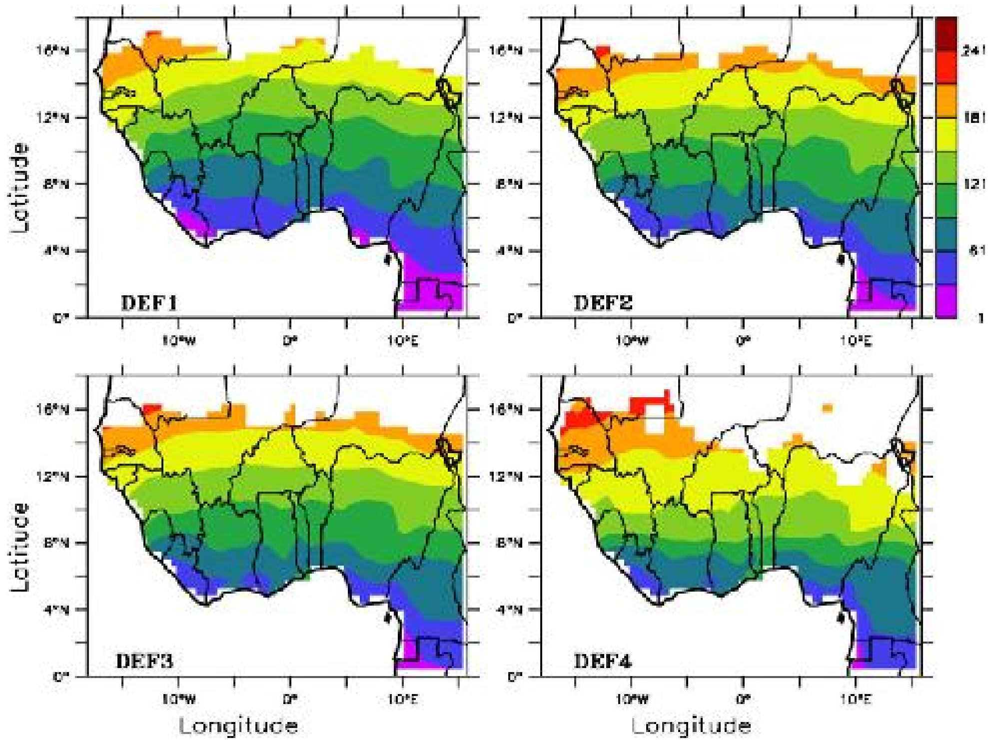

Fig. 5 CORDEX-RCMs ensemble ROD mean over West Africa (Guinea, Savanna and Sahel, respectively) for the period of 1998–2008

3.2 Evaluation of simulated rainfall-onset dates by CORDEX models

To evaluate the capability of the CORDEX models in simulating the characteristics of RODs over West Africa, we compare the simulated RODs with the observed (GPCP and TRMM) using the four onset definitions. The evaluation focuses on how well the models simulate the mean, inter-annual variability of RODs for the period 1998–2008 using each definition.

3.2.1 Spatial distribution of RODs over West Africa

Figures 3 and 4 compare the spatial distribution of the stimulated RODs over West Africa with observations (GPCP and TRMM) for DEF1 and DEF4, respectively. Corresponding figures for DEF2 and DEF3 are similar to those of DEF1; therefore, they are not shown. With all the definitions, the observed RODs (Figs. 3a, b and 4a, b) are generally zonal; the values increase gradually from the coast to inland. However, the distribution is more zonal in DEF1 than in DEF4, and the ROD is earlier north of 8°N in DEF1 than in DEF4. With all the definitions, ERAIN does not capture the spatial distribution of the RODs as observed in GPCP and TRMM. With DEF1, it produces earlier RODs (than observed) south of 8°N, and with DEF4, it gives much earlier RODs over most areas in West Africa, especially north of 8°N and fails to meet the criteria for RODs north of 12°N. The reason for the shortcomings of ERAIN may be related to formulations and physical parameterization (i.e. rainfall parameterization schemes) used to produce ERAIN and the rainfall parameterization schemes in the GCM used for its forecast.

Some RCMs show remarkable improvements over the ERAIN in simulating the RODs, while other RCMs perform worse than the reanalysis (Figs. 3 and 4); however, the performance of some RCMs in simulating the RODs depends on the ROD definition used. Regardless of the definition, the RODs produced by CRCM5, RCA35, REMO, RegCM3 and WRF show remarkable improvement over that of ERAIN when compared with observations, except that RegCM3 produces earlier RODs over Guinea. ARPEGE, RACMO, PRECIS and CCLM also show some improvement over ERAIN when DEF1, DEF2 or DEF3 are used, but not when DEF4 is used. With DEF4, ARPEGE simulates similar ROD patterns as in ERAIN, overestimates the RODs north of 8°N and fails to meet DEF4 ROD criteria north of 10°N; CRCM5 underestimates the RODs north of 10°N; and RACMO fails to reproduce the zonal pattern of RODs in 8°N–12°N, producing a local maximum ROD in the northern part of Ghana. Regardless of the definition used, CCLM fails to reproduce the observed zonal distribution south of 12°N; instead, it produces a local maximum over Cote d'Ivoire in DEF4.

Figure 5 shows the spatial distribution of the RCMs' ensemble mean ROD for each definition. The results are similar

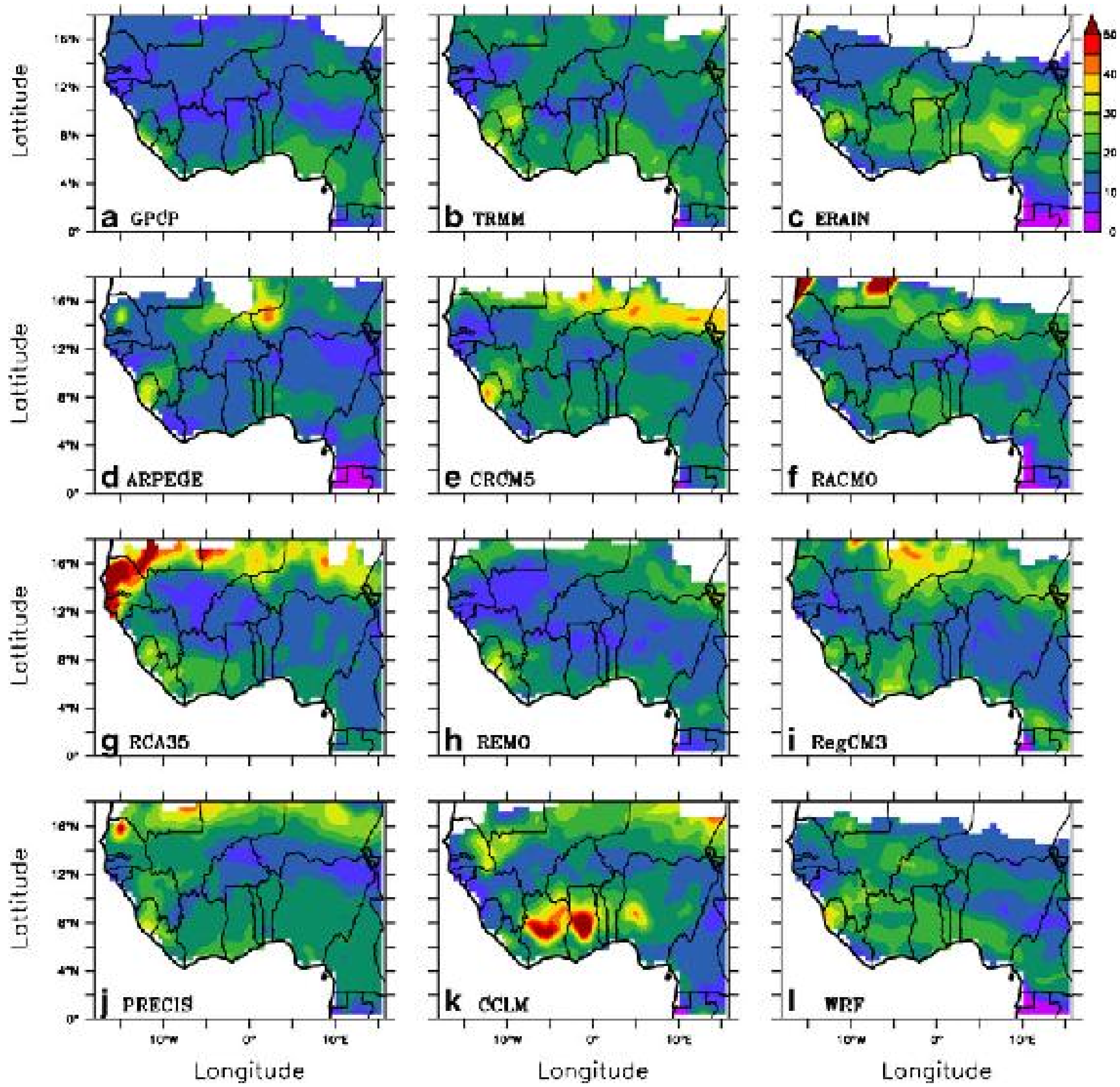

Fig. 6 Standard deviation of onset dates as observed (GPCP/TRMM) and simulated (CORDEX RCM) in DEF1 over West Africa for the period of 1998–2008

to the observed (GPCP and TRMM). The ROD of the RCMs' ensemble mean varies from February to April in DEF2, DEF3 and DEF4 over Guinea and varies from February to March in DEF1. Over the Savanna, the multi-RCMs' mean in DEF1 gives the earliest ROD and the latest RODs in DEF4 (from April to May). As a result, the multi-RCMs' mean improves the simulated ROD over Guinea, the Savanna and the southern part of the Sahel for all the definitions. However, the results are different over the northern part of the Sahel for all the definitions. For instance, in DEF4, the RCMs' mean fails to simulate RODs over the central and eastern part of the Sahel (over northern Mali, Burkina Faso and Niger). The improvement of the multi-RCMs' mean over individual RCM results found in this study is consistent with previous studies (e.g. Paeth et al. 2011, Diallo et al. 2012a, b, Sylla et al. 2013) that attribute the improvement to the cancelling of individual RCM errors in the multi-RCMs' mean; this is true for the multi-RCMs' ROD mean.

Figures 6 and 7 compare the simulated ROD standard deviation (σ) with the observed (GPCP and TRMM) for DEF1 and DEF4, respectively. The results for DEF2 and DEF4 are similar to those of DEF1 and therefore are not shown. The σ is the spread of RODs around the temporal mean; hence, it is a measure of the inter-annual variability of the RODs: high σ indicates high inter-annual variability, while low σ indicates low inter-annual variability. However, it should be noted that the 1998–2008 period is too short, and estimations of the standard deviation can be noisy, one outlier can strongly affects the results obtained. With DEF1, both observations show similar patterns of σ over Guinea and the Savanna, except that TRMM shows a local maximum in the western part of the Savanna (i.e. over Republic of Guinea).

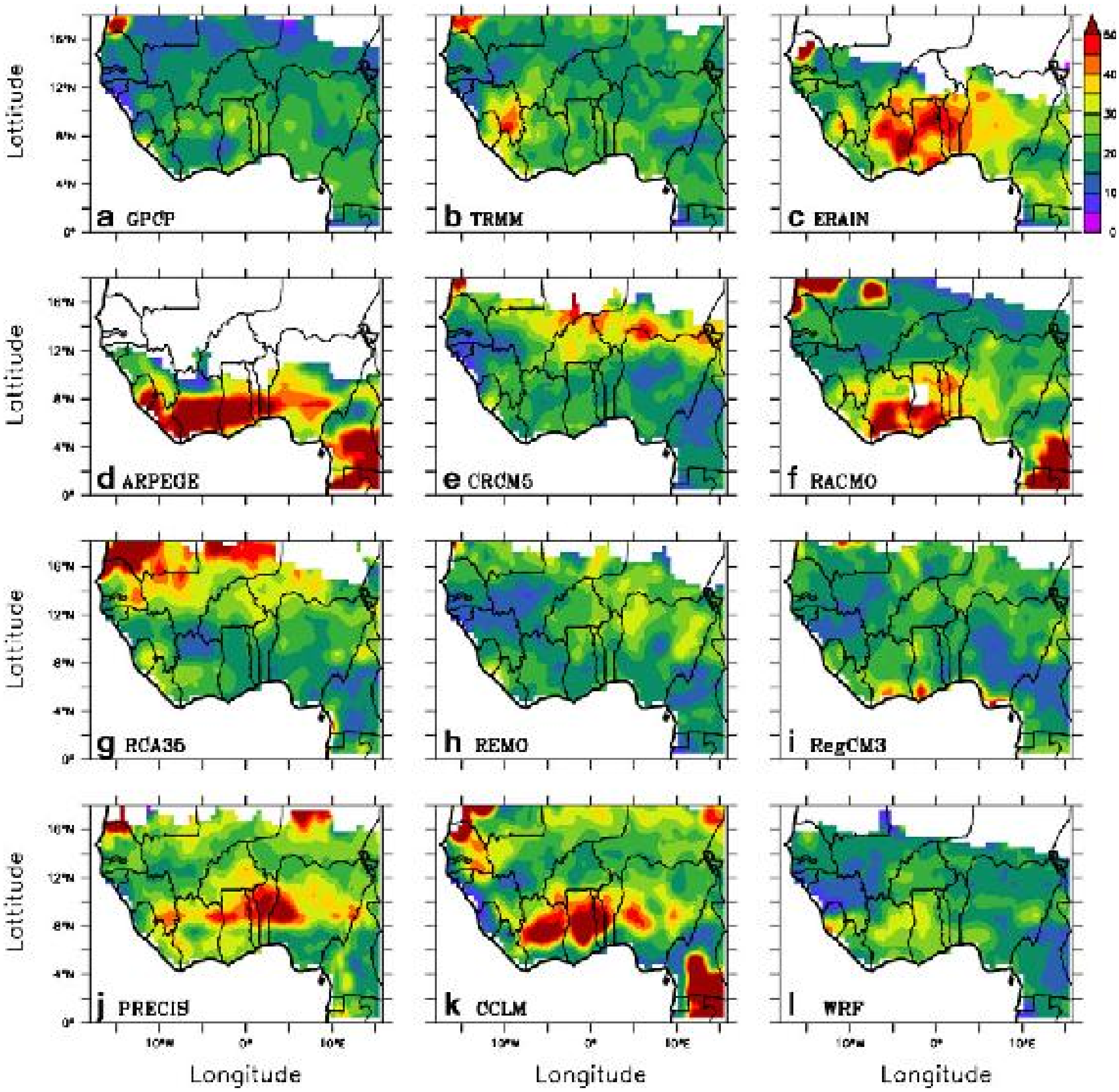

Fig. 7 Standard deviation of onset dates as observed (GPCP/TRMM) and simulated (CORDEX RCM) in DEF4 over West Africa for the period of 1998–2008

However, with DEF4, the magnitude of σ is the same over the three zones, but the local maximum of σ (over Republic of Guinea) produced by TRMM is higher with DEF4 than with DEF1. Nevertheless, ERAIN does not capture the distribution of σ in the observation (GPCP or TRMM) regardless of the definitions used. With DEF1, the reanalysis overestimates the ROD standard deviation (i.e. the inter-annual variability) by about 10 days over the Savanna, especially over the eastern Cote d'Ivoire, northern Ghana, Benin, Togo and southern Nigeria (Fig. 6). The overestimation is worst over the zone with DEF4 (Fig. 7). In addition, ERAIN fails to reproduce σ north of 14°N using any of the definitions because the reanalysis does not meet the criteria for obtaining RODs with DEF4 north of 14°N.

Most of the RCMs do not capture the distribution of σ (i.e. the inter-annual variability). They overestimate it, particularly over the northern part of the Sahel (RCA35, PRECIS, CRCM5 and CCLM), central Savanna (CCLM, RACMO and PRECIS) and along the coast (ARPEGE, CCLM and RACMO) depending on the definitions used. Some RCMs (ARPEGE, CCLM, PRECIS, RACMO and RCA35) simulate worse ROD standard deviation distribution than ERAIN regardless of the definitions used. For instance, ARPEGE fails to satisfy DEF4 criteria north of 10°N, while CCLM largely overestimates σ south of 10°N for each DEF. Nevertheless, some RCMs perform better than ERAIN depending on the definitions used and the geographical location considered (i.e. ARGEGE with DEF1 over Guinea and CRCM5 with DEF3 and 4 over Guinea and the Savanna), showing a lower bias in the simulated standard deviation (i.e. weaker the inter-annual variability). However, three RCMs (REMO, RegCM3 and WRF) produce better results than ERAIN, regardless of the

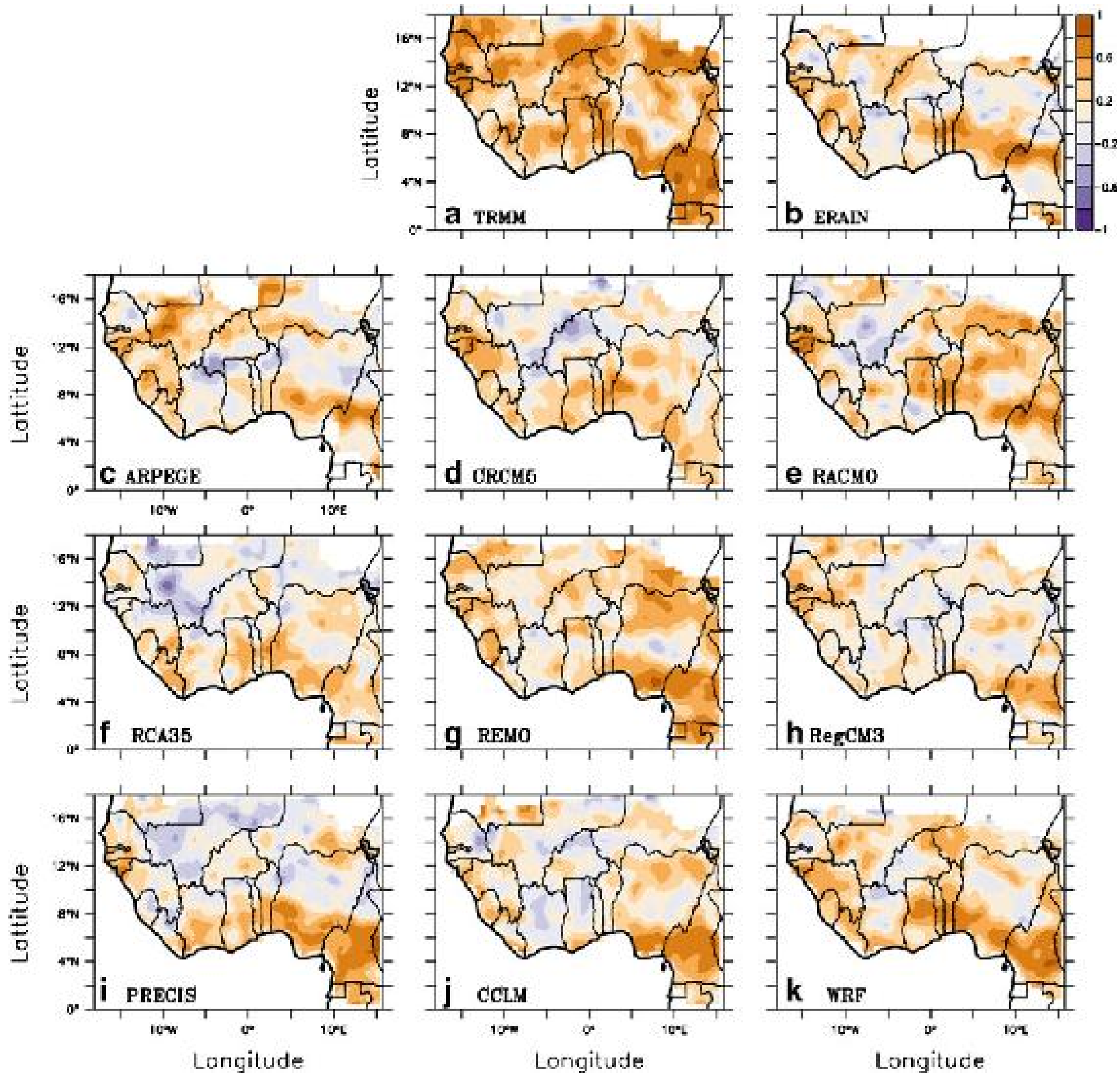

Fig. 8 Correlation of onset dates with respect to observed (GPCP) and simulated (CORDEX RCMs) in DEF1 over West Africa for the period of 1998–2008

definition used. Overall, REMO reproduces the σ pattern better than any other RCM does, regardless of the definition used.

We evaluate the spatial distribution of the correlation (r) between observation (GPCP) and RCMs. A high correlation (typically $r>0.5$) implies a good agreement between the simulated and observed RODs, while a low correlation implies a weak agreement ($r<0.5$) or no agreement ($r<0.0$) between the simulated and observed RODs. The spatial correlation between TRMM and GPCP over West Africa is high and uniform over most of the region, though the value is higher and more uniform in DEF1 than DEF4 (Figs. 8a and 9a), especially over the eastern part of the Savanna. The maximum values ($r\approx0.9$) are over the northern Sahel and along the coast. The correlation coefficient between TRMM and ERAIN changes between positive and negative values over the domain, with the negative values dominating over more areas with DEF4 than with DEF1. The best agreement between TRMM and ERAIN results occurs along the coast south of 5°N over southern Nigeria. For the RCMs, the distribution of r is higher in DEF1 than in DEF4. Regardless of the definitions used, most of the RCMs simulate positive r (Figs. 8 and 9) along the coast of Guinea (ARPEGE, REMO, WRF, PRECIS, RCA35, CRCM5 and CCLM), western Sahel (RCA35, REMO, CRCM5, WRF, PRECIS and RACMO) and northern Sahel (ARPEGE, REMO, RACMO and WRF). Consequently, the RCMs (ARPEGE, REMO, WRF, CRCM5 and PRECIS) perform remarkably well and better than ERAIN as observed in TRMM in all the definitions, except for ARPEGE in DEF4. However, the models have negative r with GPCP over the central and eastern part of the Savanna and give similar or lower results than that of ERAIN in DEF1 and DEF4. Most RCMs show high (positive) correlations with observation

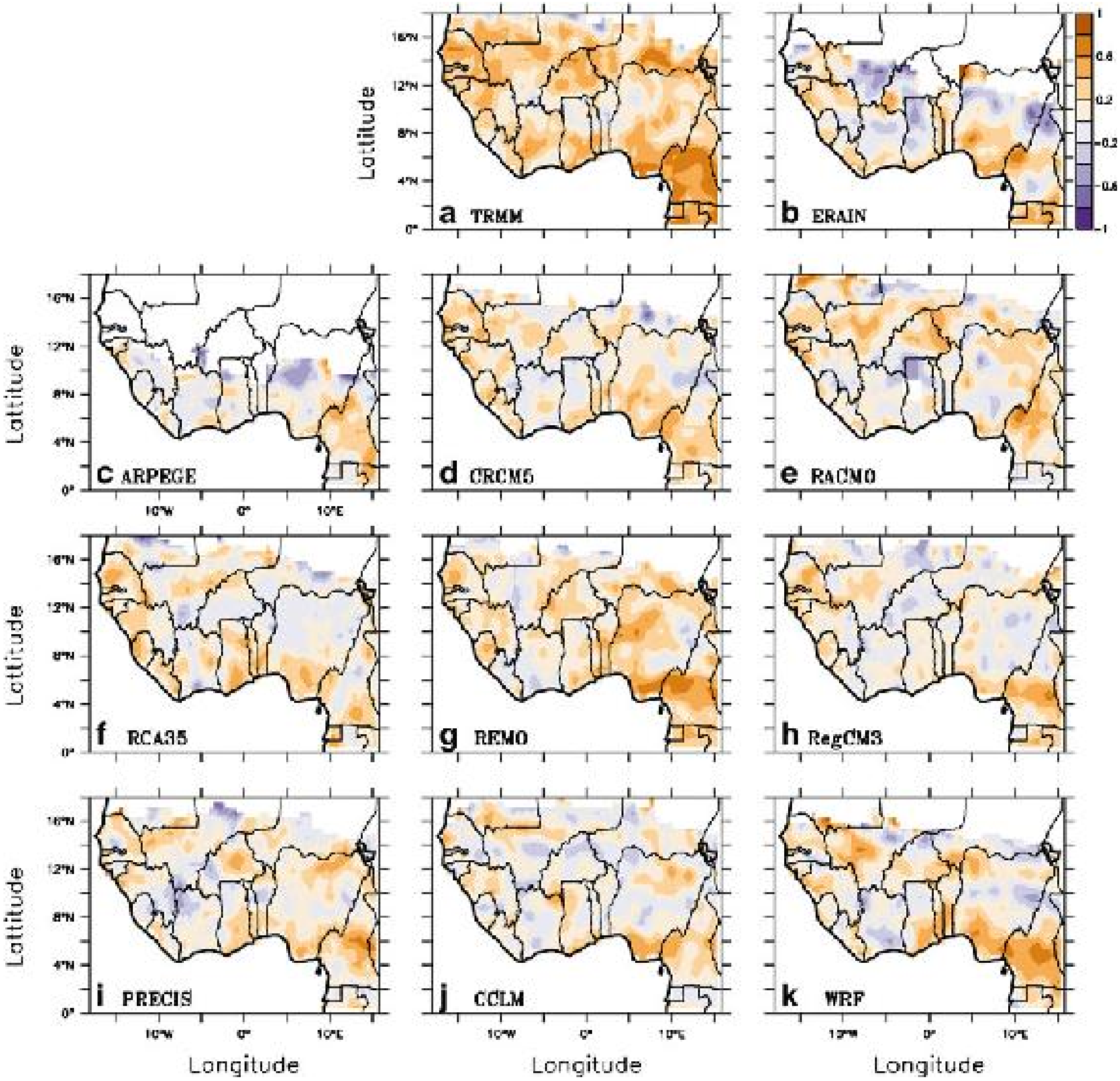

Fig. 9 Correlation of onset dates with respect to observed (GPCP) and simulated (CORDEX RCMs) in DEF4 over West Africa for the period of 1998–2008

over Guinea and the Sahel, but weak (positive and negative) correlations with observation over the Savanna. However, the RCMs' correlation outperforms ERAIN regardless of the definitions used, except along the coast at 5°N over southern Nigeria where it produces a higher correlation.

In general, the RCMs give a realistic simulation of the RODs over West Africa, though the quality of the simulate RODs depends on the definition of ROD used. Using DEF1, DEF2 or DEF3 enhances the performance of the model more than when using DEF4. Regardless of definition used, some RCMs (i.e. CRCM5, RCA35, REMO, RegCM3 and WRF) perform better than ERAIN in simulating the RODs, but some RCMs perform worse. The good performance of the RCMs in simulating the ROD in the present study is consistent with results of Nikulin et al. (2012), who found that the RCMs skillfully simulate the bimodal rainfall pattern over Guinea, the northward monsoon jump from Guinea to the Sahel and the position of the maximum rain band over the Savanna.

3.2.2 The ROD and WAMS

Here, we link the ROD with the northward progression of the WAMS. The monsoon is associated with atmospheric features like the Saharan heat low (SHL), the dry north-easterly Harmattan flow, the inter-tropical discontinuity (ITD) and the African easterly waves (AEW), the AEJ, TEJ (e.g. Omotosho and Abiodun 2007; Abiodun et al. 2011, 2012). Since the complex interaction of the features dictates the onset, intensity and location the monsoon, it is of interest to see how the RCMs link the RODs with them. Unfortunately, the first evaluation output of CORDEX available for the present study did not archive data needed to analyze all these features, but using the available data, we discuss the

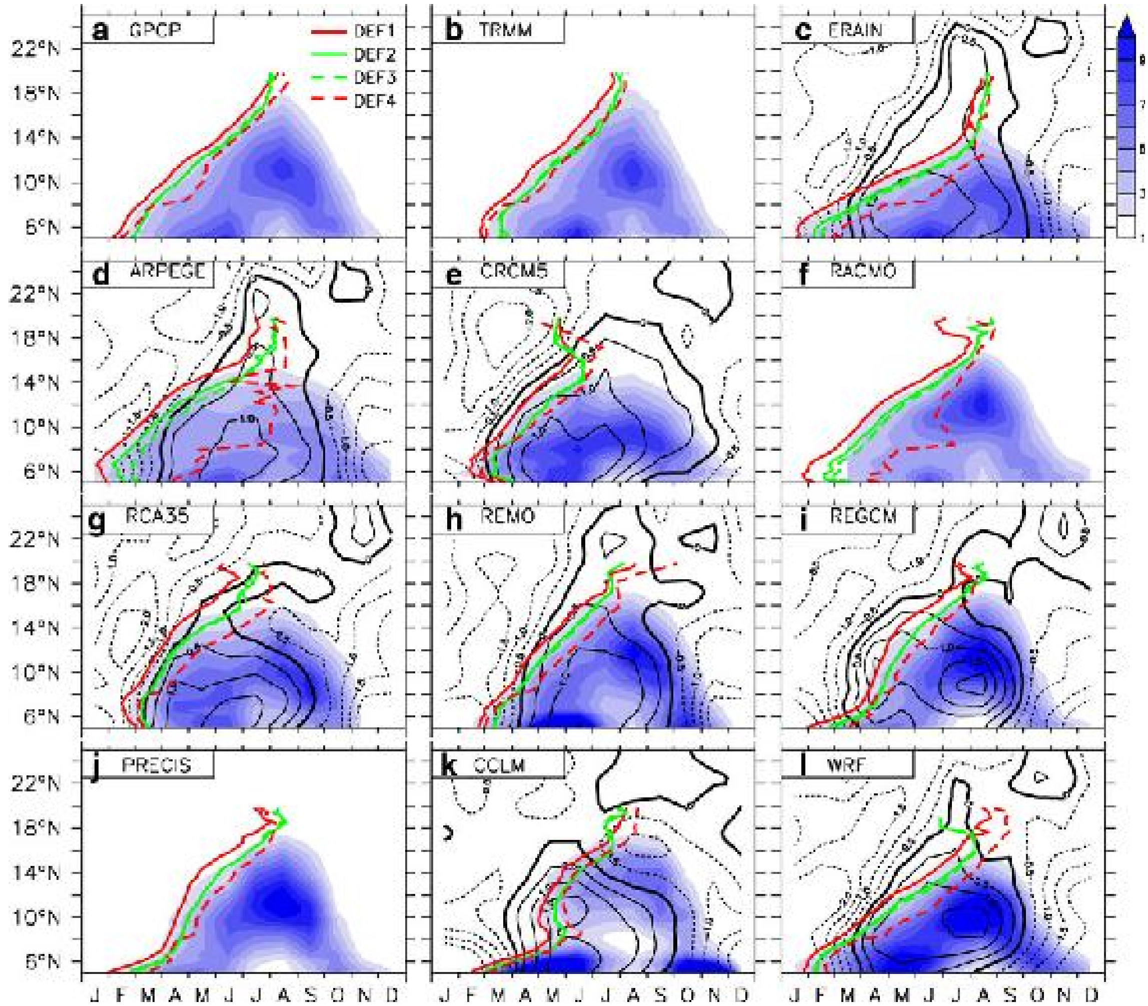

Fig. 10 Time–latitude cross-section of monthly rainfall (millimetres per day; shaded) and onset of monsoon rainfall (green and red thick lines) averaged over 10°W–10°E for observations (GPCP, TRMM) and CORDEX RCMs over West Africa for the period of 1998–2008. The corresponding zonal winds (contours) are shown in the background. Panels a, b, e and i have no wind data

relationship between RODs and the temperature maximum, moist south-westerly monsoon flow, ITD and the associated rainfall.

The observations (GPCP and TRMM; Fig. 10a, b) show that WAMS can be characterized into three different phases: the onset, the peak and the cessation of rainfall in agreement with previous studies (e.g. Le Barbe et al. 2002; Abiodun et al. 2011, 2012; Sylla et al. 2013). The onset of rainfall corresponds to the northward progression of the rain belt from the coast (about 6°N) to 16°N, and it is also associated with the position of ITD (Sultan and Janicot 2003, Omotosho and Abiodun 2007). Both observations (GPCP and TRMM) agree that the monsoon rainfall starts over the Guinea coast (5°N) in February–March and progresses inland (northward) to reach its northernmost position over the Sahel (about 18°N) in August. In ERAIN (Fig. 10c), the onset of rainfall starts earlier (i.e. January) than observed over the Guinea coast (5°N), and the northward progression is slower, reaching the northward position (about 14°N) over the Sahel. Hence, in ERAIN, the northernmost position of the monsoon rainfall is at least 3–4° latitude south of the observed position. That possibly explains why it fails to satisfy the ROD criteria north of 14°N in DEF4, while DEF1, DEF2 and DEF3 are not sensitive to that. Most RCMs (i.e. RACMO, REMO, RegCM3 and PRECIS) produce the start and inland penetration of the monsoon rainfall better than ERAIN does, although in some RCMs (i.e. CRCM5, RCA35 and WRF), the northernmost position is within 14°–15°N.

A notable feature in the northward progression of the monsoon rainfall is the so-called monsoon jump (e.g. Le Barbe et al. 2002; Abiodun et al. 2011, 2012), which signifies a break in the peak of monsoon rainfall during the northward progression. Both observations (GPCP and TRMM) show that the monsoon jump occurs over the Savanna (8°–10°N in June–July), with a local rainfall peak over Guinea (6°N in May–June) and another over the Sahel (11°N in August).

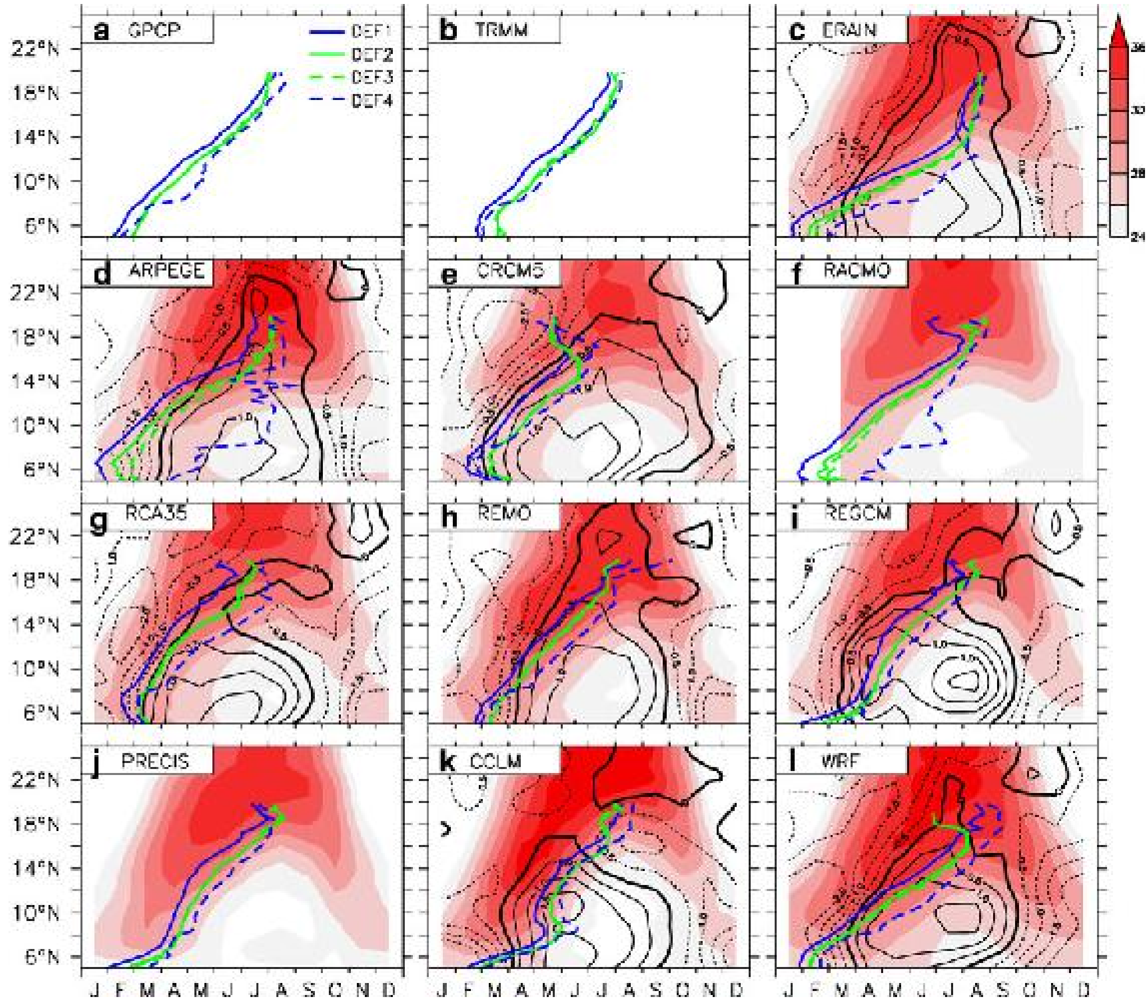

Fig. 11 Time–latitude cross-section of monthly temperature (degrees Celsius; shaded) and onset of monsoon rainfall (green and blue thick lines), averaged over 10 °W–10 °E for observations (GPCP, TRMM) and CORDEX RCMs over West Africa for the period of 1998–2008. The corresponding zonal winds (contours) are shown in the background. Panels a, b, e and i have no wind data

ERAIN poorly represents the monsoon jump. In ERAIN, the location is south of the observed and the values are higher than observed. In addition, the August rainfall peak is located over the Savanna (9°N) instead of over the Sahel (11°N) in the observation. While some RCMs (i.e. REMO, RegCM3) simulate the monsoon jump better than ERAIN does, ARPEGE simulates a worse monsoon jump than ERAIN does. However, Fig. 10 shows that the ROD definitions are sensitive to the rain jump (i.e. Fig. 10d, k) and, in this regard, DEF4 seems to be the most sensitive definition.

Despite the huge discrepancies in the monsoon rainfall produced by the RCMs (and ERAIN), there is a good agreement between their monsoon flows (Figs. 10 and 11). Figure 11 links the monsoon flows with the temperature fields that drive them. In all the RCMs (and ERAIN), the temperature maximum starts from Guinea in January–February and progresses northward (with higher values) to reach the northernmost position between 20° and 22°N (with a value of about 36 °C). The location of ITD, which indicates the northward boundary of the moist southwest monsoon flow, roughly lies over the temperature maximum, and the strength of the flow decreases northward but with a maximum value (about 1–2 ms^{-1}) over the Savanna in July–August. Note that the disagreement (or discrepancy) among the RCMs in simulating monsoon rainfall pattern (or RODs) is the highest between ARPEGE and REMO, yet these two models simulate similar monsoon flow pattern. This suggests that the main source of discrepancy among the RCMs in simulating the RODs is in their representation of the processes that convert the monsoon moisture to rainfall (i.e. rainfall or convection parameterization schemes), the soil moisture and the atmospheric feedback in the models, surface albedo, cloudiness, advection of temperature and energy fluxes (Sylla et al. 2012; Gbobaniyi et al. 2013). Various studies have indentified the convection scheme as a major bottleneck in simulating monsoon flow (e.g. Giorgi and Marinucci 1996; Fulakeza et al. 2002; Krishna et al.

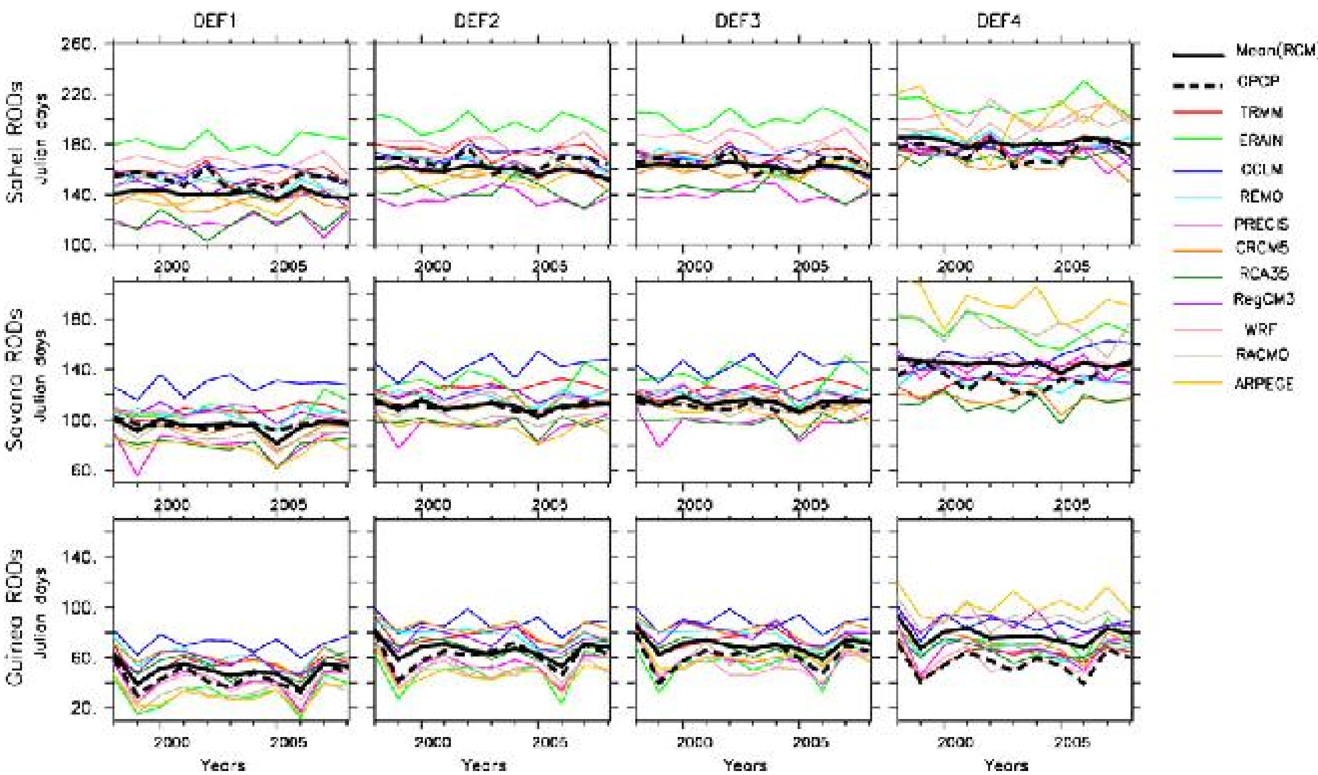

Fig. 12 Inter-annual variability of onset dates as observed (GPCP/TRMM; dash lines) and simulated (CORDEX RCM; lines) in DEF1 and 4 for the period 1998–2008 over West Africa (Guinea, Savanna and Sahel, respectively)

2011). Hence, applying empirical method/definition (e.g. Drobinski et al. 2005; Fontaine et al. 2008) to compute the ROD directly from RCMs' dynamic and thermo-dynamical fields (wind, temperature and moisture), instead of rainfall, may produce better and more consistent RODs from the RCMs. However, this is beyond the scope of the present study.

3.2.3 The inter-annual variation of RODs over the zones

Figure 12 shows the spread among the RCMs in simulating the inter-annual variation of RODs over the three climatic zones (Guinea, Savanna and Sahel) in West Africa. The spread, which can be roughly characterized by the range of the simulated RODs, indicates the uncertainty in the simulated ROD owing to physical parameterization errors in the RCMs. Over Guinea, most RCMs show that the earliest ROD occurs in 1999 and 2006, but the spread among the simulated RODs is more than 50 days using any of the definitions. ARPEGE consistently shows the earliest ROD with the first three definitions in agreement with Nikulin et al. (2012) that show that ARPEGE underestimates the rainfall over Guinea. Nevertheless, ARPEGE also shows the latest ROD with DEF4. CCLM consistently shows the latest ROD in DEF1, DEF2 and DEF3. Over the Savanna, the spread among the RCMs is widest with DEF4 (about 100 days). However, with the first three definitions, CCLM consistently shows the latest ROD while PRECIS shows the earliest ROD, and with DEF4, ARPEGE produces the latest ROD while RCA35 produces the earliest. Over the Sahel, the spread among the RCMs is narrowest with DEF4. PRECIS and RCA35 consistently show the earliest ROD in the first three definitions, while WRF shows the latest ROD in all the definitions. In most cases (except with DEF4 over Guinea), the observed RODs (GPCP) fall within the spread of the simulated RODs. Hence, the RCMs' ensemble ROD shows a lower bias than that of individual RCMs (Fig. 12). The ensemble ROD has the lowest bias (less than 5 days) with DEF2 and DEF3 over the Savanna and the highest bias (about 20 days) with DEF4 over Guinea.

The Taylor diagrams (Fig. 13), which plot the correlations (r) between the simulated and observed RODs against the normalised standard deviations (σ′), show different patterns over the three climatic zones. Over the Guinean zone, all RCMs and reanalysis cluster around a point (r≈0.85, σ′≈ 0.90) with all definitions. This implies that the RCMs and reanalysis show a very good and similar capability in simulating the inter-annual variability and standard deviation of RODs, though with different biases (Tables 4 and 5, Fig. 12). The correlation of the ensemble ROD is about 0.9 with DEF1 and DEF4, but about 0.8 with DEF2 and DEF3. Over the Savanna, the Taylor diagrams show a scatter pattern, except with DEF4, where most RCMs aligned on r≈0.35; REMO

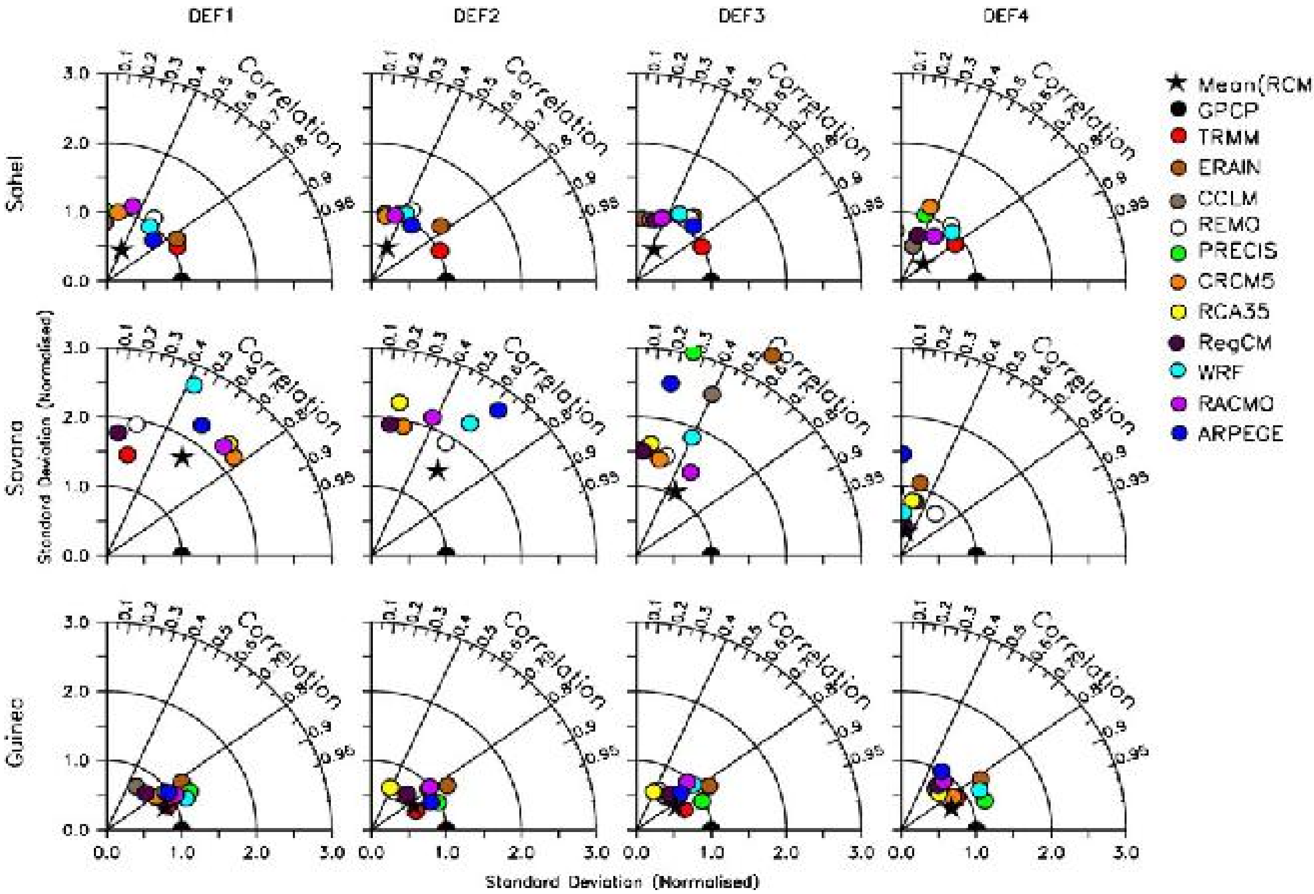

Fig. 13 Taylor diagram of ROD with respect to observed (GPCP) for simulated (CORDEX RCMs) in DEF1 and 4 over West Africa (Guinea, Savanna and Sahel, respectively) for the period of 1998–2008

produces the highest correlation (r = 0.6) and the best standard deviation (σ′ = 1). This indicates that most RCMs perform poorly and differently in simulating the inter-annual variability and standard deviation of ROD over the Savanna. For the ensemble ROD, r = 0.6 with the first three definitions, but r = 0.30 with DEF4; σ′ ≈ 1.5, 1.5, 1.0 and 0.2 with DEF1, DEF2, DEF3 and DEF4, respectively. Over the Sahel, the results are similar to those over Guinea, except that the RCMs aligned on

Table 4 A comparison of simulated and observed RODs over Guinea, showing the mean, the bias in the mean (ΔM) and root mean square error (using GPCP as reference) in DEF1 for the period 1998–2008.

Models	Guinea			Savanna			Sahel		
	Mean	ΔM	RMSE	Mean	ΔM	RMSE	Mean	ΔM	RMSE
GPCP	13 Feb			5 Apr			31 May		
TRMM	30 Jan	14	5	18 Mar	18	6	15 May	16	4
ERAIN	22 Feb	9	5	20 Mar	16	5	28 Apr	33	11
ARPEGE	9 Feb	4	5	20 Mar	16	10	27 Apr	34	8
RCA35	24 Feb	11	3	16 Apr	11	5	3 Jun	3	3
PRECIS	28 Feb	16	5	1 Apr	5	5	13 May	18	7
CRCM5	29 Feb	17	5	13 Apr	8	6	24 May	7	6
REMO	11 Mar	28	8	6 May	31	8	6 Jun	6	8
CCLM	30 Jan	14	6	13 Apr	31	10	1 Jul	31	3
RACMO	31 Jan	12	5	28 Mar	8	5	29 May	2	7
RegCM3	25 Feb	12	6	15 Apr	10	6	24 May	7	9
WRF	9 Feb	4	4	10 Apr	5	7	12 Jun	12	5

Table 5 A comparison of simulated and observed RODs over Guinea, showing the mean, the bias in the mean (ΔM) and root mean square error (using GPCP as reference) in DEF4 for the period 1998–2008

Models	Guinea			Savanna			Sahel		
	Mean	ΔM	RMSE	Mean	ΔM	RMSE	Mean	ΔM	RMSE
GPCP	25 Feb			12 May			22 Jun		
TRMM	2 Mar	6	5	11 May	1	13	24 Jun	3	5
ERAIN	11 Mar	15	7	20 Jun	39	11	29 Jul	37	6
ARPEGE	11 Apr	46	9	11 Jul	60	15	21 Jul	29	20
RCA35	6 Mar	10	7	21 Apr	20	10	19 Jun	3	10
PRECIS	7 Mar	11	4	21 May	10	13	20 Jun	2	9
CRCM5	11 Mar	16	5	25 Apr	17	11	12 Jun	9	9
REMO	9 Mar	13	6	10 May	2	7	28 Jun	6	7
CCLM	27 Mar	31	8	30 May	19	10	23 Jun	1	8
RACMO	31 Mar	35	8	20 Jun	39	15	11 Jul	19	7
RegCM3	27 Mar	31	8	13 May	1	9	23 Jun	2	8
WRF	28 Feb	3	6	23 May	11	10	19 Jul	28	6

$\sigma' \approx 1.5$ with r varying from 0.0 to 0.7 and with DEF4 where models cluster around a point ($r \approx 0.6$, $\sigma' \approx 0.70$). The correlation for the ensemble ROD is about 0.4 with the first three definitions and 0.8 with DEF4; nevertheless, the standard deviation of the ensemble ROD is lower than that of any RCM. Hence, the best performance of the RCMs in simulating the inter-annual variability of ROD (i.e. correlation, standard deviation and root mean square errors) is over Guinea and their worst performance is over the Savanna.

4 Conclusion

In this study, we have compared and used four definitions (DEF1, DEF2, DEF3 and DEF4) of rainfall onset dates in evaluating the capability of CORDEX-Africa RCMs to simulate the characteristics of RODs over West Africa. The evaluation focuses on how well the CORDEX-Africa regional climate models (RCMs) simulate the mean, standard deviation and inter-annual variability of RODs as observed in GPCP and TRMM for the period 1998–2008. ERA-Interim (ERAIN) is also used for the RCMs' performance evaluation. Using the four definitions with observed datasets (GPCP and TRMM), DEF1 consistently produces the earliest ROD, while DEF4 gives the latest ROD.

The spatial distribution of the observed mean ROD is generally zonal and the values increase inland from the coast, but the distribution is more zonal in DEF1 than in DEF4. The ROD is earlier north of 8°N than in DEF1 and in DEF4. ERAIN does not capture the spatial distribution of the ROD as observed in GPCP and TRMM, regardless of the ROD definition. Regardless of the definition used, some RCMs perform better than the ERAIN in simulating the spatial distribution of the ROD, while some RCMs perform worse than ERAIN. Other RCMs (ARPEGE, RACMO, PRECIS and CCLM) perform better than ERAIN when DEF1 (DEF2 or DEF3) is used, but perform worse than ERAIN when DEF4 is used. Observations show that monsoon rainfall starts over the Guinea coast (5°N) in February–March and progresses inland (northward) to reach its northernmost position over the Sahel (about 18°N) in August, but ERAIN produces a monsoon that starts earlier (i.e. January) and progresses slower than the observed, and the northernmost position of the monsoon rainfall in ERAIN is located south of the observed position. Some RCMs produce the start and inland penetration of the monsoon rainfall better than ERAIN does.

The good agreement among the RCMs and ERAIN in simulating temperature fields and monsoon flows over West Africa suggests that the main source of discrepancy among the RCMs in simulating the RODs is owing to the difference in the models representation of rainfall processes. In simulating the inter-annual variability of ROD, the RCMs perform best over Guinea and worst over the Savanna. The RCMs' ensemble mean outperforms individual RCMs and ERAIN in simulating the mean and inter-annual variability of RODs over West Africa, regardless the definition used. This study suggests that the performance of RCMs may be improved by using the ROD definition that uses the simulated dynamic and thermodynamic fields rather than rainfall fields.

Acknowledgments This research was supported through the Graduate Research Program in West African Climate System (GRP-WACS) of the West African Science Service Centre for Climate Change and Adapted Land Use (WASCAL) hosted by the Federal University of Akure (FUTA, Nigeria). We thank the Climate Systems Analysis Group (CSAG) of the University of Cape Town (UCT, South Africa) for the CORDEX data. We thank the two anonymous reviewers whose comments significantly has improved the quality of this manuscript.

References

Abiodun BJ, Pal JS, Afiesimama EA, Gutowski WJ, Adedoyin A (2008) Simulation of West African monsoon using RegCM3 part II: impacts of deforestation and desertification. Theor Appl Climatol 93: 245–261. doi:10.1007/s00704-007-0333-1

Abiodun BJ, Gutowski W, Abatan AA, Prusa JM (2011) CAM-EULAG: a non hydrostatic atmospheric climate model with grid stretching. Acta Geophys 59(6):1158–1167

Abiodun BJ, Adeyewa ZD, Oguntunde PG, Salami AT, Ajayi VO (2012) Modelling the impacts of reforestation on future climate in West Africa. Theor Appl Climatol. doi:10.1007/s00704-012-0614-1

Afiesimama EA, Pal JS, Abiodun BJ, Gutowski WJ, Adedoyin A (2006) Simulation of West African monsoon using the RegCM3. Part I: model validation and interannual variability. Theor Appl Climatol 86:23–37

AGRHYMET (1996) Méthodologie de suivi des zones à risque. AGRH YMET FLASH, Bulletin de Suivi de la Campagne Agricole au Sahel 0/96, Vol. 2, 2 pp. [Available at Centre Regional AGRH YMET, B.P. 11011, Niamey, Niger.]

Ati FO, Stitger CJ, Oladipo EO (2002) A comparison of methods to determine the onset of the growing season in northern Nigeria. Int J Climatol 22:731–742

Cocheme J, Franquin P (1967) An agro-climatology survey of a semi-arid area in Africa, South of Sahara, FAO/WMO Technical Bulletin 86

Cook KH, Vizy EK (2006) Coupled model simulations of the West African monsoon system: twentieth- and twenty-first-century simulations. J Clim 19:3681–3703

Dee DP et al (2011) The ERA-Interim reanalysis: configuration and performance of the data assimilation system. Q.J.R. Meteorol Soc 137:553–597. doi:10.1002/qj.828

Diallo I, Sylla MB, Giorgi F, Gaye AT, Camara M (2012a) Multi-model GCM-RCM ensemble-based projections of temperature and precipitation over West Africa for the early 21st century. Int J Geophys, Article ID 972896

Diallo I, Sylla MB, Camara M, Gaye AT (2012b) Interannual variability of rainfall and circulation features over the Sahel based on multiple regional climate models simulations. Theor Appl Climatol. doi:10.1007/s00704-012-0791-y

Djiotang et al (2010) Sensitivity of the simulated African monsoon of summers 1993 and 1999 to convective parameterization schemes in RegCM3. Theor Appl Climatol 100:207–220

Drobinski P, Sultan B, Janicot S (2005) Role of the Hoggar massif in the West African monsoon onset. Geophys Res Lett 32, L01705. doi:10.1029/2004GL020710

Druyan LM, Feng J, Cook KH, Xue Y, Fulakeza M, Hagos SM, Konare A, Moufouma-okia W, Rowell DP, Vizy EK, Ibrah SS (2010) The WAMME regional model intercomparison study. Clim Dyn 35:175–192

Eltahir E, Gong C (1996) Dynamics of wet and dry years in West Africa. J Clim 9:1030–1042

Fontaine B, Louvet S, Roucou P (2008) Definition and predictability of an OLR-based West African monsoon onset. Int J Climatol 28: 1787–1798

Fulakeza M, Druyan L, Krishnamurti T (2002) A simple soil moisture scheme for climate simulations in the tropics. Atmos Phys 79:105–126

Gbobaniyi E, Sarr A, Sylla MB, Diallo I, Lennard C, Dosio A, Dhiédiou A, Kamga A, Klutse NAB, Hewitson B, Nikulin G, Lamptey B (2013) Climatology, annual cycle and interannual variability of precipitation and temperature in CORDEX simulations over West Africa. Int J Climatol. doi:10.1002/joc.3834

Giorgi F, Marinucci M (1996) An investigation of the sensitivity of simulated precipitation to model resolution and its implication for climate studies. Mon Weather Rev 124:148–166

Hourdin, F, Mustat, I, Guichard, F, Ruti, PM, & Favot, F. Pham MMA, Grandpeix JY, Polcher J, Marquet P, Boone A, Lafore JP, Redelsperger JL, Dell'Aquilla A, Losada Doval T, Traore AK, Gallee H (2010) AMMA-Model intercomparison project. Bull Am Meteorol Soc

Huffman GJ, Bolvin DT (2011) TRMM and other data precipitation data set documentation. NASAGSFC Rep., 29 pp. ftp://precip.gsfc.nasa.gov/pub/trmmdocs/3B42_3B43_doc.pdf. Accessed 23 July 2013

Huffman GJ, Adler RF, Morrissey MM, Bolvin DT, Curtis S, Joyce R, McGavock B, Susskind J (2001) Global precipitation at one-degree daily resolution from multi-satellite observations. J Hydrometeorol 2:36–50

Huffman GJ et al (2007) The TRMM multisatellite precipitation analysis (TMPA): quasi-global, multiyear. combined-sensor precipitation estimates at fine scales. J Hydrometeorol 8:38–55

Huffman GJ, Adler RF, Bolvin DT, Gu G (2009) Improving the global precipitation record: GPCP version 2.1. Geophys Res Lett 36, L17808. doi:10.1029/2009GL040000

Janicot S, Harzallah A, Fontaine B, Moron V (1998) West African monsoon dynamics and eastern equatorial Atlantic and Pacific SST anomalies (1970–88). J Clim 11:1874–1882

Krishna et al (2011) Customization of WRF-ARW model with physical parameterization schemes for the simulation of tropical cyclones over North Indian Ocean. Nat Hazards. doi:10.1007/s11069-011-9862-0

Lamb PJ, Peppler RA (1992) Further case studies of tropical Atlantic surface atmospheric and oceanic patterns associated with sub-Saharan drought. J Clim 5:476–488

Laux P, Kunstmann H, árdossy AB (2008) Predicting the regional onset of the rainy season in West Africa. Int J Climatol 28:329–342

Le Barbe L, Lebel T, Tapsoba D (2002) Rainfall variability in West Africa during the years 1950–1990. J Clim 15(2):187–202

Nicholson SE, Some B, Kone B (2000) An analysis of recent rainfall conditions in West Africa, including the rainy seasons of the 1997 El Niño and the 1998 La Niña years. J Clim 13:2628–2640

Nikulin G et al (2012) Precipitation climatology in an ensemble of CORDEX-Africa regional climate simulations. J Clim 25:6057–6078

Odekunle TO (2006) Determining rainy season onset and retreat over Nigeria from precipitation amount and number of rainy days. Theor Appl Climatol 83:193–201

Oduru AK (1989) On the mean monthly equivalent potential temperature and rainfall in West Africa. Theor Appl Climatol 39:188–193

Omotosho JB (1990) Onset thunderstorms and precipitation over northern Nigeria. Int J Climatol 10:849–860

Omotosho JB (1992) Long-range prediction of the onset and end of the rainy season in the West African Sahel. Int J Climatol 12:369–382

Omotosho JB, Abiodun BJ (2007) A numerical study of moisture build-up and rainfall over West Africa. Meteorol Appl 14:209–225

Omotosho JB, Balogun AA, Ogunjobi K (2000) Predicting monthly and seasonal rainfall, onset and cessation of the rainy season in West Africa using only surface data. Int J Climatol 20:865–880

Paeth H, Hall NMJ, Gaertner MA, Alonso MD, Moumouni S, Polcher J, Ruti PM, Fink AH, Gosset M, Lebel T, Gaye AT, Rowell DP, Moufouma-Okia W, Jacob D, Rockel B, Giorgi F, Rummukainen M (2011) Progress in regional downscaling of West African precipitation. Atmos Sci Lett 12:75–82. doi:10.1002/asl.306

Pu B, Cook KH (2010) Dynamics of the West African westerly jet. J Clim 23:6263–6276

Ramel R, Gallée H, Messager C (2006) On the northward shift of the West African monsoon. Clim Dyn Res 26:429–440. doi:10.1007/s00382-005-0093-5

Reynolds RW, Smith TM, Liu C, Chelton DB, Casey KS, Schlax MG (2007) Daily high-resolution-blended analyses for sea surface temperature. J Clim 20:5473–5496

Ruti PM et al (2011) The West African climate system: a review of the AMMA model inter-comparison initiatives. Atmos Sci Lett 12:116–122. doi:10.1002/asl.305

Sarria-Dodd DE, Jolliffe IT (2001) Early detection of the wet season in semiarid tropical climates of western Africa. Int J Climatol 21:1251–1262

Sijikumar S, Roucou P, Fontaine B (2006) Monsoon onset over Sudan-Sahel: simulation by the regional scale model MM5. Geophys Res Lett 33: L03814. doi:10.1029/2005GL024819

Sivakumar MVK (1988) Predicting rainy season potential from the onset of rains in the Southern Sahelian and Sudanian climatic zones of West Africa. Agric For Meteorol 42:295–305

Stern RD, Dennett MD, Garbutt DJ (1981) The start of the rains in West Africa. J Clim 1:59–68

Sultan B, Janicot S (2003) The West African monsoon dynamics. Part II: the "preonset" and "onset" of the summer monsoon. J Clim 16: 3407–3427

Sylla MB et al (2009) High-resolution simulations of West African climate using regional climate model (RegCM3) with different lateral boundary conditions. Theor Appl Climatol 98:293–314

Sylla MB, Dell'Aquila A, Ruti PM, Giorgi F (2010) Simulation of the intraseasonal and the interannual variability of rainfall over West Africa with a RegCM3 during the monsoon period. Int J Climatol 30:1865–1883

Sylla MB, Giorgi F, Coppola E, Mariotti L (2012) Uncertainties in daily rainfall over Africa: assessment of gridded observation products and evaluation of a regional climate model simulation. Int J Climatol

Sylla MB, Diallo I, Pal JS (2013) West African monsoon in state-of-the-science regional climate models. doi. 10.5772/55140

Van der Linden, Mitchell (2009) ENSEMBLES: climate change and its impacts: summary of research and results from the ENSEMBLES project. Met Office Hadley Centre: Exter

Vanvyve E, Hall N, Messager C (2007) Internal variability in a regional climate model over West Africa. Clim Dyn. doi 10.1007/s00382-007-0281-6

Vigaud N et al (2009) WRF/ARPEGE-CLIMAT simulated climate trends over West Africa. Clim Dyn 36:925–944. doi:10.1007/s00382-009-0707-4

Xue Y et al (2010) Intercomparison and analyses of the climatology of the West African Monsoon in the West African monsoon modeling and evaluation project (WAMME) first model intercomparison experiment. Clim Dyn 35:3–27. doi:10.1007/s00382-010-0778-2